2013

Frost-heave and thaw-weakening of pavement foundation materials

YANG ZHANG
Iowa State University

Frost-heave and thaw-weakening of pavement foundation materials

by

Yang Zhang

A thesis submitted to the graduate faculty

In partial fulfillment of the requirements for the degree of

MASTER OF SCIENCE

Major: Civil Engineering (Geotechnical Engineering)

Program of Study Committee:
David J. White, Major Professor
Robert Horton
Peter C. Taylor
Pavana K. R. Vennapusa

Iowa State University

Ames, Iowa

2013

DEDICATION

For

My parents, Xiaolin Zhang and Demei Liu

献给

我的爸爸妈妈，张晓林先生和刘德梅女士

TABLE OF CONTENTS

LIST OF TABLES

LIST OF FIGURES

ABSTRACT

Freeze-thaw cycles are common in cold regions and lead to frost heave and thaw weakening that influence pavement construction, maintenance, safety, and longevity. Because there is limited research about frost heave and thaw weakening of pavement foundation geomaterials, this research focused on the frost heave and thaw weakening performance of geomaterials stabilized with various combinations of fly ash, cement, fibers, and fibers with cement.

The first objective of this research was to conduct laboratory tests according to ASTM D5918 to compare the effects of these stabilizers on frost susceptibility. The second objective of this research was to further associate laboratory results with in situ freeze-thaw performance of pavements with similar stabilized foundation geomaterials.

For sandy lean clay, fly ash decreased frost susceptibility, and 15% fly ash performed better than 5%, 10%, and 20% fly ash. Cement decreased the frost susceptibility to very low to negligible levels for both sandy lean clay and silty sand with gravel. For silty sand with gravel, fibers alone did not significantly affect frost susceptibility, but fibers with cement performed better than the other stabilizers. Findings related to variations in compaction delay, cure time, setting time for chemical stabilizers, and cost are also reported.

In situ stiffness testing conducted during frozen and after thaw conditions indicated that frozen pavements were stiffer than after thaw pavements. The trends in seasonal variation in stiffness were similar for pavement systems with all kinds of stabilization. Layers stabilized with cement and cement with fibers had the lowest stiffness changes after freeze-thaw cycles. These findings correlate with laboratory test results.

This research provides guidance for selecting stabilizers to improve the frost susceptibility of pavement foundation materials.

CHAPTER 1. INTRODUCTION

In climates like Iowa, pavement foundation materials are subject to freezing and thawing, which influence pavement systems associated with design, construction, and maintenance. This physical process is called the freeze-thaw cycle and results in frost heave and thaw weakening in pavement foundation layers. In earthwork engineering, freeze-thaw cycles are a common problem that influences the construction, safety, serviceability (e.g., user comfort or confidence), durability, and maintenance costs of pavements for pavement designers, transportation agencies, contractors, road users, and taxpayers.

The research reported in this thesis is part of a larger project at the Boone County Test Sections site jointly conducted by the Center for Earthworks Engineering at Iowa State University and the Iowa Department of Transportation. This chapter describes the industry and technical problems with respect to the goals, objectives, and significance of this research. The final section of this chapter presents the organization of this thesis.

TECHNICAL PROBLEM

Non-uniform heave and changes in the stiffness of geomaterials are the most immediate problems caused by freeze-thaw cycles. Although research into the effects of freeze-thaw cycles has been conducted (Cassagrande et al. 1931; Johnson 2012; Beskow 1935; Chamberlain 1986), there is limited research about the effects of frost heave and thaw weakening on relationships between the wide range of geomaterials used in modern construction, moisture contents, and stabilizers (e.g., cement, polymer fibers, and geosynthetics). To provide effective pavement designs, changes in the in situ pavement foundation stiffness and heave rates during and after freeze-thaw cycles need to be better quantified. In this study, laboratory testing following ASTM D5918 provides a basis for comparing the behavior of various geomaterials and studying the effects of various stabilizers. Whether laboratory data can accurately predict pavement performance after freeze-thaw cycles is an extended technical problem because laboratory and in situ freeze-thaw tests have not yet been correlated.

GOALS OF THE RESEARCH

The first goal of this research was to compare the stabilization effects of various stabilizers for geomaterials based on frost susceptibility. The second goal of this research was to further associate laboratory results with the in situ freeze-thaw performance.

OBJECTIVES

The objectives of this research are to:

- conduct laboratory freeze-thaw tests to evaluate the frost susceptibility of pavement foundation materials;
- conduct laboratory freeze-thaw tests with pavement foundation materials stabilized with cement, fly ash, geo-fibers, and geotextiles and determine the stabilization effect; and
- evaluate frost action of in situ pavement foundation.

SIGNIFICANCE OF THE RESEARCH

Improving the freeze-thaw performance of geomaterials is critically related to the stabilization methods applied. This research provides guidance for selecting stabilization methods in order to derive minimum frost susceptibility of various pavement foundation materials.

The benefits to industry from this research are to improve the safety and durability of pavement systems, to reduce the costs of construction and maintenance, and to provide comfortable serviceability for road users.

This research also compares laboratory freeze-thaw results to in situ freeze-thaw performance to begin to fill gaps in the limited research about predictions for field frost action based on laboratory tests.

ORGANIZATION OF THE DOCUMENT

Following this introductory chapter, this thesis is organized into six additional chapters. Chapter 2 reviews previous literature and provides background information for the study. Chapter 3 describes the laboratory and field test methods, and chapter 4 summarizes the laboratory and in situ properties that characterize the tested materials. Chapter 5 presents the results and analyses for the tests performed and discusses these findings. Chapter 6

summarizes the conclusions and outcomes derived from this research. The final chapter discusses how these conclusions can be applied in construction practice and offers suggestions for future research. Supporting materials are included as appendices that follow the list of works cited.

KEY TERMS

Freeze-thaw, frost susceptibility, stabilization, pavement foundations.

CHAPTER 2. BACKGROUND/LITERATURE REVEIW

This chapter illustrates four topics: context for the research, freeze-thaw problems of geomaterials, frost-heave and thaw-weakening laboratory test, soil stabilization methods, and costs of stabilization methods.

CONTEXT OF THE PROJECT

This research is part of a larger project that was funded by the Iowa DOT and jointly carried out by the Iowa DOT, Boone County, and the Center for Earthworks Engineering at Iowa State University. This larger project applied new stabilization technologies such as cement, fly ash, geofibers, and mechanical compaction on the site. The field construction was conducted from May to July in 2012. The Boone County test sections are located near Boone, Iowa (Figure 1) where the average monthly temperatures range from -13 °C to 29 °C (Weather.com 2013).

Figure 1. Location of the Boone County Test Sections site (Map data: Google 2013)

The project site consists of 4.8 miles of roadway with thirteen roads oriented in the North-South direction (denoted as 1st St. to 13th St.) and three roads oriented in the East-

West direction (denoted as South Ave., Central Ave., and North Ave.). Re-construction occurred on all roads except 13th St, which was paved with HMA earlier in 2012. Construction of test sections required removing the existing chip seal surface and subbase, and 6 to 12 in. of subgrade. The subgrade consisted primarily of wet soils classified as CL or A-6(5). Pore water pressure measurements from cone penetration tests (CPTs) indicated ground water elevations at depths of about 3 to 6 ft below original grade across the site, and at about 12 ft or greater near drainage features.

Sixteen test sections were constructed on the North-South roads that used woven and non-woven geotextiles at subgrade/subbase interfaces; triaxial and biaxial geogrids at subgrade/subbase interfaces; 4 in. and 6 in. geocells in the subbase layer + non-woven geosynthetics at subgrade/subbase interfaces; portland cement (PC) and fly ash stabilization of subgrades; PC stabilization of recycled subbase; PC + fiber stabilization of recycled subbase with polypropylene fibers and monofilament-polypropylene fibers; mechanical stabilization (mixing subgrade with existing subbase); and high-energy impact compaction. Triaxial and biaxial geogrids were used at subgrade/subbase interfaces at select locations on East-West roads. Individual techs brief provide detailed information for each technology (http://ceer.iastate.edu/research/).

All test sections except one were topped with a nominal 6 in. of modified subbase material (MSB) classified as GP-GM or A-1-a (7% fines content); the 6 in. geocell section required 7 in. of MSB. Crushed limestone was used in the MSB layer on all North-South roads, and a mixture of recycled concrete and recycled asphalt was used in the MSB layer on all East-West roads. Six test sections (North and South sections of 6th St., 7th St., and 9th St.) consisted of 6 in. of recycled subbase material classified as SM (USCS) or A-1-a (AASHTO) (14% fines content) between the subbase and subgrade layers (CEER 2013). Table 1 shows the tech summary on the test sections. Field and lab tests were conducted both during and after construction. These tests included light weight deflectometer (LWD); falling weight deflectometer (FWD); dynamic cone penetration (DCP) tests; soil classification; strength; compaction; and frost-heave and thaw-weakening tests. The research reported in this thesis focuses on the frost-heave and thaw-weakening lab tests of samples of stabilized subbase and subgrade materials from the site that simulate site construction.

Table 1. Stabilization technologies implemented at the Boone Test Sections site

Street	Segment	Foundation Layer Profile (above natural subgrade)	
1st St.	North	6 in. CLSB	12 in. compacted subgrade
	South		
2nd St.	North	6 in. CLSB	12 in. mechanically stabilized subgrade
	South		
3rd St.	North	2 in. CLSB	4 in. geocell reinforced MSB, NW geotextile
	South	1 in. CLSB	6 in. geocell reinforced MSB, NW geotextile
4th St.	North	6 in. CLSB	NW geotextile
	South	6 in. CLSB	woven geotextile
5th St.	North	6 in. CLSB	triaxial geogrid
	South	6 in. CLSB	biaxial geogrid
6th St.	North	6 in. CLSB	6 in. recycled subbase + 5% cement + 0.4% PP fibers
	South	6 in. CLSB	Synthetic Subsurface Drainage Layer, 6 in. recycled subbase + 5% cement + 0.4% MF fibers
7th St.	North	6 in. MSB	6 in. recycled subbase + 5% cement
	South		
8th St.	North	6 in. CLSB	12 in. compacted subgrade
	South		
9th St.	North	6 in. CLSB	6 in. reclaimed subbase
	South		
10th St.	North	6 in. CLSB	Compacted subgrade
	South		Natural subgrade
11th St.	North	6 in. CLSB	12 in. 10% cement stabilized subgrade
	South	6 in. CLSB	12 in. 20% fly ash (Port Neal) stabilized subgrade
12th St.	North	6 in. CLSB	12 in. 15% fly ash (Ames) stabilized subgrade
	South	6 in. CLSB	12 in. 10% fly ash (Muscatine and Port Neal) stabilized subgrade

Legend: CLSB = crushed limestone subbase GP-GM or A-1-a (7% fines content), NW = non-woven.

FREEZE-THAW PERFORMANCE OF GEOMATERIALS

Frost-heave results from ice forming within the soil during freezing conditions in the atmosphere. Continuous ice lens grows to expand the volume of voids potentially. The overlying pavement surface or upper layer reflects this action as cracks or bulges (Figure 2). Thaw-weakening results from ice melting within the soil. The stiffness of the soil decreases as the status of moisture changes from solid to liquid.

Figure 2. Frost-heave pavement damage in Norway (Ystenes 2011)

According to PavementInteractive.org (2006), the three elements necessary for ice lenses and thus frost heave are: frost susceptible soil (significant amount of fines); subfreezing temperatures (freezing temperatures must penetrate the soil and, in general, the thickness of an ice lens will be thicker with slower rates of freezing), water (must be available from the groundwater table, infiltration, an aquifer, or held within the voids of fine-grained soil). Remove any of the three conditions above and frost effects will be eliminated or at least minimized. If the three conditions occur uniformly, heaving will be uniform; otherwise, differential heaving will occur resulting in pavement cracking and roughness. Differential

heave is more likely to occur at locations such as: where subgrades change from clean not frost susceptible (NFS) sands to silty frost susceptible materials; abrupt transitions from cut to fill with groundwater close to the surface; where excavation exposes water-bearing strata; drains, culverts, etc., frequently result in abrupt differential heaving due to different backfill material or compaction and the fact that open buried pipes change the thermal conditions (i.e., remove heat resulting in more frozen soil) (Pavementinteractive.org 2006). Figure 3 illustrates the seasonal pavement deflection changes as thaw-weakening of a portion of State Route 172 in Washington State.

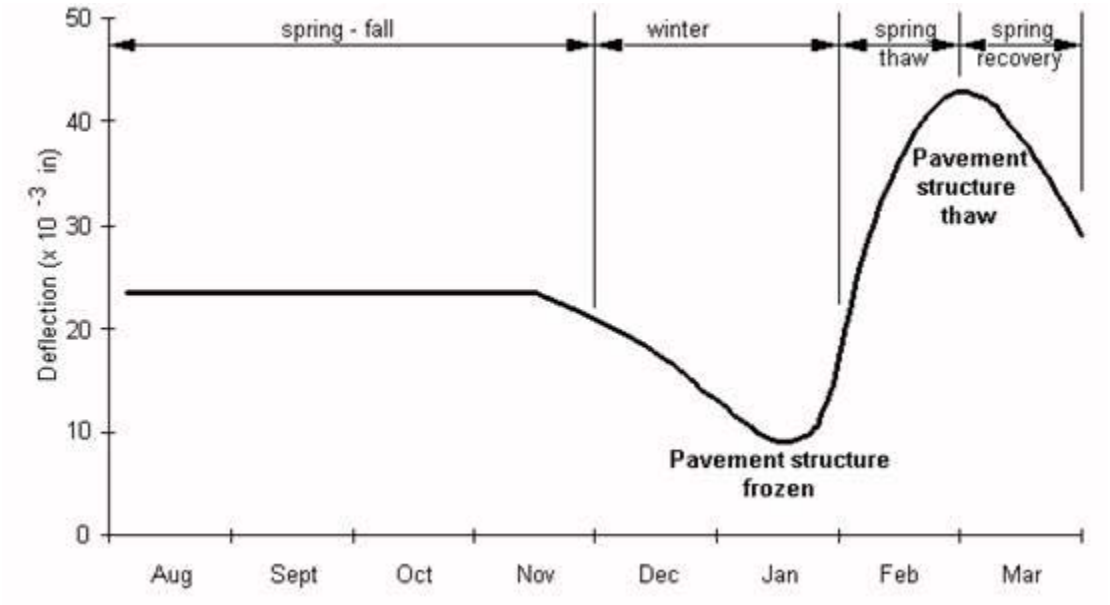

Figure 3. Typical pavement deflections illustrating seasonal pavement strength changes (Pavementinteractive.org 2006)

Uniform frost heave causes little damage to pavement structures, but differential frost heave weakens pavement foundation layers and increases stress concentrations in the pavement layer. Three important factors influence frost heave, the size and percentage of voids in soil, the size of soil particles, and the water content of soil (Taber 1929). Water content correlates to the supply of available water that influences the amount of heave. The size and percentage of voids in soil determines the height to which water may be lifted above the water table by surface tension. The size distribution of soil particles controls the segregation of water during freezing. The U.S. Army Cold Regions Research Engineering

Laboratory (CRREL) and the U.S. Army Corps of Engineers (USACE) proposed a frost susceptibility classification system based on the grain size criteria (Figure 4). The grain size criteria is a commonly used method to determine the frost susceptibility, and Chamberlain (1981) confirmed that this method is a reliable and system.

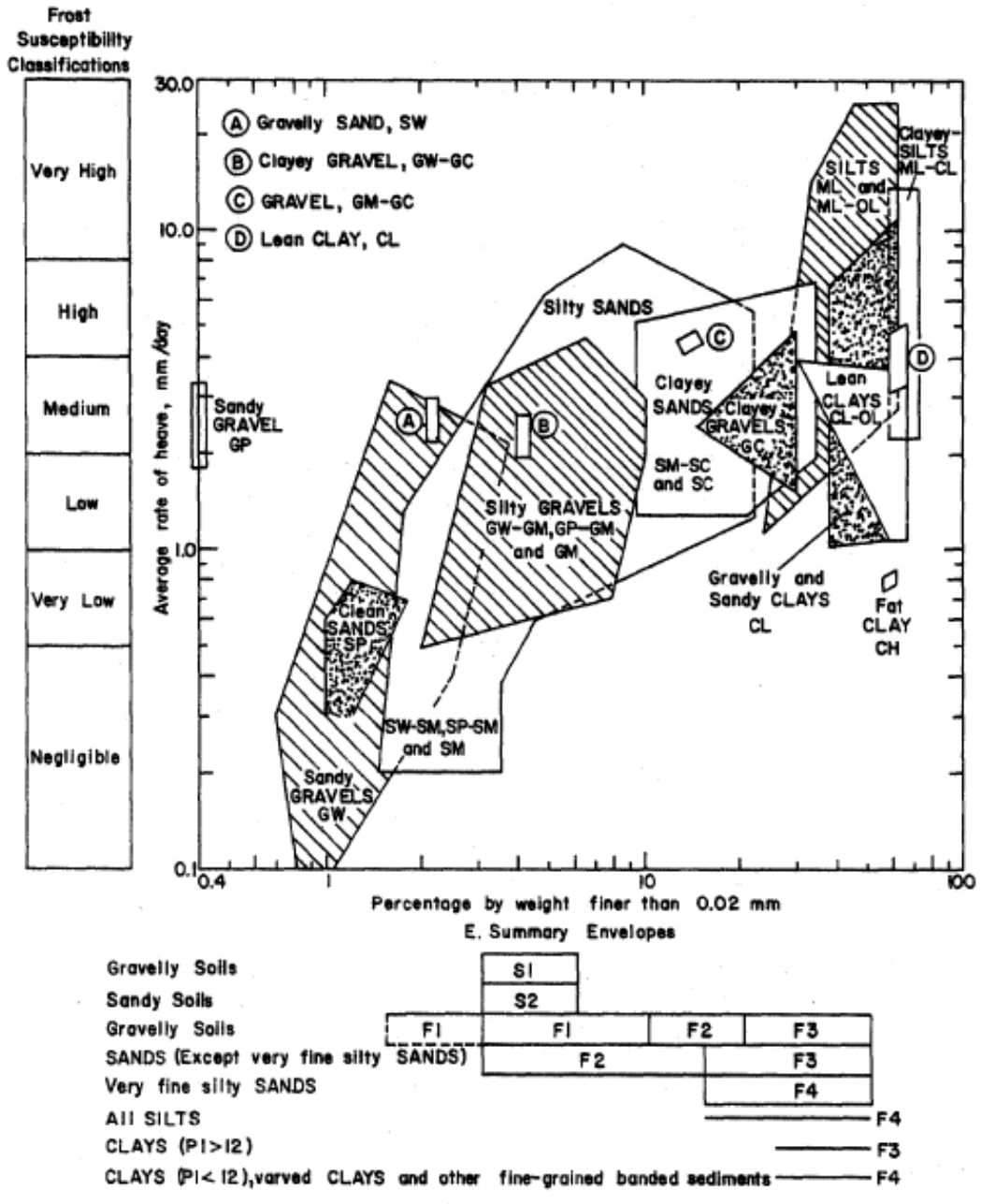

Figure 4. Frost susceptibility classification of soils (Joint Departments of the Army and Air Force 1985)

Under natural freezing conditions and with sufficient water supply one should expect considerable ice segregation in non-uniform soils containing more than 3% of grains smaller than 0.02 mm, and in very uniform soils containing more than 10 % smaller than 0.02 mm. No ice segregation was observed in soils containing less than 1% of grains smaller than 0.02 mm, even if the groundwater level is as high as the frost line (Casagrande 1932). Brandl (2008) identified other factors that influence the freeze-thaw behavior of geomaterials:

- grain size distribution;
- mineral composition of the fine grains;
- soil chemistry;
- water content and degree of saturation;
- density;
- groundwater level;
- availability of water (e.g., precipitation, seepage, groundwater);
- temperature, hydraulic gradient, and chemistry of groundwater;
- temperature conditions (e.g., magnitude and duration of freezing temperatures, temperature gradient); and
- local climate, especially freeze-thaw cycles.

Ice lens formation is the generally accepted cause for frost heave. The volume expansion of water limits the total amount of heave to around 5 cm in situ (Taber 1929). A 1,300 kPa pressure can be exerted by a growing ice lens, and the tensile strength reduces because of freeze-thaw. Higher water contents mean that ice lenses form more easily. Cassagrande (1931) agreed with Taber that a constant supply of water to the freezing front results in frost heave. Capillary stress is related to the pore sizes of soils and determines the degree of frost heave. The main factors that influence capillary stress are the soil particle size and the distance to water table. The degree of frost heave decreases for coarse silty clays as particle size increases, and it decreases for fine materials as particle size decreases (Beskow [1935] 1991). A heat balance must be reached between the extraction of heat moving through frozen layers and heat moving through unfrozen layers. The ice lens will continue to grow if the heat balance is maintained. Penner (1966) performed freeze-thaw experiments and stated that

the relationship between the supply of water and the movement of heat determines the thicknesses of ice lenses.

Janoo et al. (1997) studied on a well-graded sandy material which was used as pavement subbase layer. The laboratory frost heave tests presented low to medium frost susceptibility for unsaturated condition and high frost susceptibility for saturated condition. Four computer simulations were also developed. For both simulations with unsaturated condition, the frost penetration depth reached about halfway into the simulated layer and the average frost heave value was only around 10 to 15% of the values at saturated condition (Janoo et al. 1997)

Lime stabilized Illinoian till and cement stabilized Ridgeville fine sandy loam were tested to determine the effects of freeze-thaw parameters on the durability of stabilized geomaterials. The evaluation factors were unconfined compressive strength change, moisture content change, and unit length change. Cooling rate turned out to be more important on affecting soil durability than the other three selected parameters: freezing temperature, length of freezing period, and thawing temperature. Geographic location, climatic conditions, and position of the stabilized layer should be three factors to determine the number of freeze-thaw cycles for laboratory testing. 0.2℉/hr. was the recommended cooling rate that simulates the field condition at Illinois area. This value was heavily detrimental to durability (Dempsey et al. 1973). Konrad (1988) stated that the segregation potential increases significantly with time in a freezing test in which the cooling rate is maintained constant. Chen et al. (1988) studied on the factors influencing frost heave. The factors included initial water content, initial dry unit weight, ground water level, plasticity index, and frost penetration rate. The test results are shown in Figure 5. From the figures, lower frost heave ratio can be resulted from higher frost penetration rate, lower initial moisture content, lower initial dry unit weight, higher ground water level, or lower plastic index.

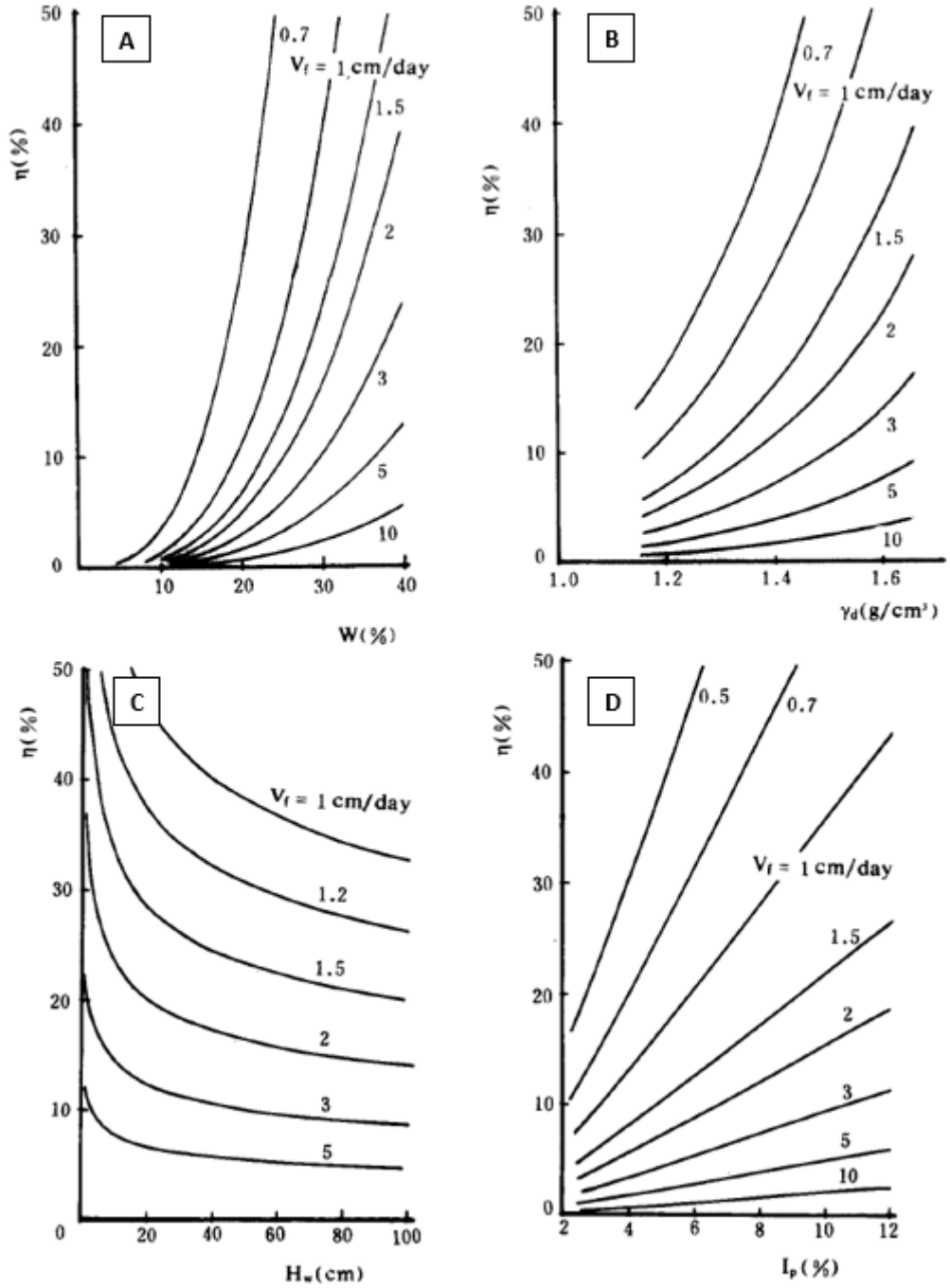

Figure 5. Frost heave ratio (Ƞ) at various frost penetration rates (V_f) versus (A). Initial moisture content; (B). Initial dry unit weight; (C). Ground water level; (D). Plasticity index (Chen et al. 1988)

FROST-HEAVE AND THAW-WEAKENING LABORATORY TESTS

Laboratory freeze-thaw tests include various tests for different testing materials and testing factors (i.e., durability, frost heave, stiffness changes). Table 2 summarizes the test methods that are related to laboratory freeze-thaw tests.

Table 2. Test methods related to laboratory freeze-thaw tests

Test Method	Test
ASTM C593	Standard Specification for Fly Ash and Other Pozzolans for Use with Lime
ASTM D559	Standard Test Methods for Wetting and Drying Compacted Soil-cement Mixtures
ASTM D560	Standard Test Methods for Freezing and Thawing Compacted Soil-Cement Mixtures
ASTM D5918	Standard Test Methods for Frost Heave And Thaw Weakening Susceptibility Of Soils
TEX-135-E	Test Procedure For Freezing and Thawing Tests of Compacted Soil-cement Mixture

Chamberlain (1981) reported that the five bases for the index tests that indicate the frost susceptibility of soils are: particle size characteristics void sizes, soil-water interaction, soil-water-ice interaction, and frost heave. A five-day freezing test was developed with two freeze-thaw cycles and the California bearing ratio test (Chamberlain 1987). Silt and silty sand were tested (Henry 1990) based on the CRREL frost heave test, which was presented by Chamberlain and Carbee (1981). The test sample assembly is shown in Figure 6. The freezing chamber was divided into four parts that include the space for ice bath. Acrylic sheets were used to reduce heat loss and the freezer temperature was controlled manually. For the initial step, the top plate was set to -4 °C (25 °F) and the bottom plate was set to 1 °C (33.8 °F), so that the frost penetration rate can be kept at 1.27 cm/day (0.5 in./day).

Two tests are used to understand typical frost-heave and thaw-weakening performance of geomaterials. ASTM D5918 “Standard Test Methods for Frost Heave and Thaw Weakening Susceptibility of Soils” is the index test for estimating the relative degree of frost susceptibility of geomaterials. California bearing ratio (CBR) values are calculated from penetration test results according to ASTM D1883 and reflect the mechanical strength of pavement foundation materials.

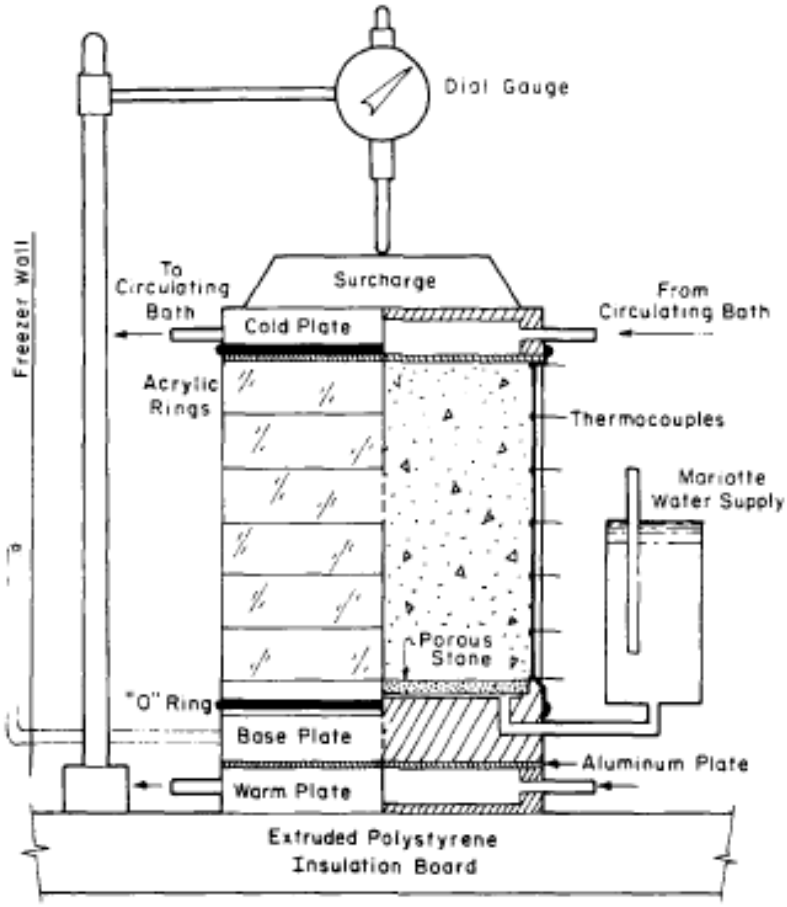

Figure 6. CRREL frost heave test sample assembly (Chamberlain and Carbee 1981)

Konrad (1988) defined the freezing test with constant temperature boundary conditions as "step-freezing" test and the freezing in which the temperature at each end of the sample is changed at a specified rate as "ramped-freezing" test. The total heave and heave rate from these two types of freezing tests were different because of the freezing path differences. The step-freezing tests resulted in frost heave curves generally concave downwards while ramped-freezing presented frost heave curves concave upwards.

However, Svec (1989) stated two drawbacks of the five-day test: the thermal boundary conditions cannot reflect the real ground freezing conditions; the frost heave rate changes as the temperature gradient changes during a CRREL frost-heave test. Svec (1989) and Penner (1967) both calculated the field temperature gradient at southeastern Ontario area, which was

smaller than the value used for laboratory frost-heave test. Svec (1989) also described temperature gradient influence based on ice-lens formation and rhythmic ice-lensing theory. Therefore, Svec (1989) reported another modified idea to determine the maximum frost heave potential. The modified test equipment was developed by Penner and Eldred (1985) and is shown in Figure 7.

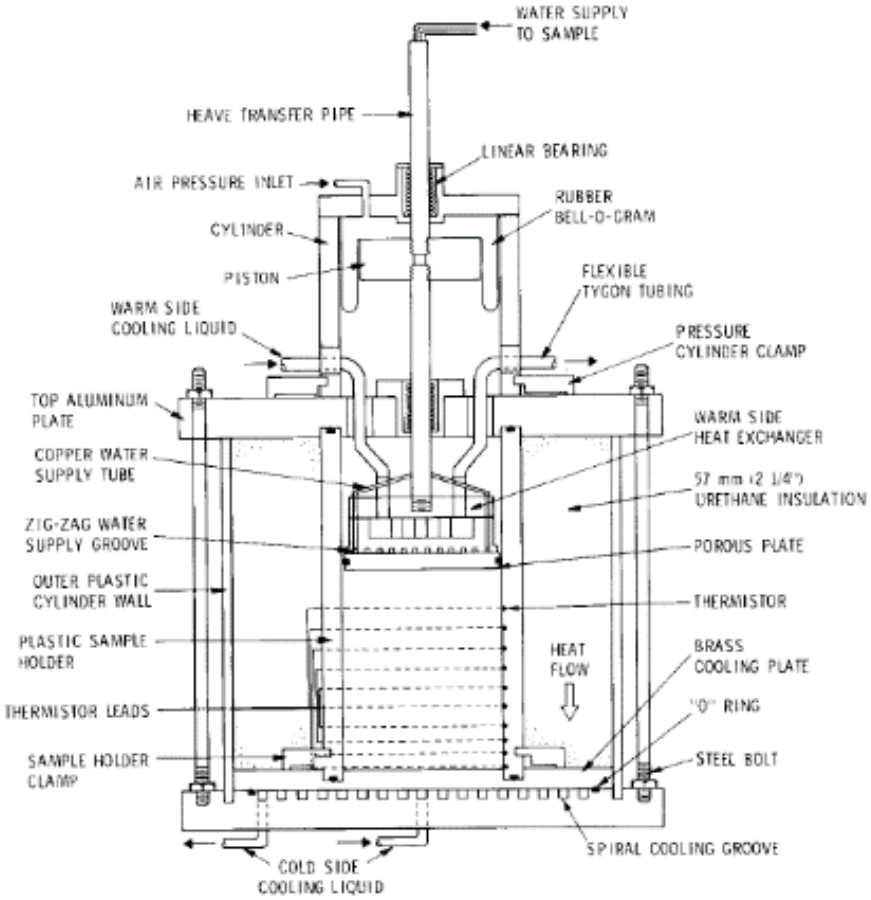

Figure 7. Modified frost heave test equipment (Penner and Eldred 1985)

Johnson (2012) constructed laboratory equipment for conducting freeze-thaw tests according to ASTM D5918. There are four major steps of this test: remold the samples, fully saturate the samples, put the samples in the temperature-controlled chamber for freeze-thaw cycles, and perform California bearing ratio tests (Figure 8).

Figure 8. Laboratory freeze-thaw test steps showing (1) sample remolding; (2) fully saturation; (3) freeze-thaw process; (4) CBR test

Six-inch samples are fully saturated before they are put into the freezer, then they are connected to Mariotte water supplies that maintain the water pressure. Two disks that connect to the water bath are applied to control the temperatures at the top and bottom of the sample. Lasers are set above the samples to measure the heave values during tests. For each sample, six thermocouples are inserted into the six 1-inch layers to monitor the temperatures during the entire freeze-thaw process. A computer program called "DasyLab" records the outputs of thermocouples, pressure transducers, and lasers (Figure 1). The entire freeze-thaw process takes around 120 hours, and includes two 8-hour freezing processes.

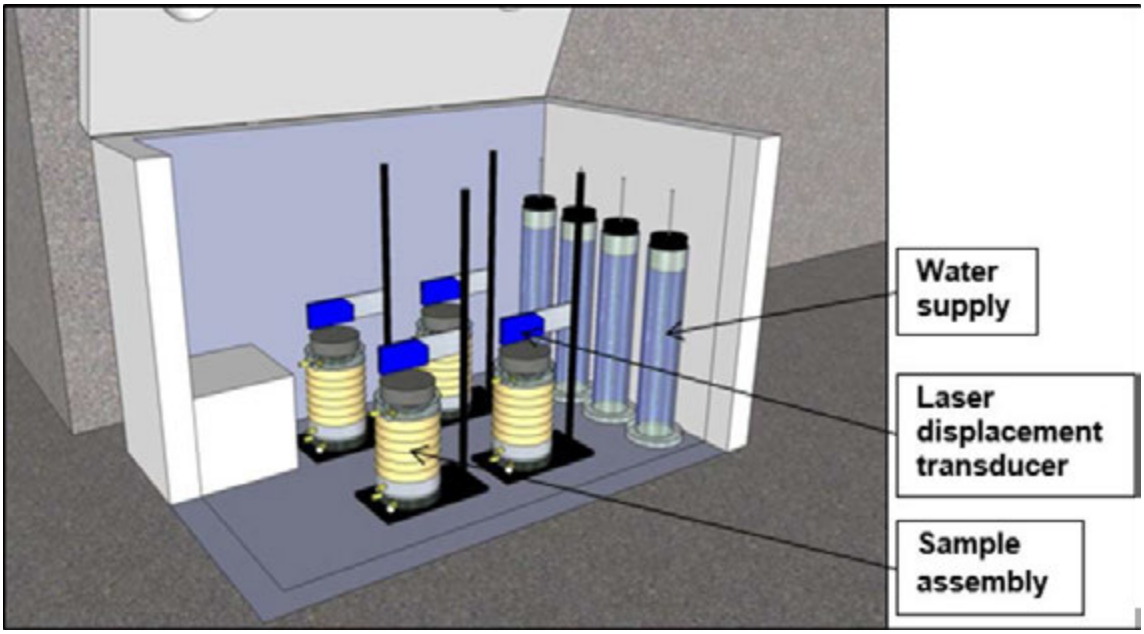

Figure 9. Idealized view of the temperature control chamber (Johnson 2012)

After freeze-thaw testing, CBR tests are conducted on the samples, and those values are compared to the CBR values of unsaturated control samples. This test method is used to evaluate the potential strength of geomaterials, and it is intended for but not limited to evaluating the strength of cohesive materials having maximum particle sizes less than 3/4 in. (19 mm) (ASTM D1883-05). By comparing the results from the after freeze-thaw testing and the control testing, the stiffness changes can be determined as the thaw-weakening performance.

Frost susceptibility classifications can be determined by comparing heave rates or CBR after thaw values with ASTM D5918 classifications (Table 3). Because the second 8-hr heave rates are always larger than the first ones, the second 8-hr heave rates are used to be compared. An exception is the recycled portland cement concrete (RPCC) subbase from US-30, that it heaves more during the first freeze-thaw cycle than the second (Figure 10) (Johnson 2012).

Table 3. ASTM D5918 frost susceptibility classification

Frost susceptibility classification	2nd 8-hr heave rate (mm/d)	CBR after thaw (%)
Negligible	<1	>20
Very low	1 to 2	20 to 15
Low	2 to 4	15 to 10
Medium	4 to 8	10 to 5
High	8 to 16	5 to 2
Very High	>16	<2

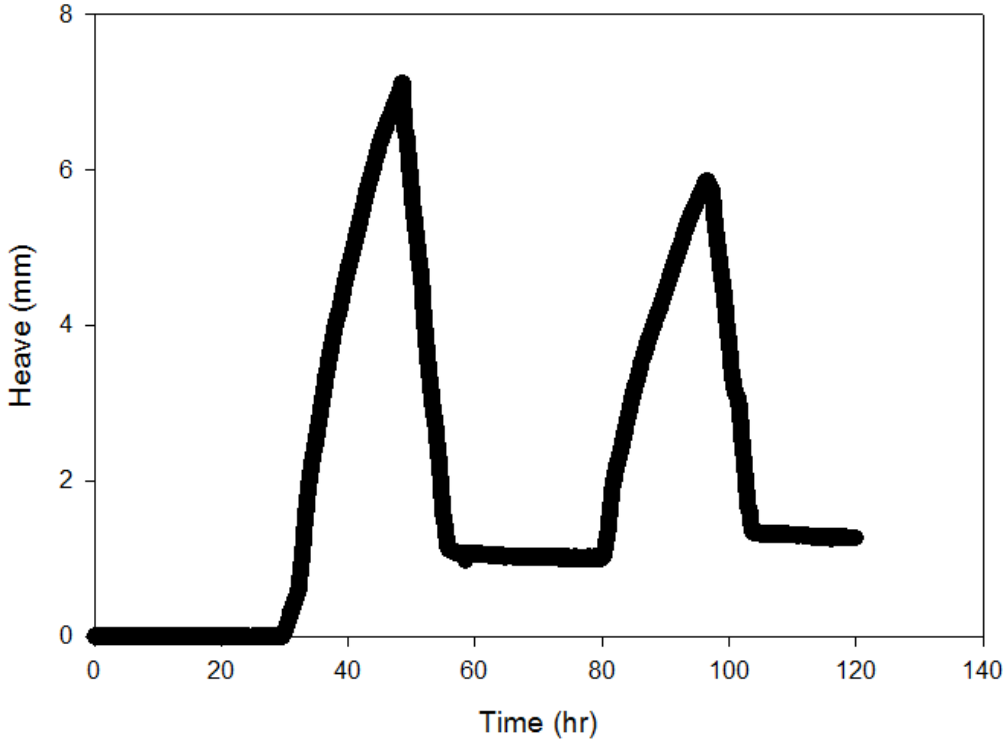

Figure 10. IA US-30 RPCC heave value with time (Johnson 2012)

SOIL STABLIZATION METHODS

Pavement foundation stabilizers are commonly used for improving pavement freeze-thaw performance. The following sections discuss basic mechanisms and performance of the stabilizers that were installed at the Boone County Test Sections site and investigated in this study: cement, fly ash, polypropylene fibers, and geosynthetics.

Cement

Cement is one of the most widely applied chemical stabilizers in pavement foundation construction to improve geomaterial behaviors during freezing and thawing. Cement hydrates

and sets after it is mixed with soil because pore water reacts with cement to form calcium silicate and aluminate hydrates. These cemented products effectively decrease the amount of pore water; bond soil grains; and improve soil stability, frost heave behavior, and thaw weakening. Texas Department of Transportation (TxDOT) provided test procedure for freezing and thawing tests of compacted soil-cement mixtures. This method determines the frost heave values of cement stabilized soil during freeze-thaw cycles.

Non-stabilized loess is among the most frost susceptible geomaterials. Johnson (2012) reported that the average heave rate of cement-stabilized western Iowa loess was 0.0 mm/d, and seven of eight cement-stabilized samples had CBR values over 100%. Johnson (2012) also stated that both frost susceptibility and thaw weakening are negligible after cement stabilization because cement-stabilized materials can absorb large amounts of water without increasing frost susceptibility (Table 4). Therefore, the effect of cement stabilization to control the frost action of loess material is considerable.

Table 4. Frost susceptibility of cement stabilized western Iowa loess

Material	Cement content (%)	Initial moisture content (%)	Frost-heave susceptibility rating	Thaw-weakening susceptibility rating
Loess	0.0	17.5	Very high	Very high
	3.0	13.0	Negligible	Negligible
	3.0	20.0	Negligible	Negligible
	5.0	20.0	Negligible	Negligible
	7.0	20.0	Negligible	Negligible
	9.0	13.0	Negligible	Negligible
	9.0	20.0	Negligible	Negligible
	11.0	20.0	Negligible	Negligible
	13.0	22.0	Negligible	Negligible

For the frost susceptibility of stabilized (lime and portland cement) soils, a minimum of 3% lime or cement is required to reduce frost heave by about 50%. In cohesionless soils, about 3 to 8% cement is required to reduce frost heave. For frost susceptible gravel soils, 2% cement is required to change it to a non-frost susceptible material. For cement treated soils, the tensile strength of the materials decreased with increasing freeze-thaw cycles. The tensile

strength did not reduce after 12 freeze-thaw cycles, when 15% cement was added to the soil. (Janoo et al., 1997).

Shrinkage cracking, water ingress, structural deterioration, and pavement roughness may occur because of the addition of excessive cement (Crane et al. 2006, George 1968, and Norling 1973). Guthrie et al. (2007) conducted laboratory freeze thaw tests to evaluate the effect of reduced cement contents on frost heave. A silty soil (ML USC classification) was stabilized with three contents of cement: 2.0%, 3.5%, and 5.0%. Cement contents corresponding to 7-day unconfined compression strength 400 psi (3.5%) and 600 psi (5.0%) reduced the frost heave effectively. Comparing the frost heaves (Figure 11), weights gained (Figure 12), and final moisture contents (Figure 13) to the non-stabilized controlled test leads to the following conclusions:

- Insufficient cement addition might lead to greater frost heave than non-stabilized silty soil, and suction and permeability properties can explain this behavior;
- Significant water ingress occurs whatever how much cement was added into the soil samples;
- Excessive cement might cause pavement damage like shrinkage cracking (Guthrie 2007).

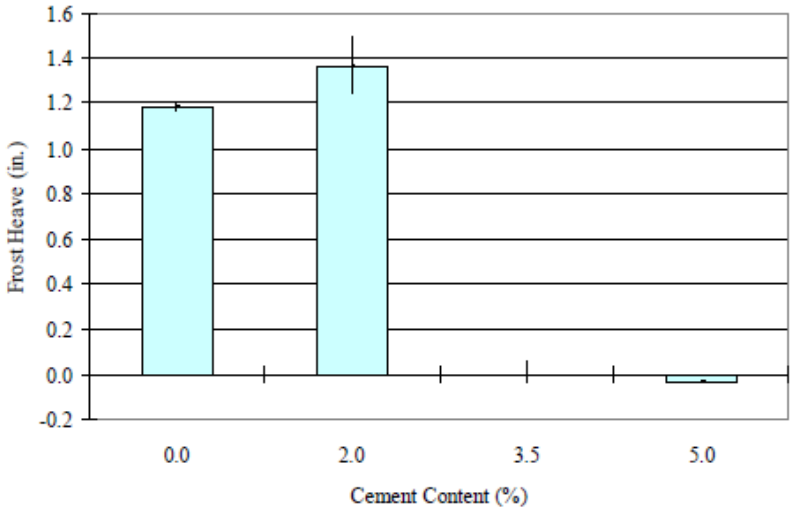

Figure 11. Frost heave versus cement content (Guthrie et al. 2007)

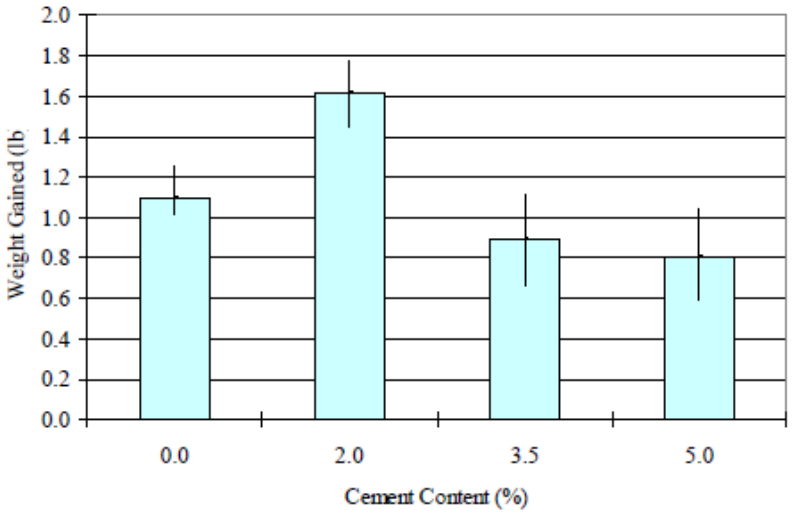

Figure 12. Weight gained versus cement content (Guthrie et al. 2007)

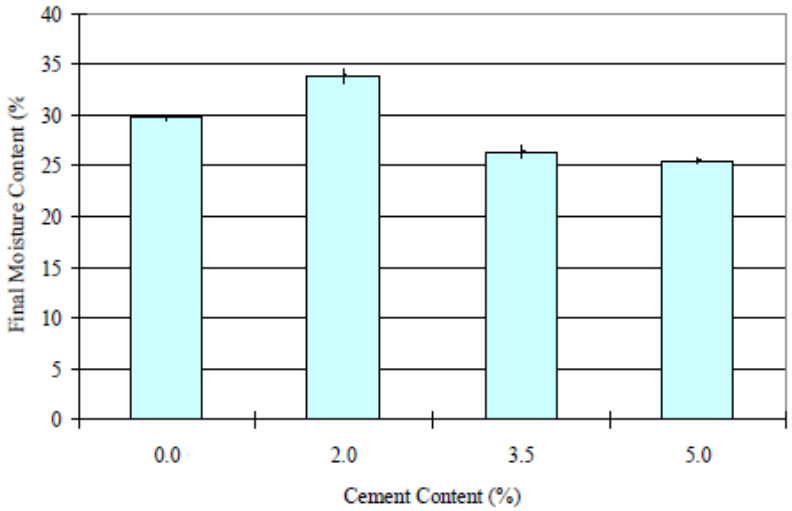

Figure 13. Final moisture content versus cement content (Guthrie et al. 2007)

Fly ash

Fly ash (FA) is a residual product of coal combustion, and the main components are silicon dioxide and calcium oxide. Nowadays FA is collected by recycling equipment instead of being released into atmosphere. ASTM C593 provides the standard specification for fly ash and other Pozzolans for use with lime. The methods for sample mixing, curing, and saturating can be referred to this standard.

Johnson (2012) compared the frost heave and thaw weakening performance of FA-stabilized loess samples and non-stabilized loess samples and reported that there is not

obvious improvement. The frost susceptibility of these samples keeps at a high level, but generally decreases as the FA content increases. All the stabilized samples heaved, and some heaved even more than non-stabilized samples. The thaw weakening susceptibility of the stabilized samples ranged from negligible to high and post CBR values range from 5.0% to 25.5% as the FA content varies from 10% to 22% (Table 5) (Johnson 2012).

Table 5. Frost susceptibility of FA stabilized western Iowa loess

Material	Fly ash content (%)	Initial moisture content (%)	Frost-heave susceptibility rating	Thaw-weakening susceptibility rating
Loess	10.0	10.0	High	High
	10.0	19.0	Very high	High
	15.0	19.0	high	Medium
	20.0	22.0	High	Negligible

Six different mixtures of fly ash and recycled base materials were cured for 7 days as normally practiced in pavement construction (Cetin et al., 2010). These specimens were subjected to resilient modulus (an estimate of soil's modulus of elasticity and a measure of soil's stiffness) tests following a group of freeze-thaw cycles. The specimens either gain or lose 3-12% of their initial resilient modulus after four cycles, and then the summary resilient modulus ratio (SM_R) (the ratio of summary resilient modulus after n freeze-thaw cycles to the initial summary resilient modulus) starts to decrease indicating the freeze-thaw effects. The highest decreasing rate of SM_R is between the fourth and eighth cycle, and the specimens lose 31-67% of the initial moduli after twelve freeze-thaw cycles. Rosa (2006) also reported a 20-66% reduction in SM_R of various coarse and fine-grained soils. Such high changes in SM_R are attributed to the frost susceptibility of mixtures due to their high gravel content and nonplastic nature. For cohesive soils, the effect of freeze-thaw was negligible when the stress at 1% strain in the unconfined compression test ($S_{u1\%}$) is less than 8 psi (55 kPa), and the effect of freeze-thaw increases as the $S_{u1\%}$ increases (Lee et al. 1995).

Though fly ash improves the soil stiffness, fly ash stabilized soil also causes tensile strength reduction and shrink-swell potential changes (Cokca 2001). Solanki et al. (2013) stated that Class C fly ash increased the freeze-thaw durability of CL-ML, CL, and CH materials based on the unconfined compressive strength and resilient modulus. However, the

improvement of fly ash on controlling the effect of freeze-thaw cycles is less than hydrated lime and cement kiln dust. Bin-Shafique et al. (2011) studied on the effect of freezing-thawing cycles on performance of fly ash stabilized expansive soil subbases. Class C fly ash and artificial fibers were used to stabilize two types of high plasticity clay (CH). Unconfined compression tests, tensile tests, and freeze-thaw tests were conducted under both good and poor drainage conditions. Good drainage was better than poor drainage to reduce the influence of freeze-thaw cycles to soil strength. A maximum of 50% strength reduction was measured for 20% fly ash stabilized samples after 24 freeze-thaw cycles. The plasticity and swell potential also increased significantly after the test. The test results were shown in Figure 14, Figure 15, and Figure 16.

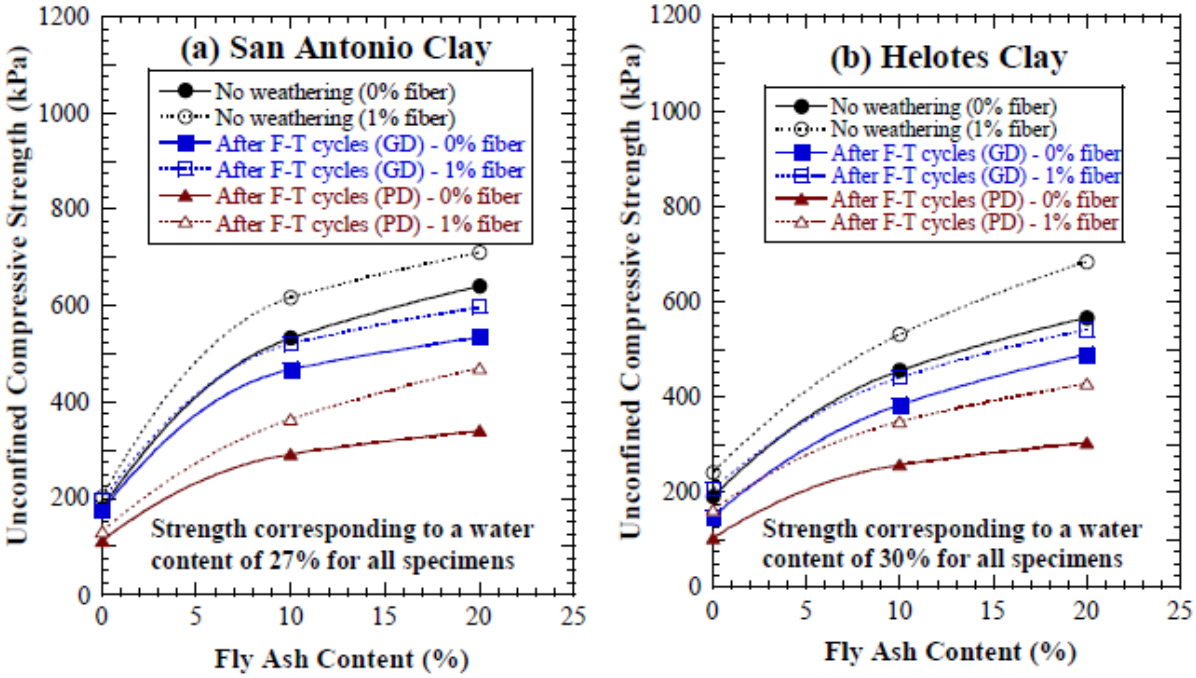

Figure 14. Unconfined compressive strength of fly ash and fiber stabilized clay (Bin-Shafique et al. 2011)

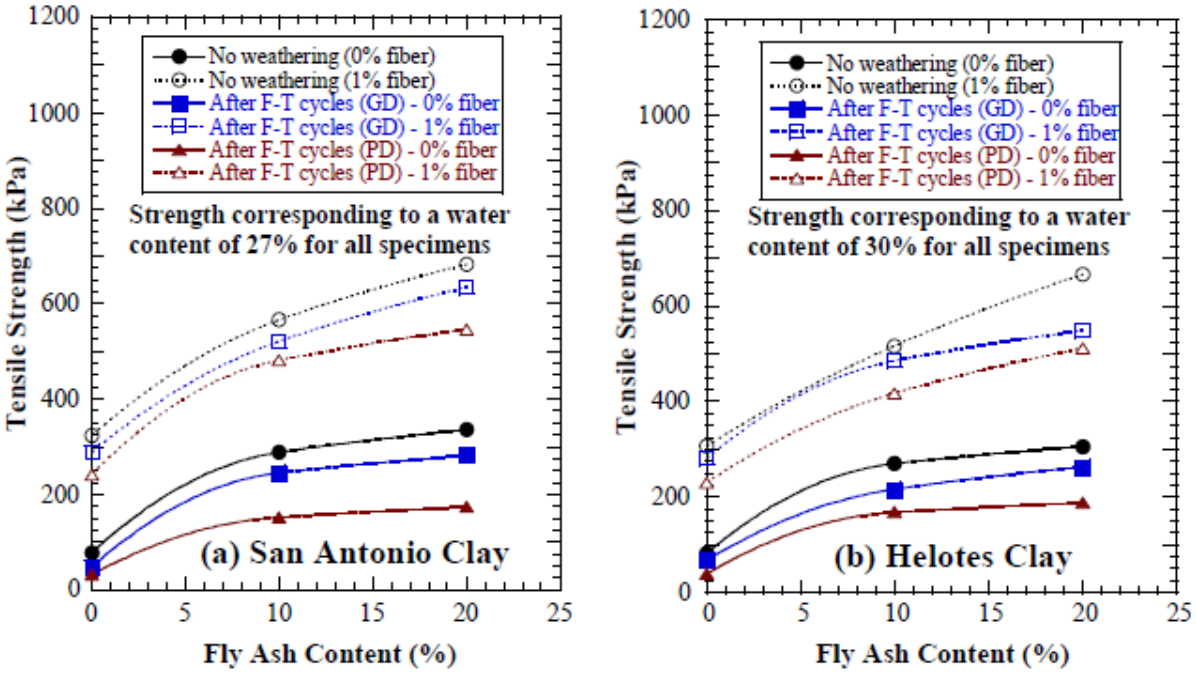

Figure 15. Tensile strength of fly ash and fiber stabilized clay (Bin-Shafique et al. 2011)

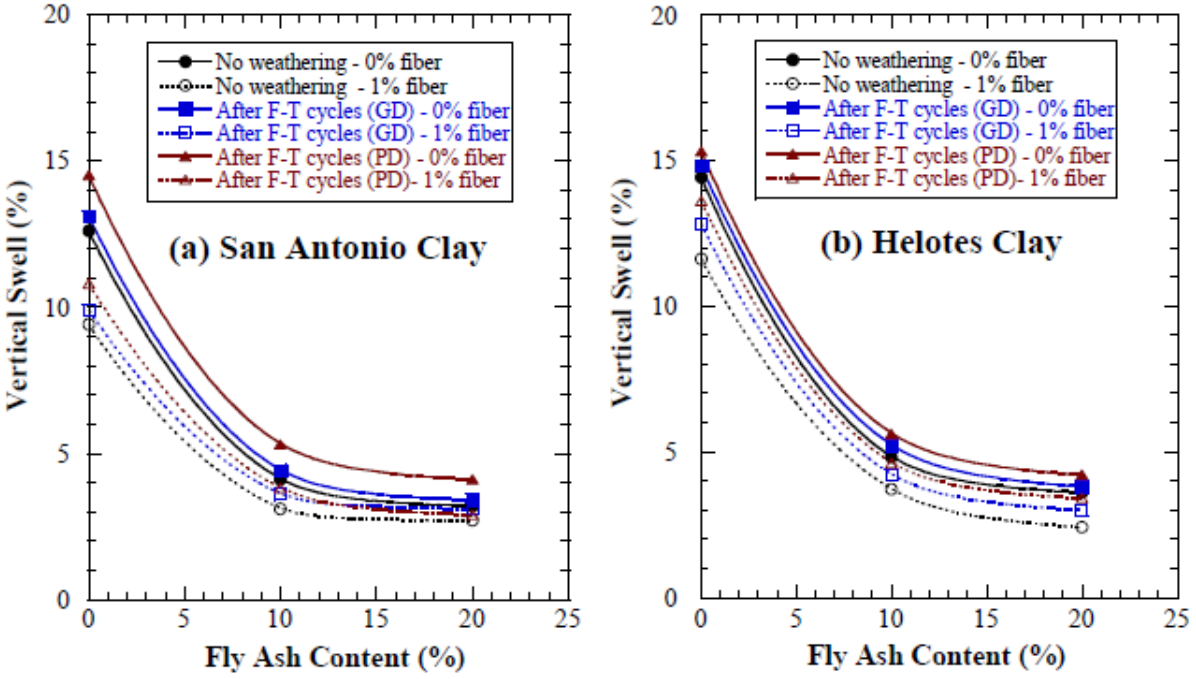

Figure 16. Vertical swell of fly ash and fiber stabilized clay (Bin-Shafique et al. 2011)

Geofiber and other geosynthetics

The two advantages of applying fibers in soil stabilization are: easy to install and mix with soils; potential weakening planes are limited to parallel to oriented reinforcement (Tang et al. 2007). It is predicted that geofibers can help to improve the freeze-thaw performance of pavement foundation materials. For example, Gray and Ohashi (1983) tested beach sand stabilized with geofibers and concluded that geofibers increase the shear strength of clean sand, but they did not conduct freeze-thaw tests. Collins (2011) recommended that samples treated with geofibers should be subjected to lab freeze-thaw conditions to evaluate the effects of this stabilization method. However, there is little research regarding freeze-thaw effects on geofiber stabilized materials.

Several researchers have studied using geofibers as a stabilization technology for geomaterials and reported that geofibers are effective in some conditions. Hazirbaba et al. (2007) studied fine-grained soil and reported that the CBR value at optimum moisture content without stabilizers was 31, and the optimum geofiber content, which corresponds to the largest CBR value, appears to be about 0.5%. Addition of 0.5% geofiber at optimum moisture content of 11% increased the CBR value from 31 to 62 and got much higher values at larger penetrations. Viswanadham (2009) stated that geofiber stabilization is a very effective method for controlling soil deformation. Use of the fibers decreased freeze-thaw volumetric changes on the order of 40% as compared with the untreated soil. The soil-fiber mixtures provided up to 40% improvement in composite stiffness than untreated soil, as evaluated through the cyclic load test following 10 freeze-thaw cycles (Hoover et al., 1982). The addition of 3% of fibers increases the unconfined compression strength of soil. For polypropylene fibers and steel fibers, the increases are 220% and 13% respectively. By adding 3% polypropylene fibers, the sample height decreases up to 70%, whereas for the same content of steel fibers, the sample height decreases up to about 20% (Figure 17) (Ghazavi and Roustaie 2009). Bin-Shafique et al. (2011) reported that the addition of fiber into fly ash stabilized clay samples improved the freeze-thaw performance of the mixtures. A maximum of 50% reduction in unconfined compressive strength loss and 45% reduction of tensile strength loss were determined by adding 1% fibers. The addition of fiber also reduced

the swelling potential of the stabilized soil. The test results can be referred to Figure 14, Figure 15, and Figure 16.

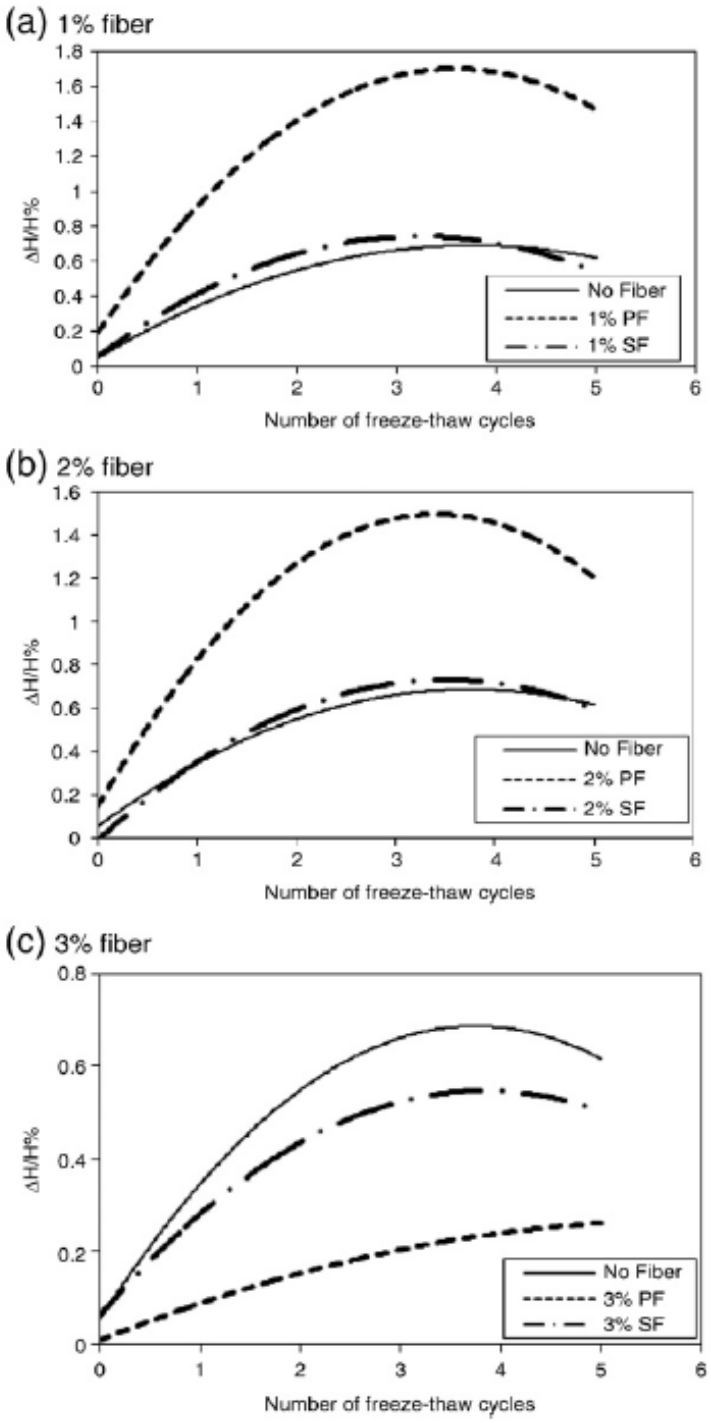

Figure 17. Height changes of polypropylene and steel fibers stabilized clayey samples (Ghazavi, and Roustaie 2009)

Henry (1990) reported that a silty sand sample heaved more than a layered silty sand-silt sample and after 25 hours heave rates were approximately equal. It was reported that Fibertex 300 and Typar 3401 better reduced the frost heave rate than other geotextiles. The greater hydrophobicity of Typar 3401 resulted in the better effect for controlling frost heave (Allen et al. 1983). Fibertex 400 and Typar 3401 were used to stabilize silt and silty sand samples. One layer of either the Fibertex or Typar reduce frost heave rate by 40 to 50%, while two layers of Fibertex reduced frost heave by about 50 to 55%. The three reasons that these two geotextiles are able to reduce frost heave are: larger pore sizes of the geotextiles, the surface properties of the fibers, and the unsaturated hydraulic conductivity of the geotextiles (Henry 1990).

Zaimoglu (2010) conducted unconfined compression tests and freeze-thaw durability tests for polypropylene fibers stabilized MH materials. The fiber contents ranged from 0.25% to 2%. As shown in Figure 18, the addition of 2% polypropylene fibers increased the unconfined compressive strength from 311 kPa to 1335 kPa. However, the stresses at the first 3% strains of all the non-stabilized and stabilized samples were similar. In the durability test, 12 freeze-thaw cycles were subjected to the samples. The addition of 0.75% polypropylene fiber reduced the mass loss from 40% to 15%, and the samples with other contents of fiber lost around 20% mass after the freeze-thaw cycles (Figure 19). According to the statement from Chamberlain et al. (1990) that surface strength cannot be significantly affected by mass losses around 10-15% after 12 freeze-thaw cycles, fiber stabilized silt was effectively durable under freeze-thaw periods.

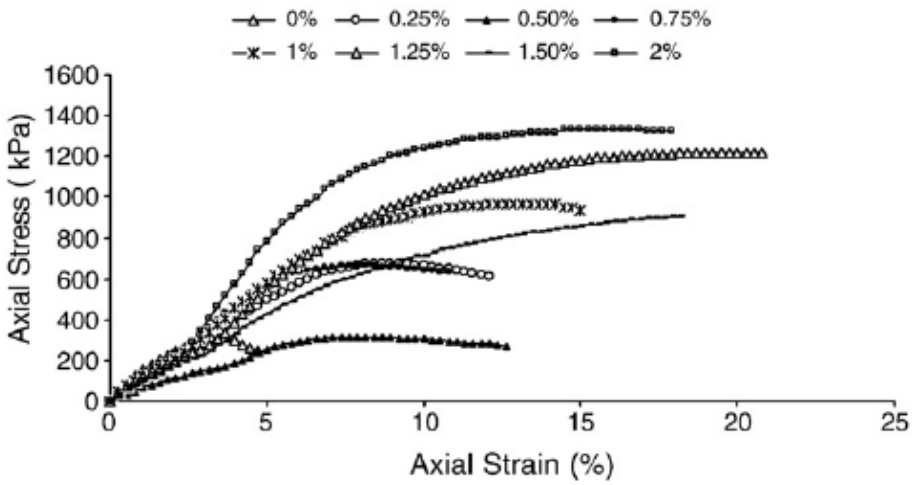

Figure 18. After freezing-thawing stress-strain curves of non-stabilized and fiber stabilized silt (Zaimoglu 2010)

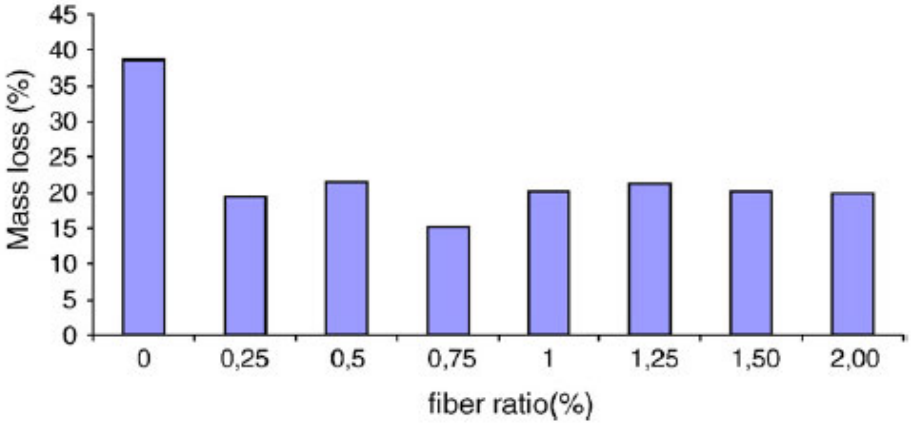

Figure 19. Mass loss of fiber stabilized silt after freezing-thawing (Zaimoglu 2010)

In order to evaluate the strength and mechanical behavior of polypropylene fiber stabilized clay and clay-cement mixtures, Tang et al. (2007) conducted unconfined compression tests, direct shear tests, and scanning electron microscopy (SEM) tests on these materials. The soil symbol was CL (lean clay) according to the uniformed soil classification system (USCS). The fiber contents ranged from 0.05% to 0.25% (0.05%, 0.15%, and 0.25%) and the cement contents ranged from 0% to 8% (0%, 5%, and 8%). The general conclusion from this study was the addition of fiber into clay and clay-cement mixtures improved the unconfined compressive strength, shear strength, and axial strain at failure. The test results indicated that the strength of non-stabilized was slightly improved by fiber only, and the

addition of cement caused the significant improvement in strength. The test results are presented in Figure 20 and Figure 21.

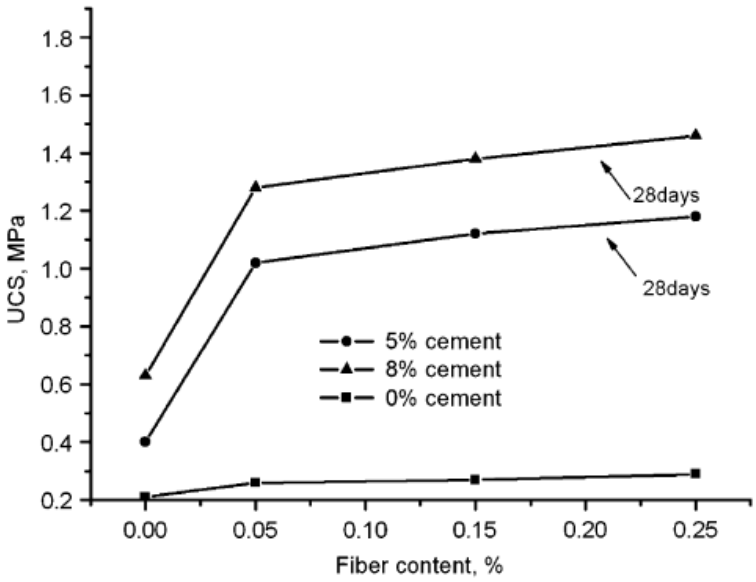

Figure 20. Unconfined compressive strength versus fiber content (Tang et al. 2007)

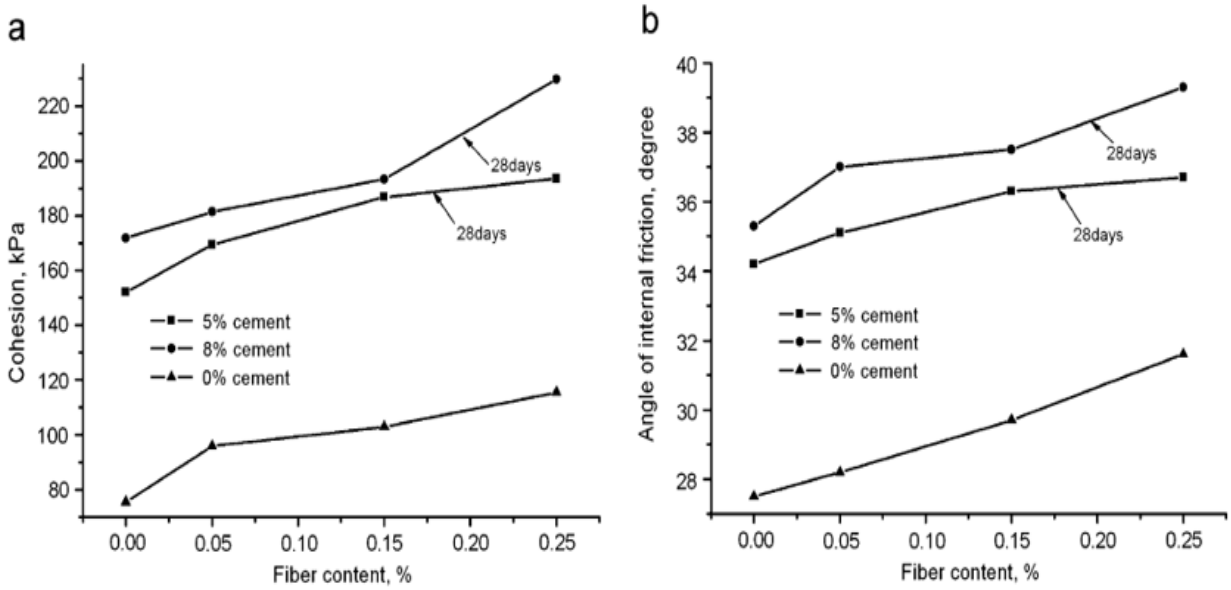

Figure 21. Shear strength parameters versus fiber content including (a). Cohesion versus fiber content; (b). Internal friction angle versus fiber content (Tang et al. 2007)

COSTS OF STABILIZATION METHODS

The cost for stabilization is an important factor in earthwork engineering. Figure 22 shows the range of bid prices for the Central Iowa Expo project for 13 methods of stabilization materials and installations from the Center for Earthworks Engineering Research (CEER) at Iowa State University.

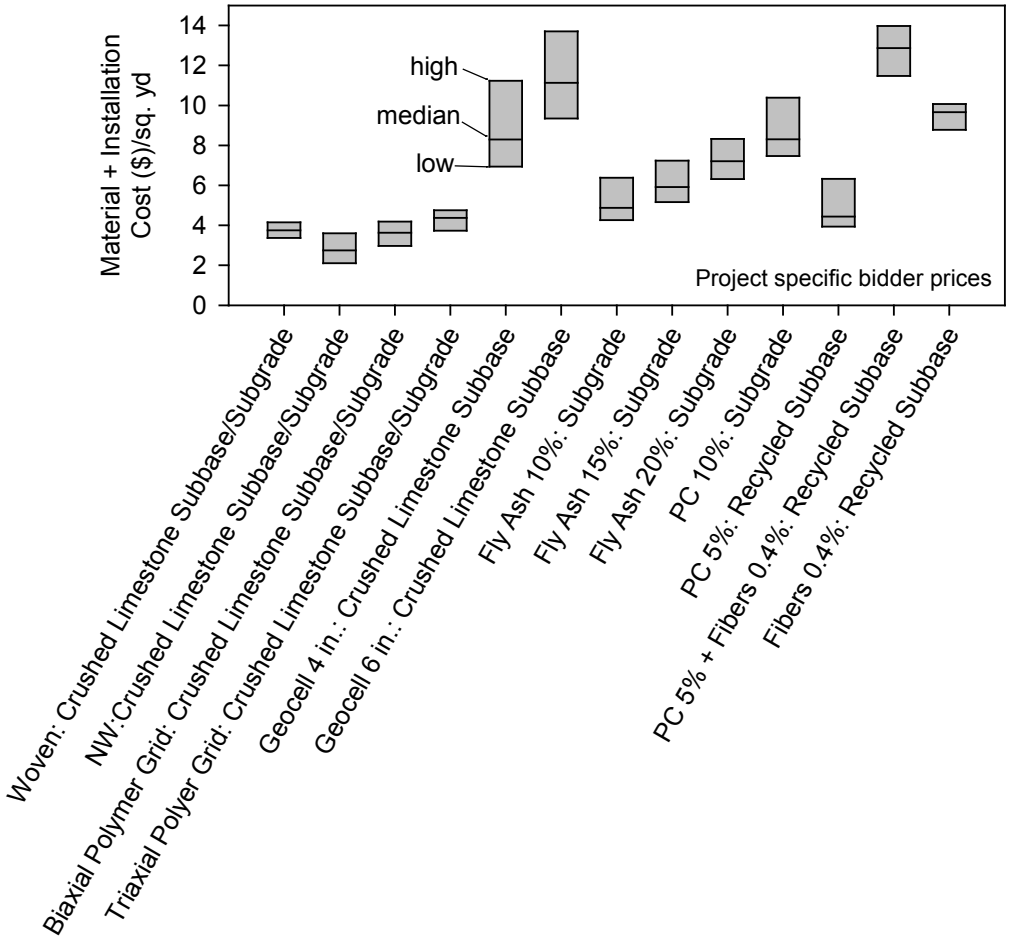

Figure 22. Cost for stabilization material and installation (White et. al 2012)

A lot of engineers and researchers had studied on comparing the costs of different stabilization methods and the stabilization effect. The major stabilization effects that are considered include soil shear strength, permeability, plastic and liquid limits, and density. Johnson (2012) reported that cement is more cost effective than fly ash based on the unconfined compressive strength (Table 6). Freeze-thaw performance was not a significant

role in evaluating the stabilization effects. However, freeze-thaw is an important factor influencing the durability, serviceability, and safety of pavement system, and must be considered when comparing the costs and effects of different stabilization methods.

Table 6. Cost efficiency of cement and fly ash (Johnson 2012)

UCS (kPa)	Average cement $/yd^2	Approximate cement content (%)	Average fly ash $/yd^2	Approximate fly ash content (%)
345	—	—	—	—
517	—	—	5.11	10
690	—	—	6.05	15
861	—	—	7.23	20
1034	3.31	3	—	—
2069	4.90	5	—	—
2758	6.50	7	—	—
3448	8.09	9	—	—
4137	9.69	11	—	—
4827	11.29	13	—	—
5516	—	—	—	—

CHAPTER 3. METHODS

The main goal of this research is to evaluate the frost heave performance of pavement foundation materials during freeze-thaw cycles. The methods used in this study were selected to address these objectives:

- to conduct laboratory freeze-thaw tests to evaluate the frost susceptibility of pavement foundation materials;
- to conduct laboratory freeze-thaw tests with pavement foundation materials stabilized with cement, fly ash, geo-fibers, and geotextiles and determine the stabilization effect; and
- to evaluate frost action of in situ pavement foundation.

To address the objectives of this study, the following laboratory tests were conducted: soil classification and index tests, compaction tests, strength tests, and frost-heave and thaw-weakening tests. Falling weight deflectometer (FWD) tests and dynamic cone penetrometer (DCP) tests were conducted at the Boone County Test Sections site. Information about laboratory tests is presented first, followed by information about the field tests.

LABORATORY TESTS

Frost-heave and thaw-weakening results can be influenced by the soil types and compactions methods. Soil classification and index tests were conducted to derive the soil types and basic geotechnical properties. Compaction tests were conducted to guide the soil preparation design for frost-heave testing. Strength tests were conducted to determine the strength variation at different conditions, such as no freeze-thaw and after thawing. Frost-heave and thaw-weakening test were the major part for this research to evaluate the frost susceptibility. Table 7 summarizes the laboratory tests conducted in this study.

Table 7. Laboratory test methods

Test Method	Test
Soil classification and index tests	
ASTM D422-63	Standard Test Method for Particle-Size Analysis of Soils
ASTM C117-04	Standard Test Method for Materials Finer than 75-µm (No. 200) Sieve in Mineral Aggregates by Washing
ASTM C136-06	Standard Test Method for Sieve Analysis of Fine and Coarse Aggregates
ASTM D4318-05	Standard Test Methods for Liquid Limit, Plastic Limit, and Plasticity Index of Soils
ASTM D2487-06	Standard Practice for Classification of Soils for Engineering Purposes (Unified Soil Classification System)
ASTM C127-07	Standard Test Method for Density, Relative Density (Specific Gravity), and Absorption of Coarse Aggregate
Compaction tests	
ASTM D698-07	Standard Test Methods for Laboratory Compaction Characteristics of Soil using Standard Effort
O'Flaherty et al. 1963	2-in. x 2-in. Iowa State Compaction Method
Strength tests	
ASTM D1883-05	Standard Test Method for CBR (California Bearing Ratio) of Laboratory-Compacted Soils
O'Flaherty et al. 1963	2-in. x 2-in. Compressive Strength Tests
Frost heave and thaw weakening test	
ASTM D5918-96	Standard Test Methods for Frost Heave and Thaw Weakening Susceptibility of Soils

Soil Classification and Index Tests

Laboratory sieve tests and hydrometer tests were conducted for particle size analyses according to ASTM D422-63, ASTM C117-04, and ASTM C136-06 (Figure 23). Atterberg limit tests were conducted according to ASTM D4318-05 to determine the liquid limits (LL), plastic limits (PL), and plasticity index (PI) (Figure 23).

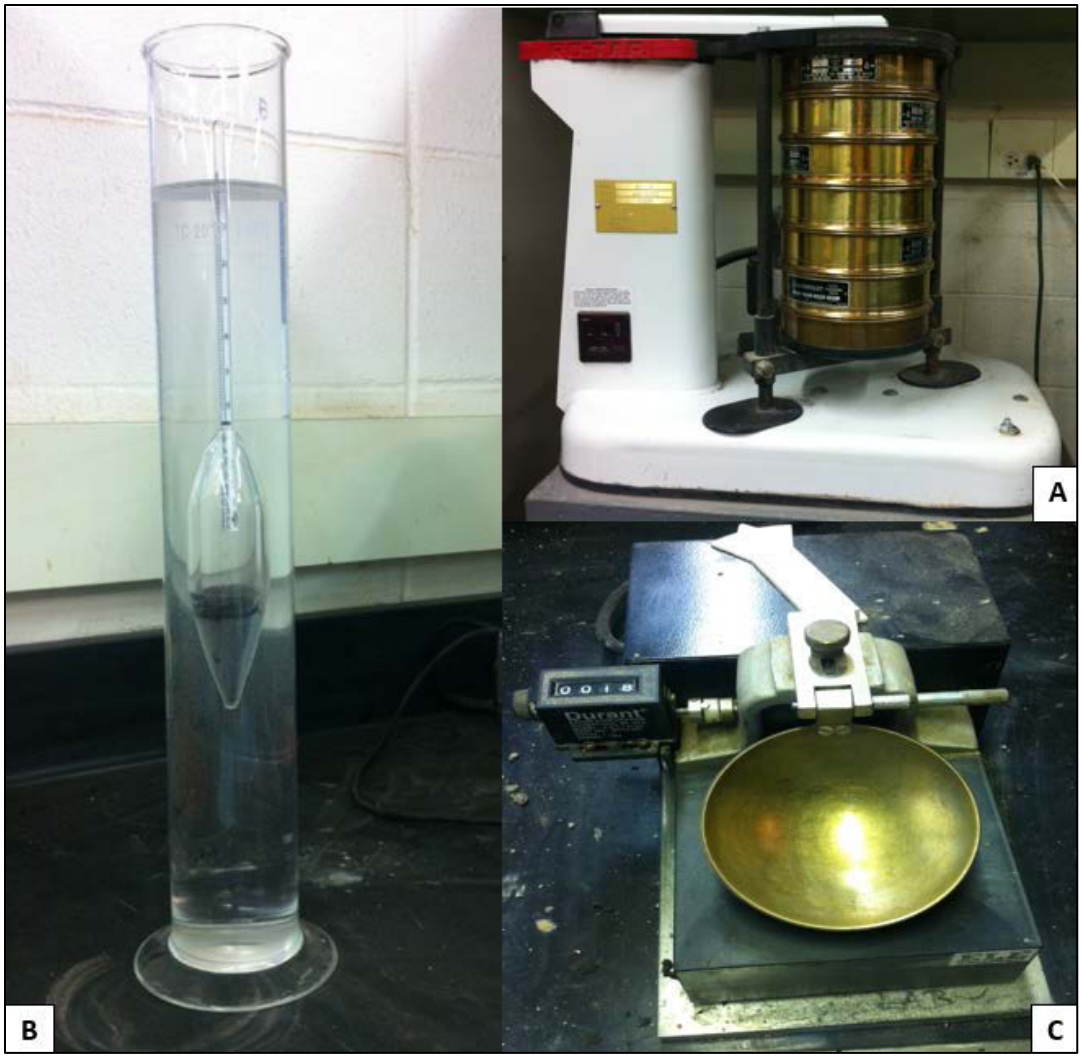

Figure 23. Soil classification tests showing (a) Sieve test; (b) Hydrometer test; (c) Atterberg limits test.

Compaction Tests

Standard Proctor compaction tests were conducted according to ASTM D698-07 (Figure 24). The relationship between moisture content and dry unit weight determines the specific moisture content for optimum dry unit weight. This specific moisture content was used to batch and prepare the soil materials for later frost-heave and thaw-weakening tests.

Figure 24. Standard Proctor compaction test

The 2-in. x 2-in. tests were conducted according to O'Flaherty et al. (1963). The results from these tests can be used to determine the specific moisture content and stabilizer content for peak compressive strength. Soils were moisture conditioned at selected target values and then stabilizers were added based on dry soil weight and then mixed with the soil. 2268 g (5 lb.) hammer was used to compact the soils by dropping it from a 305 mm (12 in.) height (Figure 25). The number of blow was calculated according to the target density. Compacted soil samples were sealed with plastic wrap and aluminum foil to keep the moisture, and then cured at 38 °C (100 °F) for 7 days.

Figure 25. 2-in. x 2-in. compaction test

Strength Tests

Unconfined compressive strength tests were performed to determine the failure stresses of the 2-in. x 2-in. samples. O'Flaherty et al. (1963) also provided the procedure of the unconfined compressive test (Figure 26). The applied loading rate was 0.05 in/min. ASTM D2166 provide the standard test method for unconfined compressive strength of cohesive soil.

Figure 26. 2-in. x 2-in unconfined compressive strength test

California bearing ratio (CBR) tests were conducted according to ASTM D1883-05 to evaluate the potential strength of pavement foundation materials. The CBR test device is shown in Figure 27. The test is performed by measuring the pressure required to penetrate a soil sample with a piston. The measured pressure is then divided by the pressure required to achieve an equal penetration on a standard crushed rock material. The treating conditions for the CBR tests samples were the same to the frost-heave and thaw-weakening test.

Figure 27. CBR test device

Frost-heave and Thaw-weakening Test

ASTM D5918-96 "Standard Test Methods for Frost Heave and Thaw Weakening Susceptibility of Soils" is the index test for estimating the relative degree of frost-susceptibility of soils used in pavement systems. Johnson (2012) constructed the laboratory equipment used in this study for conducting freeze-thaw tests. Six-inch samples are fully saturated before they are put into the freezer, then they are connected to Mariotte water supplies that maintain the water pressure. Two disks that connect to the water bath are applied to control the temperatures at the top and bottom. Lasers are set above the samples to measure the heave values during testing, and the computer program records the outputs of thermocouples, pressure transducers, and lasers. The entire freeze-thaw process takes around 120 hours, and includes two 8-hour freezing cycles.

Prepare the sample materials

The following is the procedure for preparing the materials that will be used as samples.

1. Use geomaterials passing 3/4 in. (1.91 cm) sieve.
2. Measure the moisture content and calculate the difference to the target moisture.
3. Adjust the moisture content.
    A. Add required amount of water if the target moisture content is larger than the measured value; or
    B. Oven dry the materials (100℉) to reduce the moisture content if the target value is less than the measured value.
4. Add stabilizers according to the test design. Mixing time depends on achieving a uniform distribution of the stabilizer.
    A. Incorporate chemical stabilizers (e.g., cement, fly ash) with a laboratory soil mixer (Figure 28).
    B. Incorporate geofibers may by hand.
5. Seal the mixed materials in zip sample bags for later use.
6. Record compaction delay time for chemically stabilized soils.

Figure 28. Soil sample mixer

Remold and compact the samples

The sample consists of six acrylic rings, each with a hole for a thermocouple and alignment grooves on the top and bottom rings; two acrylic spacer disks; a rubber membrane; a split cylinder mold; four clamps; and a top collar (Figure 29).

Figure 29. Sample assembly showing (a). Sample setup; (b). Six acrylic rings

1. Record the weight of the six acrylic rings, top and bottom acrylic spacer disks, and rubber membranes.
2. Place a spacer disk with a rubber membrane wrapped around it into the bottom of one side of the mold.
3. Put the acrylic rings into the mold and vertically align the thermocouple holes and grooves.
4. Place the other side of the cylinder mold around the assembled rings.
5. Place the clamps around the mold and top with collar.
6. Pull up the rubber membrane and stretch it over the top edge of the assembly until no ripple appears on the rubber.

7. Compact the mixed materials prepared in zip bags with five layers. Each compacted layer should have the same height of 1.2 in. (3.05 cm).
8. Use the standard Proctor rammer to compact layer for forty blows per layer. This number is determined by the dry unit weight.
9. Split the assembly and take out the sample after compaction.
10. Use straight edges to flatten the top surface and record the total weight of the sample, membrane, acrylic rings, and two spacer disks (Figure 30).
11. Seal the sample with a zip sample bag. Cure the sample according to the design curing level (e.g., time and temperature).

Figure 30. Remolded sample

Saturating samples

In order to eject the air between soil particles, full saturation is required. A water supply is connected to the sample through the inlet and base plate with a porous stone (Figure 31). A glass tube inside the water supply controls the water head through lifting it up or down.

1. Tightly close the clamp on the outlet after dewatering.

2. Place the bottom of the glass tube at the same height of the bottom layer of the sample.
3. Open the valve and leave it for one hour.
4. Repeat the same procedure for the other five layers above.
5. Put the glass tube down to the sixth layer after the top layer is saturated.
6. Leave the sample for a minimum of 8 hours.

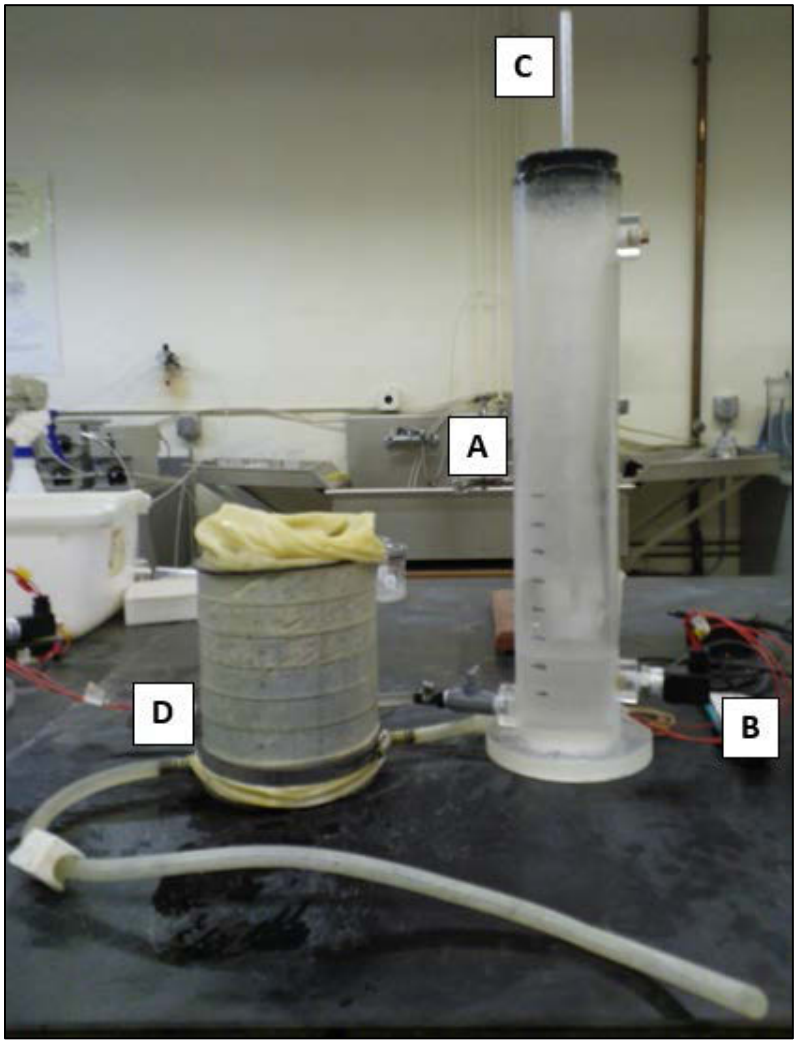

Figure 31. Saturation assembly showing (a) Mariotte tube; (b) Pressure transducer; (c) Bubble tube; (d) Base plate with porous stone

Conducting freeze-thaw tests

1. Disassemble the saturation set and dig shallow holes on the sample through the thermocouple holes and grooves.

2. Put the fully saturated sample into the freezer on the aluminum side of the temperature control end plate (Figure 32) and reconnect the saturation assembly to the sample.
3. Place the acrylic side of the temperature control end plate (Figure 32) at the top of sample and then put two 2268 g (5 lb.) steel disks as surcharge weight above the plate.

Figure 32. Temperature control end plates

4. Turn on the temperature control baths (Figure 33) to cool down the 50% ethylene glycol-water.

Figure 33. Water bath

5. Connect the pressure transducers to the data receiver.
6. Insert the thermocouples into the holes through the grooves.
7. Set up the laser displacement transducer above the sample assembly within required height range (Figure 34).

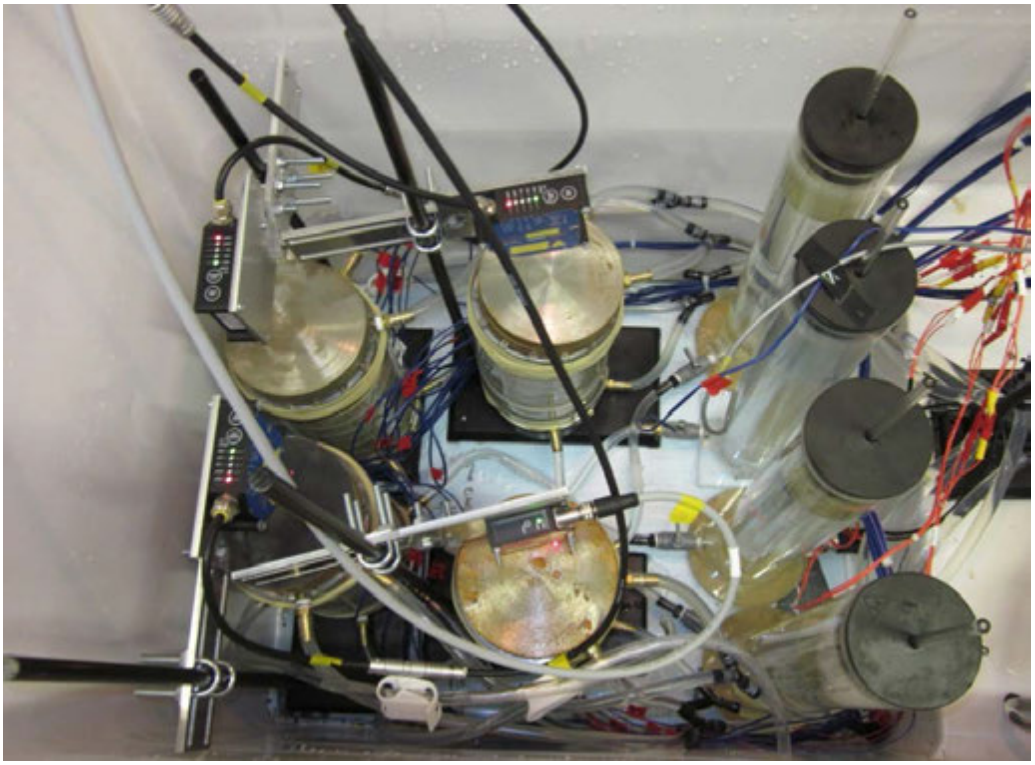

Figure 34. Freeze-thaw test assembly in the freezer

8. Run the computer program as an initial test to determine if every index meets the requirement (Figure 35).

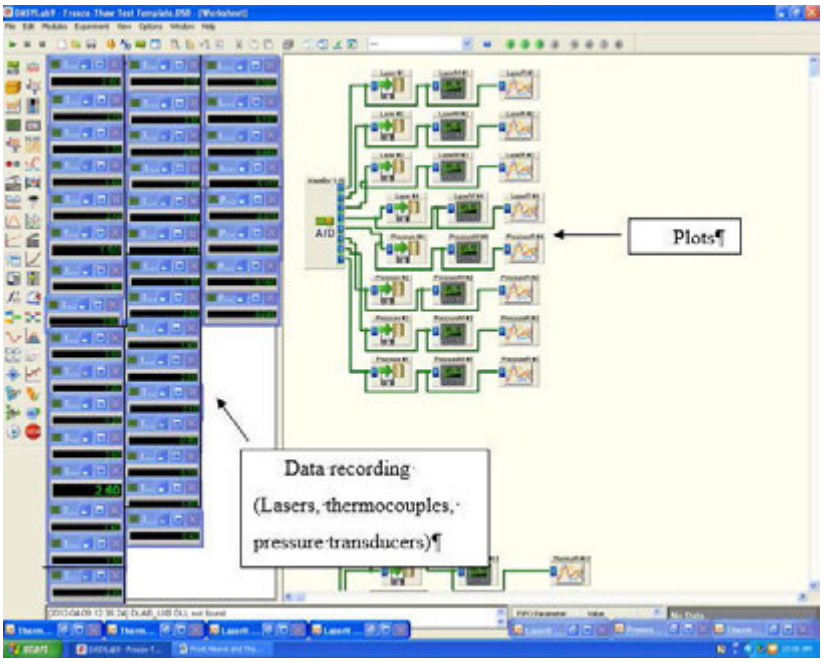

Figure 35. Computer program (DasyLab) interface

9. Close the freezer and rerun the program.
10. Leave the program running for 120 hours (5 days) (Table 8), and then take out the sample for strength testing.

Table 8. Freezing schedule based on computer program settings

Day	Elapsed Time, hr	Top Plate Temperature, °C	Bottom Plate Temperature, °C	Comments
1	0	3	3	24-hr conditioning
2	24	3	3	First 8-hr freeze
	32	12	0	Freeze to bottom
3	48	12	3	First thaw
	64	3	3	—
4	72	3	3	Second 8-hr freeze
	80	12	0	Freeze to bottom
5	96	12	3	Second thaw
	112 to 120	3	3	—

11. Run California bearing ratio (CBR) test on the after-thaw sample (Figure 36).

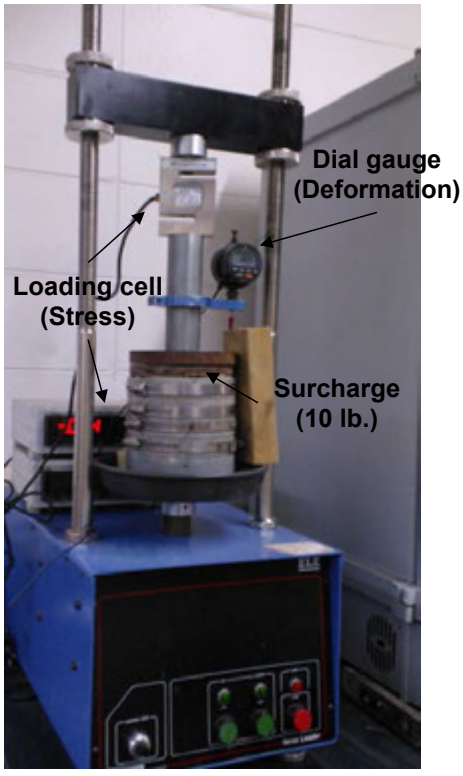

Figure 36. After thawing CBR test

12. Cut the sample into six layers along with the six acrylic rings (Figure 37). Take part each layer of material to measure the moisture contents.

Figure 37. Cut the sample into six layers

FIELD TESTS

To evaluate frost action of in situ pavement foundations and to compare the freeze-thaw performance with laboratory findings, field tests were conducted at the Boone County Test Section site. Falling weight deflectometer (FWD) tests and dynamic cone penetrometer (DCP) tests were conducted at the Boone County Test Sections site (Table 9).

Table 9. Field test methods

Test Method	Test
ASTM D6951-03	Standard Test Method for Use of the Dynamic Cone Penetrometer in Shallow Pavement Applications
FHWA 2000	Falling weight deflectometer (FWD)

Dynamic Cone Penetrometer

Dynamic cone penetrometer (DCP) tests were conducted according to ASTM D6851-03 to determine the field CBR values of pavement foundation systems (Figure 38). An 8 kg (17.64 lb.) hammer was dropped from a height of 575 mm (22.64 in.).

Equation 1 uses the penetration index in mm/blow to determine CBR values as follows

$$\text{CBR} = \frac{292}{\text{PI}^{1.12}} \quad (1)$$

where

CBR = California bearing ratio and

PI = penetration index (mm/blow).

Figure 38. In situ DCP test

Falling Weight Deflectometer

Falling weight deflectometer (FWD) tests were performed according to FHWA 2000 to evaluate the stiffness-related parameters of the pavement structures. A Kuab FWD setup (Figure 39) with a 300 mm (11.81 in.) diameter loading plate was used to directly test the pavement foundation layers with various loads. A load cell recorded actual applied forces and seismometers recorded deflections.

Elastic modulus values were determined by using the outputs from FWD tests based on Equation (2).

$$E_{SB-LWD} = \frac{(1-\eta^2)\sigma_0 r}{D_o} \times F \quad (2)$$

where

E = elastic modulus (psi),

D_0 = measured deflection under the plate (in.),

η = Poisson's ratio (assumed as 0.4),

σ_0 = applied stress (psi),

r = radius of the plate (in.),

F = shape factor depending on stress distribution (assumed as 8/3) (Vennapusa and White, 2009).

Figure 39. Kuab FWD Setup

CHAPTER 4. MATERIALS

This chapter describes the two kinds of materials, geomaterials and stabilizers, used in this research This research is part of a larger project, the Boone County Test Section project located at the Iowa Expo site that was funded by the Iowa DOT and jointly carried out by the Iowa DOT, Boone County, and the Center for Earthworks Engineering at Iowa State University. Table 10 shows the geomaterials and stabilization methods for laboratory tests according to the construction.

Table 10. Test materials and stabilization methods

Materials	Stabilization
Recycled subbase	No
Subgrade	No
Subgrade	5% Ames fly ash
Subgrade	10% Ames fly ash
Subgrade	15% Ames fly ash
Subgrade	20% Ames fly ash
subgrade	5% Muscatine fly ash
subgrade	10% Muscatine fly ash
subgrade	15% Muscatine fly ash
subgrade	20% Muscatine fly ash
Subgrade	5% Port Neal fly ash
Subgrade	10% Port Neal fly ash
Subgrade	15% Port Neal fly ash
Subgrade	20% Port Neal fly ash
Recycled subbase	2.5% cement
Recycled subbase	5.0% cement
Recycled subbase	2.5% cement
Recycled subbase	5.0% cement
Recycled subbase	7.5% cement
Recycled subbase	10.0% cement
Recycled subbase	0.2% PP
Recycled subbase	0.4% PP
Recycled subbase	0.6% PP
Recycled subbase	0.2% MF
Recycled subbase	0.4% MF
Recycled subbase	0.6% MF
Recycled subbase	0.2% PP + 3.75% cement
Recycled subbase	0.4% PP + 3.75% cement
Recycled subbase	0.6% PP + 3.75% cement
Recycled subbase	0.2% MF+ 3.75% cement

Table 10. Test materials and stabilization methods (continued)

Materials	Stabilization
Recycled subbase	0.4% MF+ 3.75% cement
Recycled subbase	0.6% MF+ 3.75% cement
Subgrade	5% cement
Subgrade	10% cement
Western Iowa Loess	12% fly ash 90 days curing
Western Iowa Loess	12% fly ash 180 days curing

GEOMATERIALS

Three types of geomaterials were tested for this research. With the exception of Western Iowa loess, the materials for this research are from the Iowa Expo site (Table 11).

Table 11. Material types and source locations

Material type	Source location
Recycled subbase	Boone County Test Section, Iowa
Subgrade	Boone County Test Section, Iowa
Loess	Pottawattamie County, Iowa

Three kinds of standard tests to determine soil index properties of the three materials, soil classification and index tests, compaction tests, and strength tests (Table 12).

Table 12. Lab tests methods

Test Method	Test
Soil classification and index tests	
ASTM D422-63	Standard Test Method for Particle-Size Analysis of Soils
ASTM C117-04	Standard Test Method for Materials Finer than 75-µm (No. 200) Sieve in Mineral Aggregates by Washing
ASTM C136-06	Standard Test Method for Sieve Analysis of Fine and Coarse Aggregates
ASTM D4318-05	Standard Test Methods for Liquid Limit, Plastic Limit, and Plasticity Index of Soils
ASTM D2487-06	Standard Practice for Classification of Soils for Engineering Purposes (Unified Soil Classification System)
Compaction tests	
ASTM D698-07	Standard Test Methods for Laboratory Compaction Characteristics of Soil using Standard Effort
O'Flaherty et al. 1963	2-in. x 2-in. Iowa State Compaction Method

Table 12. Lab tests methods (continued)

Test Method	Test
Strength tests	
ASTM D1883-05	Standard Test Method for CBR (California Bearing Ratio) of Laboratory-Compacted Soils
O'Flaherty et al. 1963	2-in. x 2-in. Compressive Strength Tests
Frost heave and thaw weakening test	
ASTM D5918-96	Standard Test Methods for Frost Heave and Thaw Weakening Susceptibility of Soils

Boone County Test Sections Recycled Subbase

Figure 40. Recycled subbase from the Boone County Test Sections site

Recycled subbase was collected from the Boone County Test Sections site (Figure 40). The soil index properties tests were conducted (Table 13). It was classified as silty sand with gravel (SM) based on USCS classification and A-1-a based on AASHTO classification. Figure 41 shows the grain size distribution curve of the material. Atterberg limits test

resulted in non-plastic. The optimum moisture content and maximum dry unit weight from standard Proctor test are 7.9% and 19.6 kN/m^3 (Figure 42).

Table 13. Recycled subbase index properties

Parameter	Recycled Subbase
Specific Gravity	2.5 (Assumed)
Gravel Content (%) (>4.75 mm)	37.2
Sand Content (%) (4.75 – 75 μm)	48.4
Silt content (%) (75 μm – 2 μm)	6.3
Clay content (%) (<2 μm)	8.1
D_{10} (mm)	0.02
D_{30} (mm)	0.45
D_{60} (mm)	4
Coefficient of Uniformity, C_u	160
Coefficient of Curvature, C_c	2
Liquid Limit, LL (%)	NP
Plasticity Index, PI (%)	
AASHTO	A-1-a
USCS Group Symbol	SM
USCS Group Name	Silty sand with gravel
Maximum Dry Unit Weight, $\gamma_{d,max}$ (kN/m^3)	19.62
Optimum Moisture Content, w_{opt} (%)	7.9

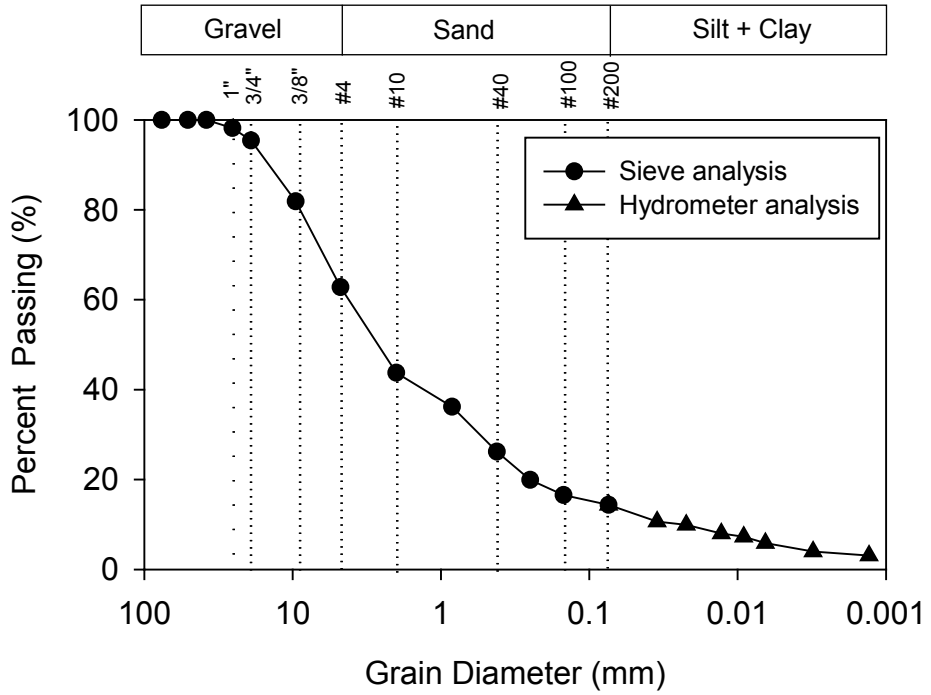

Figure 41. Recycled subbase grain size distribution

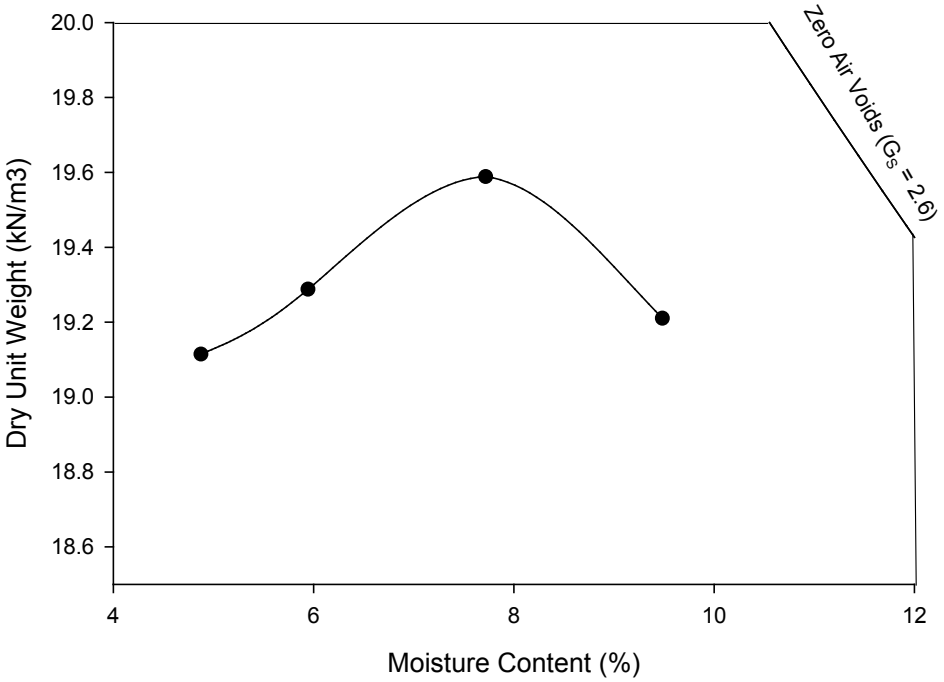

Figure 42. Recycled subbase standard Proctor curve

Boone County Test Sections Subgrade

Natural subgrade was collected from the Boone County Test Sections site (Figure 43). The soil index properties tests were conducted (Table 14). Figure 44 shows the grain size distribution of the material. It was classified as sandy lean clay (CL) based on USCS classification and A-6(5) based on AASHTO classification. Atterberg limits test resulted in 33 as the liquid limit and 18 as the plastic limit. The optimum moisture content and maximum dry unit weight from standard Proctor test are 13.5% and 18.2 kN/m^3 (Figure 45).

Figure 43. Subgrade from the Boone County Test Sections site

Table 14. Subgrade soil index properties

Parameter	Subgrade
Specific Gravity	2.7 (Assumed)
Gravel Content (%) (>4.75 mm)	5.3
Sand Content (%) (4.75 – 75 µm)	39.7
Silt + Clay content (%) (75 µm – 2 µm)	21.4
Clay content (%) (<12 µm)	33.6
D_{10} (mm)	-

Table 14. Subgrade soil index properties (continued)

Parameter	Subgrade
D_{30} (mm)	0.01
D_{60} (mm)	0.12
Coefficient of Uniformity, C_u	-
Coefficient of Curvature, C_c	-
Liquid Limit, LL (%)	33
Plasticity Index, PI (%)	15
AASHTO	A-6(5)
USCS Group Symbol	CL
USCS Group Name	Sandy lean clay
Maximum Dry Unit Weight, $\gamma_{d,max}$ (kN/m^3)	18.15
Optimum Moisture Content, w_{opt} (%)	13.5

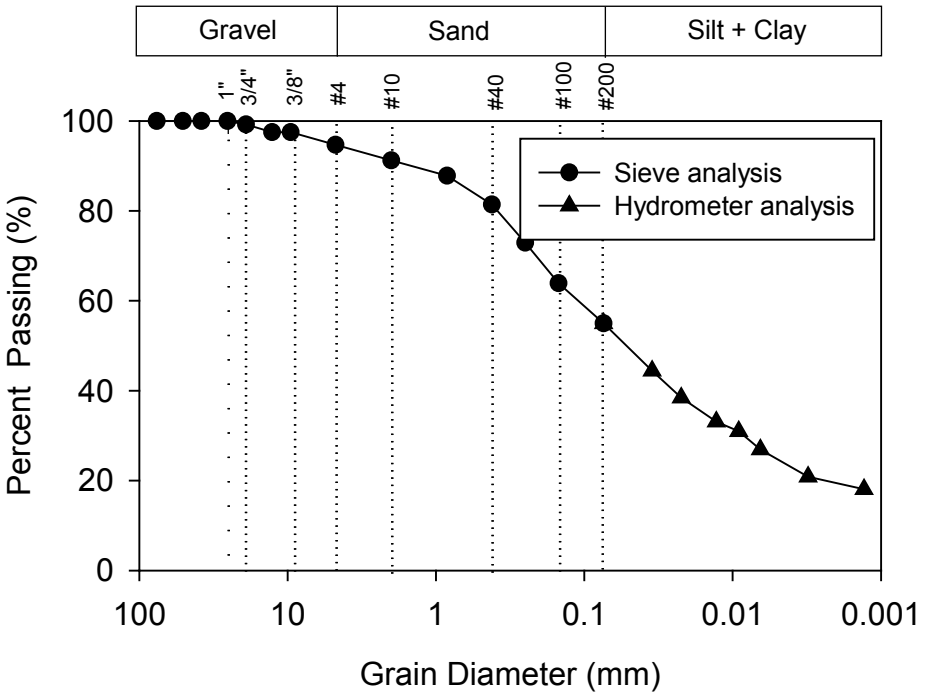

Figure 44. Subgrade grain size distribution

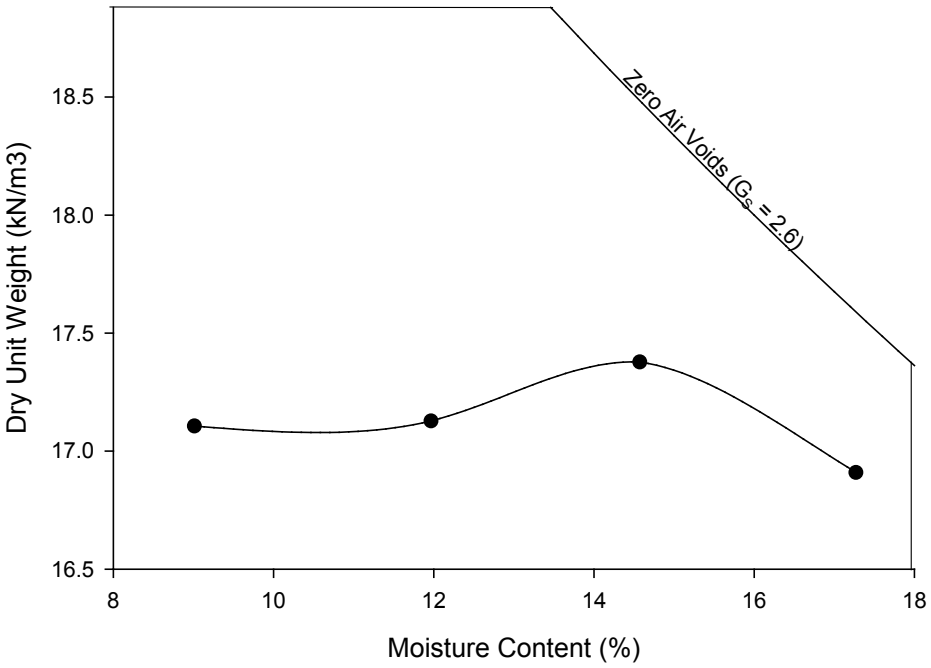

Figure 45. Subgrade standard Proctor curve

Western Iowa Loess

Figure 46. Western Iowa loess (WIL)

Loess material were collected from western Iowa local deposits (Figure 46). In this research, western Iowa loess (WIL) was used to determine the influence of various curing time to the effect of controlling freeze-thaw performance. Table 15 shows the soil index properties of non-stabilized and FA stabilized western Iowa loess. Both of the soils were classified as silt (ML) according to USCS classification. Figure 47 and Figure 48 show the grain size distribution of the soils. Figure 49 and Figure 50 show the standard Proctor results between dry unit weight and moisture content.

Table 15. Soil index properties of non-stabilized and FA stabilized western Iowa loess

Parameter	Non-stabilized WIL	FA stabilized WIL
Specific Gravity, G_s	2.72	2.68
Gravel Content (%) (>4.75 mm)	0	0
Sand Content (%) (4.75 – 75 μm)	0	3.0
Silt content (%) (75 μm – 2 μm)	82.0	82.0
Clay content (%) (<2 μm)	18.0	15.0

Table 15. Soil index properties of non-stabilized and FA stabilized western Iowa loess (continued)

Parameter	Non-stabilized WIL	FA stabilized WIL
Coefficient of Uniformity, C_u	-	-
Coefficient of Curvature, C_c	-	-
Liquid Limit, LL (%)	29	29
Plasticity Index, PI (%)	6	6
AASHTO	A-4(0)	A-4(2)
USCS Group Symbol	ML	ML
USCS Group Name	Silt	Silt
Maximum Dry Unit Weight, $\gamma_{d,max}$ (kN/m^3)	16.2	16.9
Optimum Moisture Content, w_{opt} (%)	16.7	16.7

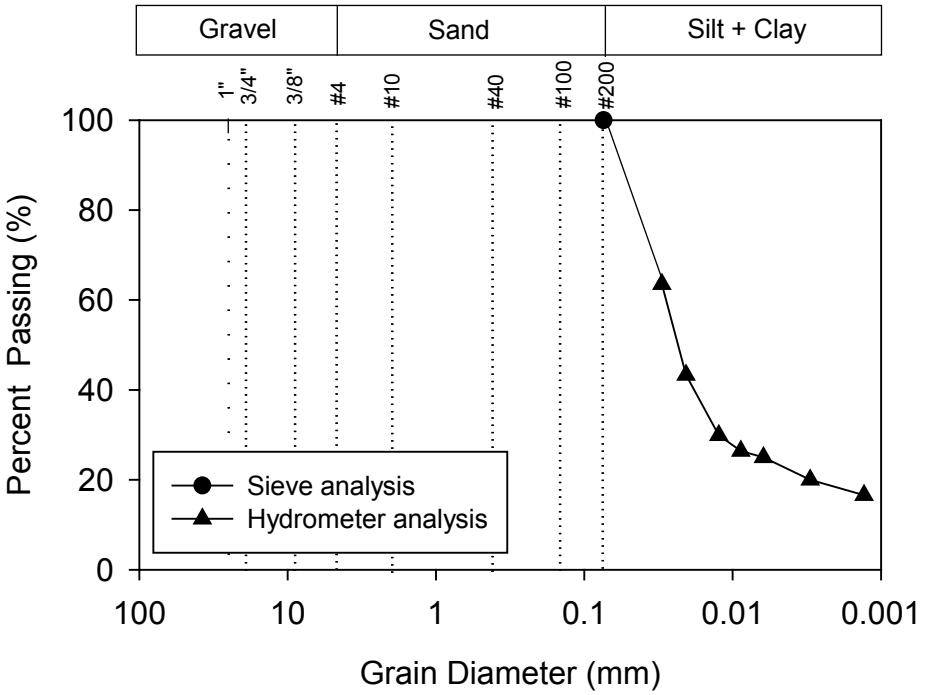

Figure 47. Non-stabilized WIL grain size distribution (Johnson 2012)

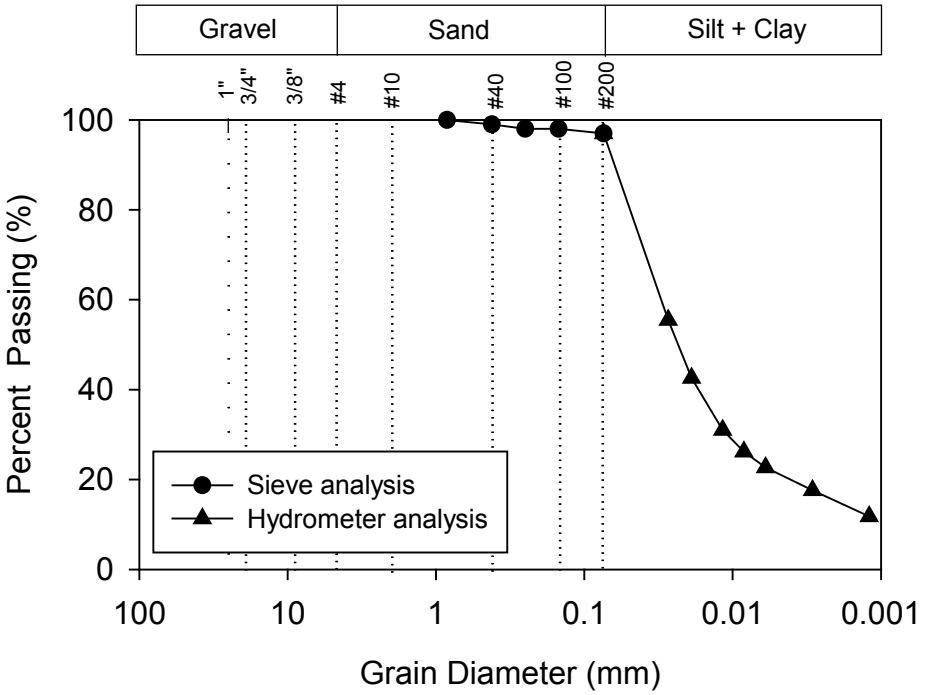

Figure 48. FA stabilized WIL grain size distribution (Johnson 2012)

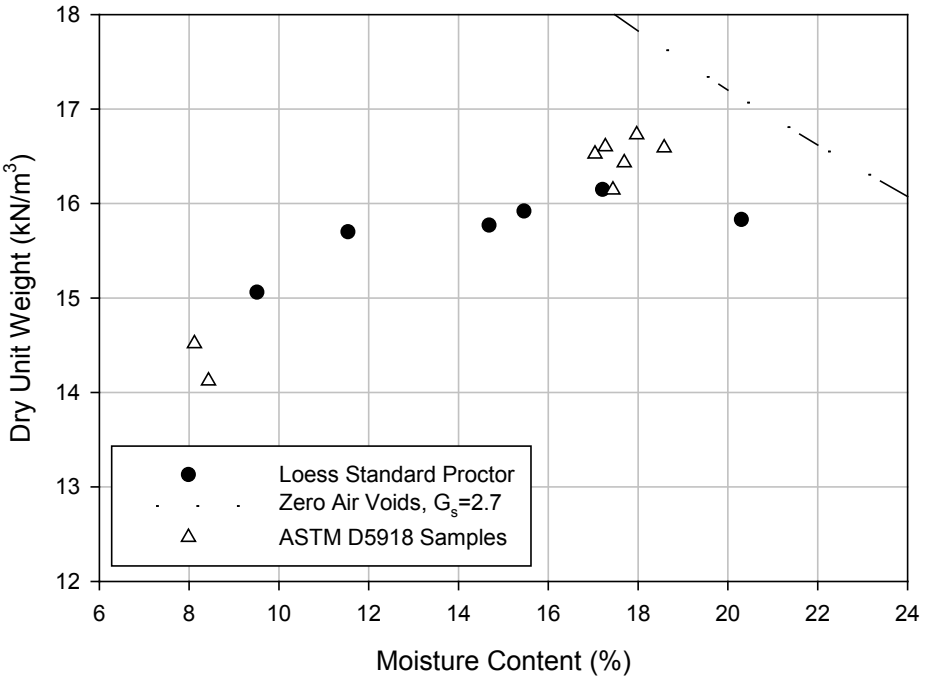

Figure 49. Non-stabilized WIL standard Proctor curve (Johnson 2012)

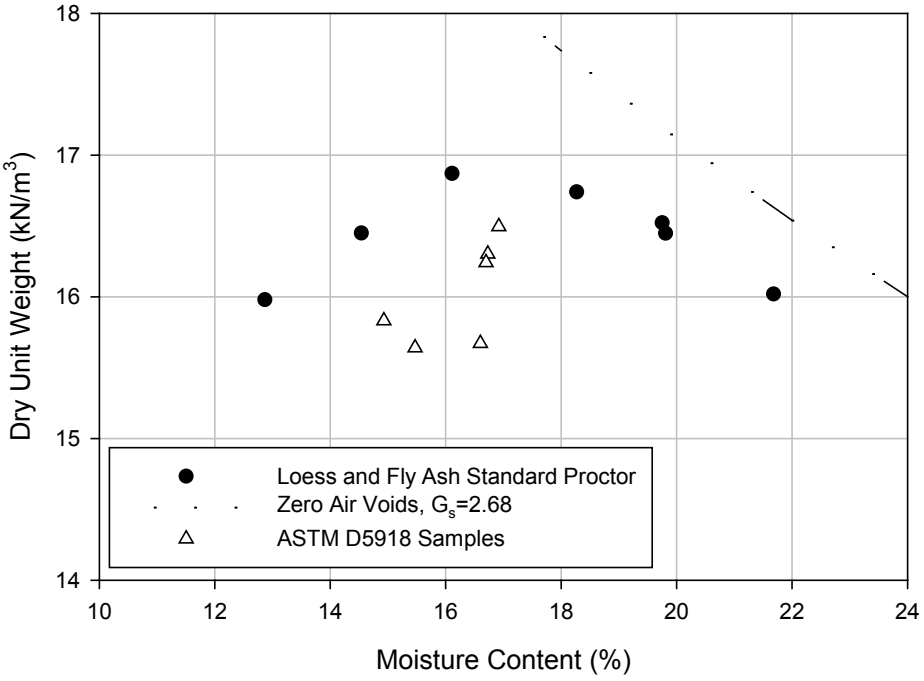

Figure 50. FA stabilized WIL standard Proctor curve (Johnson 2012)

STABILIZERS

Pavement foundation stabilizers are commonly used for improving pavement freeze-thaw performance. The following sections discuss basic mechanisms and performance of the stabilizers that were installed at the Boone County Test Sections site and investigated in this study: fly ash, cement, and geofabrics.

Fly ash

Fly ash (FA) (Figure 51) is a residual product of coal combustion, and the main components are silicon dioxide and calcium oxide. Johnson (2012) compared the frost-heave and thaw-weakening performance of FA-stabilized loess samples and non-stabilized loess samples and reported that there is no obvious improvement. The frost susceptibility of stabilized samples remained at a high level, but generally decreased as the FA content increases. All the stabilized samples heaved, and some heaved even more than non-stabilized samples. The thaw-weakening susceptibility of the stabilized samples ranged from negligible to high and post CBR values range from 5.0% to 25.5% as the FA content varies from 10% to 22% (Johnson 2012).

Figure 51. Three kinds of fly ash

In this project, freeze-thaw laboratory tests were conducted on FA stabilized Boone County Test Sections site geomaterials to determine if FA stabilization effectively improves the freeze-thaw performance of these materials. Furthermore, FA stabilized loess samples with longer cure period were tested for frost susceptibility. X-ray fluorescence (XRF) tests were conducted to analyze the chemical compositions of these three FA (

Table 16). X-ray diffraction (XRD) tests were also conducted by Iowa State University to characterize crystalline materials. Figure 53, Figure 54, and Figure 55 show the XRD test results of the three FA. Setting times of the three FA were tested to determine the hydration time (Figure 52). The time recorded at the first available resistance and 4.5 tsf was treated as the initial and final set time. The influences of different composition contents of different FA to stabilization effect were analyzed according to the XRF and XRD results.

Table 16. Composition and setting time of three types of FA

Composition (%)	Port Neal FA	Ames FA	Muscatine FA
SiO_2	38.90	33.80	36.50
Al_2O_3	17.30	17.00	20.70
Fe_2O_3	5.03	5.36	7.08
SO_3	2.25	2.53	2.14
CaO	25.30	26.40	22.90
MgO	5.03	6.15	4.84
Na_2O	1.57	2.56	1.59
K_2O	0.58	0.62	0.40
P_2O_5	0.59	1.32	1.39
TiO_2	1.52	1.57	1.57
SrO	0.36	0.34	0.39
BaO	0.66	0.78	0.80
Initial sett time (min)	2.75	4.25	7.00
Final set time (min)	6.00	18.5	166.00

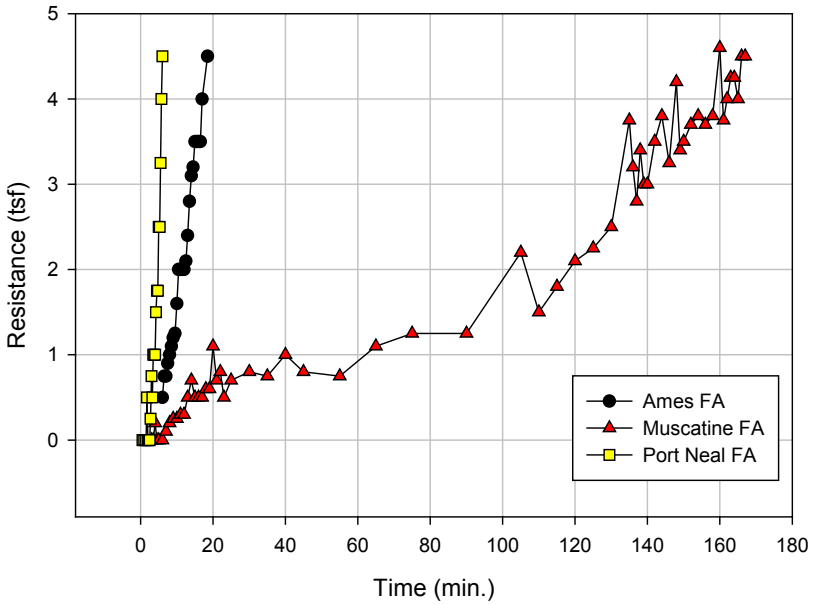

Figure 52. Set time plots of Ames, Muscatine, and Port Neal FA

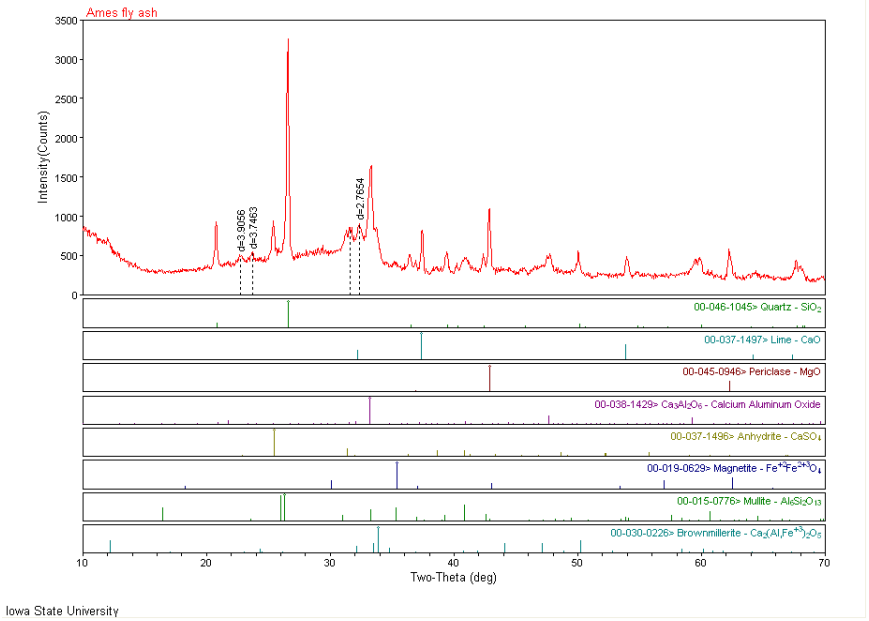

Figure 53. XRD test result of Ames FA

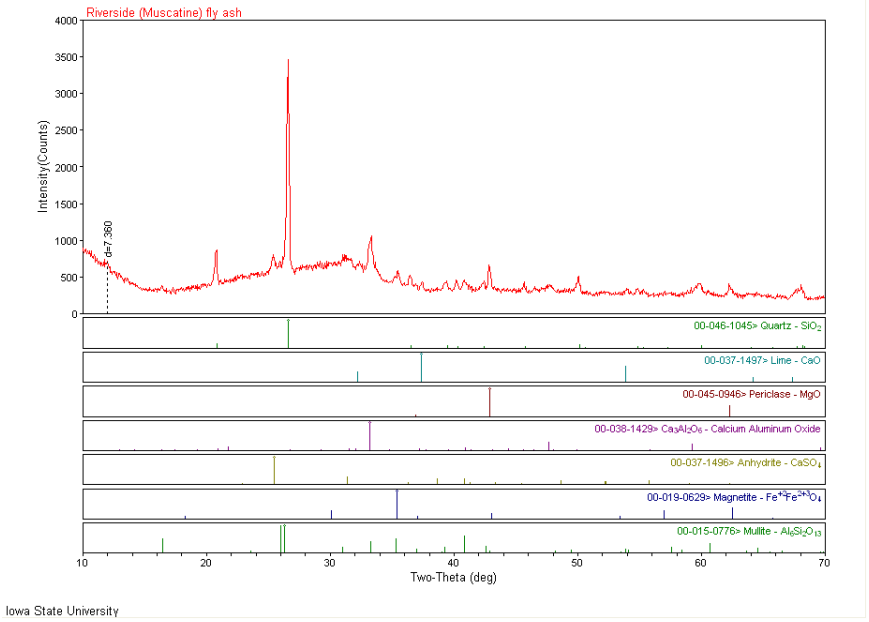

Figure 54. XRD test result of Muscatine FA

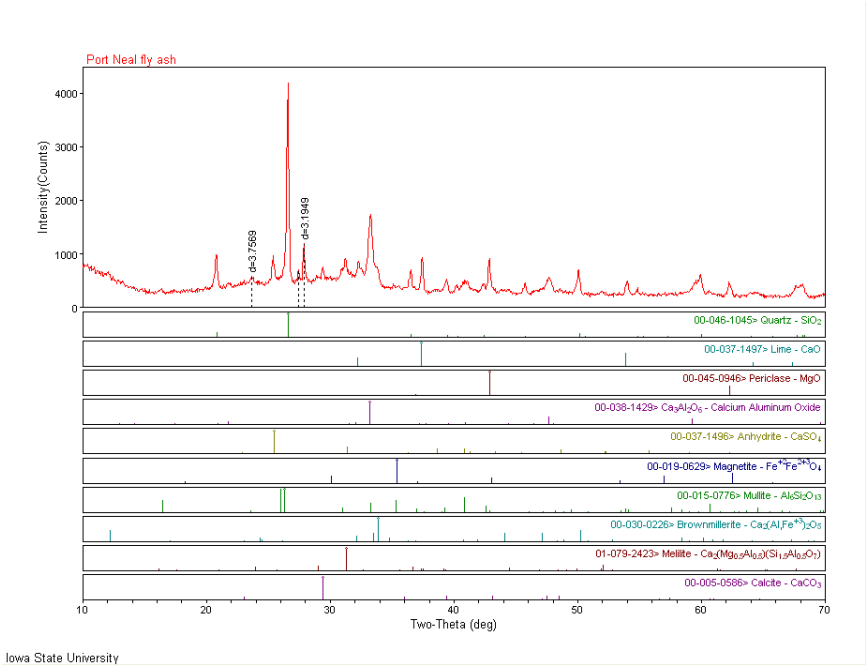

Figure 55. XRD test result of Port Neal FA

Portland cement

Figure 56. Type II Portland cement

Cement (Figure 56) is one of the most widely applied chemical stabilizers in pavement foundation construction to improve geomaterial behaviors during freezing and thawing (Joint

Department of the Army and Air Force 1985). Cement hydrates and sets after it is mixed with soil because pore water reacts with cement to form calcium silicate and aluminate hydrates. These cemented products effectively decrease the amount of pore water; bond soil grains; and improve soil stability, frost-heave behavior, and thaw-weakening.

Non-stabilized loess is among the most frost susceptible geomaterials. Johnson (2012) reported that the average heave rate of cement-stabilized Iowa loess was 0 mm/d, and seven of eight cement-stabilized samples had CBR values over 100%. Johnson (2012) also stated that both frost susceptibility and thaw-weakening are negligible after cement stabilization because cement-stabilized materials can absorb large amounts of water without increasing frost susceptibility.

This project extended Johnson's work by studying cement stabilized geomaterials from the Boone County Test Sections site to evaluate how cement stabilization affects the engineering properties of these materials. Type II Portland cement (Table 17) was used to stabilize the geomaterials. This type of cement is commonly used for general construction that is exposed to moderate sulfate attack (Wikipedia, 2013), such in the western United States where concrete is in contact with soils and ground water with high sulfur contents.

Table 17. Composition of type II portland cement

Composition	C_3S	C_2S	C_3A	C_4AF	MgO	SO_3	CaO	Ignition loss
Content	51.0%	24.0%	6.0%	11.0%	2.9%	2.5%	1.0%	0.8%

Geofibers

Figure 57. Black polypropylene geofibers (PP)

Two types of geofibers, polypropylene geofibers (Figure 57) and monofilament fibers (Figure 58), were used to evaluate the stabilization effects on improving freeze-thaw performance.

Figure 58. White monofilament fibers (MF)

Several researchers have studied using geo-fibers as a stabilization technology for geomaterials, but there is limited research regarding freeze-thaw effects on geofiber stabilized materials. Hazirbaba et al. (2007) studied native soil and reported that the CBR value at optimum moisture content without stabilizers was 31, and the optimum geofiber content, which corresponds to the largest CBR value, appears to be about 0.5%. Addition of 0.5% geofiber at optimum moisture content of 11% increased the CBR value from 31 to 62 and got much higher values at larger penetrations. Viswanadham (2009) stated that geofiber stabilization is a very effective method for controlling soil deformation. It is predicted that geofibers can help to improve the freeze-thaw performance of pavement foundation materials. For example, Gray and Ohashi (1983) tested beach sand stabilized with geo-fibers and concluded that geo-fibers increase the shear strength of clean sand, but they did not conduct freeze-thaw tests. Collins (2011) recommended that samples treated with geo-fibers should be subjected to lab freeze-thaw conditions to evaluate the effects of this stabilization method.

CHAPTER 5. RESULTS AND DISCUSSION

This chapter includes the data from the laboratory and field tests and an overview of the major points organized by frost-heave and thaw-weakening tests and in situ tests. All tests were conducted according to the methods illustrated in Chapter 3 on the materials presented in Chapter 4.

FROST-HEAVE AND THAW-WEAKENING TESTS

Freeze-thaw and California bearing ration (CBR) tests were conducted on a total of 35 non-stabilized and stabilized geomaterials. Freeze-thaw tests with two freeze-thaw cycles were conducted to determine the heave performance and water movement in the test layers. In most cases, frost heaves during the second cycle were greater and faster and were used to evaluate the frost susceptibility of the materials. When the frost heave from the first cycle was greater, that was used as the governed heave rate. Heave values and heave rates can be determined from frost heave time plots. Moisture contents were measured at each layer after the freeze-thaw tests to show trends of moisture content with depth. CBR values are calculated from stress penetrations at the depth of 0.2 in. CBR tests were performed before and after freeze-thaw testing to determine the weakening performance of the materials.

The following sections show frost-heave time plots, the after-thawing moisture contents profiles, and the frost susceptibilities based on heave rates and CBRs for the 35 materials.

Non-stabilized subgrade and recycled subbase

One set of control frost-heave and thaw-weakening test was performed. Two samples of non-stabilized recycled subbase (samples 1 and 2) and two samples of non-stabilized subgrade (samples 3 and 4) were tested. Figure 59 shows the frost heave time plots of these four samples. The slopes that represent the heave rates of non-stabilized subbase samples were similar. The governed second heave rate was 15.63 mm/day. The non-stabilized subgrade samples heaved less and more slowly than the subbase samples. The governed second heave rate was 11.43 mm/day. However, the first heave rates of the four samples were close, which was around 9.50 mm/day.

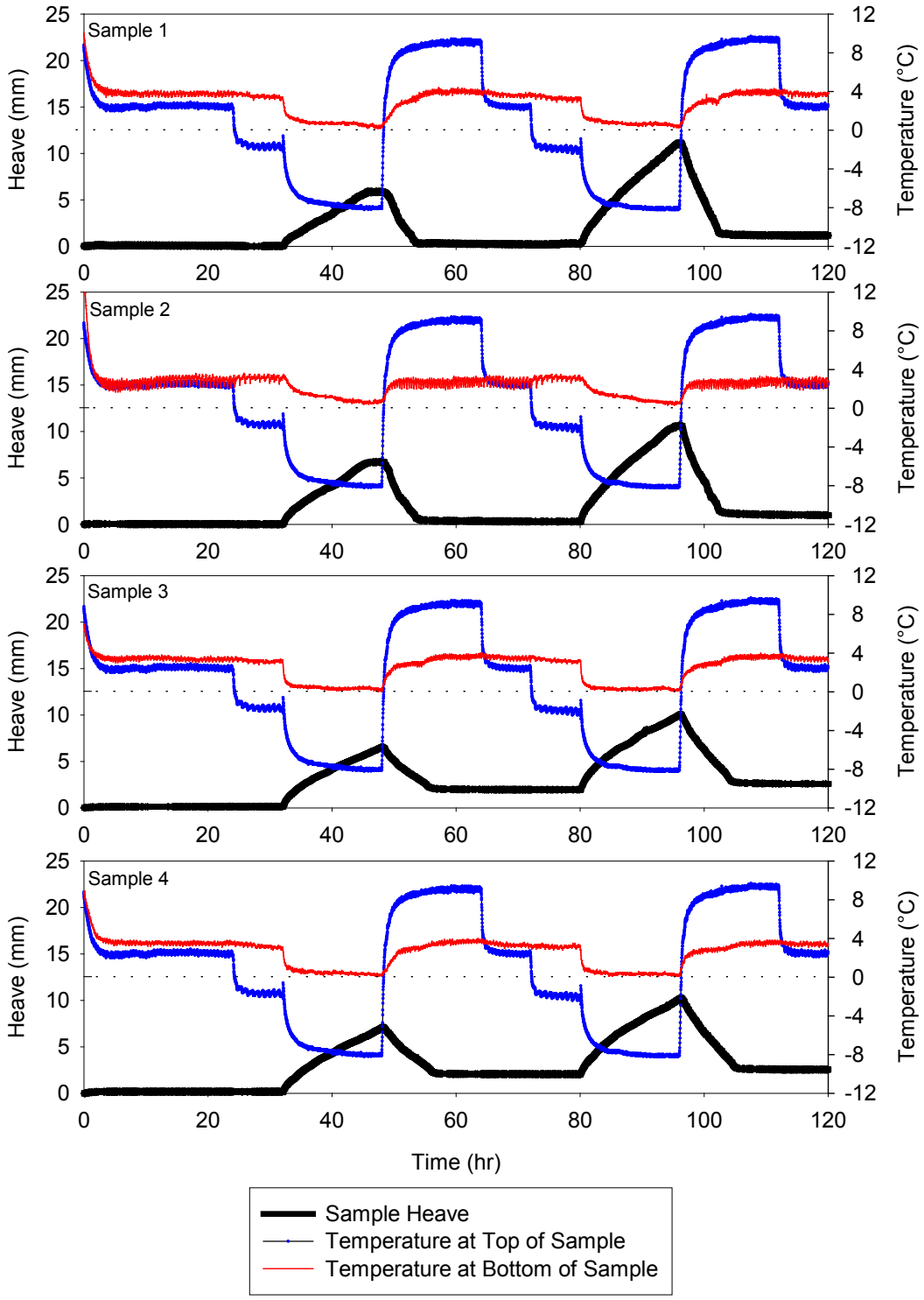

Figure 59. Non-stabilized subbase (samples 1 and 2) and subgrade (samples 3 and 4) frost heave time plots

For non-stabilized recycled subbase and subgrade samples the moisture content profiles show the moisture contents decreased as the depth increased. Figure 60 shows the moisture content profiles of the post-test samples.

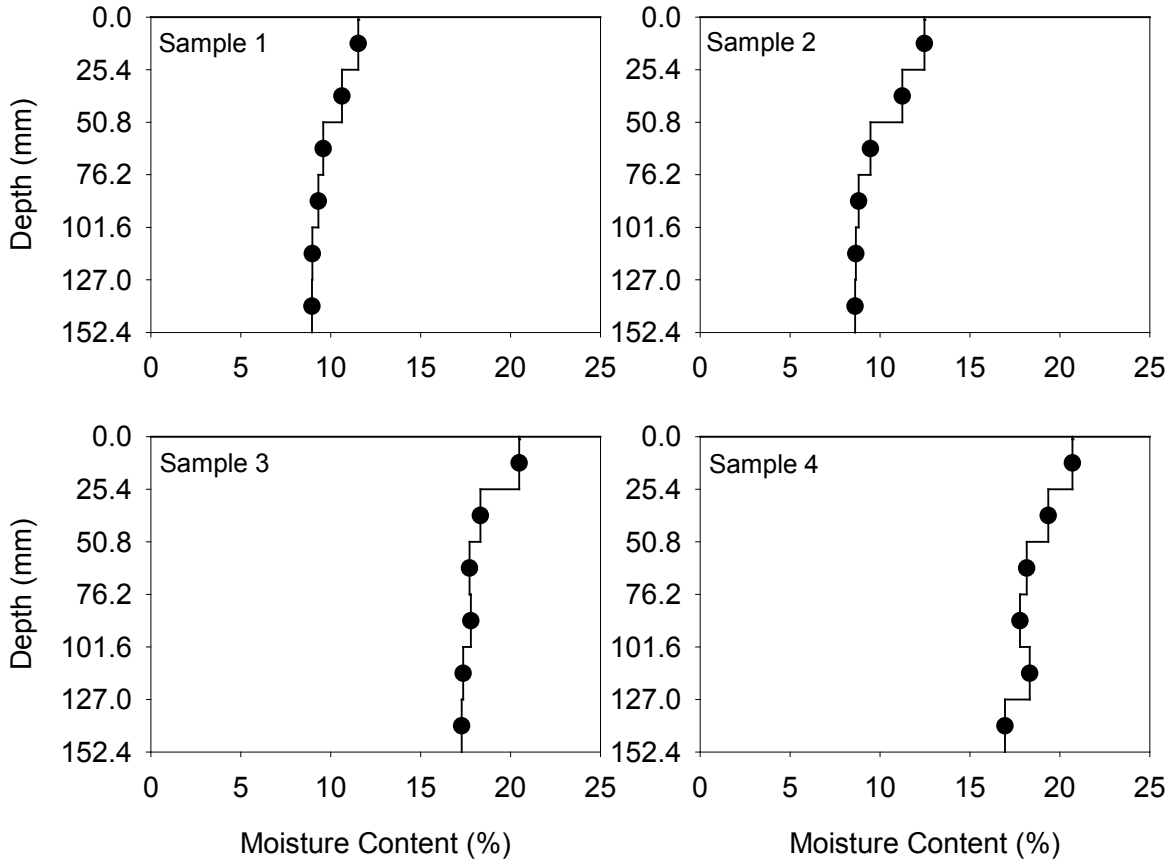

Figure 60. Non-stabilized subbase (samples 1 and 2) and subgrade (samples 3 and 4) moisture content profiles

The CBR value of non-stabilized recycled subbase after freeze-thaw testing was larger than the one without freeze-thaw test. The frost susceptibility of non-stabilized recycles subbase was classified as medium to high level. Table 18 summarizes the frost-heave and thaw-weakening test results on non-stabilized recycled subbase material.

Table 18. Non-stabilized subbase frost-heave and thaw-weakening test results

1st frost-heave rate (mm/day)	9.61
2nd frost-heave rate (mm/day)	15.63
CBR after freeze-thaw test (%)	8.8
CBR before freeze-thaw test (%)	4.6
Frost susceptibility based on heave	High
Frost susceptibility based on CBR	Medium

The CBR value of non-stabilized subgrade after freeze-thaw test was less than the one without freeze-thaw test. The frost susceptibility of this material was classified as high to very high level. Table 19 summarizes the frost-heave and thaw-weakening test results on non-stabilized subgrade material.

Table 19. Non-stabilized subgrade frost-heave and thaw-weakening test results

1st Frost-heave rate (mm/day)	9.44
2nd Frost-heave rate (mm/day)	11.43
CBR after freeze-thaw test (%)	1.4
CBR before freeze-thaw test (%)	2.8
Frost susceptibility based on heave	High
Frost susceptibility based on CBR	Very high

Subgrade stabilized with fly ash

Ten sets of fly ash-stabilized subgrade samples with different percentages of three kinds of fly ash (FA), Ames, Muscatine, and Port Neal FA, were constructed. Table 20 shows the sources, percentages in the sample mixtures, the ASTM C 618 class of the FA, and the chemical components of the FA for the 10 sets of samples.

Table 20. Fly ash percentages and active components contents

Fly ash source	Percent (%)	SiO_2 content (%)	Al_2O_3 content (%)	CaO content (%)	Initial set time (min.)	Final set time (min.)
Ames	5	33.8	17.0	26.4	2.75	6.00
Ames	10					
Ames	15					
Ames	20					
Muscatine	5	36.5	20.7	22.9	4.25	18.5
Muscatine	10					

Table 20. Fly ash percentages and active components contents (continued)

Fly ash source	Percent (%)	SiO_2 content (%)	Al_2O_3 content (%)	CaO content (%)	Initial set time (min.)	Final set time (min.)
Port Neal	5	38.9	17.3	25.3	7.00	166.00
Port Neal	10					
Port Neal	15					
Port Neal	20					

Two subgrade samples stabilized with 5% Ames fly ash were tested. The peak heave values of the samples were similar. The governed second heave rate calculated from the slopes was 8.40 mm/day. Figure 61 shows the frost heave time plots of these two samples. The heave rate was less than the non-stabilized subgrade.

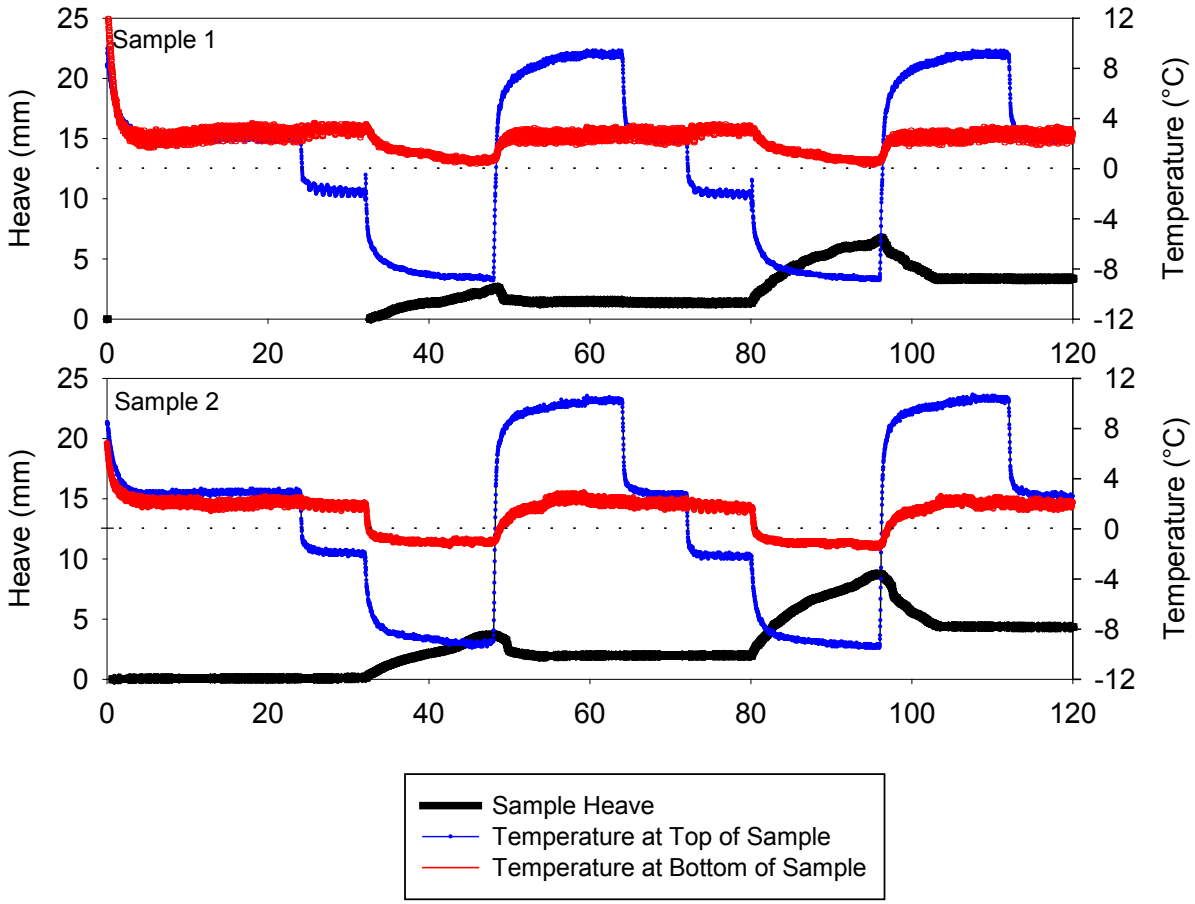

Figure 61. 5% Ames FA stabilized subgrade frost heave time plots

For the 5% Ames FA stabilized subgrade the moisture content profiles show that the moisture contents decreased as the depth increased. Figure 62 shows the moisture content profiles of the post-test samples.

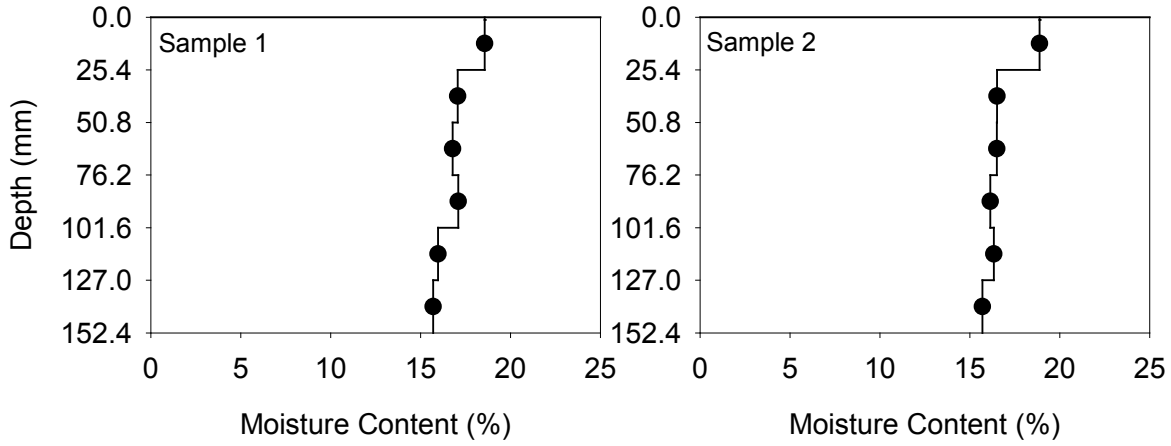

Figure 62. 5% Ames FA stabilized subgrade moisture content profiles

For 5% Ames FA stabilized subgrade, the CBR value after freeze-thaw test was less than the one without freeze-thaw test. The frost susceptibility of this material was classified as medium to high level. Table 21 summarizes the frost-heave and thaw-weakening test results on 5% Ames FA stabilized subgrade material.

Table 21. 5% Ames FA stabilized subgrade frost-heave and thaw-weakening test results

1st Frost-heave rate (mm/day)	4.51
2nd Frost-heave rate (mm/day)	8.40
CBR after freeze-thaw test (%)	6.6
CBR before freeze-thaw test (%)	15.5
Frost susceptibility based on heave	High
Frost susceptibility based on CBR	Medium

Two subgrade samples stabilized with 10% Ames fly ash were tested. The peak heave values of the samples were similar. The governed second heave rate calculated from the slopes was 6.60 mm/day. Figure 63 shows the frost heave time plots of these two samples. The heave rate was less than the non-stabilized and 5% Ames FA stabilized subgrade.

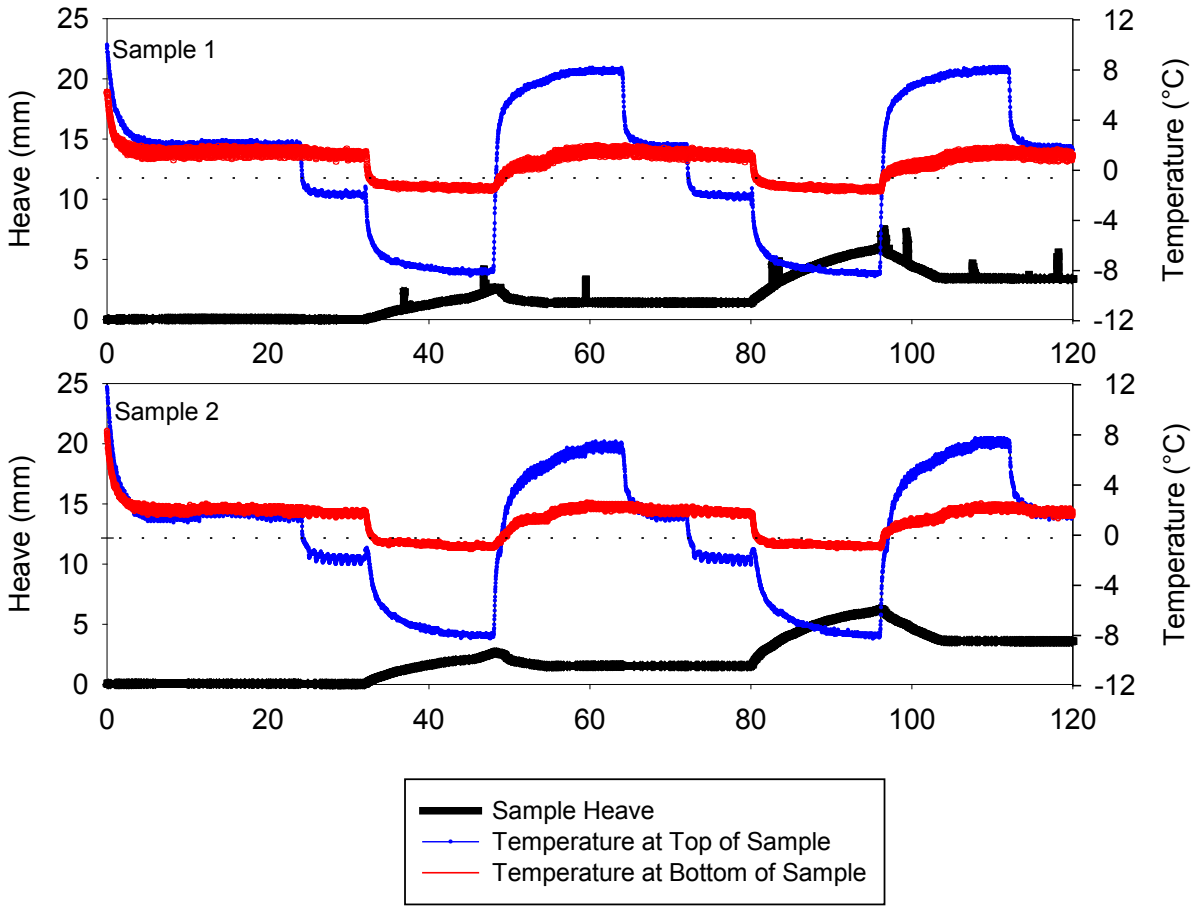

Figure 63. 10% Ames FA stabilized subgrade frost heave time plots

For 10% Ames FA stabilized subgrade the moisture content profiles show the moisture contents decreased as the depth increased. Figure 64 shows the moisture content profiles of the post-test samples.

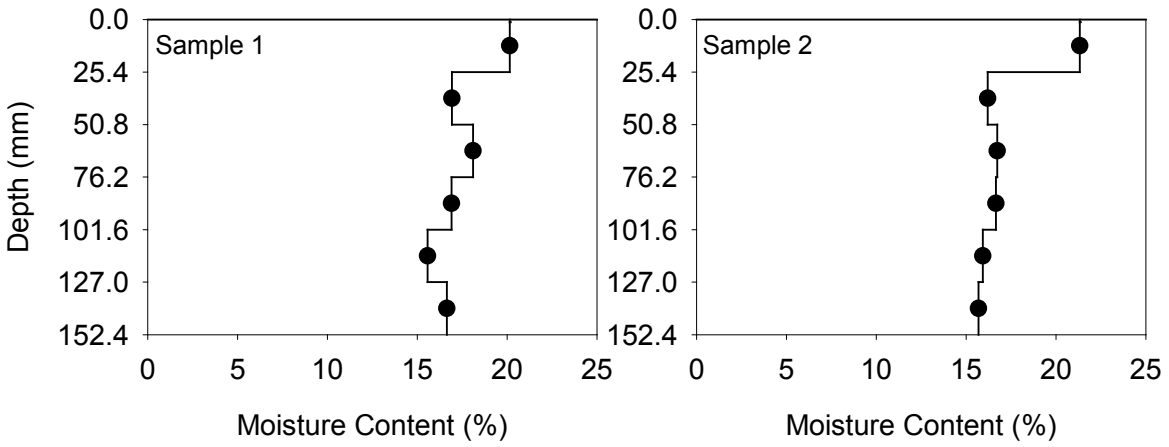

Figure 64. 10% Ames fly ash stabilized subgrade moisture content profiles

For 10% Ames FA stabilized subgrade, the CBR value after freeze-thaw test was less than the one without freeze-thaw test. The frost susceptibility of this material was classified as medium level. Table 22 summarizes the frost-heave and thaw-weakening test results on 10% Ames FA stabilized subgrade material.

Table 22. 10% Ames fly ash stabilized subgrade frost-heave and thaw-weakening test results

1st Frost-heave rate (mm/day)	3.60
2nd Frost-heave rate (mm/day)	6.60
CBR after freeze-thaw test (%)	9.6
CBR before freeze-thaw test (%)	44.6
Frost susceptibility based on heave	Medium
Frost susceptibility based on CBR	Medium

Two subgrade samples stabilized with 15% Ames fly ash were tested. The peak heave values of the samples were similar. The governed second heave rate calculated from the slopes was 6.87 mm/day. Figure 65 shows the frost heave time plots of these two samples. The heave rate was less than the non-stabilized, 5% Ames FA stabilized, and 10% Ames FA stabilized subgrade.

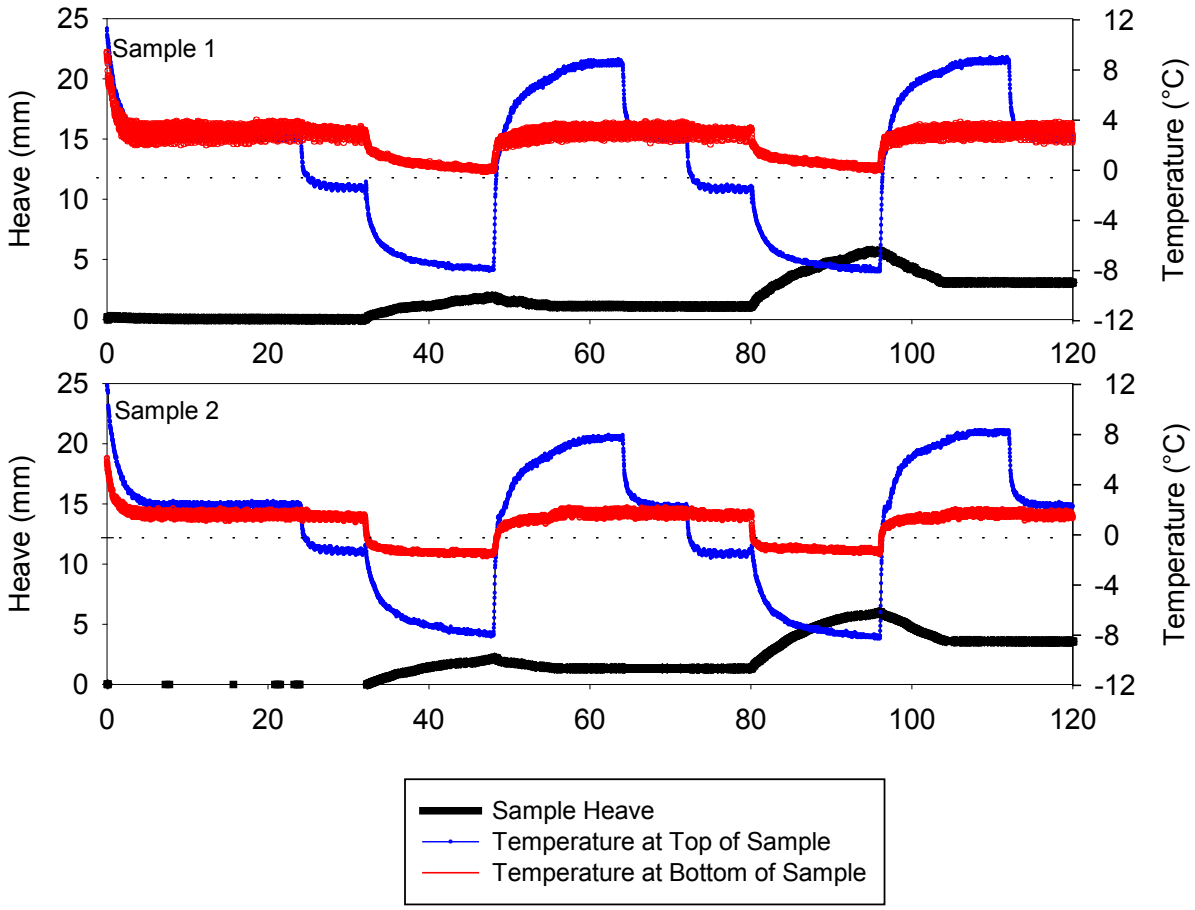

Figure 65. 15% Ames FA stabilized subgrade frost heave time plots

For both of the 15% Ames FA samples the moisture content profiles show that the moisture content decreased as the depth increased. Figure 66 shows the moisture content profiles of both post-test samples.

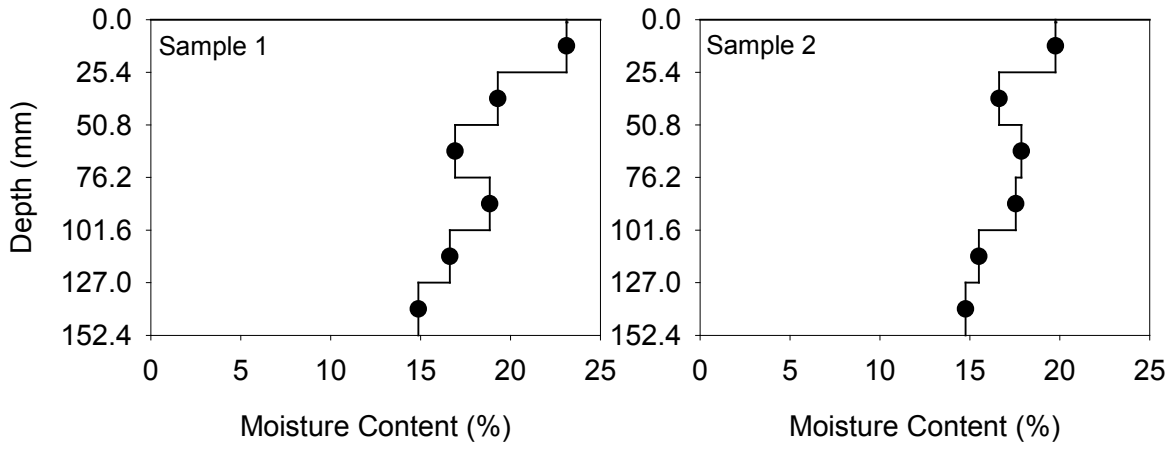

Figure 66. 15% Ames FA stabilized subgrade moisture content profiles

For 15% Ames FA stabilized subgrade, the CBR value after freeze-thaw test was less than the one without freeze-thaw test. The frost susceptibility of this material was classified as medium to negligible level. Table 23 summarizes the frost-heave and thaw-weakening test results on 15% Ames FA stabilized subgrade material.

Table 23. 15% Ames FA stabilized subgrade frost-heave and thaw-weakening test results

1st Frost-heave rate (mm/day)	2.92
2nd Frost-heave rate (mm/day)	6.87
CBR after freeze-thaw test (%)	20.1
CBR before freeze-thaw test (%)	73.2
Frost susceptibility based on heave	Medium
Frost susceptibility based on CBR	Negligible

Two subgrade samples stabilized with 20% Ames fly ash were tested. The peak heave values of the samples were similar. The governed second heave rate calculated from the slopes was 7.85 mm/day. Figure 67 shows the frost heave time plots of these two samples. The heave rate was less than the non-stabilized and 5% Ames FA stabilized subgrade, but larger than the 10% and 15% Ames FA stabilized subgrade.

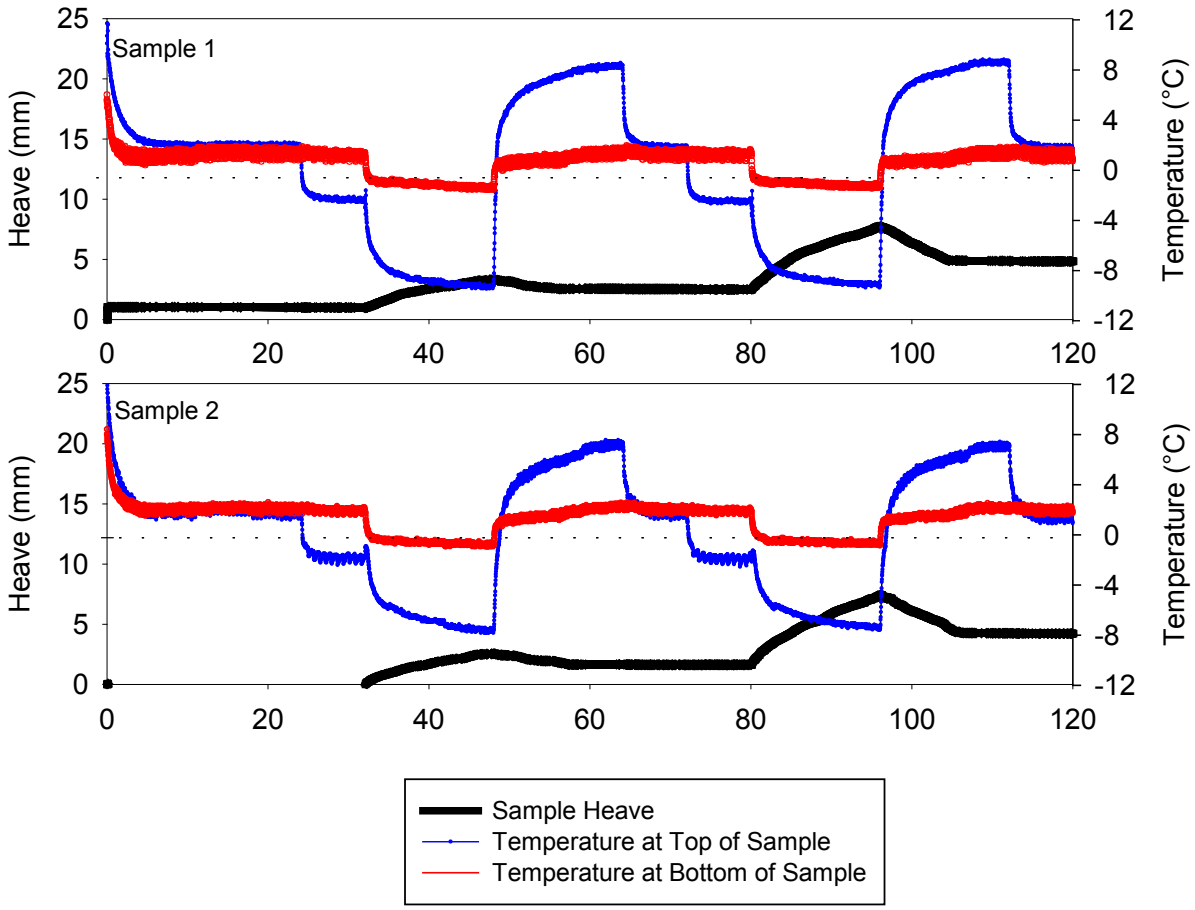

Figure 67. 20% Ames FA stabilized subgrade frost heave time plots

For 20% Ames FA stabilized subgrade the moisture content profiles show the moisture contents decreased as the depth increased. Figure 68 shows the moisture content profiles of the post-test samples.

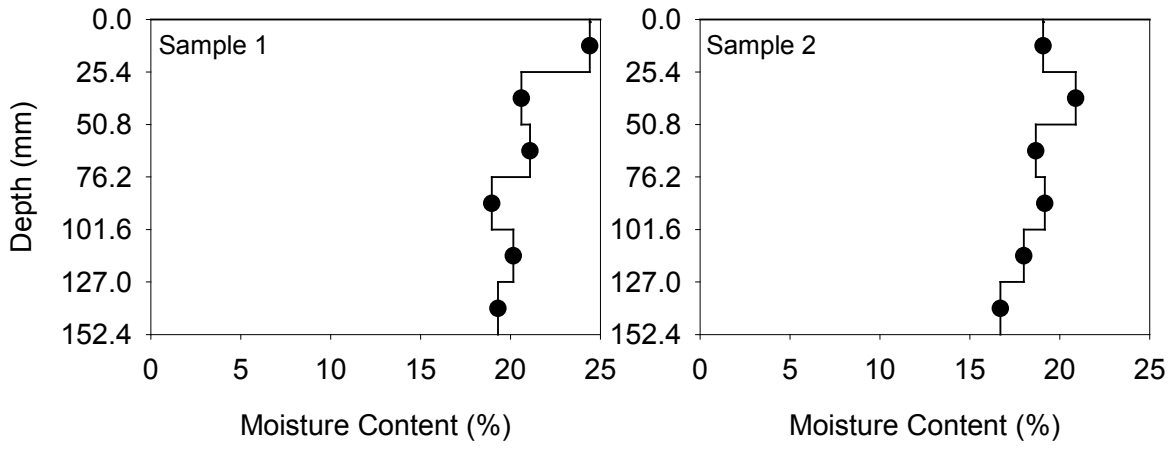

Figure 68. 20% Ames FA stabilized subgrade moisture content profiles

For 20% Ames FA stabilized subgrade, the CBR value after freeze-thaw testing was less than the one without freeze-thaw test. The frost susceptibility of this material was classified as medium to low level. Table 24 summarizes the frost-heave and thaw-weakening test results on 20% Ames FA stabilized subgrade material.

Table 24. 20% Ames FA stabilized subgrade frost-heave and thaw-weakening test results

1st Frost-heave rate (mm/day)	3.61
2nd Frost-heave rate (mm/day)	7.85
CBR after freeze-thaw test (%)	10.2
CBR before freeze-thaw test (%)	18.2
Frost susceptibility based on heave	Medium
Frost susceptibility based on CBR	Low

Two subgrade samples stabilized with 5% Muscatine fly ash were tested. The peak heave values of the samples were similar. The governed second heave rate calculated from the slopes was 9.88 mm/day. Figure 69 shows the frost heave time plots of these two samples. The heave rate was less than the non-stabilized subgrade.

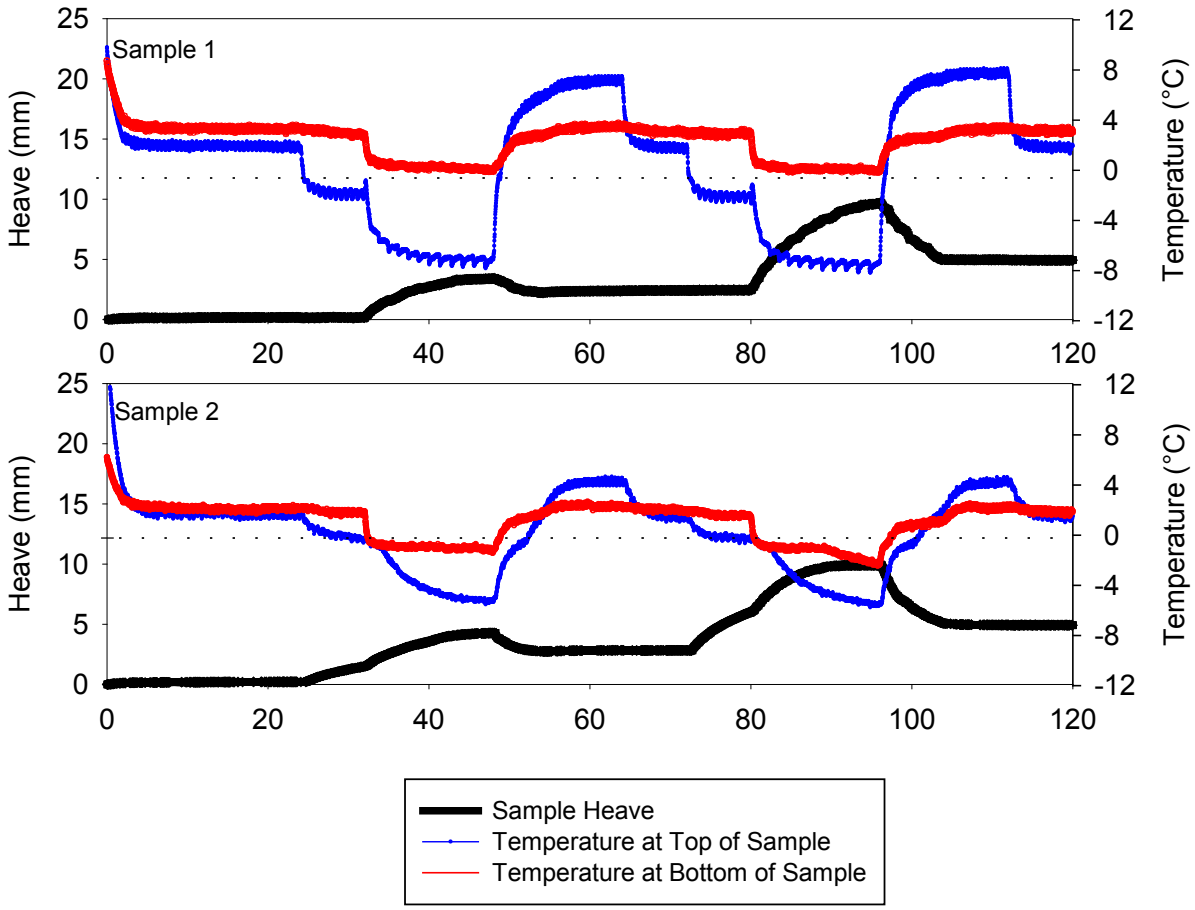

Figure 69. 5% Muscatine FA stabilized subgrade frost heave time plots

For 5% Muscatine FA stabilized subgrade the moisture content profiles show the moisture contents decreased as the depth increased. Figure 70 shows the moisture content profiles of the post-test samples.

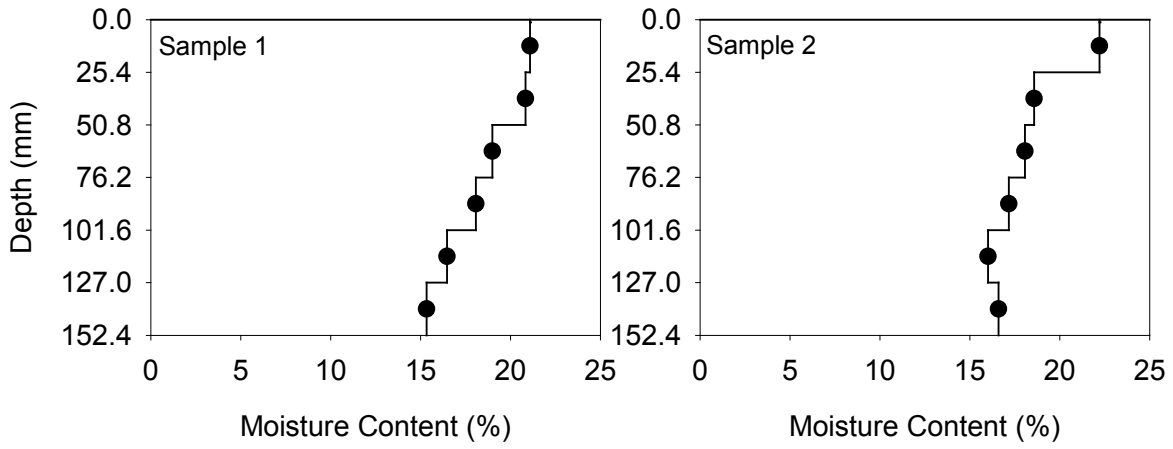

Figure 70. 5% Muscatine FA stabilized subgrade moisture content profiles

For 5% Muscatine FA stabilized subgrade, the CBR value after freeze-thaw test was less than the one without freeze-thaw test. The frost susceptibility of this material was classified as high level. Table 25 summarizes the frost-heave and thaw-weakening test results on 5% Muscatine FA stabilized subgrade material.

Table 25. 5% Muscatine FA stabilized subgrade frost-heave and thaw-weakening test results

1st Frost-heave rate (mm/day)	4.57
2nd Frost-heave rate (mm/day)	9.88
CBR after freeze-thaw test (%)	2.9
CBR before freeze-thaw test (%)	—
Frost susceptibility based on heave	High
Frost susceptibility based on CBR	High

Two subgrade samples stabilized with 10% Muscatine fly ash were tested. The peak heave values of the samples were similar. The governed second heave rate calculated from the slopes was 12.32 mm/day. Figure 71 shows the frost heave time plots of these two samples. The heave rate was less than the non-stabilized subgrade, but larger than the 5% Muscatine FA stabilized subgrade.

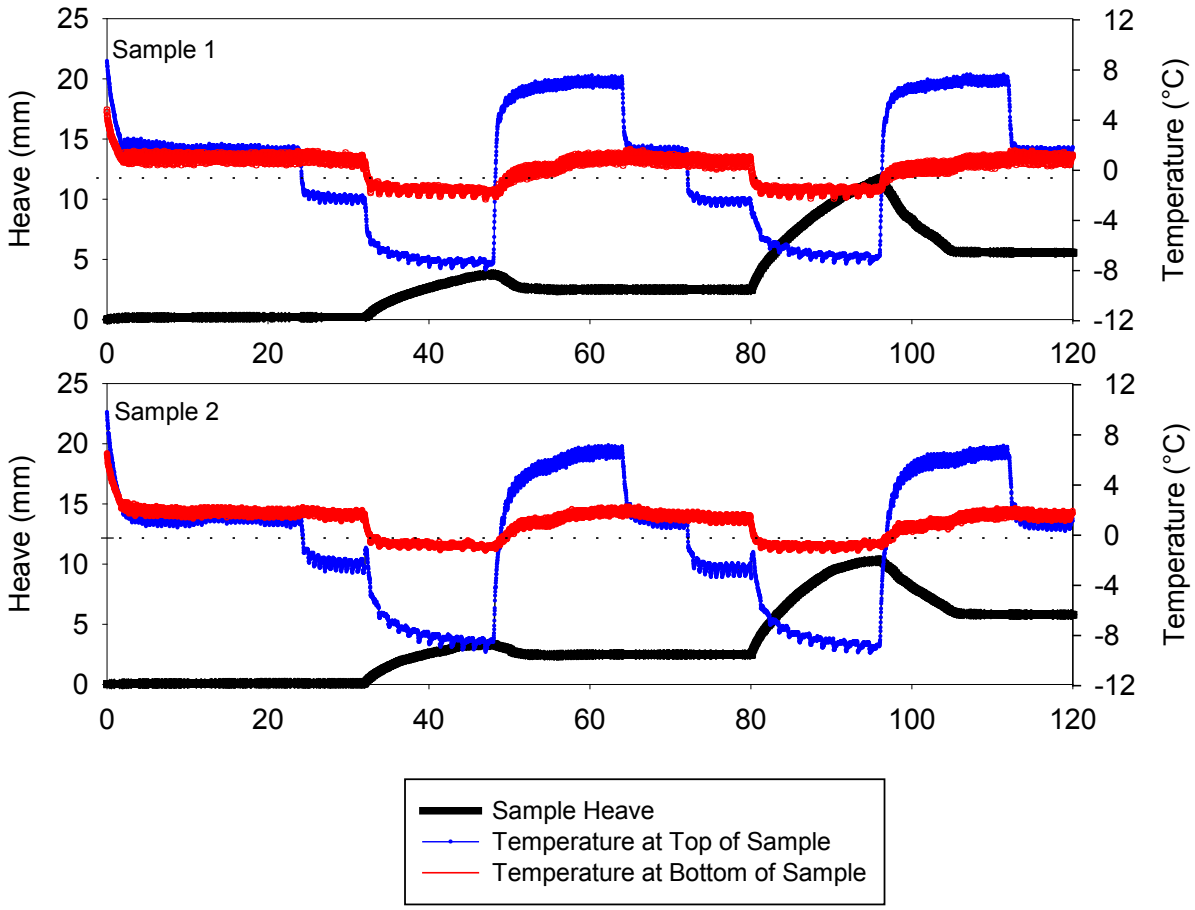

Figure 71. 10% Muscatine FA stabilized subgrade frost heave time plots

For 10% Muscatine FA stabilized subgrade the moisture content profiles show the moisture contents decreased as the depth increased. Figure 72 shows the moisture content profiles of the post-test samples.

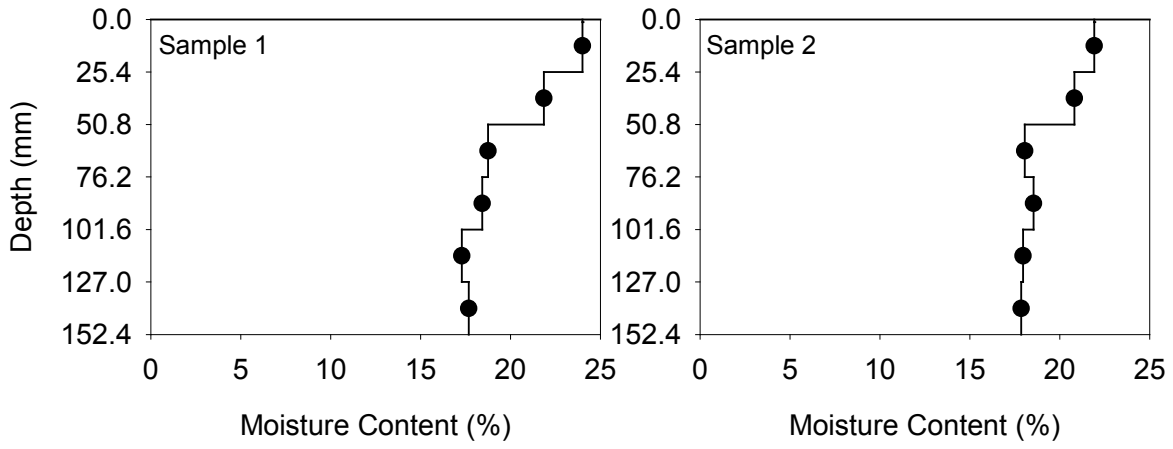

Figure 72. 10% Muscatine FA stabilized subgrade moisture content profiles

For 10% Muscatine FA stabilized subgrade, the CBR value after freeze-thaw test was less than the one without freeze-thaw test. The frost susceptibility of this material was classified as high level. Table 26 summarizes the frost-heave and thaw-weakening test results on 10% Muscatine FA stabilized subgrade material.

Table 26. 10% Muscatine FA stabilized subgrade frost-heave and thaw-weakening test results

1st Frost-heave rate (mm/day)	4.86
2nd Frost-heave rate (mm/day)	12.32
CBR after freeze-thaw test (%)	2.6
CBR before freeze-thaw test (%)	—
Frost susceptibility based on heave	High
Frost susceptibility based on CBR	High

Two subgrade samples stabilized with 5% Port Neal fly ash were tested. The peak heave values of the samples were similar. The governed second heave rate calculated from the slopes was 6.61 mm/day. Figure 73 shows the frost heave time plots of these two samples. The heave rate was less than the non-stabilized subgrade.

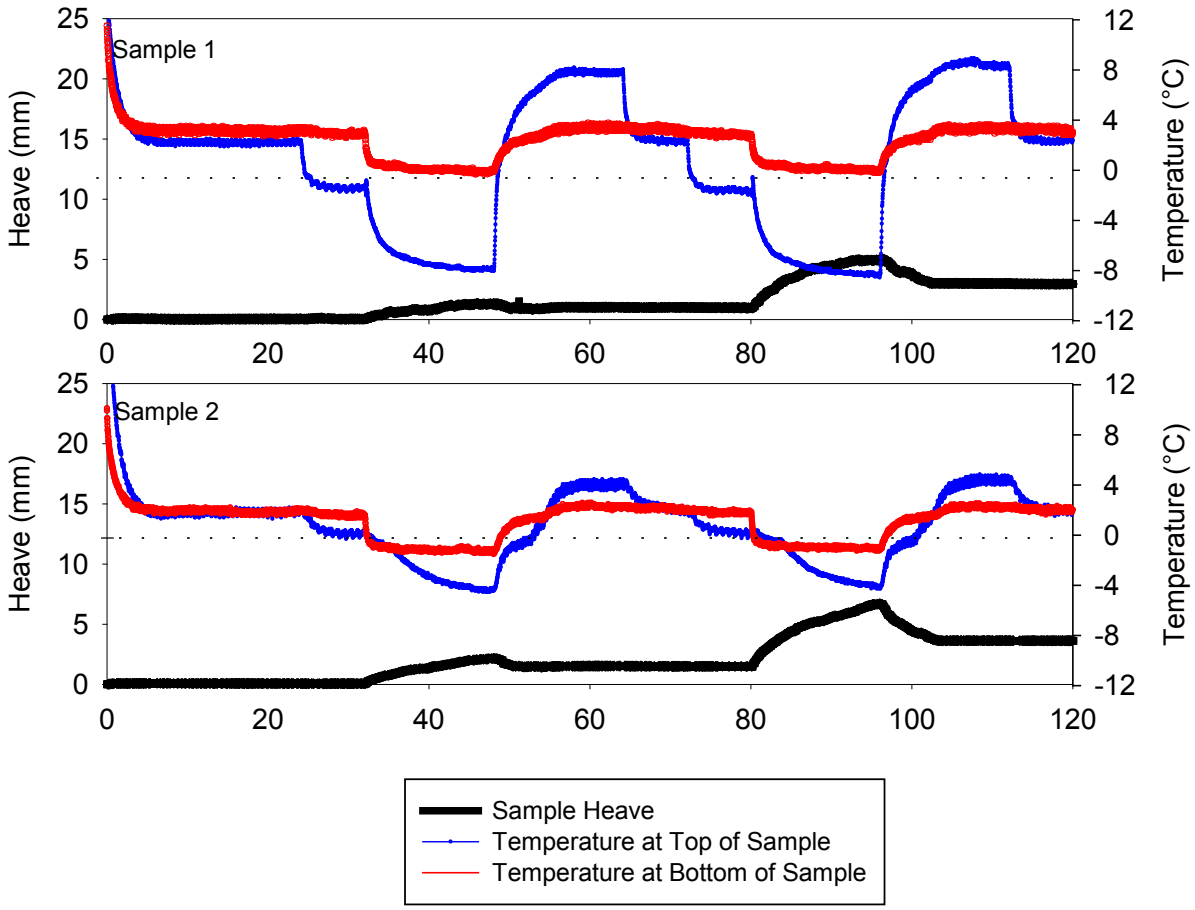

Figure 73. 5% Port Neal FA stabilized subgrade frost heave time plots

For 5% Port Neal FA stabilized subgrade the moisture content profiles show the moisture contents decreased as the depth increased. Figure 74 shows the moisture content profiles of the post-test samples.

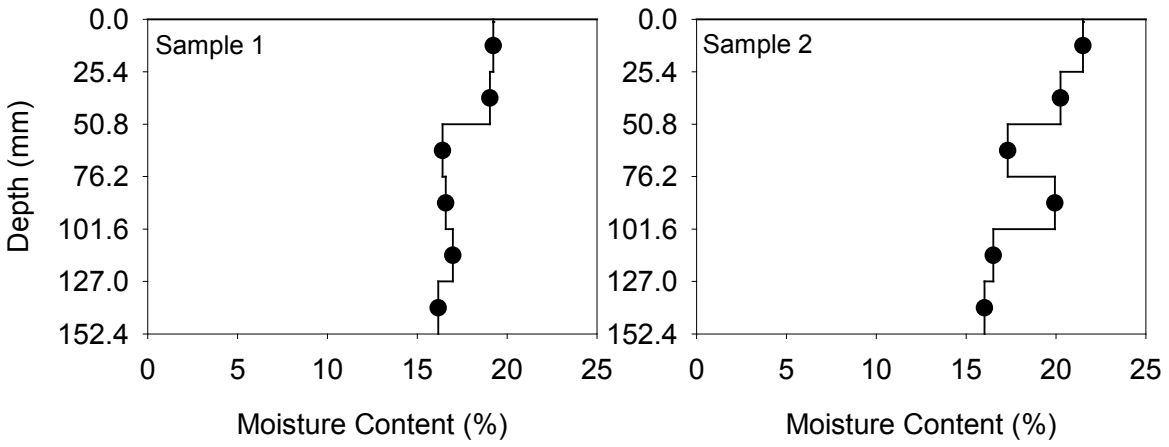

Figure 74. 5% Port Neal FA stabilized subgrade moisture content profiles

For 5% Port Neal FA stabilized subgrade, the CBR value after freeze-thaw test was less than the one without freeze-thaw test. The frost susceptibility of this material was classified as medium level. Table 27 summarizes the frost-heave and thaw-weakening test results on 5% Port Neal FA stabilized subgrade material.

Table 27. 5% Port Neal FA stabilized subgrade frost-heave and thaw-weakening test results

1st Frost-heave rate (mm/day)	2.50
2nd Frost-heave rate (mm/day)	6.61
CBR after freeze-thaw test (%)	5.7
CBR before freeze-thaw test (%)	—
Frost susceptibility based on heave	Medium
Frost susceptibility based on CBR	Medium

Two subgrade samples stabilized with 10% Port Neal fly ash were tested. The peak heave values of the samples were similar. The governed second heave rate calculated from the slopes was 8.21 mm/day. Figure 75 shows the frost heave time plots of these two samples. The heave rate was less than the non-stabilized subgrade, but larger than the 5% Port Neal FA stabilized subgrade.

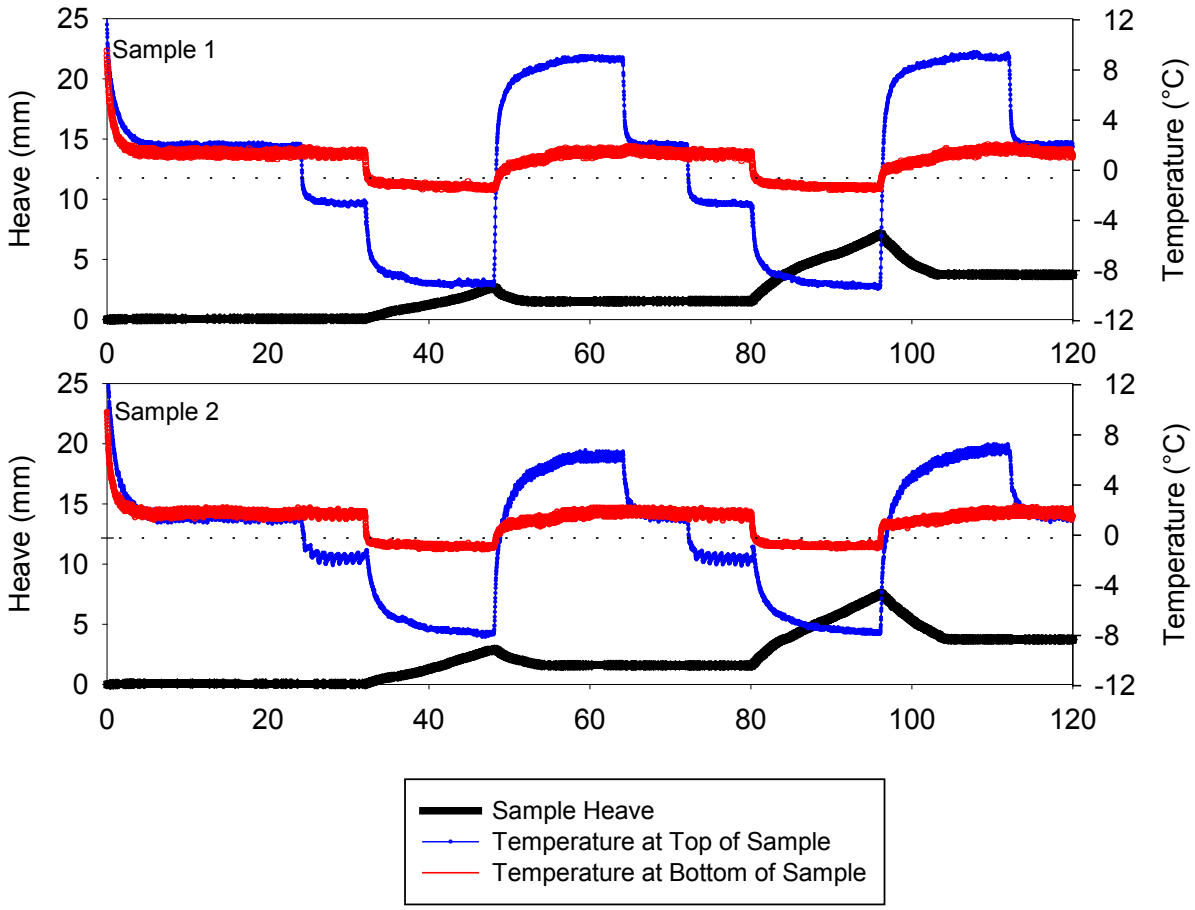

Figure 75. 10% Port Neal FA stabilized subgrade frost heave time plots

For 10% Port Neal FA stabilized subgrade the moisture content profiles show the moisture contents decreased as the depth increased. Figure 76 shows the moisture content profiles of the post-test samples.

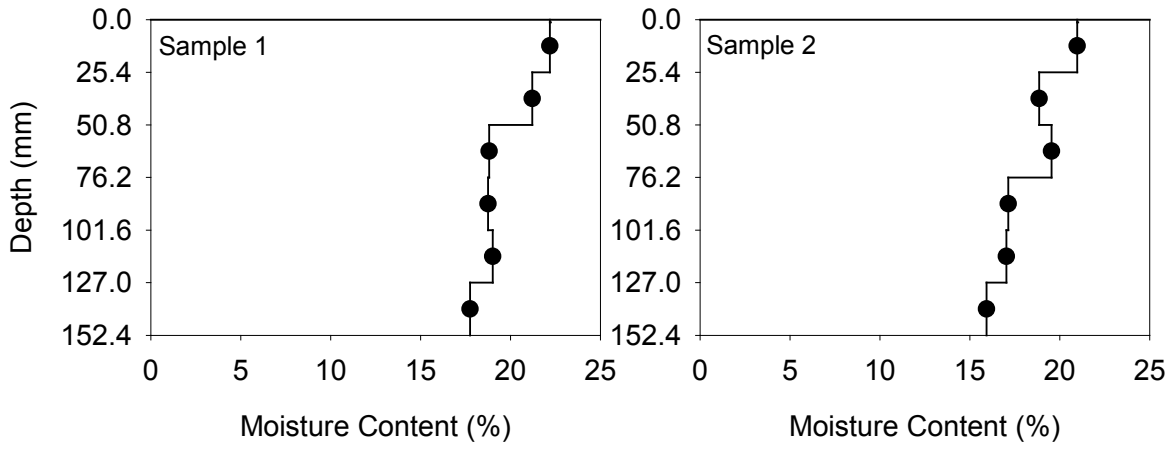

Figure 76. 10% Port Neal FA stabilized subgrade moisture content profiles

For 10% Port Neal FA stabilized subgrade, the CBR value after freeze-thaw test was less than the one without freeze-thaw test. The frost susceptibility of this material was classified as Low to high level. Table 28 summarizes the frost-heave and thaw-weakening test results on 10% Port Neal FA stabilized subgrade material.

Table 28. 10% Port Neal FA stabilized subgrade frost-heave and thaw-weakening test results

1st Frost-heave rate (mm/day)	4.04
2nd Frost-heave rate (mm/day)	8.21
CBR after freeze-thaw test (%)	11.2
CBR before freeze-thaw test (%)	15.0
Frost susceptibility based on heave	High
Frost susceptibility based on CBR	Low

Two subgrade samples stabilized with 15% Port Neal fly ash were tested. The peak heave values of the samples were similar. The governed second heave rate calculated from the slopes was 1.96 mm/day. Figure 77 shows the frost heave time plots of these two samples. The heave rate was less than the non-stabilized, 5%, and 10% Port Neal FA stabilized subgrade.

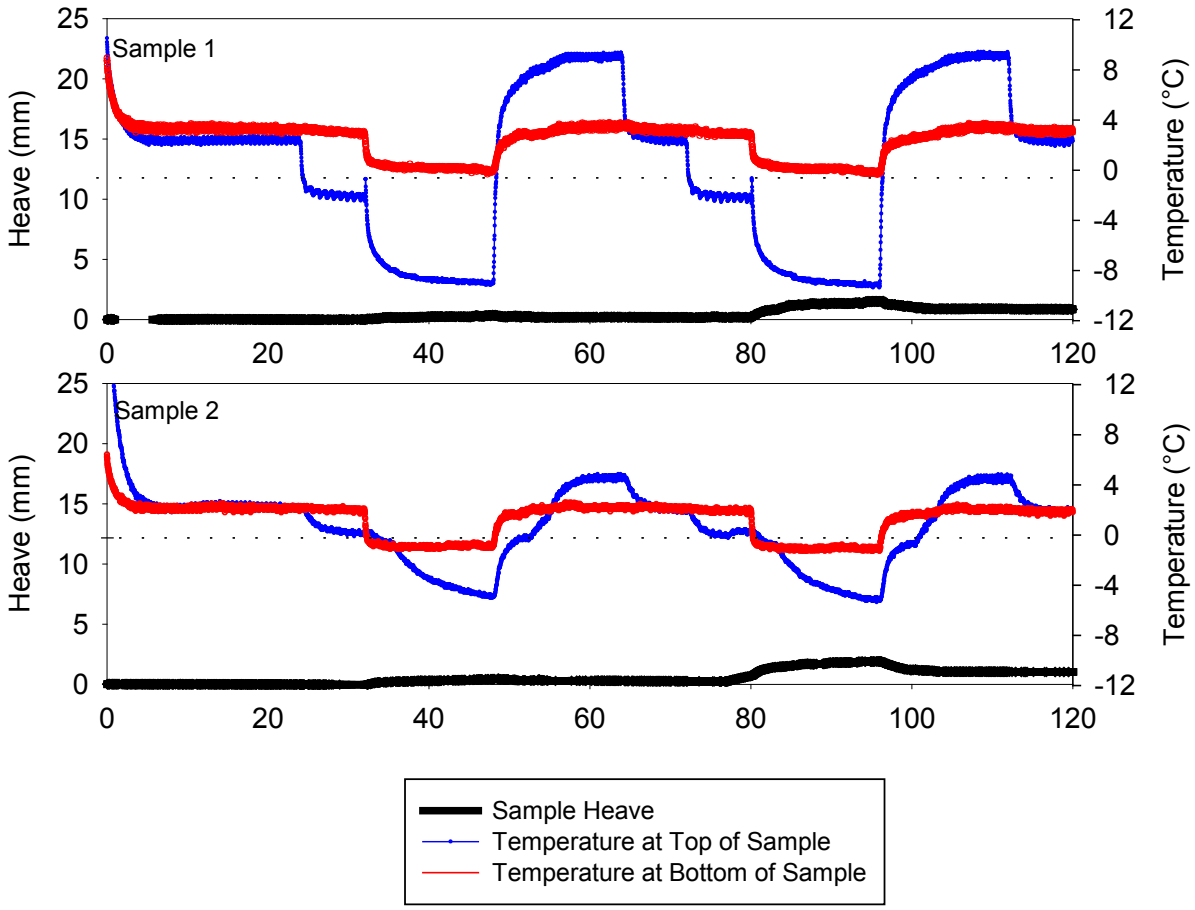

Figure 77. 15% Port Neal FA stabilized subgrade frost heave time plots

For 15% Port Neal FA stabilized subgrade the moisture content profiles show the moisture contents decreased as the depth increased. Figure 78 shows the moisture content profiles of the post-test samples.

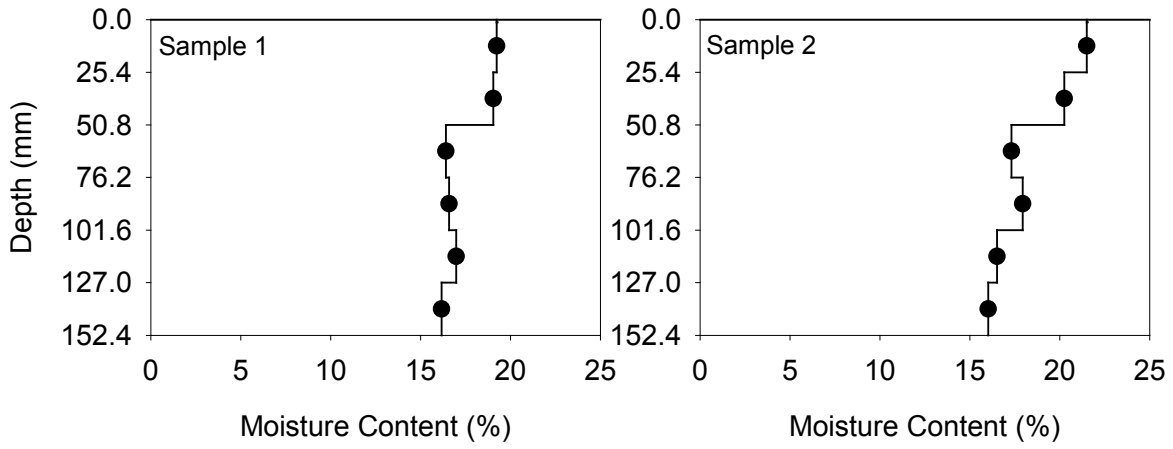

Figure 78. 15% Port Neal FA stabilized subgrade moisture content profiles

For 15% Port Neal FA stabilized subgrade, the CBR value after freeze-thaw test was less than the one without freeze-thaw test. The frost susceptibility of this material was classified as very low level. Table 29 summarizes the frost-heave and thaw-weakening test results on 15% Port Neal FA stabilized subgrade material.

Table 29. 15% Port Neal FA stabilized subgrade frost-heave and thaw-weakening test results

1st Frost-heave rate (mm/day)	0.56
2nd Frost-heave rate (mm/day)	1.96
CBR after freeze-thaw test (%)	16.9
CBR before freeze-thaw test (%)	25.8
Frost susceptibility based on heave	Very low
Frost susceptibility based on CBR	Very low

Two subgrade samples stabilized with 20% Port Neal fly ash were tested. The peak heave values of the samples were similar. The governed second heave rate calculated from the slopes was 3.16 mm/day. Figure 79 shows the frost heave time plots of these two samples. The heave rate was less than the non-stabilized, 5%, and 10% stabilized subgrade, but larger than the 15% Port Neal FA stabilized subgrade.

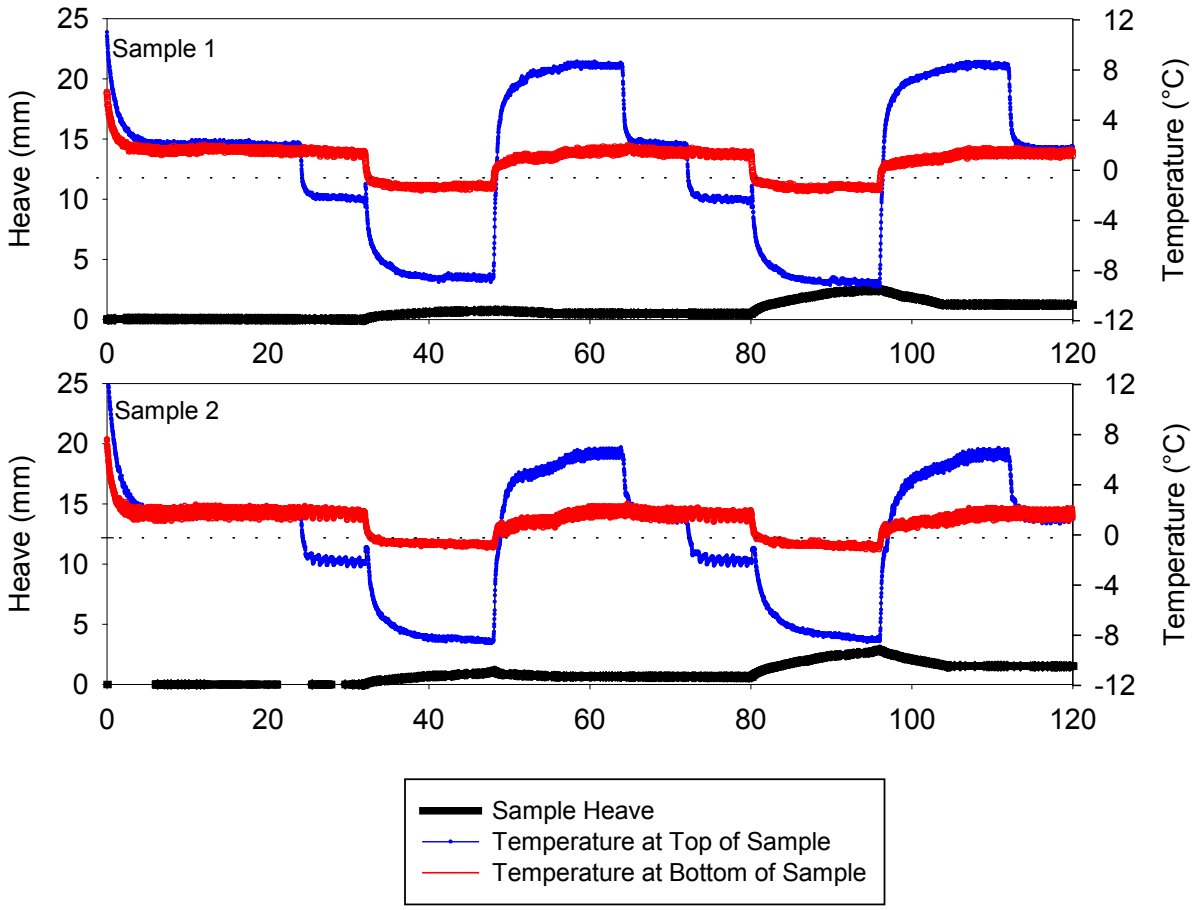

Figure 79. 20% Port Neal FA stabilized subgrade frost heave time plots

For 20% Port Neal FA stabilized subgrade the moisture content profiles show the moisture contents decreased as the depth increased. Figure 80 shows the moisture content profiles of the post-test samples.

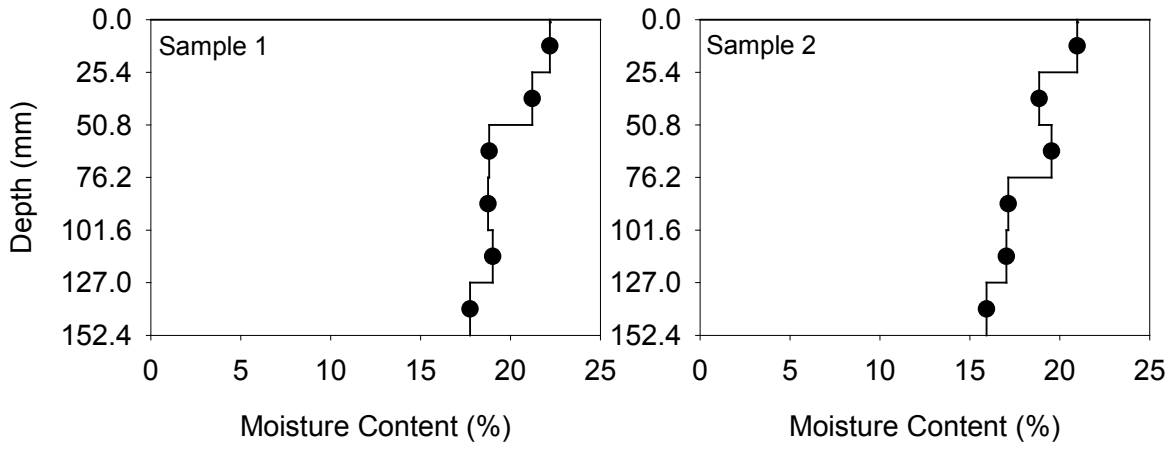

Figure 80. 20% Port Neal FA stabilized subgrade moisture content profiles

For 20% Port Neal FA stabilized subgrade, the CBR value after freeze-thaw test was less than the one without freeze-thaw test. The frost susceptibility of this material was classified as low to very low level. Table 30 summarizes the frost-heave and thaw-weakening test results on 20% Port Neal FA stabilized subgrade material.

Table 30. 20% Port Neal FA stabilized subgrade frost-heave and thaw-weakening test results

1st Frost-heave rate (mm/day)	1.24
2nd Frost-heave rate (mm/day)	3.16
CBR after freeze-thaw test (%)	17.9
CBR before freeze-thaw test (%)	—
Frost susceptibility based on heave	Low
Frost susceptibility based on CBR	Very low

Subgrade stabilized with cement

One subgrade sample stabilized with 5% cement was tested. The peak heave value of the sample was 0.25 mm. The governed second heave rate calculated from the slopes was too small to measure. Figure 81 shows the frost heave time plots of the sample. The heave rate was less than the non-stabilized subgrade.

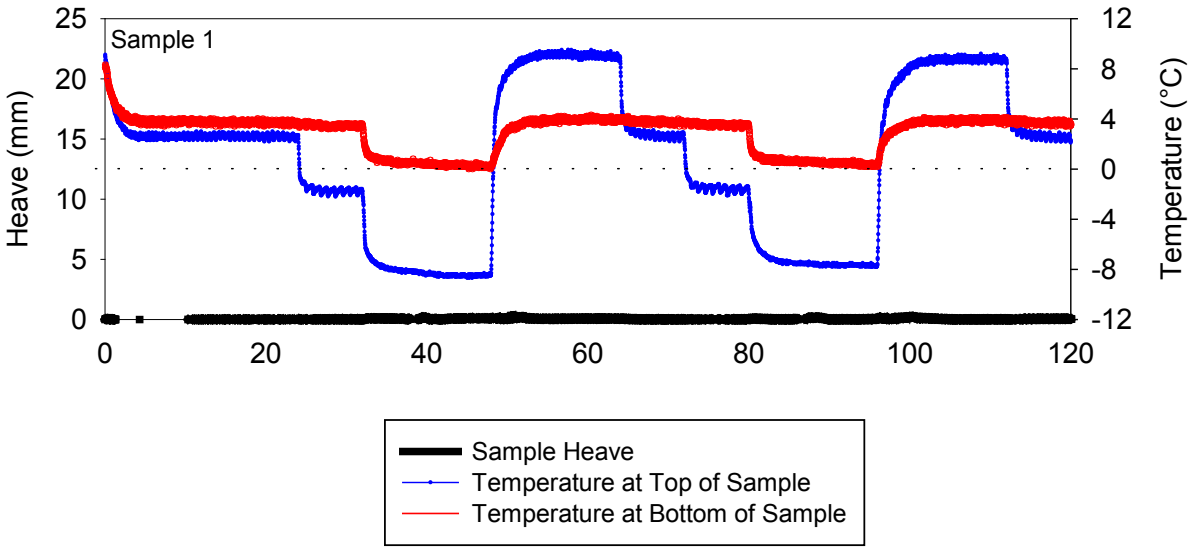

Figure 81. 5% cement stabilized subgrade frost heave time plots

For 5% cement stabilized subgrade the moisture content profiles show that there was not obvious change of moisture contents from top to bottom layer. Figure 82 shows the moisture content profiles of the post-test sample.

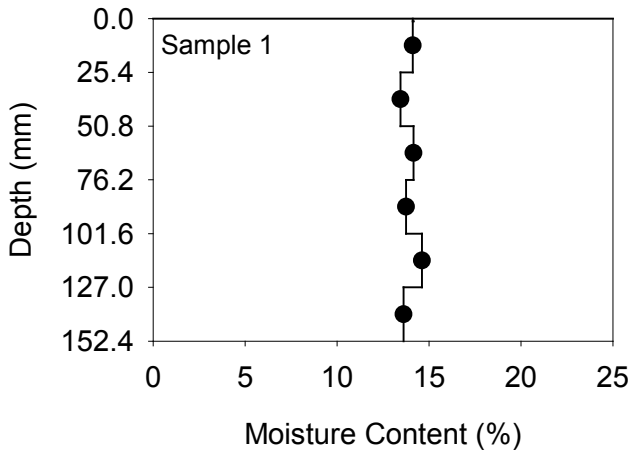

Figure 82. 5% cement stabilized subgrade moisture content profiles

For 5% cement stabilized subgrade, the CBR value after freeze-thaw test was larger than the one without freeze-thaw test. The frost susceptibility of this material was classified as

negligible level. Table 31 summarizes the frost-heave and thaw-weakening test results on 5% cement stabilized subgrade material.

Table 31. 5% cement stabilized subgrade frost-heave and thaw-weakening test results

1st Frost-heave rate (mm/day)	<1.00
2nd Frost-heave rate (mm/day)	<1.00
CBR after freeze-thaw test (%)	165.8
CBR before freeze-thaw test (%)	37.3
Frost susceptibility based on heave	Negligible
Frost susceptibility based on CBR	Negligible

One subgrade sample stabilized with 10% cement was tested. The peak heave value of the sample was 0.36 mm. The governed second heave rate calculated from the slopes was also too small to measure. Figure 83 shows the frost heave time plots of the sample. The heave rate was less than the non-stabilized and 5% cement stabilized subgrade.

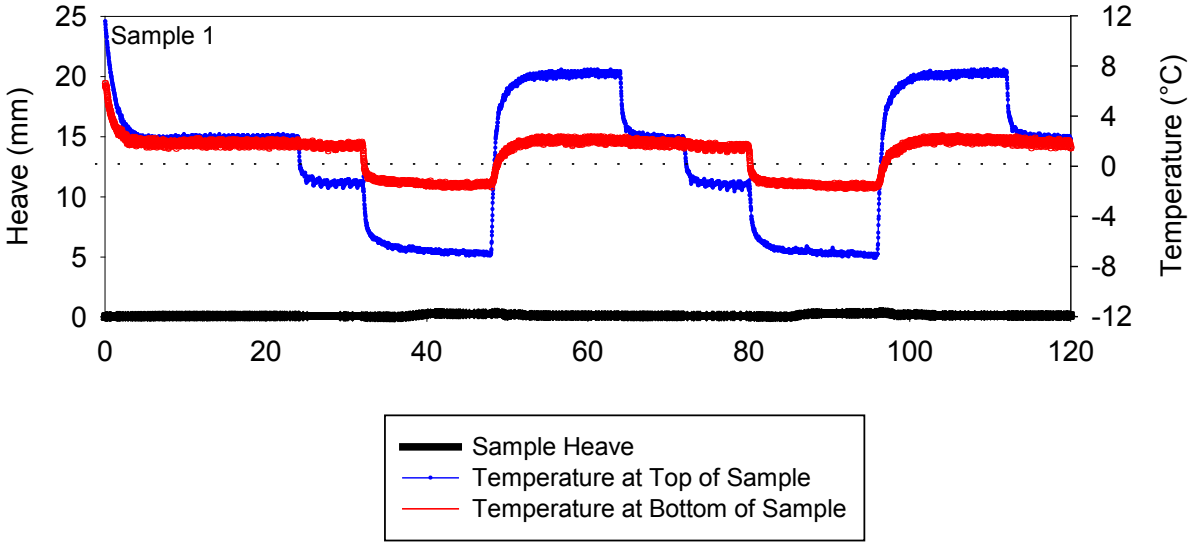

Figure 83. 10% cement stabilized subgrade frost heave time plots

For 10% cement stabilized subgrade, the CBR value after freeze-thaw test was larger than the one without freeze-thaw test. The frost susceptibility of this material was classified as negligible level. Table 32 summarizes the frost-heave and thaw-weakening test results on the 10% cement stabilized subgrade material.

Table 32. 10% cement stabilized subgrade frost-heave and thaw-weakening test results

1st Frost-heave rate (mm/day)	<1.00
2nd Frost-heave rate (mm/day)	<1.00
CBR after freeze-thaw test (%)	Too high
CBR before freeze-thaw test (%)	94.5
Frost susceptibility based on heave	Negligible
Frost susceptibility based on CBR	Negligible

Recycled subbase stabilized with cement

Two recycled subbase samples stabilized with 2.5% cement were tested. The peak heave values of the samples were similar. The governed second heave rate calculated from the slopes was 12.70 mm/day. Figure 84 shows the frost heave time plots of these two samples. The heave rate was less than the non-stabilized recycled subbase.

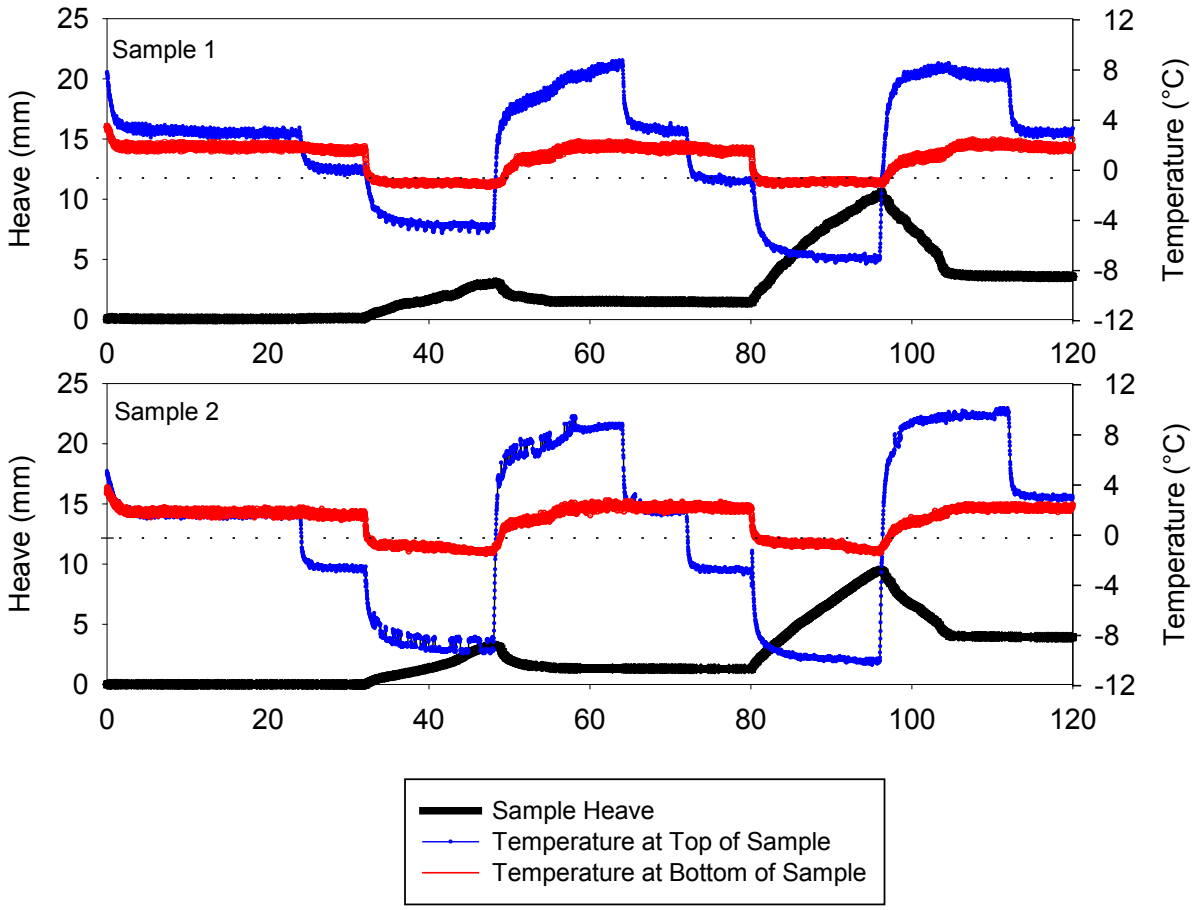

Figure 84. 2.5% cement stabilized subbase frost heave time plots

For 2.5% cement stabilized recycled subbase the moisture content profiles show the moisture contents decreased as the depth increased. Figure 85 shows the moisture content profiles of the post-test samples.

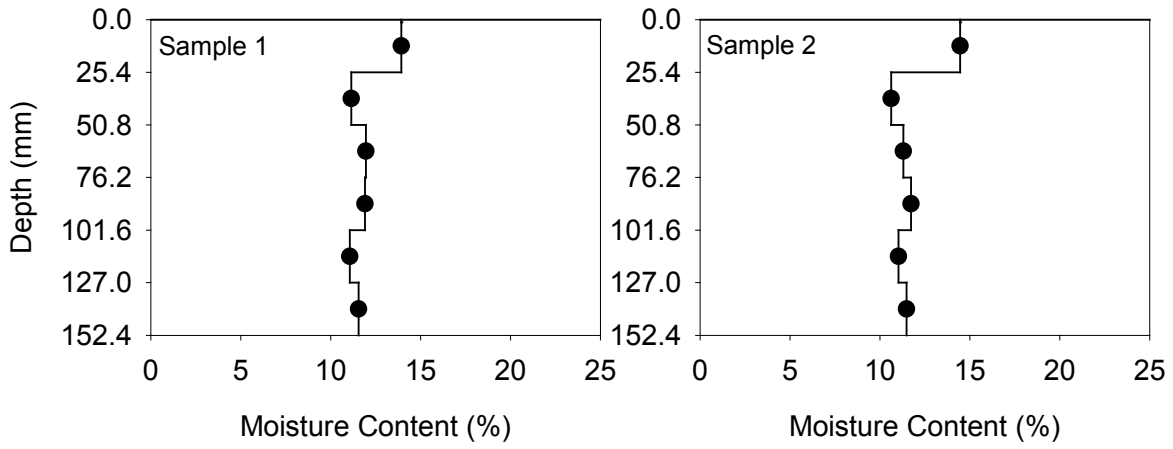

Figure 85. 2.5% cement stabilized subbase moisture content profiles

For 2.5% cement stabilized recycled subbase, the CBR value after freeze-thaw test was less than the one without freeze-thaw test. The frost susceptibility of this material was classified as low to high level. Table 33 summarizes the frost-heave and thaw-weakening test results on 2.5% cement stabilized recycled subbase material.

Table 33. 2.5% cement stabilized subbase frost-heave and thaw-weakening test results

1st Frost-heave rate (mm/day)	4.52
2nd Frost-heave rate (mm/day)	12.70
CBR after freeze-thaw test (%)	12.8
CBR before freeze-thaw test (%)	95.6
Frost susceptibility based on heave	High
Frost susceptibility based on CBR	Low

Two recycled subbase samples stabilized with 3.75% cement were tested. The peak heave values of the samples were similar. The governed second heave rate calculated from the slopes was 2.09 mm/day. Figure 86 shows the frost heave time plots of these two samples. The heave rate was less than the non-stabilized and 2.5% cement stabilized recycled subbase.

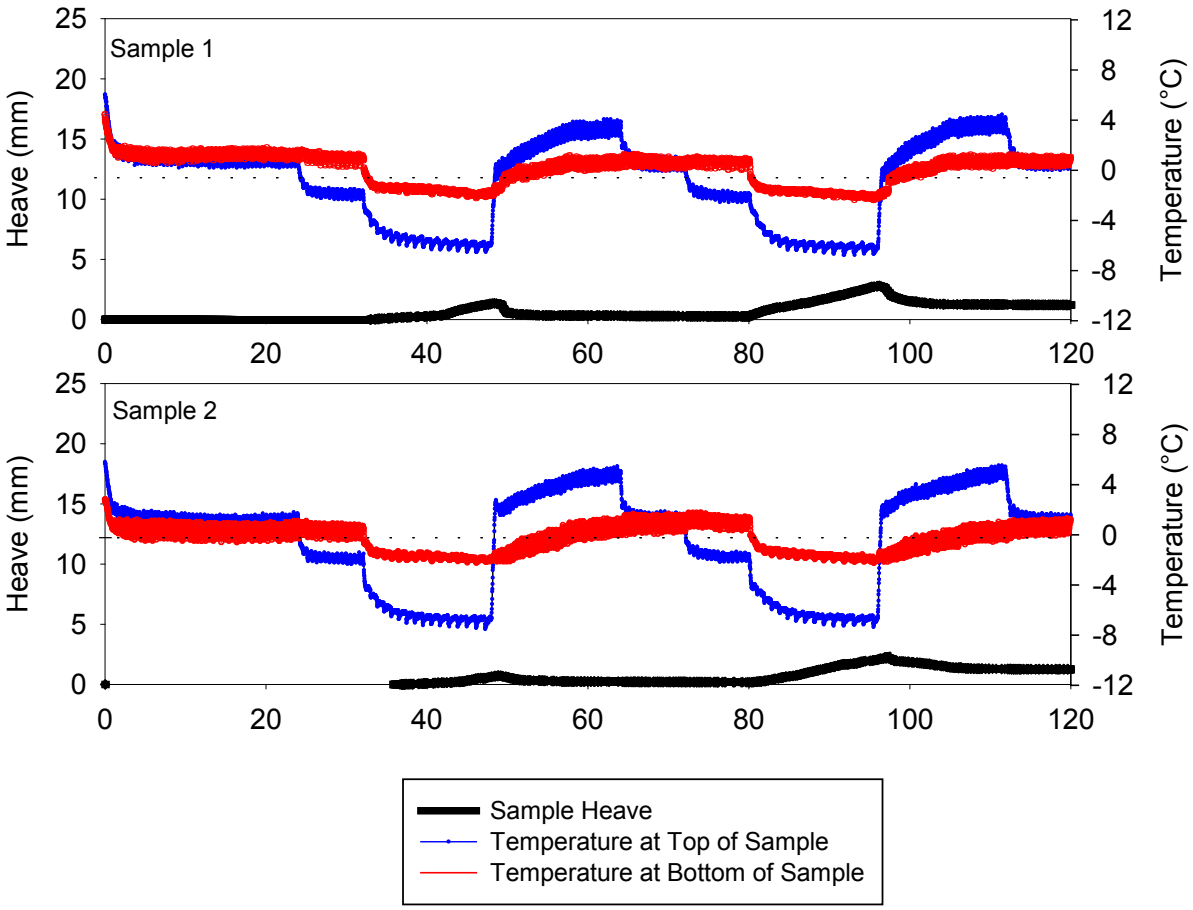

Figure 86. 3.75% cement stabilized subbase frost heave time plots

For 3.75% cement stabilized recycled subbase the moisture content profiles show the moisture contents changed slightly as the depth increased. Figure 87 shows the moisture content profiles of the post-test samples.

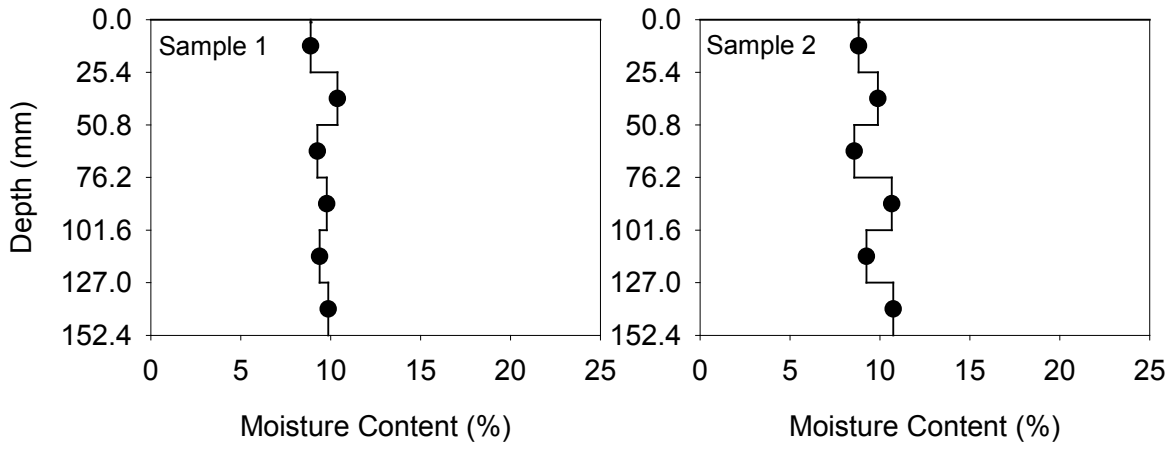

Figure 87. 3.75% cement stabilized subbase moisture content profiles

For 3.75% cement stabilized recycled subbase, the CBR value after freeze-thaw test was less than the one without freeze-thaw test. The frost susceptibility of this material was classified as low to negligible level. Table 34 summarizes the frost-heave and thaw-weakening test results on 3.75% cement stabilized recycled subbase material.

Table 34. 3.75% cement stabilized subbase frost-heave and thaw-weakening test results

1st Frost-heave rate (mm/day)	1.31
2nd Frost-heave rate (mm/day)	2.09
CBR after freeze-thaw test (%)	35.1
CBR before freeze-thaw test (%)	127.0
Frost susceptibility based on heave	Low
Frost susceptibility based on CBR	Negligible

Two recycled subbase samples stabilized with 5% cement were tested. The peak heave values of the samples were similar. The governed second heave rate calculated from the slopes was 3.35 mm/day. Figure 88 shows the frost heave time plots of these two samples. The heave rate was less than the non-stabilized recycled subbase, but larger than the 3.75% cement stabilized recycled subbase.

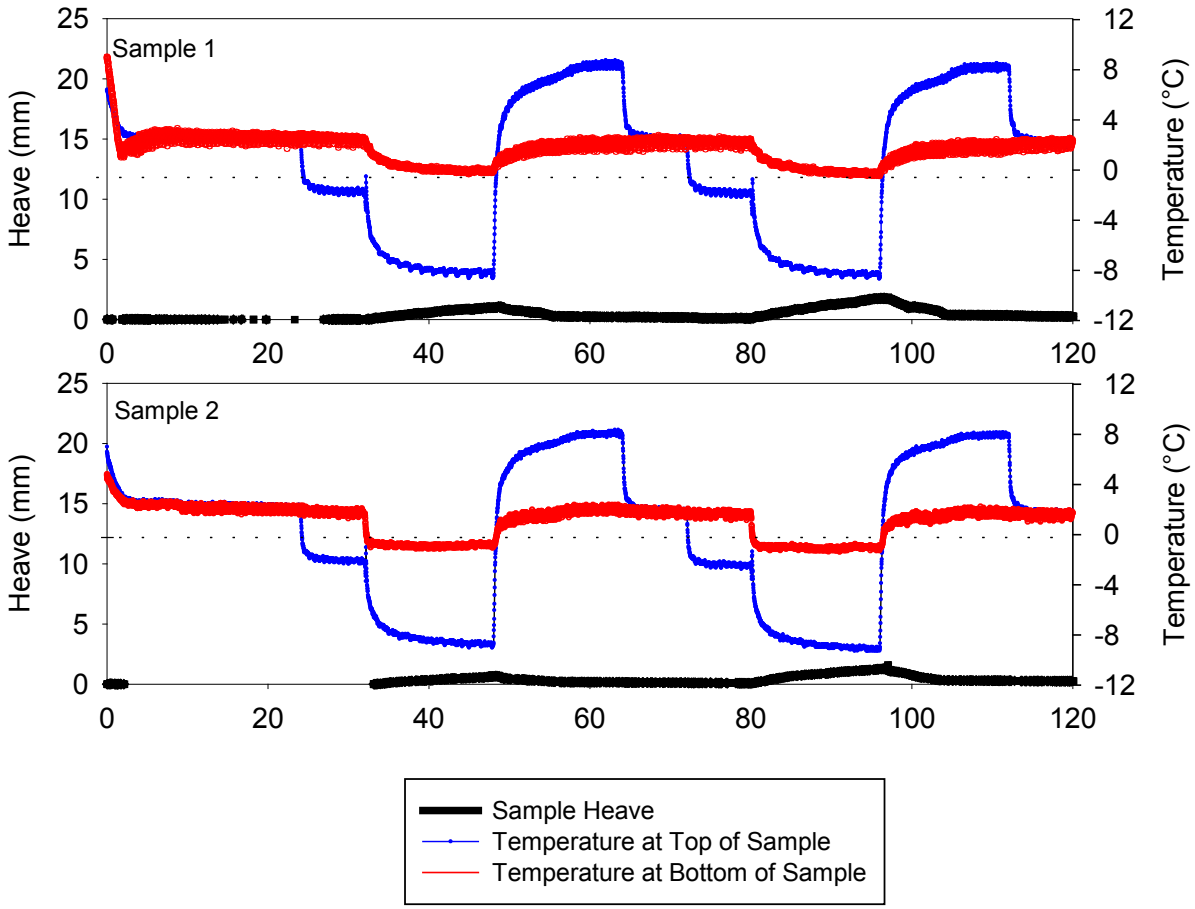

Figure 88. 5% cement stabilized subbase frost heave time plots

For 5% cement stabilized recycled subbase the moisture content profiles show the moisture contents decreased slightly as the depth increased. Figure 89 shows the moisture content profiles of the post-test samples.

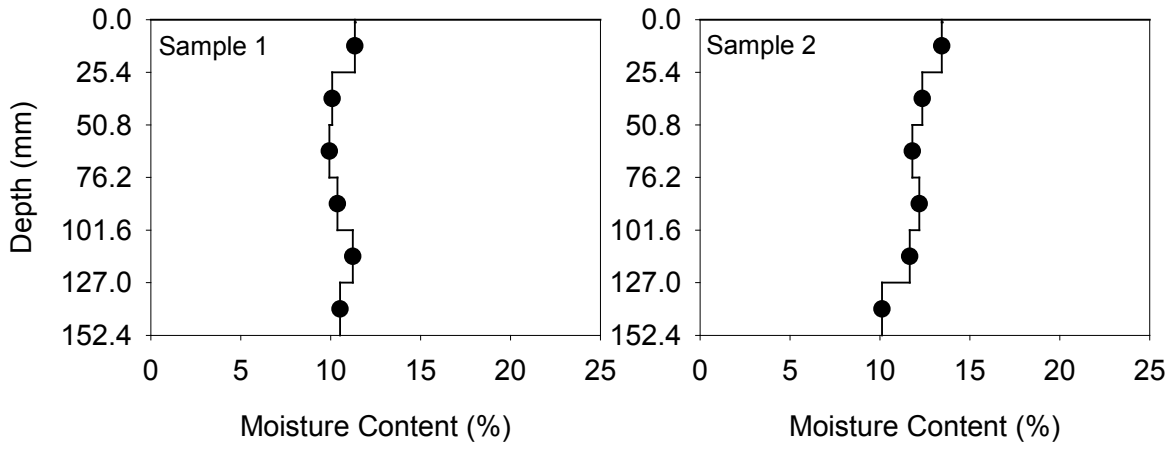

Figure 89. 5% cement stabilized subbase moisture content profiles

For 5% cement stabilized recycled subbase, the CBR value after freeze-thaw test was less than the one without freeze-thaw test. The frost susceptibility of this material was classified as low to negligible level. Table 35 summarizes the frost-heave and thaw-weakening test results on 5% cement stabilized recycled subbase material.

Table 35. 5% cement stabilized subbase frost-heave and thaw-weakening test results

1st Frost-heave rate (mm/day)	1.66
2nd Frost-heave rate (mm/day)	3.35
CBR after freeze-thaw test (%)	56.7
CBR before freeze-thaw test (%)	208.9
Frost susceptibility based on heave	Low
Frost susceptibility based on CBR	Negligible

Two recycled subbase samples stabilized with 7.5% cement were tested. The peak heave values of the samples were similar. The governed second heave rate calculated from the slopes was 1.64 mm/day. Figure 90 shows the frost heave time plots of these two samples. The heave rate was less than the non-stabilized, 2.5%, 3.75%, 5% cement stabilized recycled subbase.

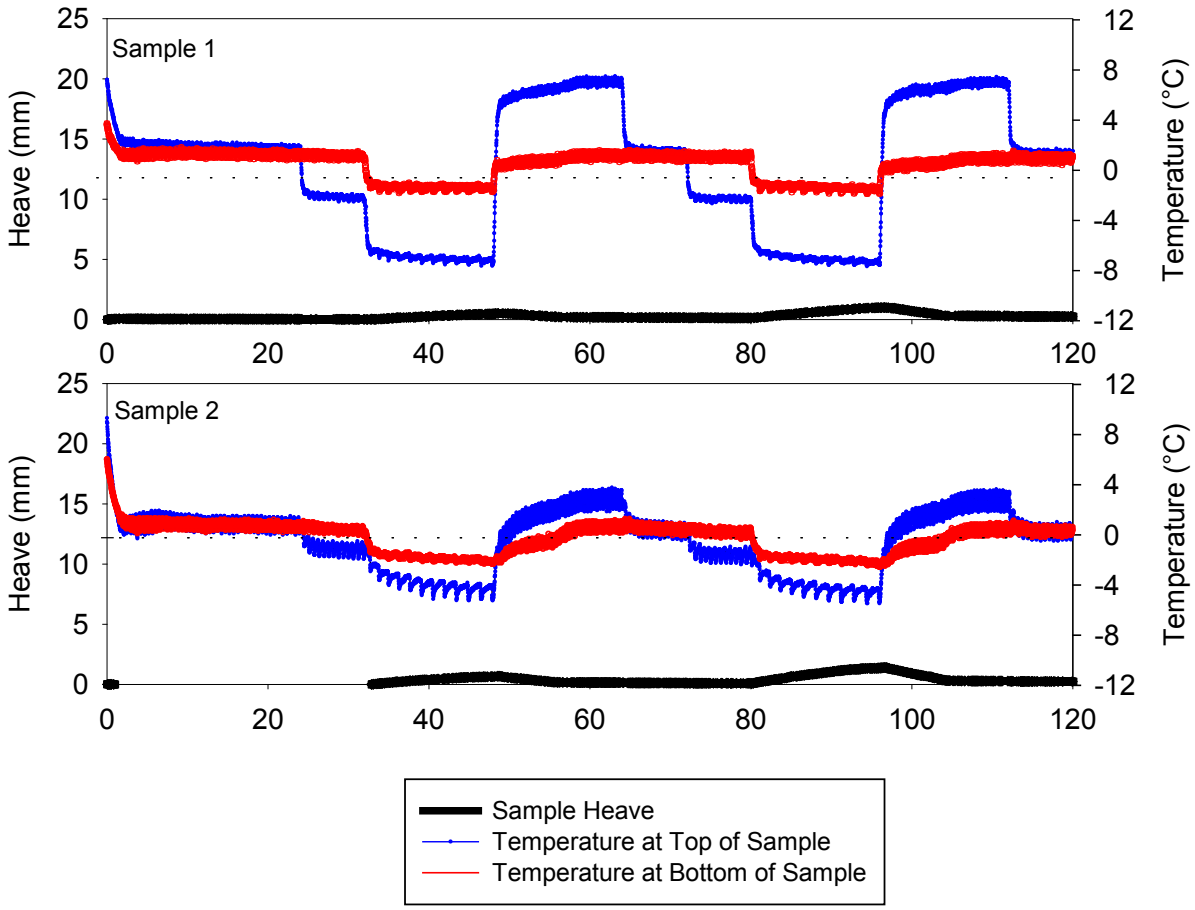

Figure 90. 7.5% cement stabilized subbase frost heave time plots

For 7.5% cement stabilized recycled subbase the moisture content profiles show the moisture contents changed slightly as the depth increased. Figure 91 shows the moisture content profiles of the post-test samples.

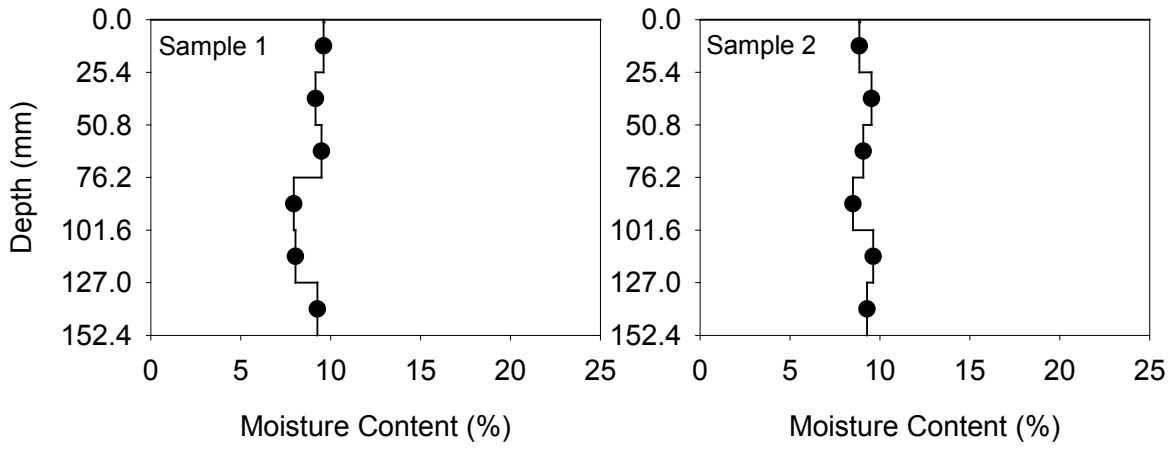

Figure 91. 7.5% cement stabilized subbase moisture content profiles

For 7.5% cement stabilized recycled subbase, the CBR value after freeze-thaw test was less than the one without freeze-thaw test. The frost susceptibility of this material was classified as very low to negligible level. Table 36 summarizes the frost-heave and thaw-weakening test results on 7.5% cement stabilized recycled subbase material.

Table 36. 7.5% cement stabilized subbase frost-heave and thaw-weakening test results

1st Frost-heave rate (mm/day)	0.91
2nd Frost-heave rate (mm/day)	1.64
CBR after freeze-thaw test (%)	43.4
CBR before freeze-thaw test (%)	Too high
Frost susceptibility based on heave	Very low
Frost susceptibility based on CBR	Negligible

Recycled subbase stabilized with fiber

Two recycled subbase samples stabilized with 0.2% polypropylene (PP) fiber were tested. The peak heave values of the samples were similar. The governed second heave rate calculated from the slopes was 12.11 mm/day. Figure 92 shows the frost heave time plots of these two samples. The heave rate was less than the non-stabilized recycled subbase.

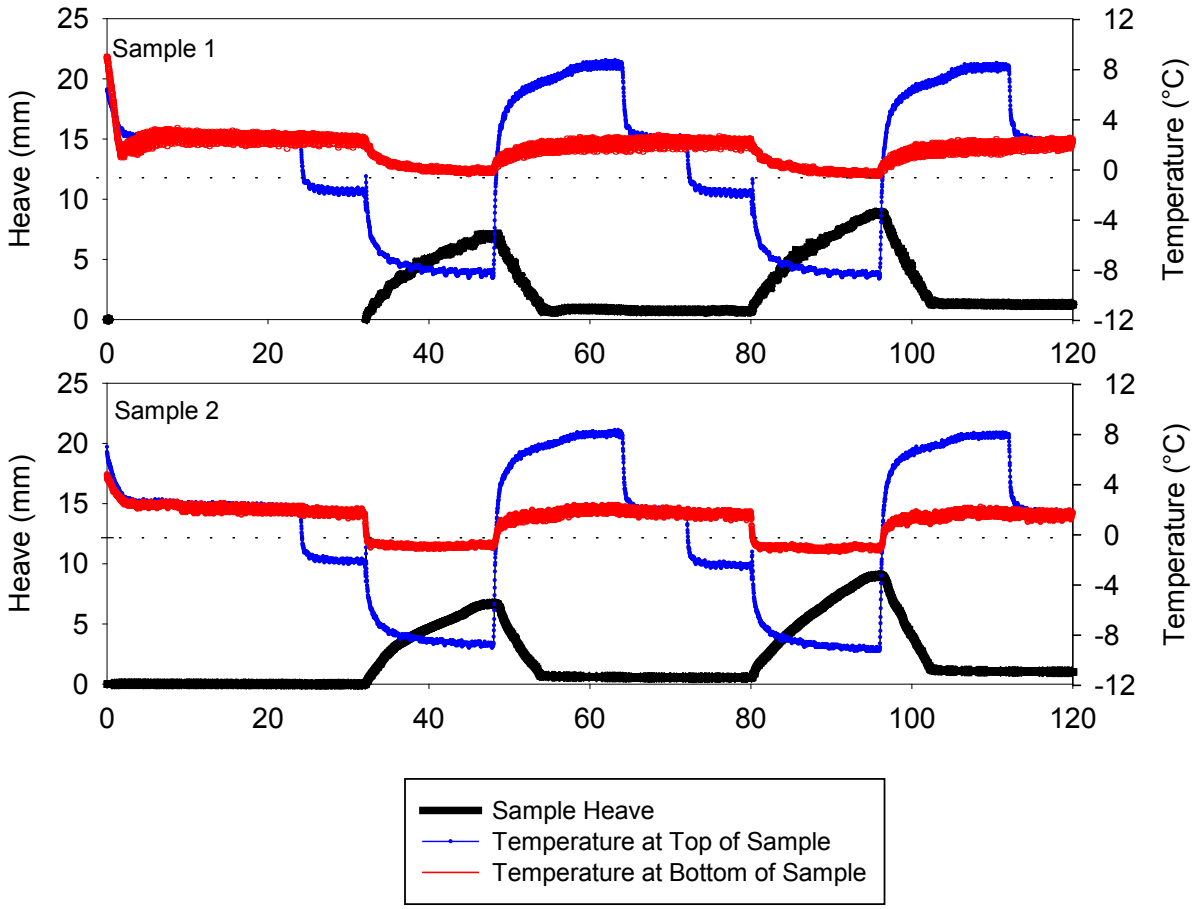

Figure 92. 0.2% PP fiber stabilized subbase frost heave time plots

For 0.2% PP fiber stabilized recycled subbase the moisture content profiles show the moisture contents decreased as the depth increased. Figure 93 shows the moisture content profiles of the post-test samples.

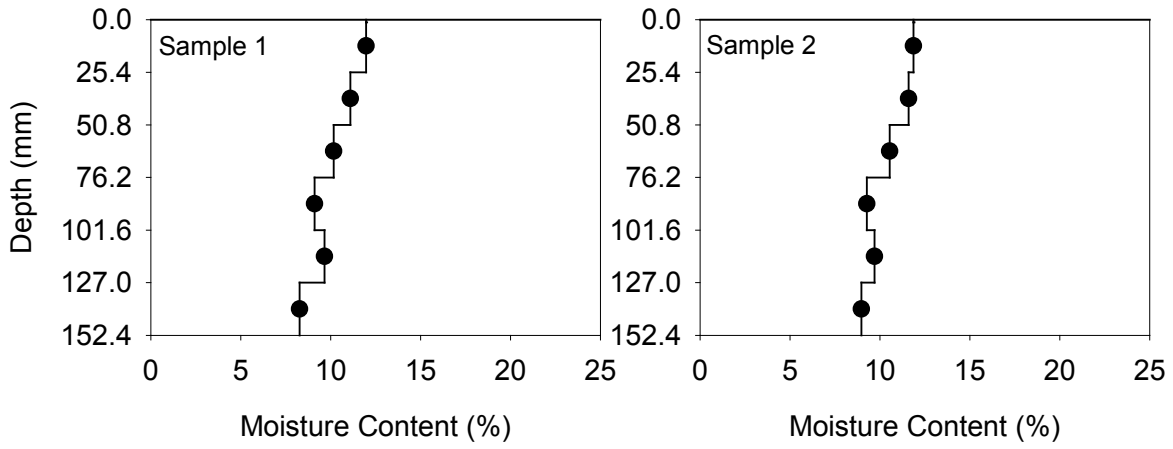

Figure 93. 0.2% PP fiber stabilized subbase moisture content profiles

For 0.2% PP fiber stabilized recycled subbase, the CBR value after freeze-thaw test was larger than the one without freeze-thaw test. The frost susceptibility of this material was classified as low to high level. Table 37 summarizes the frost-heave and thaw-weakening test results on 0.2% PP fiber stabilized recycled subbase material.

Table 37. 0.2% PP fiber stabilized subbase frost-heave and thaw-weakening test results

1st Frost-heave rate (mm/day)	10.35
2nd Frost-heave rate (mm/day)	12.11
CBR after freeze-thaw test (%)	11.4
CBR before freeze-thaw test (%)	4.6
Frost susceptibility based on heave	High
Frost susceptibility based on CBR	Low

Two recycled subbase samples stabilized with 0.4% PP fiber were tested. The peak heave values of the samples were similar. The governed second heave rate calculated from the slopes was 12.75 mm/day. Figure 94 shows the frost heave time plots of these two samples. The heave rate was less than the non-stabilized recycled subbase, but larger than the 0.2% PP fiber stabilized recycled subbase.

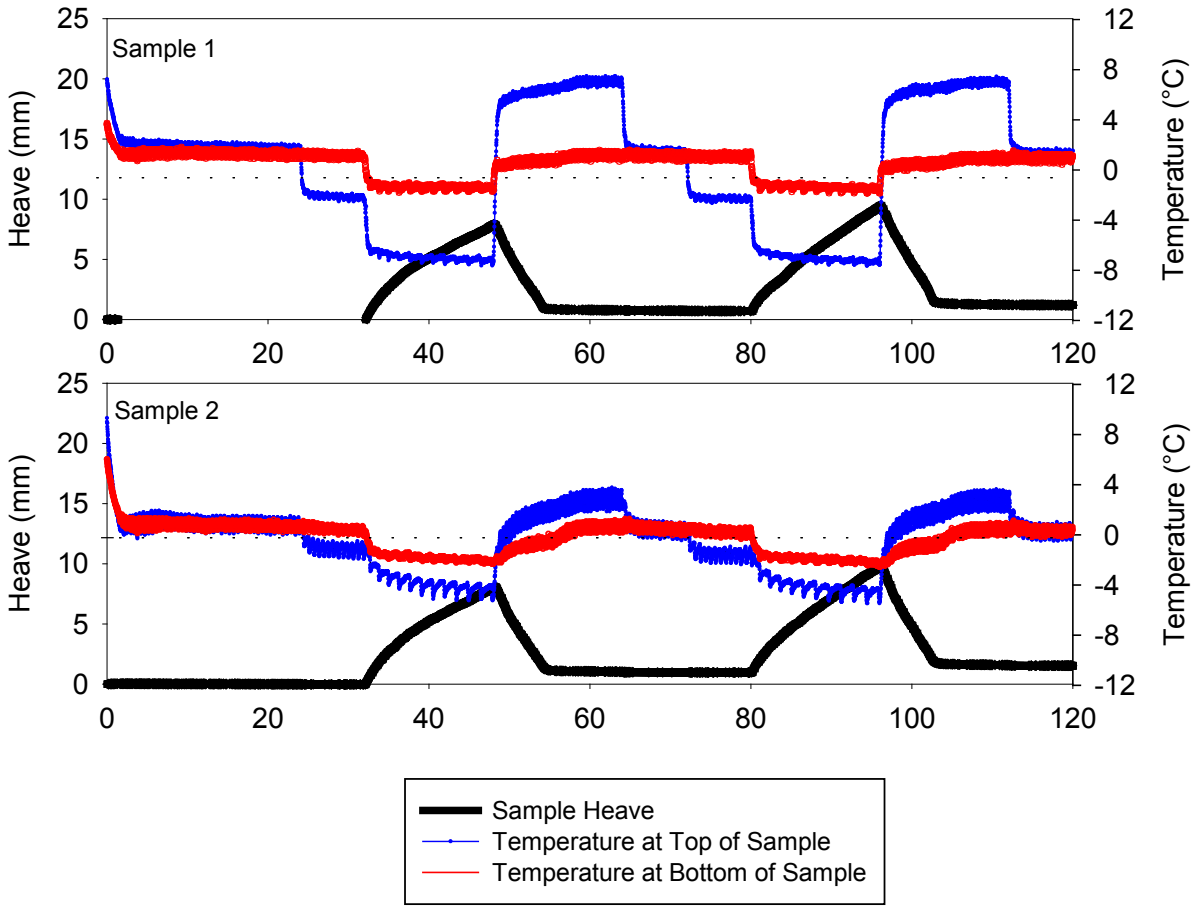

Figure 94. 0.4% PP fiber stabilized subbase frost heave time plots

For 0.4% PP fiber stabilized recycled subbase the moisture content profiles show the moisture contents decreased as the depth increased. Figure 95 shows the moisture content profiles of the post-test samples.

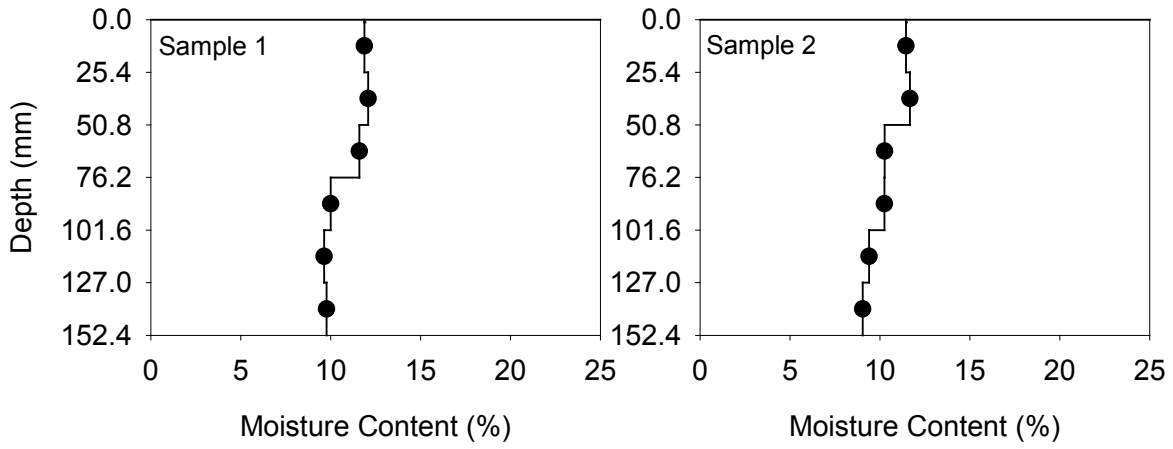

Figure 95. 0.4% PP fiber stabilized subbase moisture content profiles

For 0.4% PP fiber stabilized recycled subbase, the CBR value after freeze-thaw test was larger than the one without freeze-thaw test. The frost susceptibility of this material was classified as medium to high level. Table 38 summarizes the frost-heave and thaw-weakening test results on 0.4% PP fiber stabilized recycled subbase material.

Table 38. 0.4% PP fiber stabilized subbase frost-heave and thaw-weakening test results

1st Frost-heave rate (mm/day)	11.36
2nd Frost-heave rate (mm/day)	12.75
CBR after freeze-thaw test (%)	7.8
CBR before freeze-thaw test (%)	7.3
Frost susceptibility based on heave	High
Frost susceptibility based on CBR	Medium

Two recycled subbase samples stabilized with 0.6% PP fiber were tested. The peak heave values of the samples were similar. The governed first heave rate calculated from the slopes was 6.25 mm/day. Figure 96 shows the frost heave time plots of these two samples. The heave rate was less than the non-stabilized, 0.2%, and 0.4% PP fiber stabilized recycled subbase.

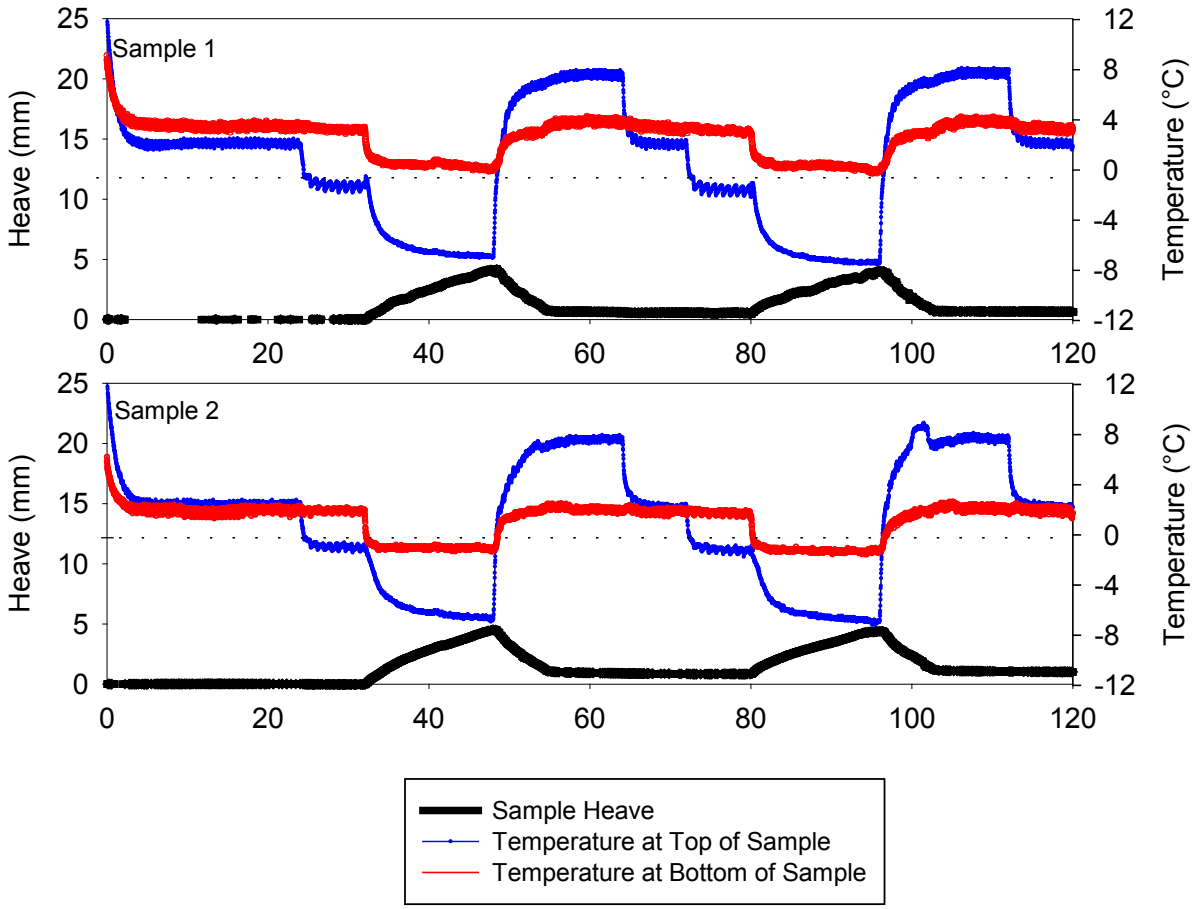

Figure 96. 0.6% PP fiber stabilized subbase frost heave time plots

For 0.6% PP fiber stabilized recycled subbase the moisture content profiles show the moisture contents decreased as the depth increased. Figure 97 shows the moisture content profiles of the post-test samples.

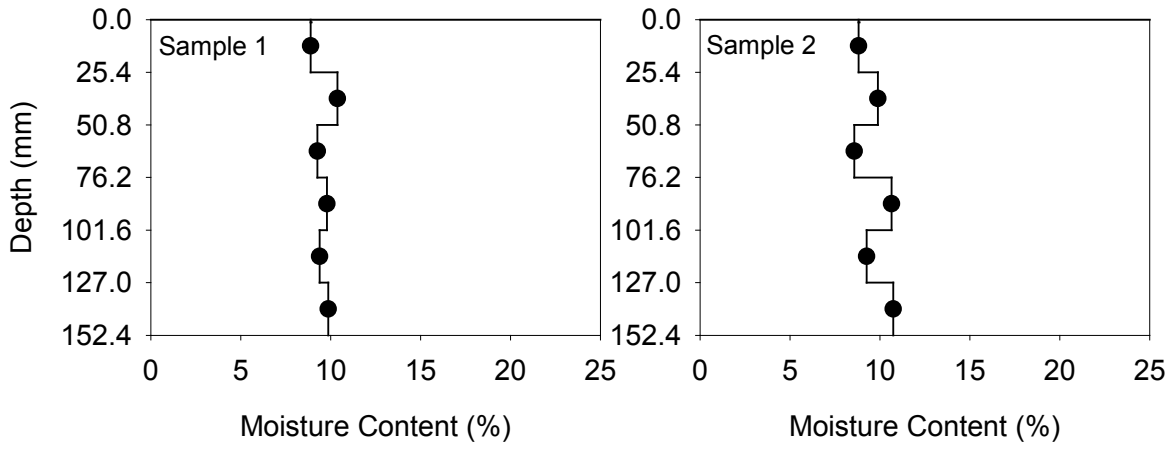

Figure 97. 0.6% PP fiber stabilized subbase moisture content profiles

For 0.6% PP fiber stabilized recycled subbase, the CBR value after freeze-thaw test was larger than the one without freeze-thaw test. The frost susceptibility of this material was classified as very low to medium level. Table 39 summarizes the frost-heave and thaw-weakening test results on 0.6% PP fiber stabilized recycled subbase material.

Table 39. 0.6% PP fiber stabilized subbase frost-heave and thaw-weakening test results

1st Frost-heave rate (mm/day)	6.25
2nd Frost-heave rate (mm/day)	5.12
CBR after freeze-thaw test (%)	16.3
CBR before freeze-thaw test (%)	5.8
Frost susceptibility based on heave	Medium
Frost susceptibility based on CBR	Very low

Two recycled subbase samples stabilized with 0.2% monofilament (MF) fiber were tested. The peak heave values of the samples were similar. The governed second heave rate calculated from the slopes was 10.34 mm/day. Figure 98 shows the frost heave time plots of these two samples. The heave rate was less than the non-stabilized recycled subbase.

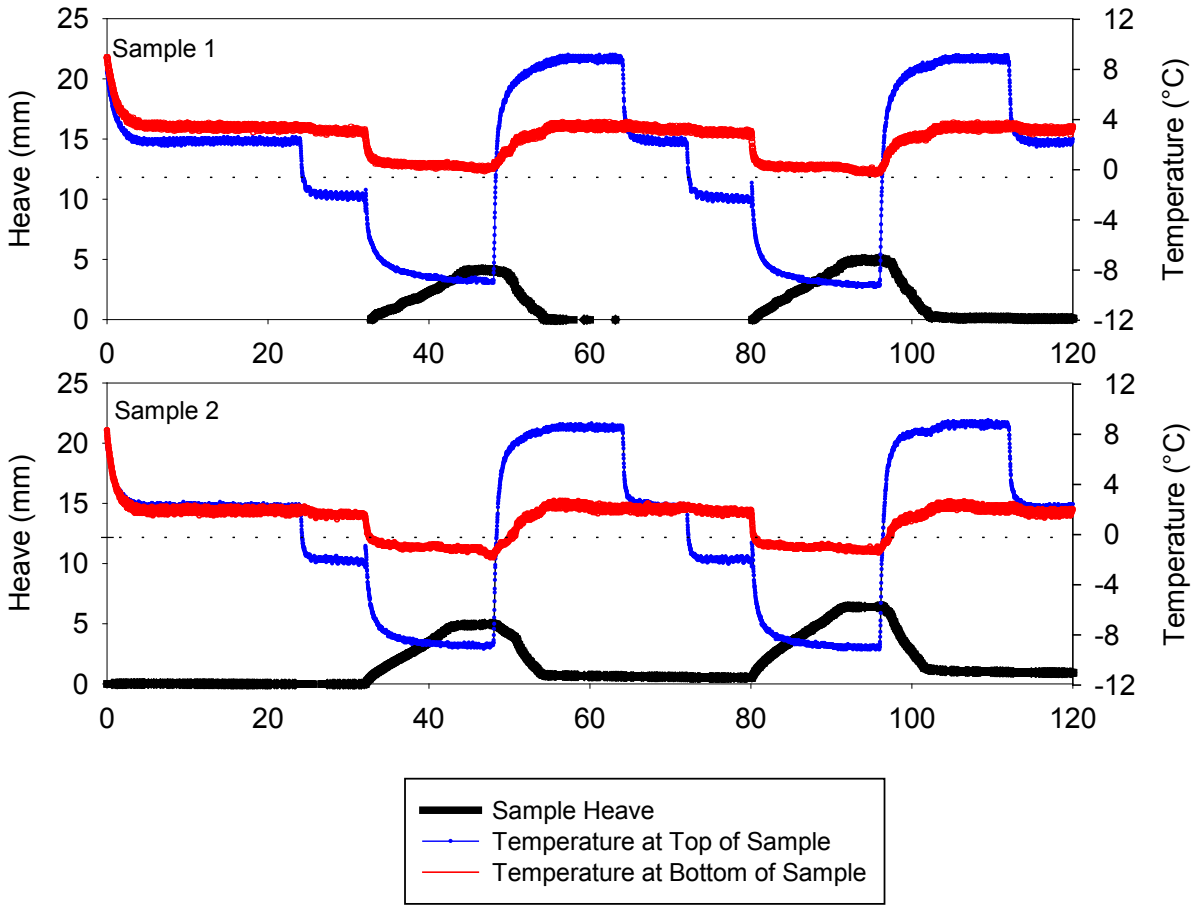

Figure 98. 0.2% MF fiber stabilized subbase frost heave time plots

For 0.2% MF fiber stabilized recycled subbase the moisture content profiles show the moisture contents decreased as the depth increased. Figure 99 shows the moisture content profiles of the post-test samples.

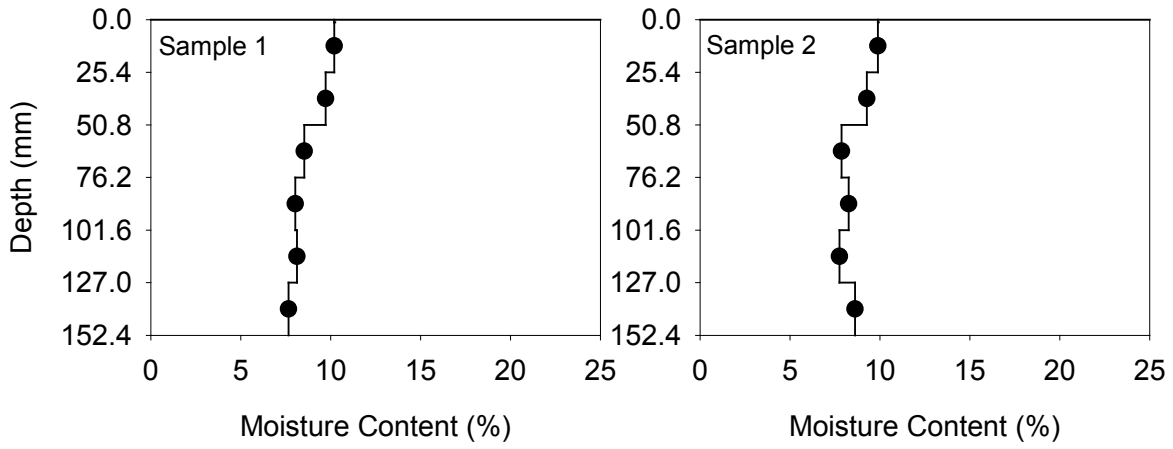

Figure 99. 0.2% MF fiber stabilized subbase moisture content profiles

For 0.2% MF fiber stabilized recycled subbase, the CBR value after freeze-thaw test was larger than the one without freeze-thaw test. The frost susceptibility of this material was classified as low to high level. Table 40 summarizes the frost-heave and thaw-weakening test results on 0.2% MF fiber stabilized recycled subbase material.

Table 40. 0.2% MF fiber stabilized subbase frost-heave and thaw-weakening test results

1st Frost-heave rate (mm/day)	8.78
2nd Frost-heave rate (mm/day)	10.34
CBR after freeze-thaw test (%)	12.1
CBR before freeze-thaw test (%)	4.1
Frost susceptibility based on heave	High
Frost susceptibility based on CBR	Low

Two recycled subbase samples stabilized with 0.4% MF fiber were tested. The peak heave values of the samples were similar. The governed second heave rate calculated from the slopes was 9.90 mm/day. Figure 100 shows the frost heave time plots of these two samples. The heave rate was less than the non-stabilized and 0.2% MF fiber stabilized recycled subbase.

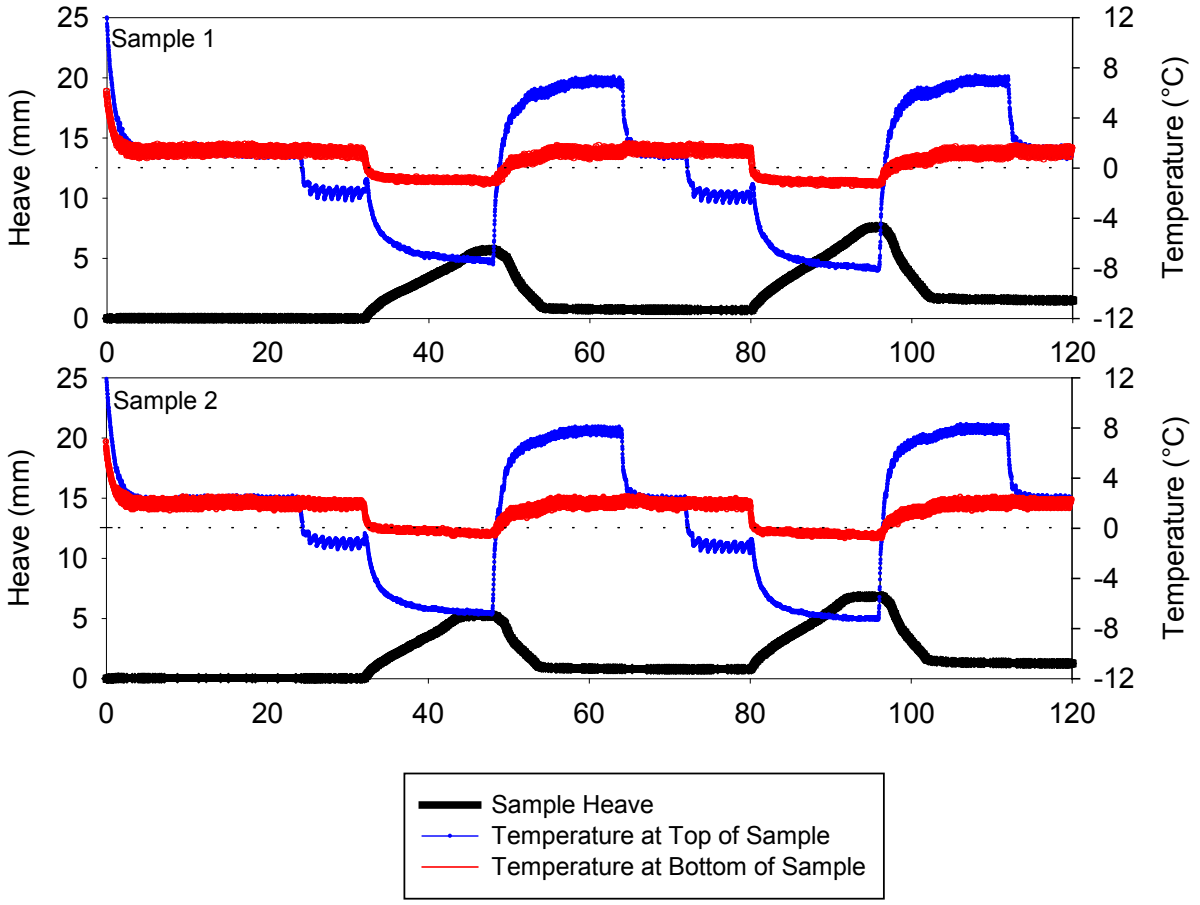

Figure 100. 0.4% MF fiber stabilized subbase frost heave time plots

For 0.4% MF fiber stabilized recycled subbase the moisture content profiles show the moisture contents decreased as the depth increased. Figure 101 shows the moisture content profiles of the post-test samples.

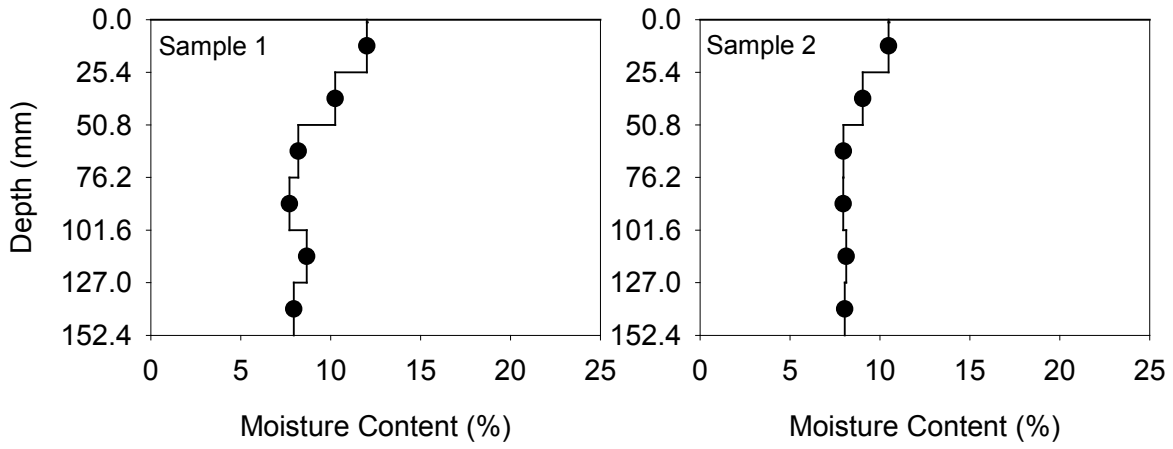

Figure 101. 0.4% MF fiber stabilized subbase moisture content profiles

For 0.4% MF fiber stabilized recycled subbase, the CBR value after freeze-thaw test was larger than the one without freeze-thaw test. The frost susceptibility of this material was classified as low to high level. Table 41 summarizes the frost-heave and thaw-weakening test results on 0.4% MF fiber stabilized recycled subbase material.

Table 41. 0.4% MF fiber stabilized subbase frost-heave and thaw-weakening test results

1st Frost-heave rate (mm/day)	8.50
2nd Frost-heave rate (mm/day)	9.50
CBR after freeze-thaw test (%)	14.8
CBR before freeze-thaw test (%)	7.9
Frost susceptibility based on heave	High
Frost susceptibility based on CBR	Low

Two recycled subbase samples stabilized with 0.6% MF fiber were tested. The peak heave values of the samples were similar. The governed first heave rate calculated from the slopes was 6.94 mm/day. Figure 102 shows the frost heave time plots of these two samples. The heave rate was less than the non-stabilized, 0.2%, and 0.4% MF stabilized recycled subbase.

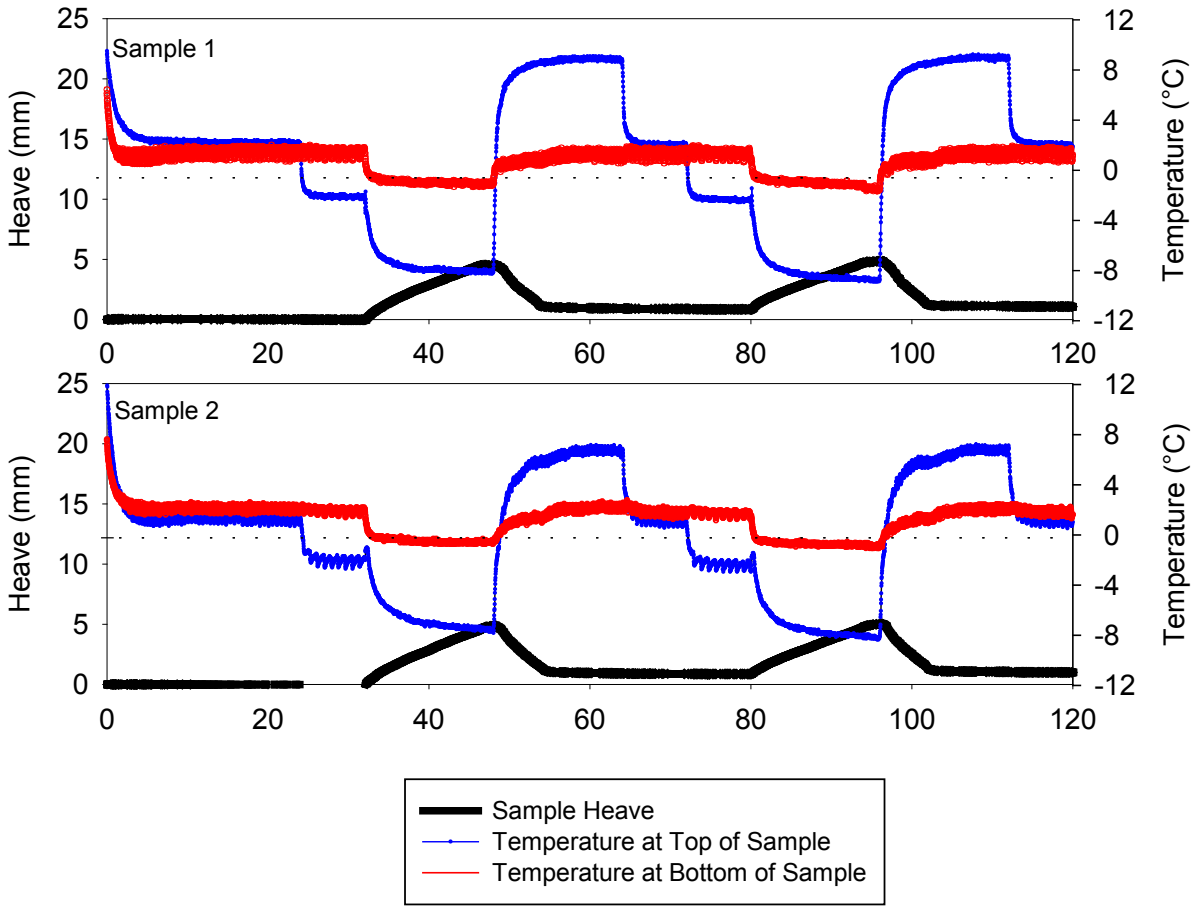

Figure 102. 0.6% MF fiber stabilized subbase frost heave time plots

For 0.6% MF fiber stabilized recycled subbase the moisture content profiles show the moisture contents decreased as the depth increased. Figure 103 shows the moisture content profiles of the post-test samples.

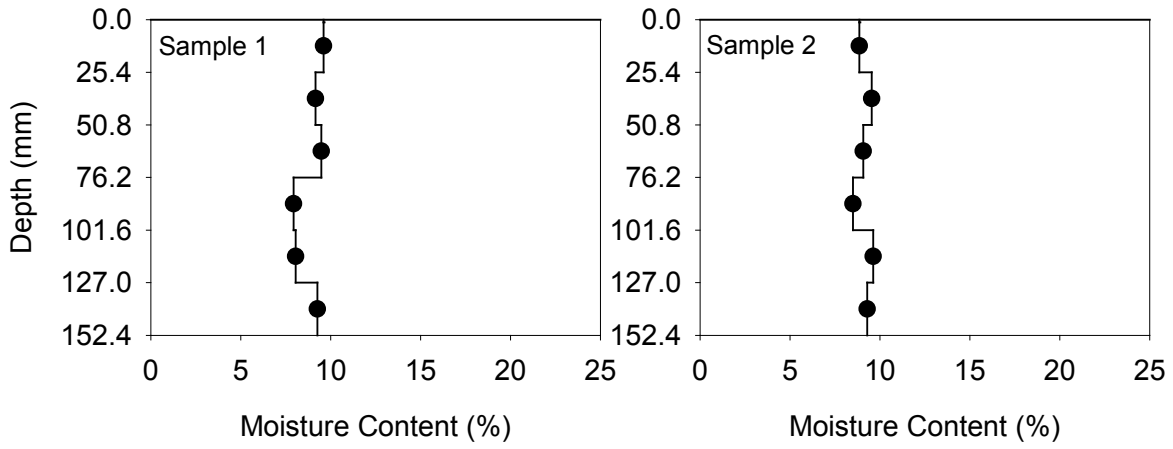

Figure 103. 0.6% MF fiber stabilized subbase moisture content profiles

For 0.6% MF fiber stabilized recycled subbase, the CBR value after freeze-thaw test was larger than the one without freeze-thaw test. The frost susceptibility of this material was classified as very low to medium level. Table 42 summarizes the frost-heave and thaw-weakening test results on 0.6% MF fiber stabilized recycled subbase material.

Table 42. 0.6% MF fiber stabilized subbase frost-heave and thaw-weakening test results

1st Frost-heave rate (mm/day)	6.94
2nd Frost-heave rate (mm/day)	6.11
CBR after freeze-thaw test (%)	18.4
CBR before freeze-thaw test (%)	8.6
Frost susceptibility based on heave	Medium
Frost susceptibility based on CBR	Very low

Recycled subbase stabilized with cement and fiber

One recycled subbase samples stabilized with 0.2% PP fiber and 3.75% cement was tested. The peak heave value of the sample was small. The governed second heave rate calculated from the slopes was 1.31 mm/day. Figure 104 shows the frost heave time plots of the samples. The heave rate was less than the non-stabilized recycled subbase.

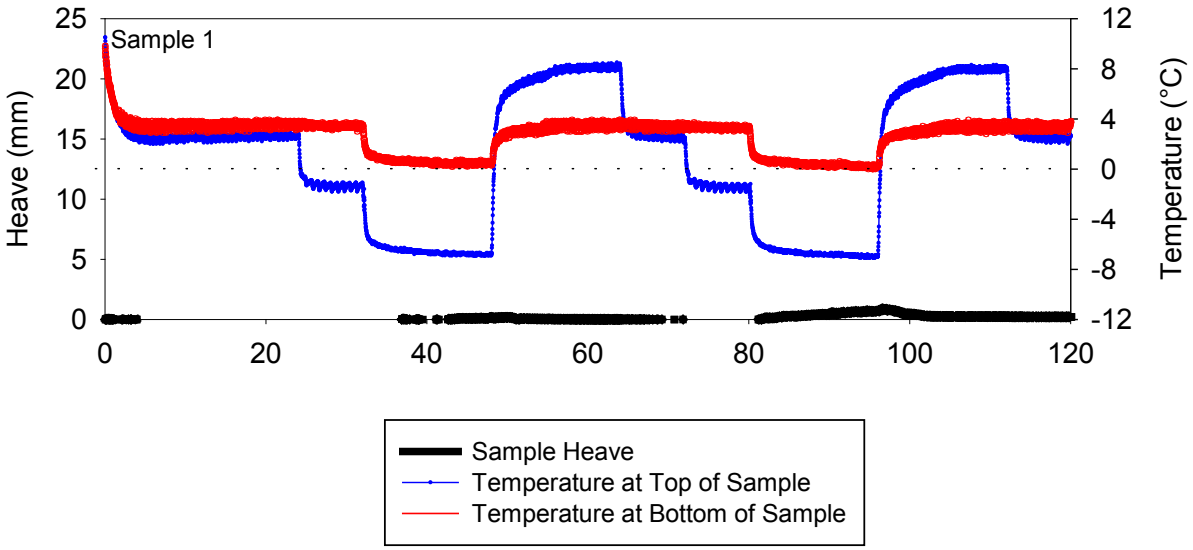

Figure 104. 0.2% PP fiber + 3.75% cement stabilized subbase frost heave time plots

For 0.2% PP fiber + 3.75% cement stabilized recycled subbase the moisture content profiles show the moisture contents increased as the depth increased. Figure 105 shows the moisture content profiles of the post-test sample.

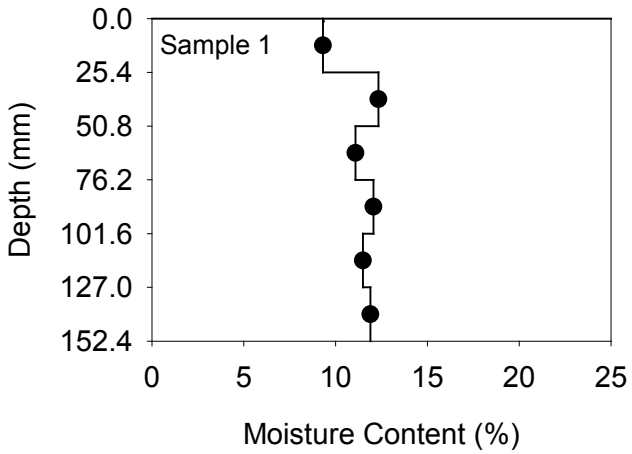

Figure 105. 0.2% PP fiber + 3.75% cement stabilized subbase moisture content profile

For 0.2% PP fiber + 3.75% cement stabilized recycled subbase, the CBR value after freeze-thaw test was larger than the one without freeze-thaw test. The frost susceptibility of this material was classified as very low to negligible level. Table 43 summarizes the frost-

heave and thaw-weakening test results on 0.2% PP fiber + 3.75% cement stabilized recycled subbase material.

Table 43. 0.2% PP fiber + 3.75% cement stabilized subbase frost-heave and thaw-weakening test results

1st Frost-heave rate (mm/day)	0.42
2nd Frost-heave rate (mm/day)	1.31
CBR after freeze-thaw test (%)	58.2
CBR before freeze-thaw test (%)	185.5
Frost susceptibility based on heave	Very low
Frost susceptibility based on CBR	Negligible

One recycled subbase samples stabilized with 0.2% PP fiber and 3.75% cement was tested. The compaction delay time was 12 hours. The peak heave value of the sample was larger than the sample without compaction delay. The governed second heave rate calculated from the slopes was 3.83 mm/day. Figure 106 shows the frost heave time plots of the samples. The heave rate was less than the non-stabilized recycled subbase, but larger than the no compaction delay sample.

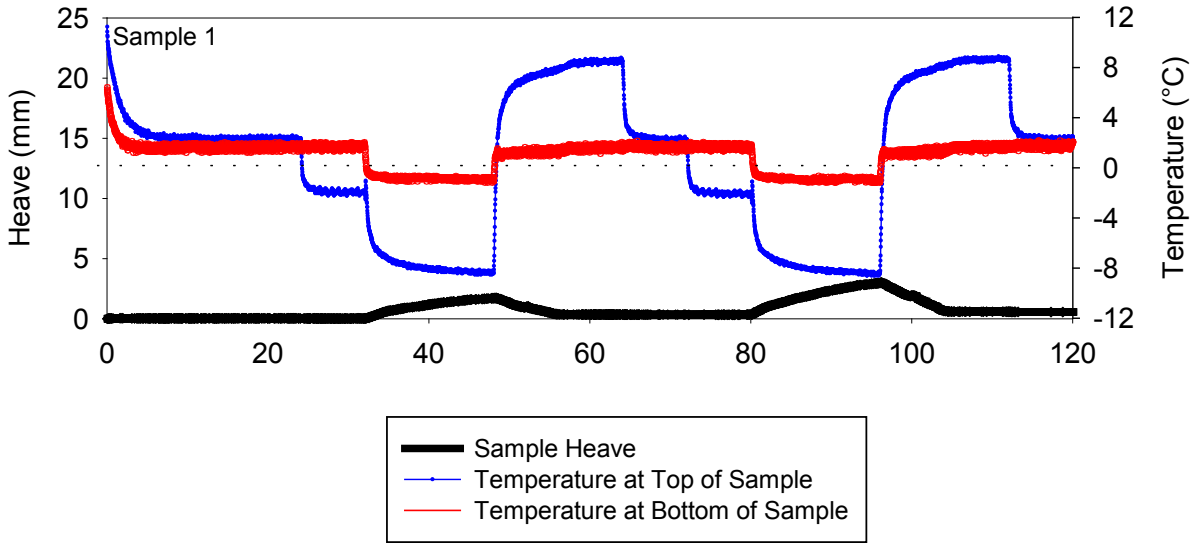

Figure 106. 0.2% PP fiber + 3.75% cement stabilized subbase frost heave time plots (12-hr compaction delay)

For 0.2% PP fiber + 3.75% cement stabilized recycled subbase with 12-hr compaction delay, the moisture content profiles show the moisture contents increased as the depth increased. Figure 107 shows the moisture content profiles of the post-test sample.

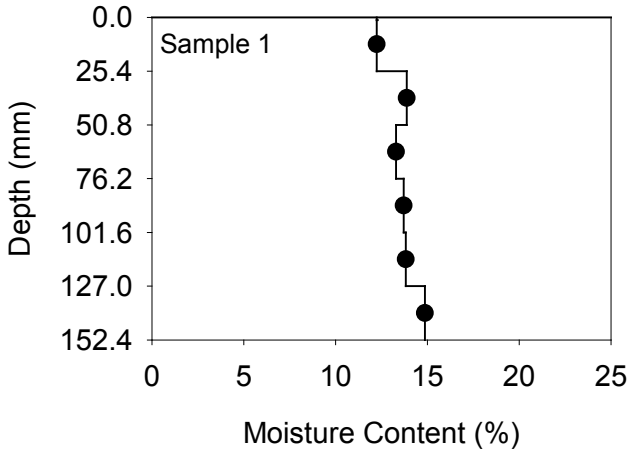

Figure 107. 0.2% PP fiber + 3.75% cement stabilized subbase moisture content profile (12-hr compaction delay)

For 0.2% PP fiber + 3.75% cement stabilized recycled subbase with 12-hr compaction delay, the after-thawing CBR value was less than the no compaction delay sample with the same stabilization method. The frost susceptibility of this material was classified as low to negligible level. Table 44 summarizes the frost-heave and thaw-weakening test results on 12-hr compaction delay 0.2% PP fiber + 3.75% cement stabilized recycled subbase material.

Table 44. 0.2% PP fiber + 3.75% cement stabilized subbase frost-heave and thaw-weakening test results (12-hr compaction delay)

1st Frost-heave rate (mm/day)	2.47
2nd Frost-heave rate (mm/day)	3.83
CBR after freeze-thaw test (%)	20.3
CBR before freeze-thaw test (%)	—
Frost susceptibility based on heave	Low
Frost susceptibility based on CBR	Negligible

Two 0.4% PP fiber + 3.75% cement stabilized recycled subbase samples were tested. The peak heave values of the samples were similar. The governed second heave rates were too

small to be calculated from the slopes. Figure 108 shows the frost heave time plots of these two samples. The heave rate was less than the non-stabilized, 0.2% PP fiber + 3.75% cement stabilized, and 0.6% PP fiber + 3.75% cement stabilized recycled subbase.

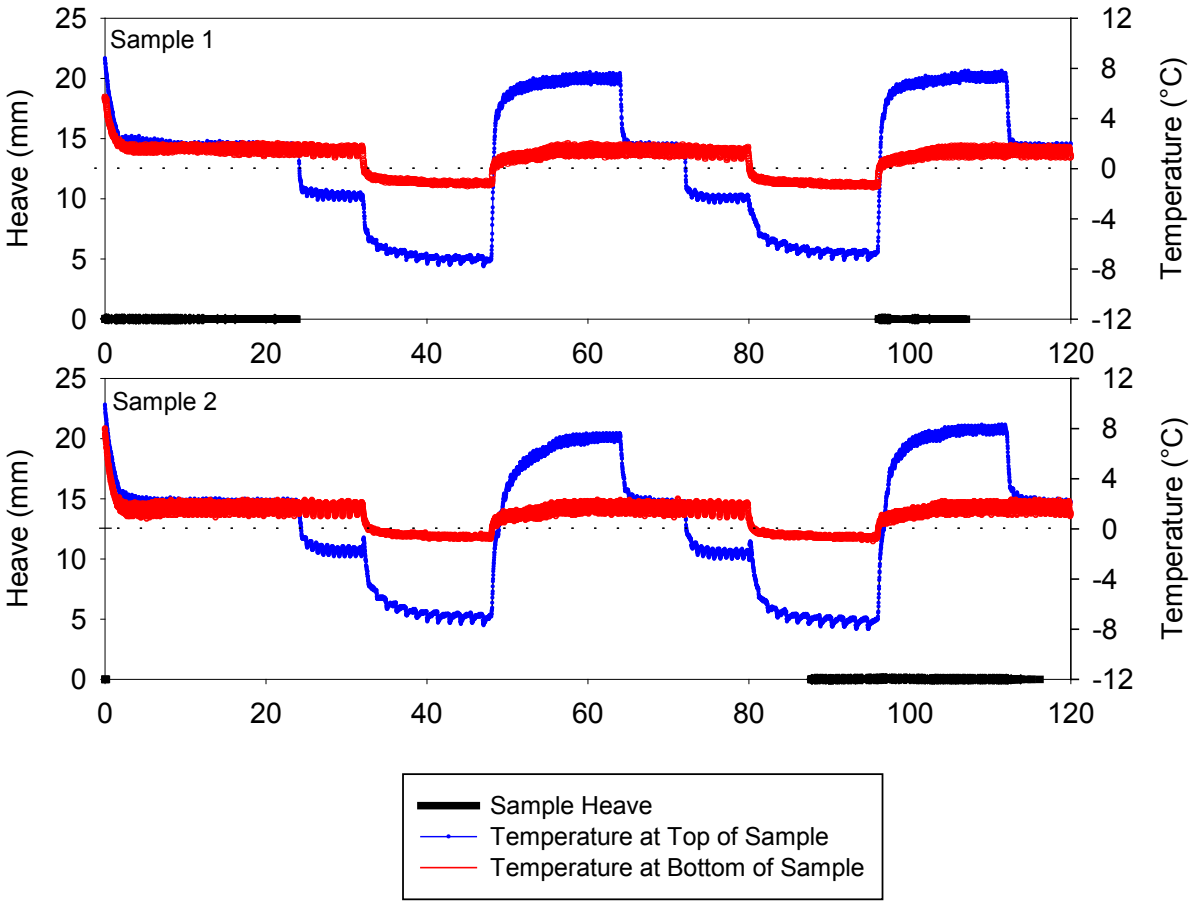

Figure 108. 0.4% PP fiber + 3.75% cement stabilized subbase frost heave time plots

For 0.4% PP fiber + 3.75% cement stabilized recycled subbase the moisture content profiles show that the moisture contents increased as the depth increased (Figure 109).

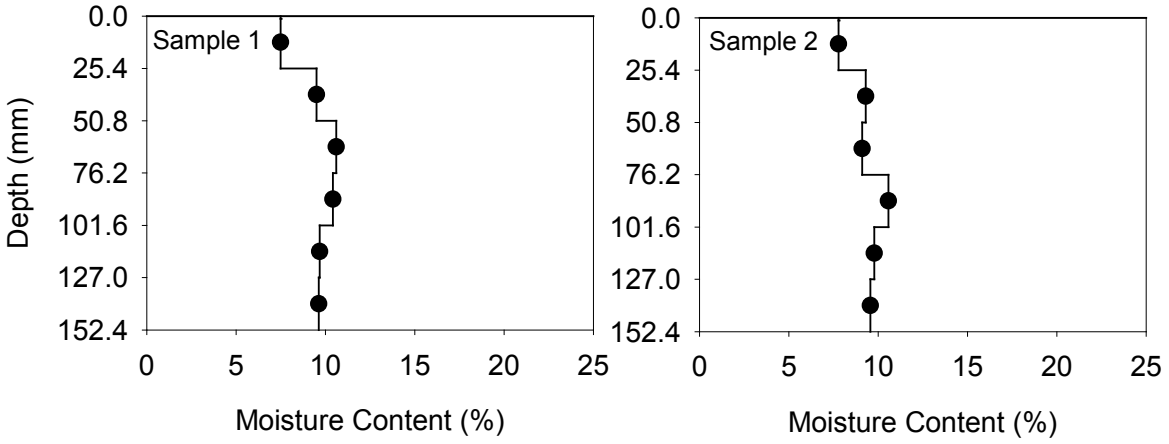

Figure 109. 0.4% PP fiber + 3.75% cement stabilized subbase moisture content profiles

For 0.4% PP fiber + 3.75% cement stabilized recycled subbase, the after-thawing CBR value was less than the sample with the same stabilization method. The frost susceptibility of this material was classified as negligible level. Table 45 summarizes the frost-heave and thaw-weakening test results of 0.4% PP fiber + 3.75% cement stabilized recycled subbase material.

Table 45. 0.4% PP fiber + 3.75% cement stabilized subbase frost-heave and thaw-weakening test results

1st Frost-heave rate (mm/day)	<1.00
2nd Frost-heave rate (mm/day)	<1.00
CBR after freeze-thaw test (%)	127.4
CBR before freeze-thaw test (%)	Too high
Frost susceptibility based on heave	Negligible
Frost susceptibility based on CBR	Negligible

Two 0.4% PP fiber + 3.75% cement stabilized recycled subbase samples with 12-hr compaction delay were tested. The peak heave values of the samples were similar. The governed second heave rate calculated from the slopes was 2.98 mm/day. Figure 110 shows the frost heave time plots of these two samples. The heave rate was less than the non-stabilized recycled subbase, but larger than the no compaction delay samples.

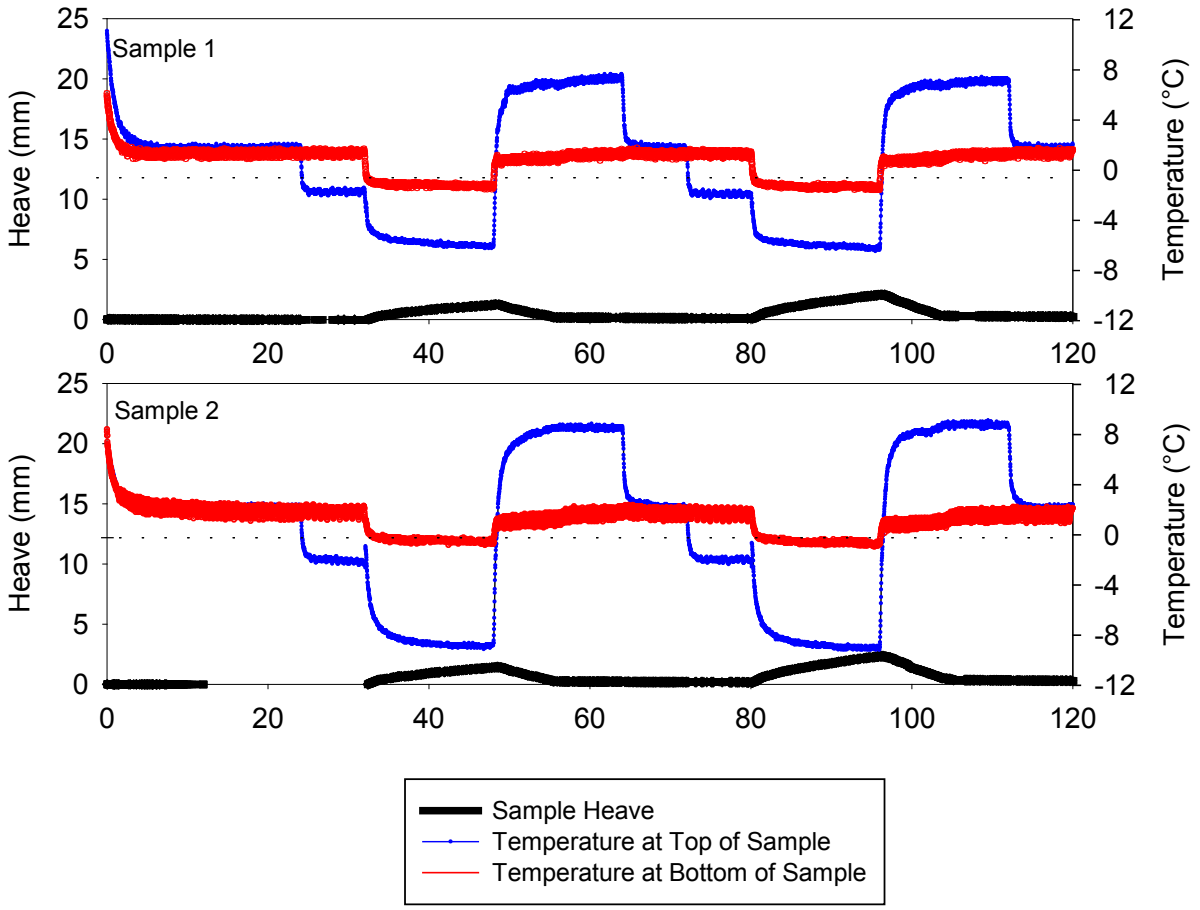

Figure 110. 0.4% PP fiber + 3.75% cement stabilized subbase frost heave time plots (12-hr compaction delay)

For 0.4% PP fiber + 3.75% cement stabilized recycled subbase with 12-hr compaction delay, the moisture content profiles show the moisture contents increased as the depth increased. Figure 111 shows the moisture content profiles of the post-test samples.

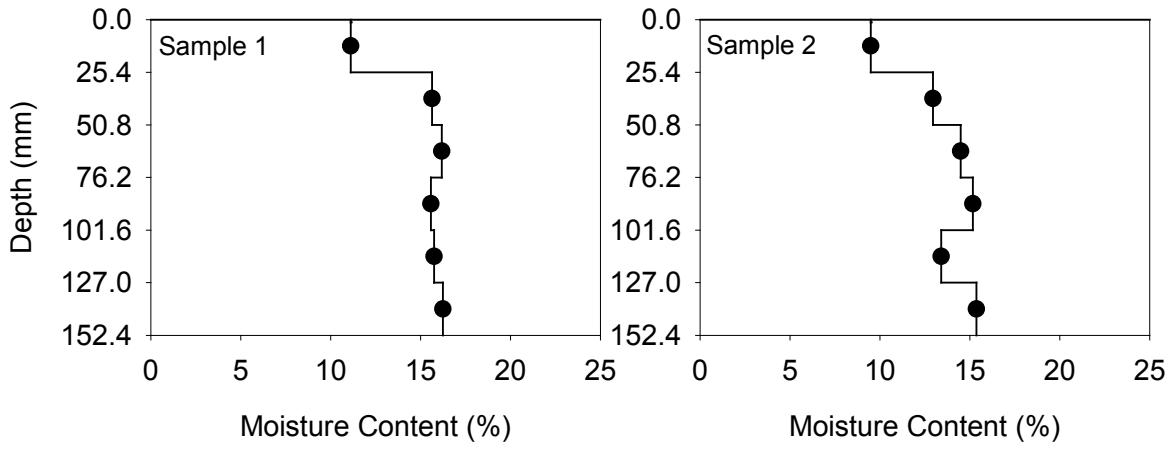

Figure 111. 0.4% PP fiber + 3.75% cement stabilized subbase moisture content profiles (12-hr compaction delay)

For 0.4% PP fiber + 3.75% cement stabilized recycled subbase with 12-hr compaction delay, the after-thawing CBR values were less than the no compaction delay samples with the same stabilization method. The frost susceptibility of this material was classified as low to negligible level. Table 46 summarizes the frost-heave and thaw-weakening test results on this material.

Table 46. 0.4% PP fiber + 3.75% cement stabilized subbase frost-heave and thaw-weakening test results (12-hr compaction delay)

1st Frost-heave rate (mm/day)	1.93
2nd Frost-heave rate (mm/day)	2.98
CBR after freeze-thaw test (%)	19.8
CBR before freeze-thaw test (%)	—
Frost susceptibility based on heave	Low
Frost susceptibility based on CBR	Negligible

One recycled subbase samples stabilized with 0.6% PP fiber + 3.75% cement was tested. The peak heave value of the sample was small. The governed first heave rate calculated from the slopes was 1.48 mm/day. Figure 112 shows the frost heave time plots of the sample. The heave rate was less than the non-stabilized recycled subbase, but larger than the 0.2% PP fiber + 3.75% cement stabilized recycled subbase.

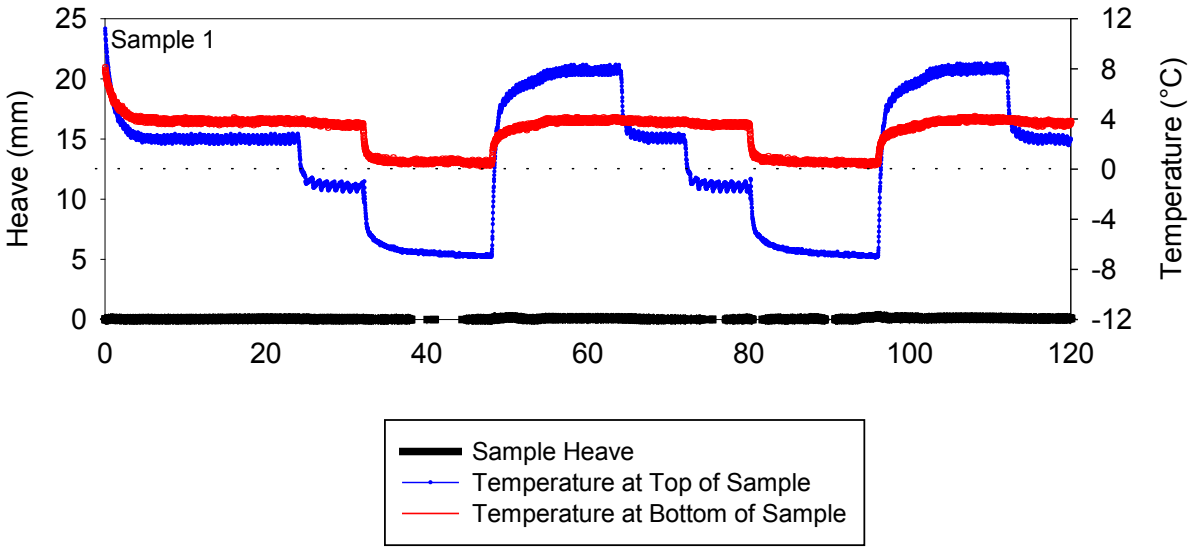

Figure 112. 0.6% PP fiber + 3.75% cement stabilized subbase frost heave time plots

For 0.6% PP fiber + 3.75% cement stabilized recycled subbase the moisture content profiles show the moisture contents increased as the depth increased. Figure 113 shows the moisture content profiles of the post-test sample.

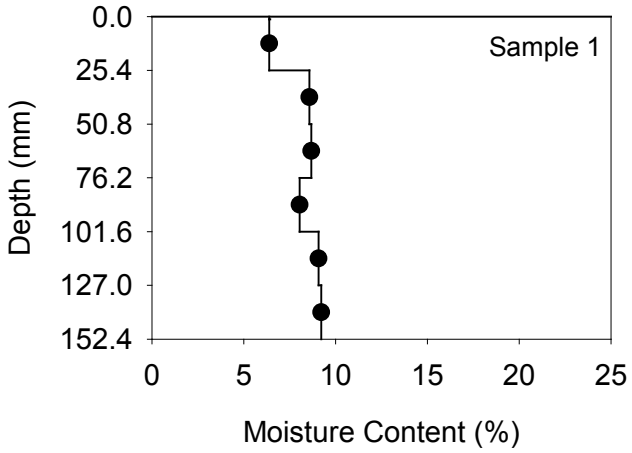

Figure 113. 0.6% PP fiber + 3.75% cement stabilized subbase moisture content profiles

For 0.6% PP fiber + 3.75% cement stabilized recycled subbase, the CBR value after freeze-thaw test was less than the without freeze-thaw test. The frost susceptibility of the

material was classified as very low level. Table 47 summarizes the frost-heave and thaw-weakening test results on 0.6% PP + 3.75% cement stabilized recycled subbase material.

Table 47. 0.6% PP fiber + 3.75% cement stabilized subbase frost-heave and thaw-weakening test results

1st Frost-heave rate (mm/day)	1.48
2nd Frost-heave rate (mm/day)	1.19
CBR after freeze-thaw test (%)	120.1
CBR before freeze-thaw test (%)	Too high
Frost susceptibility based on heave	Very low
Frost susceptibility based on CBR	Very low

One recycled subbase samples stabilized with 0.2% MF fiber + 3.75% cement was tested. The peak heave value of the sample was small. The governed first heave rate calculated from the slopes was 0.75 mm/day. Figure 114 shows the frost heave time plots of the sample. The heave rate was less than the non-stabilized recycled subbase.

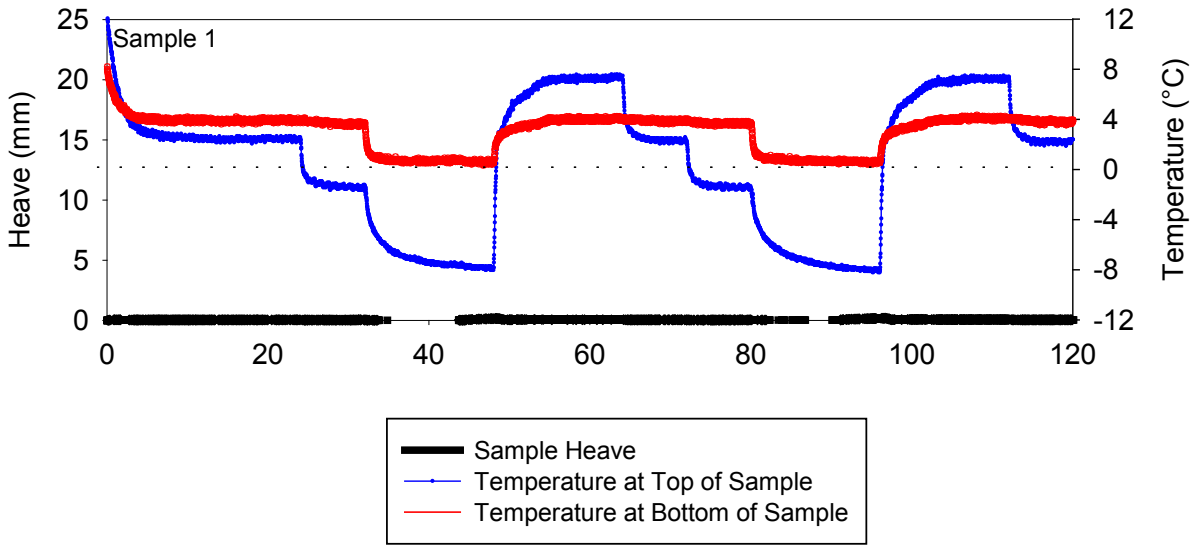

Figure 114. 0.2% MF fiber + 3.75% cement stabilized subbase frost heave time plots

For 0.2% MF fiber + 3.75% cement stabilized recycled subbase the moisture content profiles show that there was a small change of the after-thawing moisture contents of each layer from the top to the bottom. Besides a moisture content of the middle layer was around

9.0%, the other moisture contents were l around 7.5%. Figure 115 shows the moisture content profiles of the post-test sample.

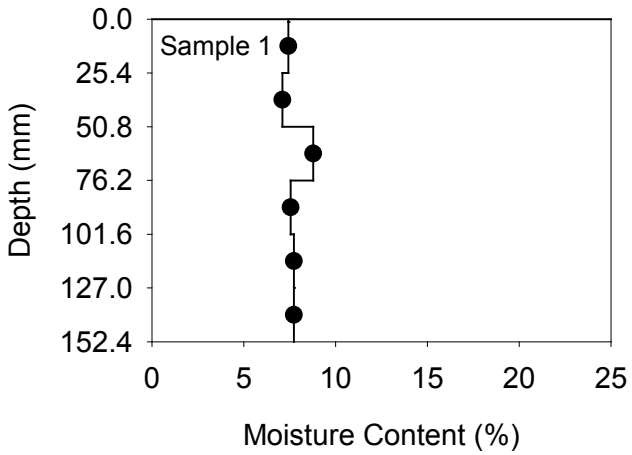

Figure 115. 0.2% MF fiber + 3.75% cement stabilized subbase moisture content profiles

For 0.2% MF fiber + 3.75% cement stabilized recycled subbase, the CBR value after freeze-thaw test was less than the one without freeze-thaw test. The frost susceptibility of this material was classified as negligible level. Table 48 summarizes the frost-heave and thaw-weakening test results on 0.2% MF fiber + 3.75% cement stabilized recycled subbase material.

Table 48. 0.2% MF fiber + 3.75% cement stabilized subbase frost-heave and thaw-weakening test results

1st Frost-heave rate (mm/day)	0.75
2nd Frost-heave rate (mm/day)	0.62
CBR after freeze-thaw test (%)	190.5
CBR before freeze-thaw test (%)	184.9
Frost susceptibility based on heave	Negligible
Frost susceptibility based on CBR	Negligible

One recycled subbase samples stabilized with 0.4% MF fiber + 3.75% cement was tested. The peak heave value of the sample was small. The governed second heave rate calculated from the slopes was 1.43 mm/day. Figure 116 shows the frost heave time plots of the sample.

The heave rate was less than the non-stabilized recycled subbase, but larger than the 0.2% MF + 3.75% cement stabilized recycled subbase.

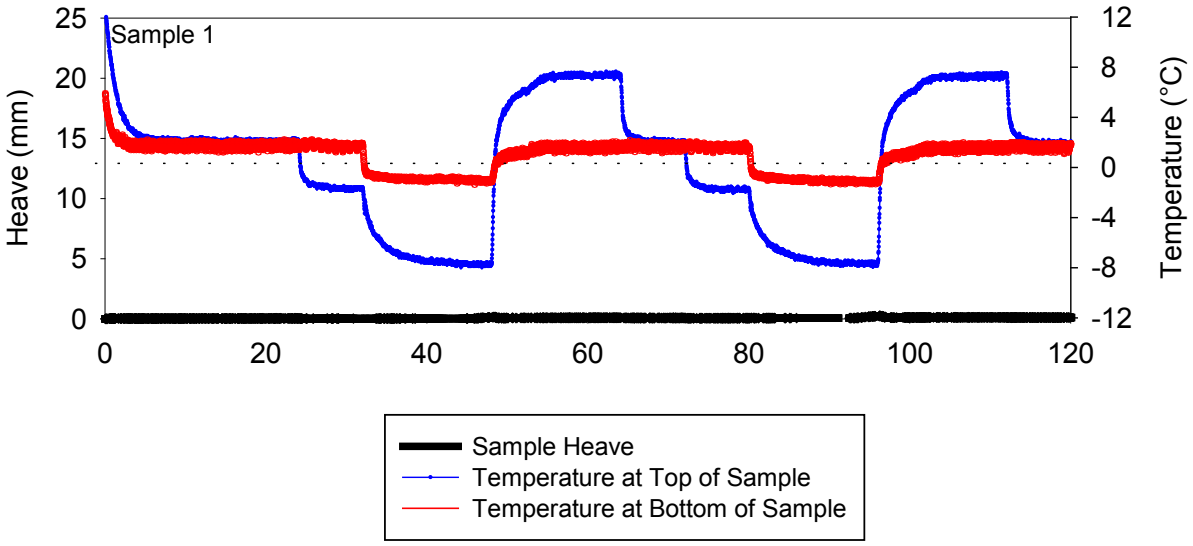

Figure 116. 0.4% MF fiber + 3.75% cement stabilized subbase frost heave time plots

For 0.4% MF fiber + 3.75% cement stabilized recycled subbase, the CBR value after freeze-thaw test was less than the one without freeze-thaw test. The frost susceptibility of this material was classified as very low to negligible level. Table 49 summarizes the frost-heave and thaw-weakening test results on 0.4% MF fiber + 3.75% cement stabilized recycled subbase material.

Table 49. 0.4% MF fiber + 3.75% cement stabilized subbase frost-heave and thaw-weakening test results

1st Frost-heave rate (mm/day)	1.11
2nd Frost-heave rate (mm/day)	1.43
CBR after freeze-thaw test (%)	203.2
CBR before freeze-thaw test (%)	143.1
Frost susceptibility based on heave	Very low
Frost susceptibility based on CBR	Negligible

One recycled subbase samples stabilized with 0.6% MF fiber + 3.75% cement was tested. The peak heave value of the sample was small. The governed first heave rate calculated from the slopes was 1.00 mm/day. Figure 117 shows the frost heave time plots of the sample. The

heave rate was less than the non-stabilized and 0.4% MF fiber + 3.75% cement stabilized recycled subbase, but larger than the 0.2% MF fiber +3.75% cement stabilized recycled subbase.

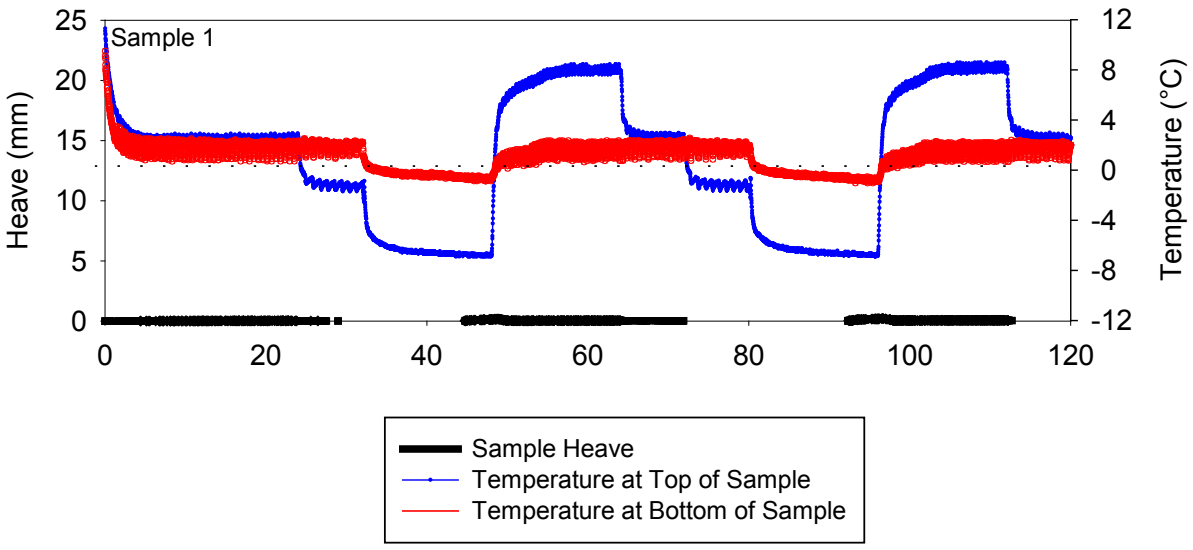

Figure 117. 0.6% MF fiber + 3.75% cement stabilized subbase frost heave time plots

For 0.6% MF fiber + 3.75% cement stabilized recycled subbase, the CBR value after freeze-thaw test was less than the one without freeze-thaw test. The frost susceptibility of this material was classified as negligible level. Table 50 summarizes the frost-heave and thaw-weakening test results on this material.

Table 50. 0.6% MF fiber + 3.75% cement stabilized subbase frost-heave and thaw-weakening test results

1st Frost-heave rate (mm/day)	0.81
2nd Frost-heave rate (mm/day)	1.00
CBR after freeze-thaw test (%)	177.0
CBR before freeze-thaw test (%)	158.7
Frost susceptibility based on heave	Negligible
Frost susceptibility based on CBR	Negligible

Western Iowa loess with long cure period

In order to evaluate the influence of cure period to improving freeze-thaw performance of geomaterials, frost-heave and thaw-weakening tests were conducted on 15% FA stabilized western Iowa loess with three cure periods, 7-day, 90-day, and 180-day.

Two western Iowa loess samples stabilized with 15% FA were tested. The samples were cured at 100 °F for 7 days before testing. The peak heave values range from 7.50 mm to 16.00 mm. The average governed second heave rate calculated from the slopes was 14.10 mm/day. Figure 118 shows the frost heave time plots of the 7-day cured 15% FA stabilized western Iowa loess.

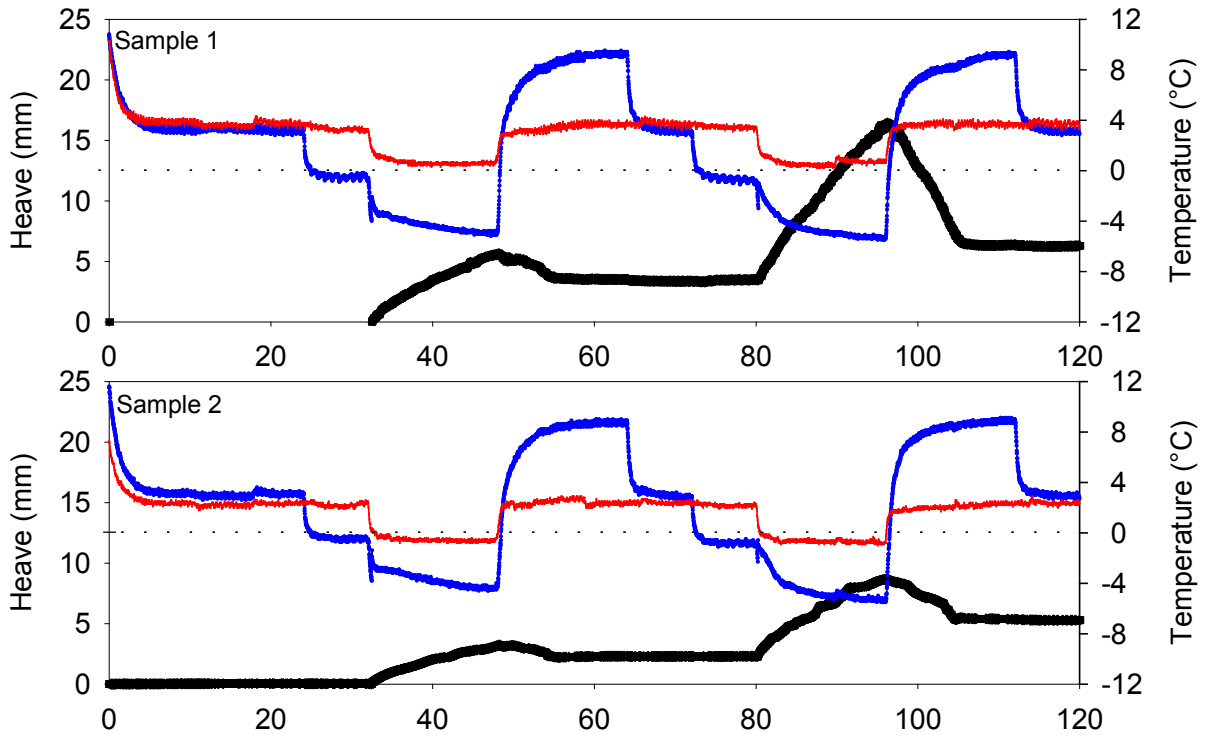

Figure 118. 7-day cured FA stabilized loess frost heave time plots

The CBR value after freeze-thaw of this material was 7.1%. The frost susceptibility was classifies as medium to high level. Table 51 summarizes the frost-heave and thaw-weakening test results of this material.

Table 51. 7-day cured FA stabilized loess frost-heave and thaw-weakening test results

1st Frost-heave rate (mm/day)	6.20
2nd Frost-heave rate (mm/day)	14.10
CBR after freeze-thaw test (%)	7.1
Frost susceptibility based on heave	High
Frost susceptibility based on CBR	Medium

Four western Iowa loess samples stabilized with 15% FA were tested. The samples were cured at 100 °F for 90 days before testing. The peak heave values range from 10.00 mm to 15.00 mm. The average governed second heave rate calculated from the slopes was 11.83 mm/day. Figure 119 shows the frost heave time plots of the 90-day cured 15% FA stabilized western Iowa loess.

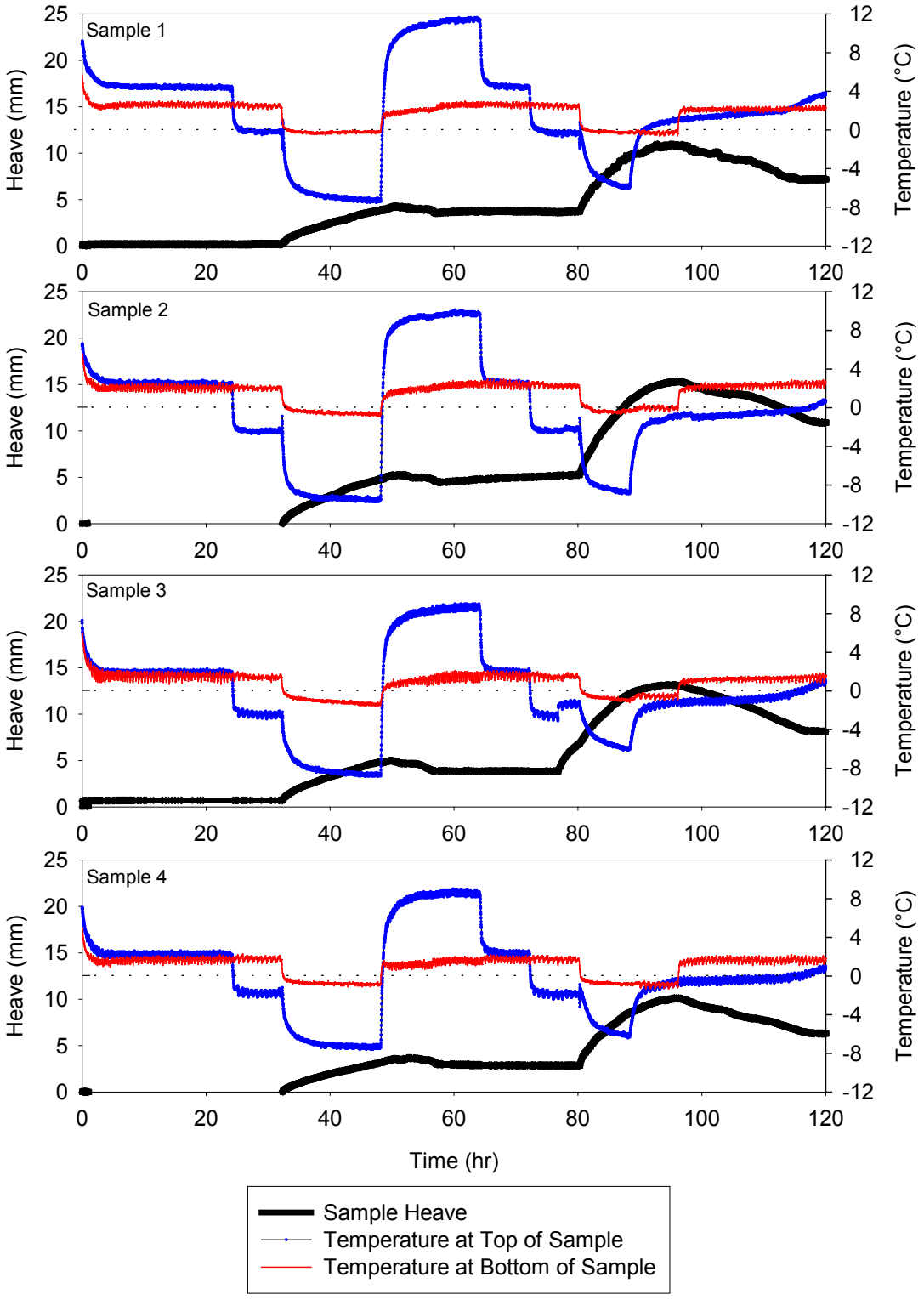

Figure 119. 90-day cured FA stabilized loess frost heave time plots

The CBR value after freeze-thaw of this material was close to the 7-day cured samples. The frost susceptibility was classifies as medium to high level. Table 52 summarizes the frost-heave and thaw-weakening test results of this material.

Table 52. 90-day cure FA stabilized loess frost-heave and thaw-weakening test results

1st Frost-heave rate (mm/day)	5.16
2nd Frost-heave rate (mm/day)	11.83
CBR after freeze-thaw test (%)	8.7
Frost susceptibility based on heave	High
Frost susceptibility based on CBR	Medium

Four western Iowa loess samples stabilized with 15% FA were tested. The samples were cured at 100 °F for 180 days before testing. The peak heave values were similar. The average governed second heave rate calculated from the slopes was 8.27 mm/day. Figure 120 shows the frost heave time plots of the 180-day cured 15% FA stabilized western Iowa loess.

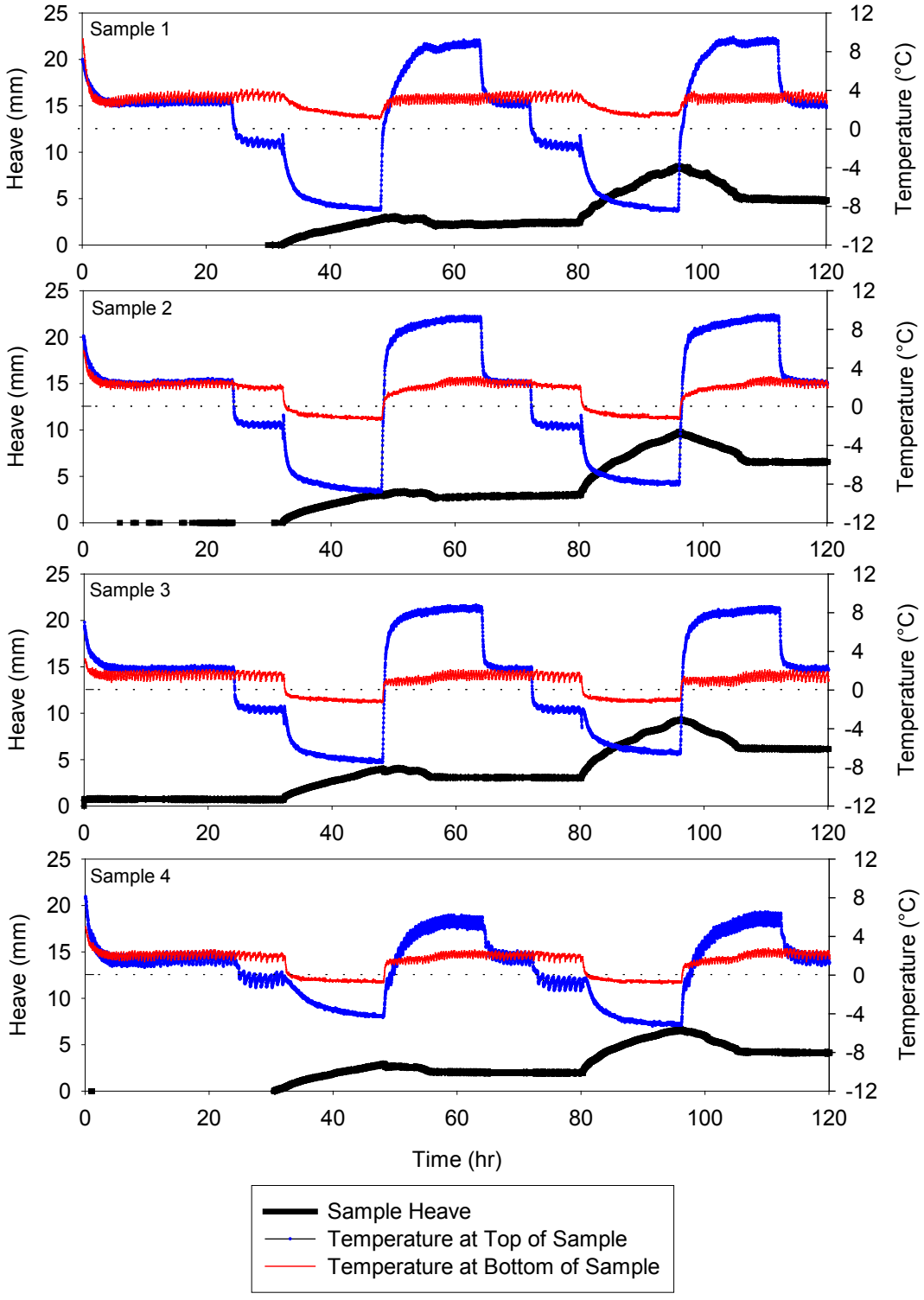

Figure 120. 180-day cure FA stabilized loess frost heave time plots

The CBR value after freeze-thaw of this material was higher than the 7-day and 90-day cured samples. The frost susceptibility was classifies as negligible to high level. Table 53 summarizes the frost-heave and thaw-weakening test results of this material.

Table 53. 180-day cure FA stabilized loess frost-heave and thaw-weakening test results

1st Frost-heave rate (mm/day)	3.74
2nd Frost-heave rate (mm/day)	8.27
CBR after freeze-thaw test (%)	32.0
Frost susceptibility based on heave	High
Frost susceptibility based on CBR	Negligible

Summary of frost-heave and thaw-weakening tests

Various combinations of geomaterials and stabilizers were tested to provide the frost susceptibility of the materials. From evaluating the test results, the improvement on the freeze-thaw performance of geomaterials can also be determined. The stabilization effects of different types and contents of stabilizers on freeze-thaw were compared based on the frost heave rates and CBR values. The stiffness changes because of freeze-thaw cycles can be presented by comparing the pre- and post-test CBRs. The post-test moisture content profiles of six layers of each sample help to understand the water movement and moisture changes during the freeze-thaw cycles.

The original non-stabilized subgrade was classified as sandy lean clay (CL) and had a heave rate of 11.43 mm/day. The non-stabilized recycled subbase was silty sand with gravel (SM) with a heave rate of 15.63 mm/day. With these heave rates, both materials were highly frost susceptible. However, the post-test CBR value of the non-stabilized subgrade was 1.4% which was less than the 8.8% post-test CBR value of the non-stabilized recycled subbase. The frost susceptibilities based on CBR values were high for the subgrade and medium for the subbase.

Fly ash stabilized subgrade

Different FA-subgrade combinations resulted in different frost susceptibilities. Of all of the FA-stabilized combinations, the 15% Ames FA and the 15% Port Neal FA were the best for improving the freeze-thaw performance. The 15% FA stabilized samples even outperformed the 20% FA samples. The Port Neal FA was more effective than the Ames or Muscatine FA for improving the frost susceptibility of the subgrade (Figure 121). Both the 15% Port Neal and Ames FA stabilized subgrade reached the very low to negligible frost susceptibility levels based on CBR, but the 15% Ames FA only decreased the heave-rate based frost susceptibility levels from high to medium. Both the heave-rate and CBR based frost susceptibilities of the 5% and 10% Muscatine FA stabilized subgrade remained at the high level. The post-test CBRs were less than the CBRs without freeze-thaw cycles.

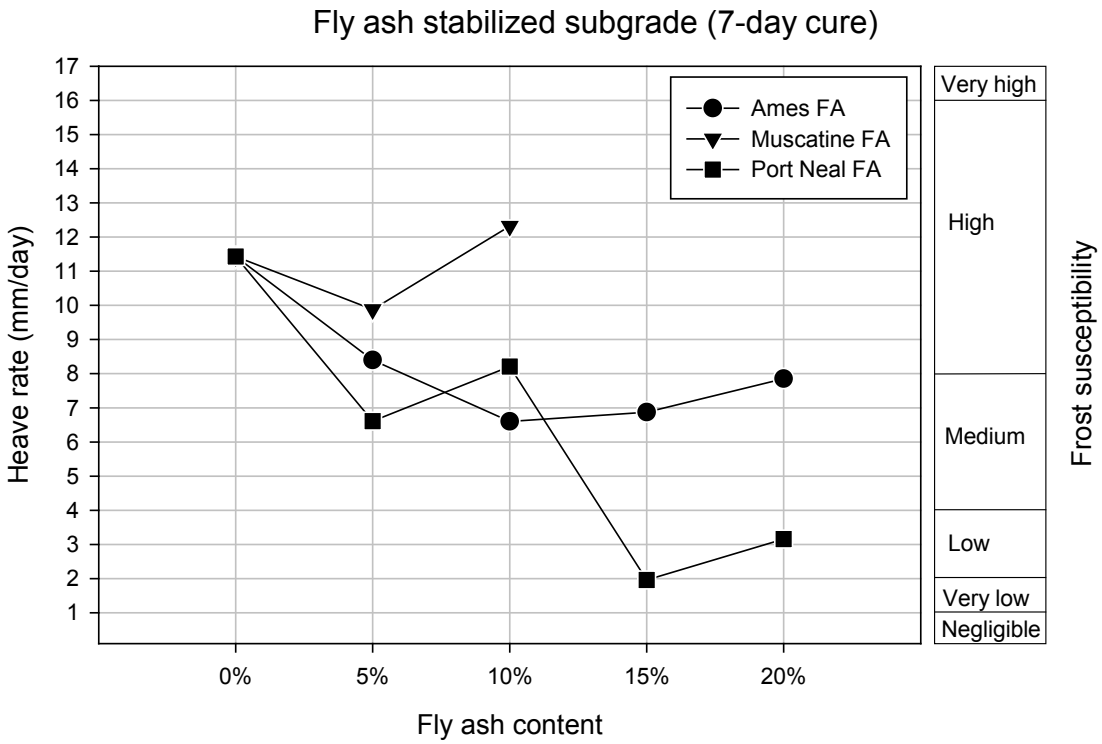

Figure 121. Frost heave rates of fly ash stabilized subgrade

SiO_2, Al_2O_3, and CaO are the three active components of these three types of FA. In this study. The chemical reactions between these components and soils were complex. Therefore, it is difficult to determine the influence of each component to the fly ash stabilization effects. Table 54 summarizes the setting time of the three types of fly ash. The fly with shorter setting time performed better on controlling the frost heave and stiffness changes during freeze-thaw cycles. Table 55 summarizes the frost susceptibility of FA stabilized subgrade and the active components of the FA.

Table 54. Setting time of three fly ash

FA source location	Port Neal	Ames	Muscatine
Initial sett time (min)	2.75	4.25	7.00
Final set time (min)	6.00	18.5	166.00

Table 55. Summary of frost susceptibility of FA stabilized subgrade and three active components content of the FA

Stabilization method	Frost susceptibility based on heave	Frost susceptibility based on CBR
5% Ames fly ash	High	Medium
10% Ames fly ash	Medium	Medium
15% Ames fly ash	Medium	Negligible
20% Ames fly ash	Medium	Low
5% Muscatine fly ash	High	High
10% Muscatine fly ash	High	High
5% Port Neal fly ash	Medium	Medium
10% Port Neal fly ash	High	Low
15% Port Neal fly ash	Very low	Very low
20% Port Neal fly ash	Low	Very low

Cement-stabilized subgrade

The cement was more effective than the same amount of FA on improving freeze-thaw performance of subgrade. No matter the frost susceptibility based on heave or CBR, it was at negligible level for both 5% and 10% cement contents. The stiffness increased after the freeze-thaw cycles. The post-test CBRs were larger than the no freeze-thaw CBRs. As the increment of cement content mixed with the subgrade, the geomaterials were less frost susceptible. Table 56 summarizes the frost susceptibility of two cement stabilized subgrade materials.

Table 56. Summary of frost susceptibility of cement stabilized subgrade

Stabilization method	Frost susceptibility based on heave	Frost susceptibility based on CBR
5% cement	Negligible	Negligible
10% cement	Negligible	Negligible

Cement stabilized recycled subbase

Cement was also used to stabilizing the recycled subbase. The frost susceptibility was decreased as the cement content increased. Besides the 2.5% cement stabilized subbase ranged from low to high frost susceptible, all 3.75%, 5.0%, and 7.5% cement stabilized samples resulted in low to negligible frost susceptibilities. Figure 122 shows the frost heave rates of cement stabilized subgrade and subbase.

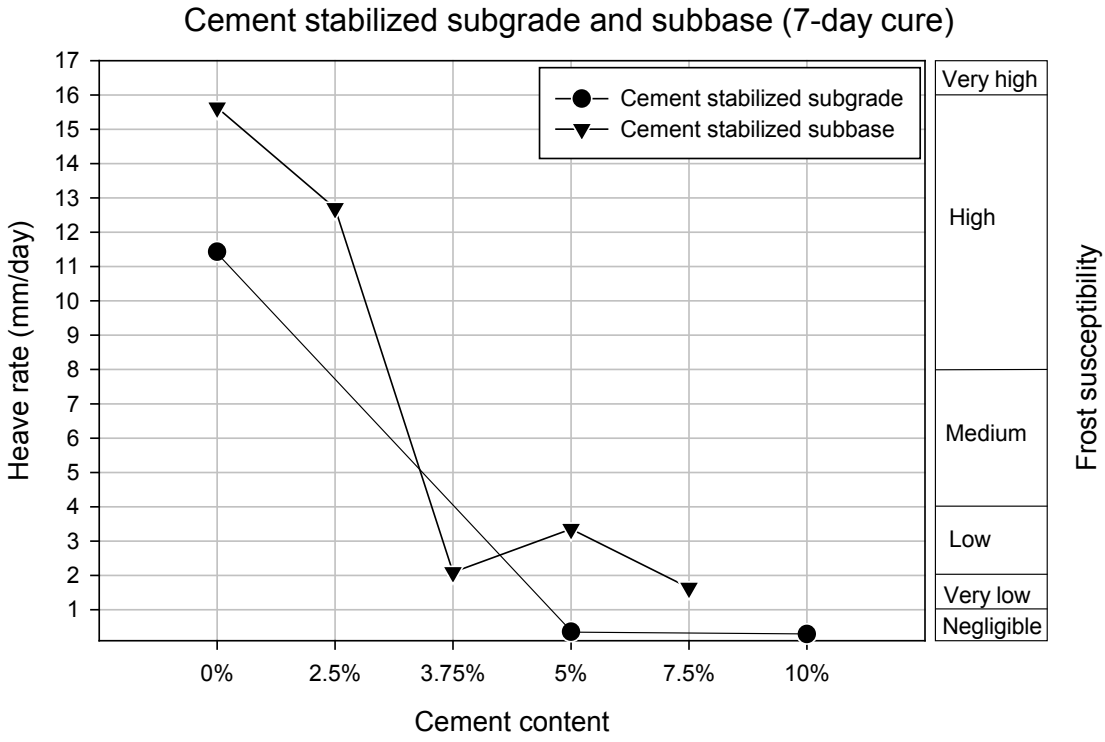

Figure 122. Frost heave rates of cement stabilized subgrade and subbase

The CBR values decreased 70-80% after the freeze-thaw cycles. The no freeze-thaw CBR values of the four materials were around or larger than 100.0%. The 0.2 in. CBR values of the 7.5% cement stabilized samples could not be obtained with the load cell with 10K lb limits. The frost susceptibility of the mixed geomaterials decreased as the cement content in the mixtures increased. Table 57 summarizes the frost susceptibility of cement stabilized recycled subbase.

Table 57. Summary of frost susceptibility of cement stabilized recycled subbase

Stabilization method	Frost susceptibility based on heave	Frost susceptibility based on CBR
2.50% cement	High	Low
3.75% cement	Low	Negligible
5.00% cement	Low	Negligible
7.50% cement	Very low	Negligible

Geofiber stabilized recycled subbase

Two types of geofiber with three different contents were mixed with the recycled subbase for freeze-thaw tests. The PP fiber provided the similar frost susceptibilities as the same amount of MF fiber. The frost susceptibilities based on heave ranged from medium to high for all six combinations. Figure 123 shows the frost heave rates of fibers stabilized recycled subbase. However, 0.6% PP and 0.6% MF stabilized samples both resulted in very low frost susceptibilities based on CBRs. The stiffness changes of fiber stabilized subbase were different to most of the materials with other stabilization methods, but the same to the non-stabilized recycled subbase. The post-test CBRs were larger than the pre-test CBRs. Table 58 summarizes the frost susceptibility of fiber stabilized recycled subbase.

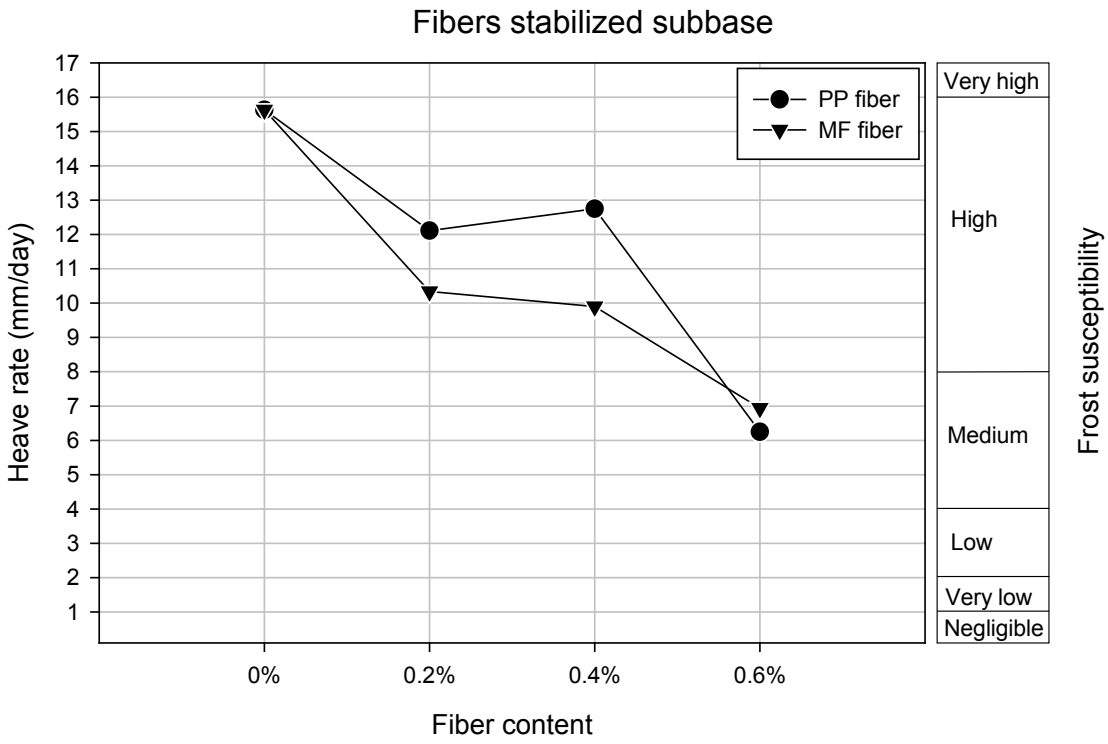

Figure 123. Frost heave rates of fibers stabilized subbase

Table 58. Summary of frost susceptibility of fiber stabilized recycled subbase

Stabilization method	Frost susceptibility based on heave	Frost susceptibility based on CBR
0.2% PP	High	Low
0.4% PP	High	Medium
0.6% PP	Medium	Very low
0.2% MF	High	Low
0.4% MF	High	Low
0.6% MF	Medium	Very low

Cement + geofiber stabilized recycled subbase

A constant cement content (3.75%) was added to each of the six geofiber combinations. The addition of cement improved the freeze-thaw performance of the materials stabilized only with geofiber. The frost susceptibilities of all the cement + fiber stabilized recycled subbase no compaction delay samples ranged from very low to negligible levels. For PP +

cement stabilized samples, 0.4% PP + 3.75% cement turned out to be more effective than the other combinations. For MF + cement stabilized samples, both 0.2% MF + 3.75% cement and 0.6% MF + 3.75% cement controlled the frost heave slightly better than 0.4% MF + 3.75% cement. Figure 124 shows the frost heave rates of cement + fibers stabilized recycled subbase.

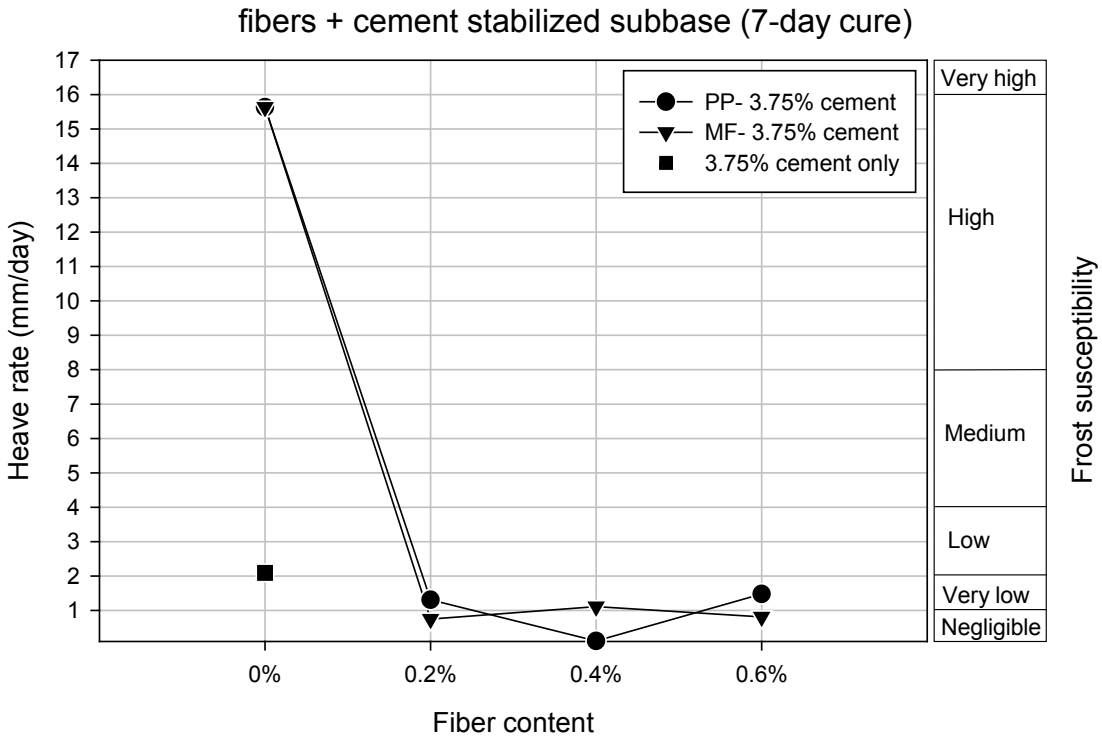

Figure 124. Frost heave rates of cement + fibers stabilized subbase

The stiffness decreased after freeze-thaw tests for PP + cement stabilized materials. However, the post-test CBRs of the MF + cement stabilized samples also increased with variable amounts to the CBRs without freeze-thaw cycles. Therefore, the cement + fiber stabilization was an effective method for controlling the freeze-thaw performance and improving the frost susceptibility of recycled subbase.

Because stabilizing frost susceptible geomaterials with 5% cement or 3.75% + 0.2% fiber reduces frost susceptibility to very low to negligible levels for a geomaterial, the pavement designers ought to balance the environmental impact with the cost. 5% cement results in less cost and higher environmental impact, while 3.75% cement + 0.2% fiber results in higher cost and lower environmental impact. Table 59 summarizes the frost susceptibility of cement + fiber stabilized recycled subbase.

Table 59. Summary of frost susceptibility of cement + fiber stabilized recycled subbase

Stabilization method	Frost susceptibility based on heave	Frost susceptibility based on CBR
0.2% PP + 3.75% cement	Very low	Negligible
0.4% PP + 3.75% cement	Negligible	Negligible
0.6% PP + 3.75% cement	Very low	Very low
0.2% MF+ 3.75% cement	Negligible	Negligible
0.4% MF+ 3.75% cement	Very low	Negligible
0.6% MF+ 3.75% cement	Negligible	Negligible

Two kinds of materials, 0.2% PP + 3.75% cement stabilized and 0.4% PP + 3.75% cement stabilized recycled subbase with 12-hr compaction delay were tested to determine the influence the compaction delay time to stabilization effects. The heave rates increased (Figure 125) and the CBR values decreased comparing with the same materials without compaction delay. The frost susceptibility of the materials with longer compaction delay slightly increased. Table 60 summarizes the frost susceptibility of cement + fiber stabilized recycled subbase with longer compaction delay.

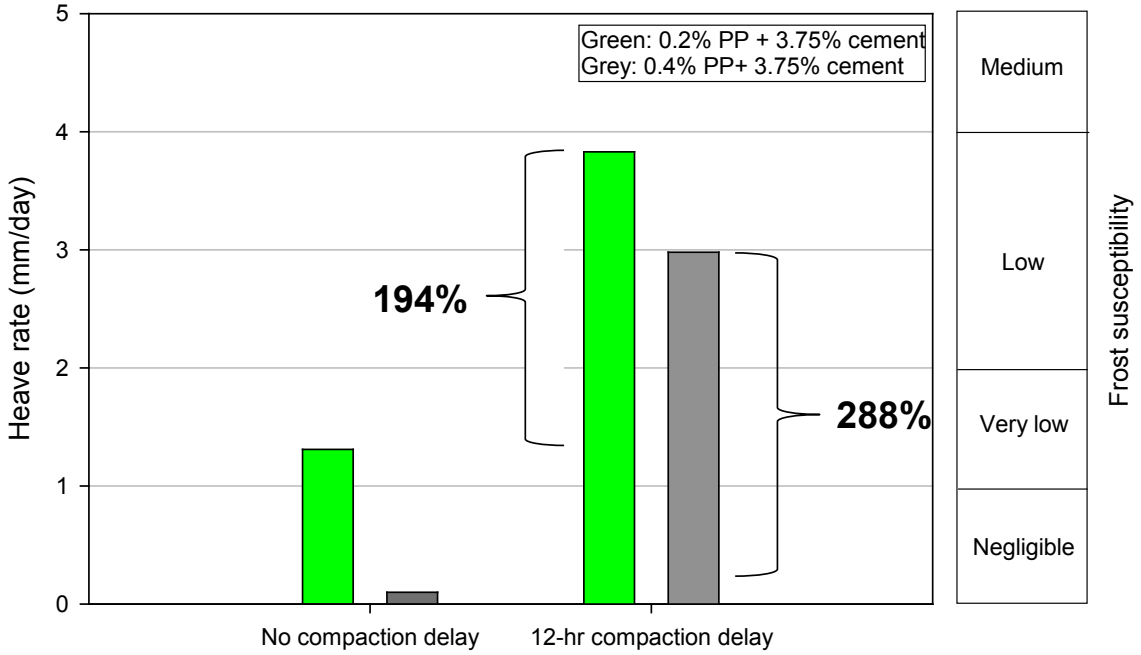

Figure 125. Frost heave rates of cement + fibers stabilized subbase with long compaction delay

Table 60. Summary of frost susceptibility of cement + fiber stabilized recycled subbase with longer compaction delay

Stabilization method	Frost susceptibility based on heave	Frost susceptibility based on CBR
0.2% PP + 3.75% cement (12-hr compaction delay)	Low	Negligible
0.4% PP + 3.75% cement (12-hr compaction delay)	Low	Negligible

Fly ash stabilized western Iowa loess

Western Iowa loess stabilized with 15% FA was tested to evaluate the influence of three cure periods to freeze-thaw performance. The freeze-thaw tests resulted in the same frost susceptibility for both 7-day and 90-day cured samples, which was medium based on heave and high based on CBR. For the 180-day cured samples, the frost susceptibility based on heave was still at high level, but the frost susceptibility based on CBR was decreased to

negligible level. CBR values changed from 7.1% to 32.0% as the cure time extended from 7 days to 180 days. Therefore, 180-day cure is more effective than 90-day cure for improving the frost susceptibility of FA stabilized western Iowa loess, and there was not effective improvement increasing the cure period from 7 days to 90 days. Figure 126 shows the frost heave rates and susceptibility of this kind of materials. Table 61 summarizes the frost susceptibility of FA stabilized western Iowa loess with longer cure period.

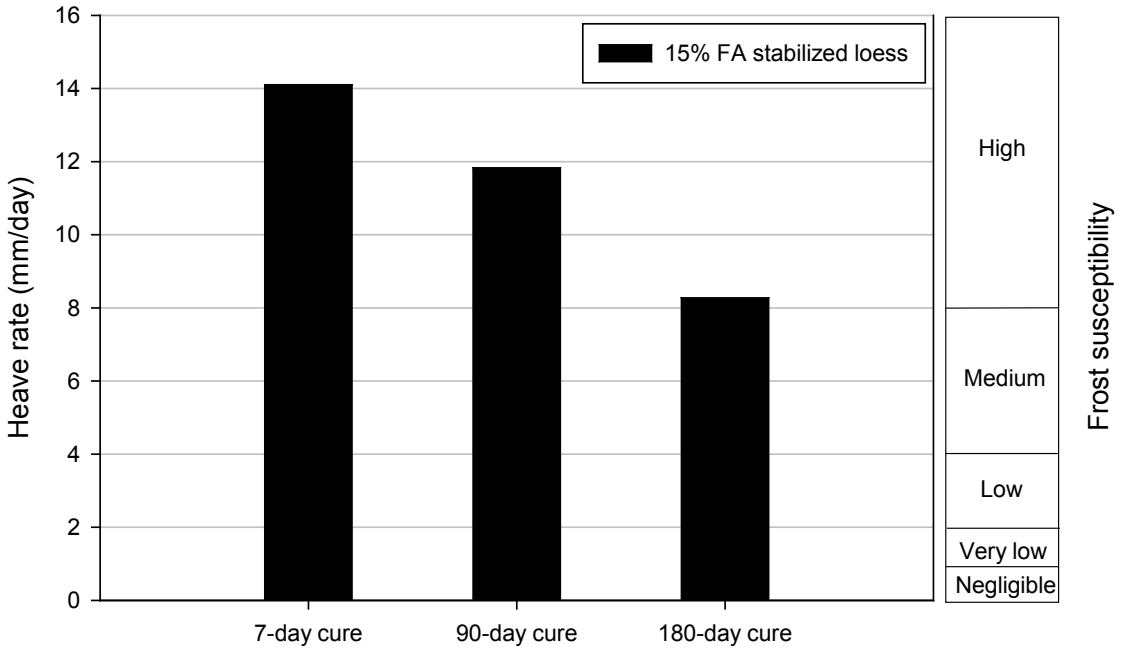

Figure 126. Frost heave rates of FA stabilized western Iowa loess

Table 61. Summary of frost susceptibility of FA stabilized western Iowa loess with longer cure period

Stabilization method	Frost susceptibility based on heave	Frost susceptibility based on CBR
15% fly ash 7 days curing	High	Medium
15% fly ash 90 days curing	High	Medium
15% fly ash 180 days curing	High	Negligible

Overall summary

By testing the frost heave rates and CBR values and comparing the frost susceptibility of each kind of non-stabilized and stabilized geomaterials, cement and cement + geofiber turned out to be more effective than other stabilization methods to improve the frost susceptibility of the geomaterials. Figure 127 shows the laboratory CBR values of non-stabilized and stabilized subgrade and recycled subbase.

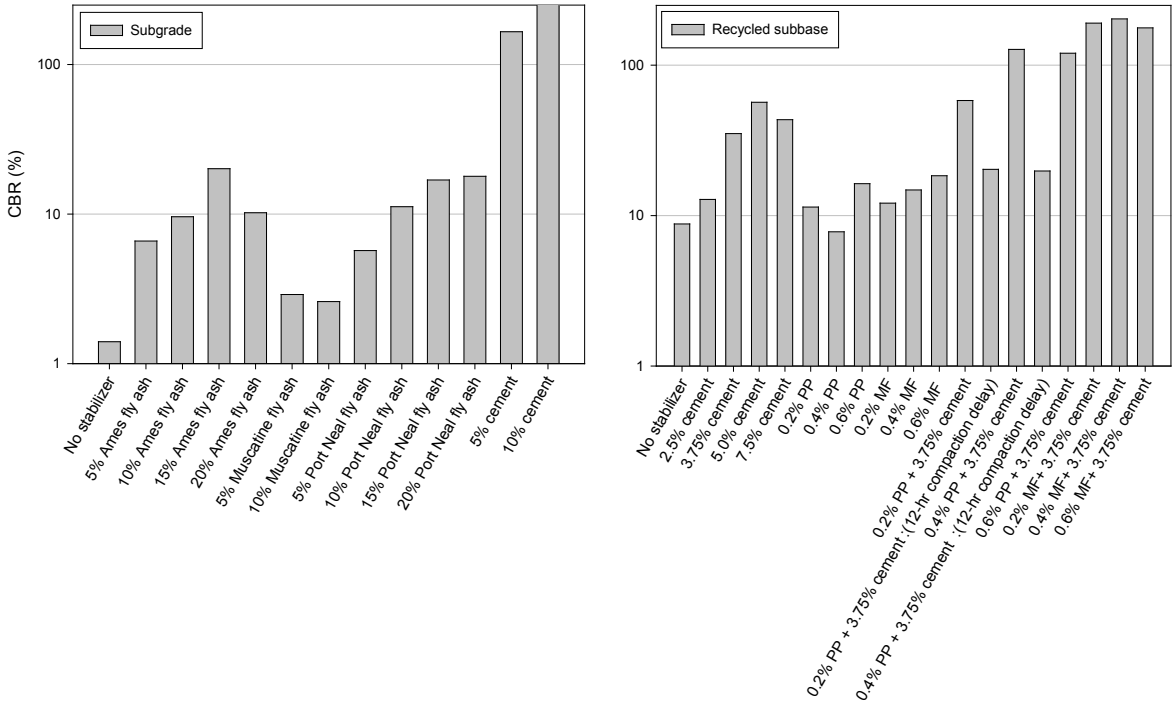

Figure 127. CBR values of non-stabilized and stabilized subgrade and subbase

Water content of each layer was tested to help understand the ice lens theory. According to ice lens theory and the effects of capillary stress, water should be moved upward to form a moisture content gradient as shown in Figure 128. The moisture content decreased as the depth increased. All of the tested samples confirmed this expected trend except for some of the fiber and fiber + cement stabilized subbase samples as shown in Figure 128. The moisture content either did not change or slightly increased as the depth increased in the fiber or fiber-cement samples. The possible reason is the different pore sizes of these two geomaterials. For all tested samples, the moisture content of each layer after freeze-thaw cycles was larger than the original moisture content of mixtures before compaction.

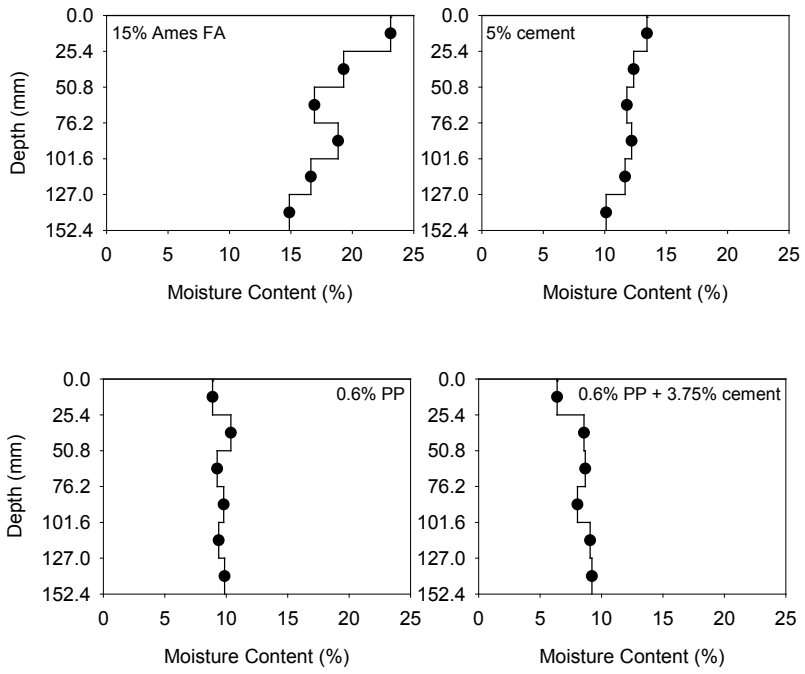

Figure 128. Two kinds of moisture content profiles

Based on the lab results and White's statement (2012), higher initial cost correlates with lower frost susceptibility. 0.4% MF fibers + 3.75% cement stabilized subbase turned out to be the most effective and also the most expensive methods for improving the frost susceptibility. Figure 129 shows the initial costs of different stabilization methods with various frost susceptibility.

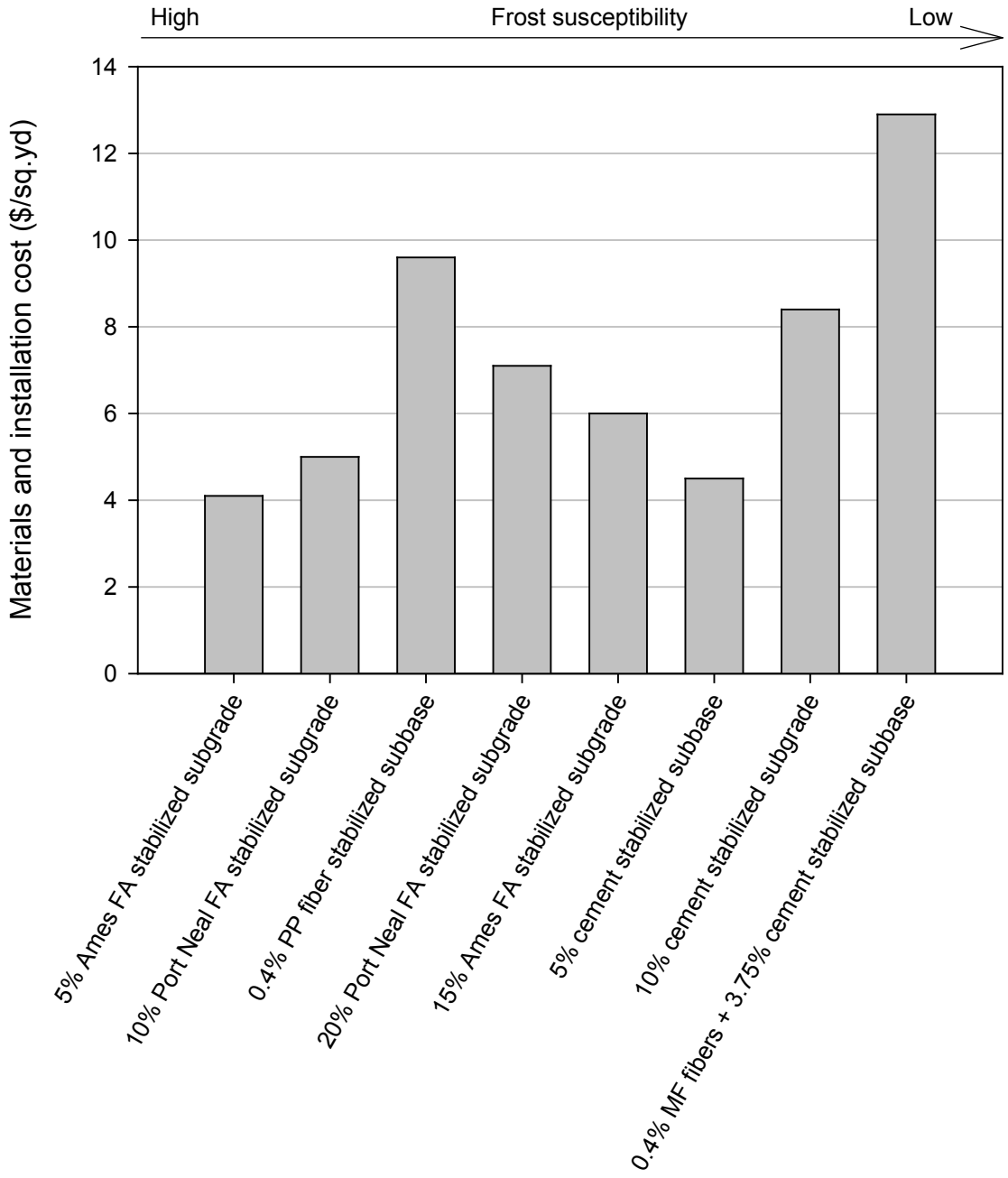

Figure 129. Initial costs of stabilization methods with various frost susceptibility

According to ASTM D5918 (Table 62), frost susceptibility of all the tested materials was classified both based on frost heave rates and CBR values.

Table 62. ASTM D5918 frost susceptibility classification

Frost susceptibility classification	2nd 8-hr heave rate (mm/d)	CBR after thaw (%)
Negligible	<1	>20
Very low	1 to 2	20 to 15
Low	2 to 4	15 to 10
Medium	4 to 8	10 to 5
High	8 to 16	5 to 2
Very High	>16	<2

The frost susceptibility of non-stabilized geomaterials, FA and cement stabilized subgrade, cement, geofiber, and mixtures of cement and geofiber stabilized recycled subbase, and FA stabilized western Iowa loess with different cure periods were classified according to ASTM D5918 based on the test results. Cement and cement + geofiber turned out to be more effective than other stabilization methods to improve the frost susceptibility of both subgrade and recycled subbase. Fly ash with 15% effectively controlled the stiffness changes of subgrade during freeze-thaw cycles. The CBR reduction factor (R_f) is defined as a ratio of two different CBRs. This factor represents the direction and rate of the change between two CBRs. Table 63 summarizes the frost-heave and thaw-weakening test results.

Table 63. Summary of frost-heave and thaw-weakening tests results

Material	Stabilizer	Heave rate (mm/d)	Post-test CBR (%)	Pre-test CBR (%)	R_f	F/S based on heave	F/S based on CBR
Subgrade	No stabilizer	11.43	1.4	2.8	0.21	High	Very high
	5% Ames fly ash	8.40	6.6	15.5	0.43	High	Medium
	10% Ames fly ash	6.60	9.6	44.6	0.22	Medium	Medium
	15% Ames fly ash	6.87	20.1	73.2	0.27	Medium	NG
	20% Ames fly ash	7.85	10.2	18.2	0.56	Medium	Low
	5% Muscatine fly ash	9.88	2.9	—	—	High	High
	10% Muscatine fly ash	12.32	2.6	—	—	High	High
	5% Port Neal fly ash	6.61	5.7	—	—	Medium	Medium
	10% Port Neal fly ash	8.21	11.2	15.0	0.75	High	Low
	15% Port Neal fly ash	1.96	16.9	25.8	0.66	Very low	Very low
	20% Port Neal fly ash	3.16	17.9	—	—	Low	Very low
	5% cement	<1.00	165.8	37.3	4.45	NG	NG

Table 63. Summary of frost-heave and thaw-weakening tests results (continued)

Material	Stabilizer	Heave rate (mm/d)	Post-test CBR (%)	Pre-test CBR (%)	R_f	F/S based on heave	F/S based on CBR
Subgrade	10% cement	<1.00	TH	94.5	—	NG	NG
Recycled subbase	No stabilizer	15.63	8.8	4.6	1.91	High	Medium
	2.5% cement	12.70	12.8	95.6	0.13	High	Low
	3.75% cement	2.09	35.1	127.0	0.28	Low	NG
	5.0% cement	3.35	56.7	208.9	0.27	Low	NG
	7.5% cement	1.64	43.4	TH	—	Very low	NG
	0.2% PP	12.11	11.4	4.6	2.48	High	Low
	0.4% PP	12.75	7.8	7.3	1.07	High	Medium
	0.6% PP	6.25	16.3	5.8	2.81	Medium	Very low
	0.2% MF	10.34	12.1	4.1	2.95	High	Low
	0.4% MF	9.90	14.8	7.9	1.87	High	Low
	0.6% MF	6.94	18.4	8.6	2.14	Medium	Very low
	0.2% PP + 3.75% cement	1.31	58.2	185.5	0.31	Very low	NG
	0.2% PP + 3.75% cement (12-hr compaction delay)	3.83	20.3	—	—	Low	NG
	0.4% PP + 3.75% cement	<1.00	127.4	TH	—	NG	NG
	0.4% PP + 3.75% cement (12-hr compaction delay)	2.98	19.8	—	—	Low	NG
	0.6% PP + 3.75% cement	1.48	120.1	TH	—	Very low	Very low
	0.2% MF+ 3.75% cement	0.75	190.5	184.9	1.03	NG	NG
	0.4% MF+ 3.75% cement	1.43	203.2	143.1	1.42	Very low	NG
	0.6% MF+ 3.75% cement	1.00	177.0	158.7	1.12	NG	NG
Western Iowa loess	15% fly ash 7 days curing	14.10	7.1	—	—	High	Medium
	15% fly ash 90 days curing	11.83	8.7	—	—	High	Medium
	15% fly ash 180 days curing	8.27	32.0	—	—	High	NG

Legend: F/T=Freeze-thaw, F/S=Frost susceptibility, TH=Too high, NG=Negligible, —=Data not available.

IN SITU TESTS

In situ tests, including dynamic cone penetration (DCP) tests and falling weight deflectometer (FWD) tests, were performed at the Boone County Test Sections site. The California bearing ratio (CBR) of each layer was determined from DCP tests. The deflection measured at the center of the loading plate (D_0) was the direct output from the FWD tests, which can be used to determine the elastic modulus (E) of the composite pavement system. Lower D_0 indicates larger elastic modulus, which stands for the pavement is stiffer. The D_0 used in this research was correlated to a loading of 14000 lbs. Table 64 shows the stabilization technology for each street segment implemented at the Boone Test Sections site.

The following sections present the DCP profiles and D_0 variations of each street segment at different time. The data from October 2012 can be treated as the before-freezing test results; the data from February 2013 can be treated as the during-freezing (frozen) test results; and the April 2013 data can be treated as the after-thawing test results. By comparing the test results at these different times, the effects of freezing and thawing on the properties of soils with different stabilization methods can be evaluated. The effectiveness of different stabilization methods on controlling the influences from freezing and thawing can also be compared.

Table 64. Stabilization technologies implemented at the Boone Test Sections site

Street	Segment	Foundation Layer Profile (above natural subgrade)	
1st St.	North	6 in. CLSB	12 in. compacted subgrade
	South		
2nd St.	North	6 in. CLSB	12 in. mechanically stabilized subgrade
	South		
3rd St.	North	2 in. CLSB	4 in. geocell reinforced MSB, NW geotextile
	South	1 in. CLSB	6 in. geocell reinforced MSB, NW geotextile
4th St.	North	6 in. CLSB	NW geotextile
	South	6 in. CLSB	woven geotextile
5th St.	North	6 in. CLSB	triaxial geogrid
	South	6 in. CLSB	biaxial geogrid

Table 64. Stabilization technologies implemented at the Boone Test Sections site (continued)

Street	Segment	Foundation Layer Profile (above natural subgrade)	
6th St.	North	6 in. CLSB	6 in. recycled subbase + 5% cement + 0.4% PP fibers
	South	6 in. CLSB	Synthetic Subsurface Drainage Layer, 6 in. recycled subbase + 5% cement + 0.4% MF fibers
7th St.	North	6 in. MSB	6 in. recycled subbase + 5% cement
	South		
8th St.	North	6 in. CLSB	12 in. compacted subgrade
	South		
9th St.	North	6 in. CLSB	6 in. reclaimed subbase
	South		
10th St.	North	6 in. CLSB	compacted subgrade
	South		Natural subgrade
11th St.	North	6 in. CLSB	12 in. 10% cement stabilized subgrade
	South	6 in. CLSB	12 in. 20% fly ash (Port Neal) stabilized subgrade
12th St.	North	6 in. CLSB	12 in. 15% fly ash (Ames) stabilized subgrade
	South	6 in. CLSB	12 in. 10% fly ash (Muscatine and Port Neal) stabilized subgrade

Legend: CLSB = crushed limestone subbase GP-GM or A-1-a (7% fines content), NW = non-woven.

1st Street South

The layer between 6 in. and 18 in. of the 1st Street South was compacted subgrade. The DCP profiles of April 2012, October 2012, and April 2013 are shown in Figure 130. The average CBR value of the layer in October 2012 was 12.0% compared with 37.0% in April 2013.

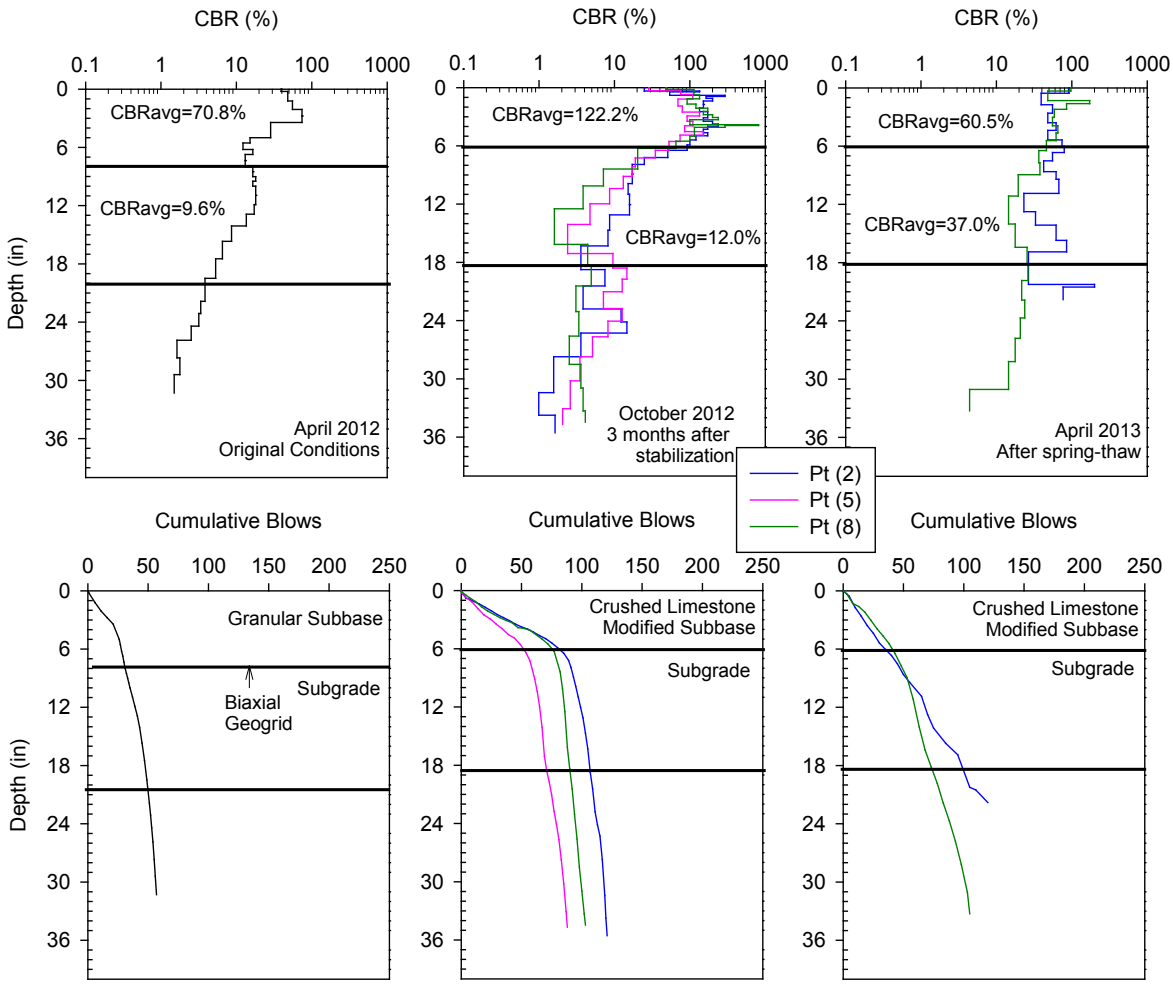

Figure 130. 1st Street South seasonal DCP variations

The variation of D_0 with time is shown in Figure 131. It presents a decrease in D_0 at February 2013 followed by an increase at April 2013. This represents the effects of freezing and thawing to the soil stiffness.

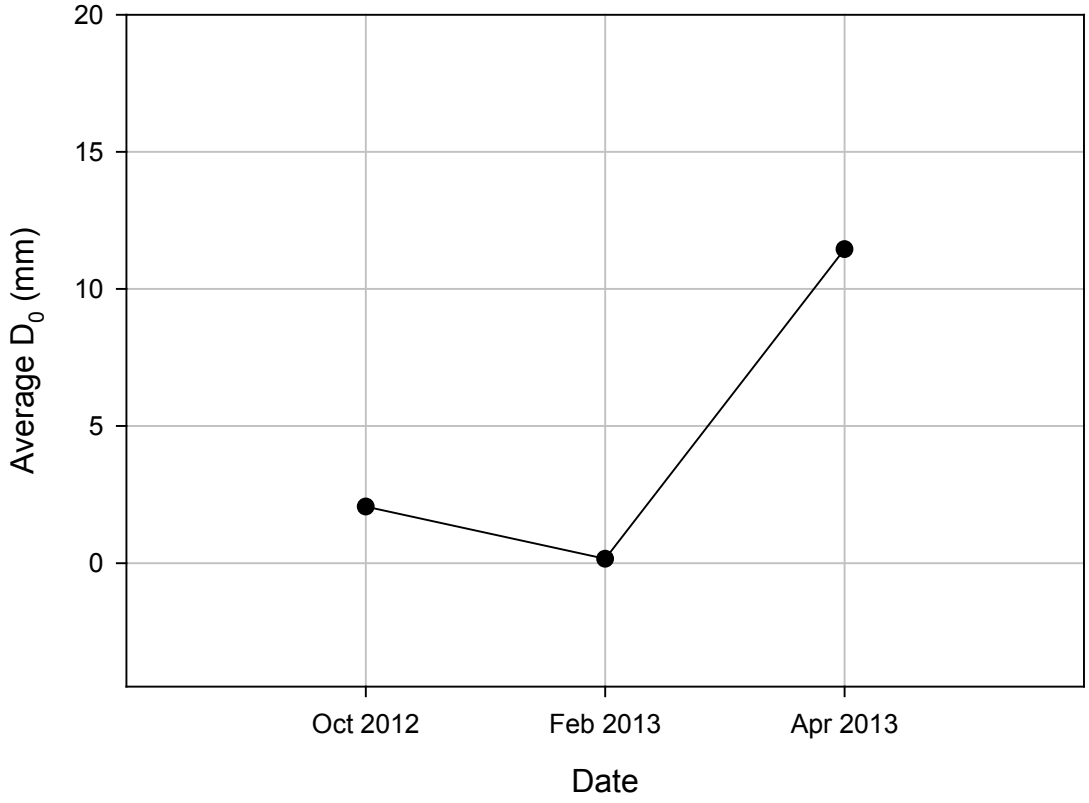

Figure 131. 1st Street South seasonal D_0 variations

1st Street North

The 6 inch to 18 inch layer of the 1st Street North was also stabilized with compacted subgrade. The DCP profiles of April 2012, October 2012, and April 2013 are shown in Figure 132. The average CBR value of stabilized layer at October 2012 was less than the April 2013 value.

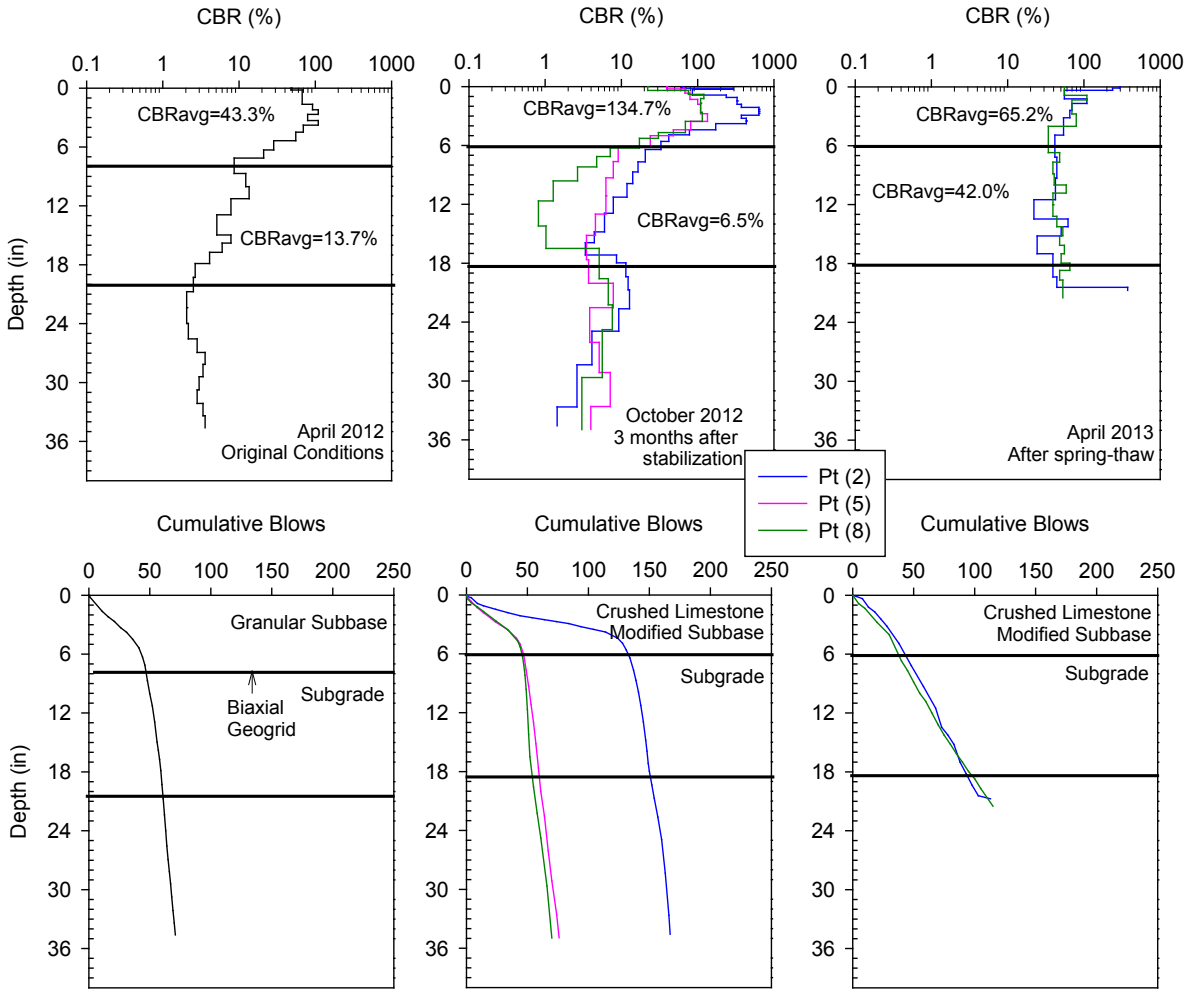

Figure 132. 1st Street North seasonal DCP variations

The variation of D_0 with time is shown in Figure 133. It presents a decrease in D_0 at February 2013 followed by an increase at April 2013. This represents the effects of freezing and thawing on the soil stiffness.

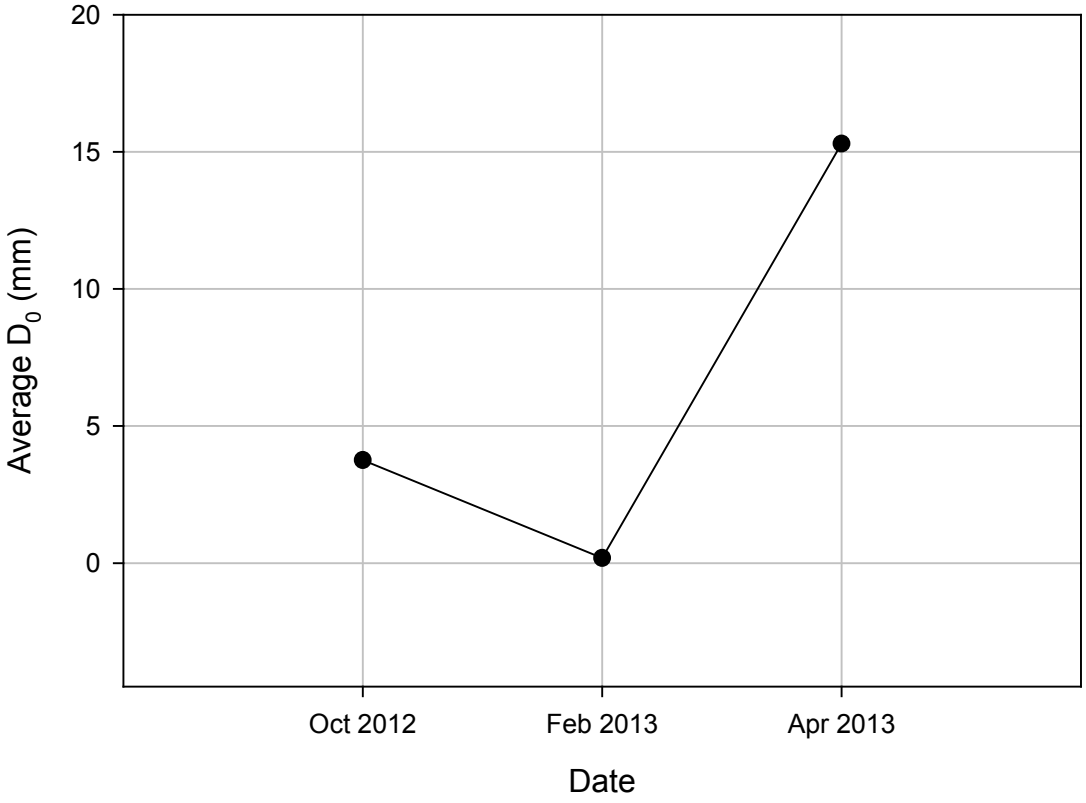

Figure 133. 1st Street North seasonal D_0 variations

2nd Street South

The 6 inch to 18 inch layer of the 2nd Street South was stabilized with mechanically stabilized subgrade. The DCP profiles of April 2012, October 2012, and April 2013 are shown in Figure 134. The average CBR value of stabilized layer at October 2012 was less than the April 2013 value.

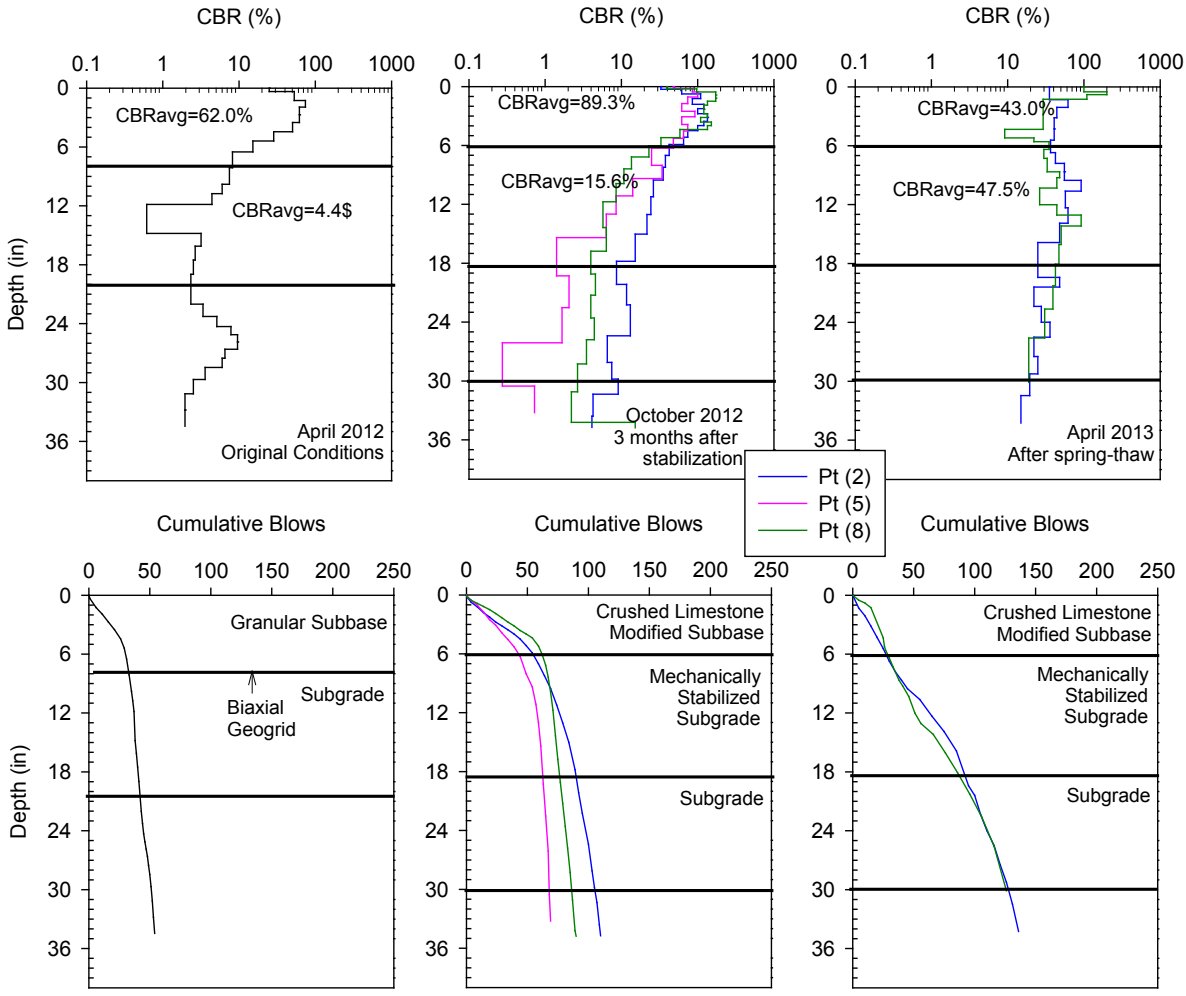

Figure 134. 2nd Street South seasonal DCP variations

The variation of D_0 with time is shown in Figure 135. It presents a decrease in D_0 at February 2013 followed by an increase at April 2013. This represents the effects of freezing and thawing to the soil stiffness.

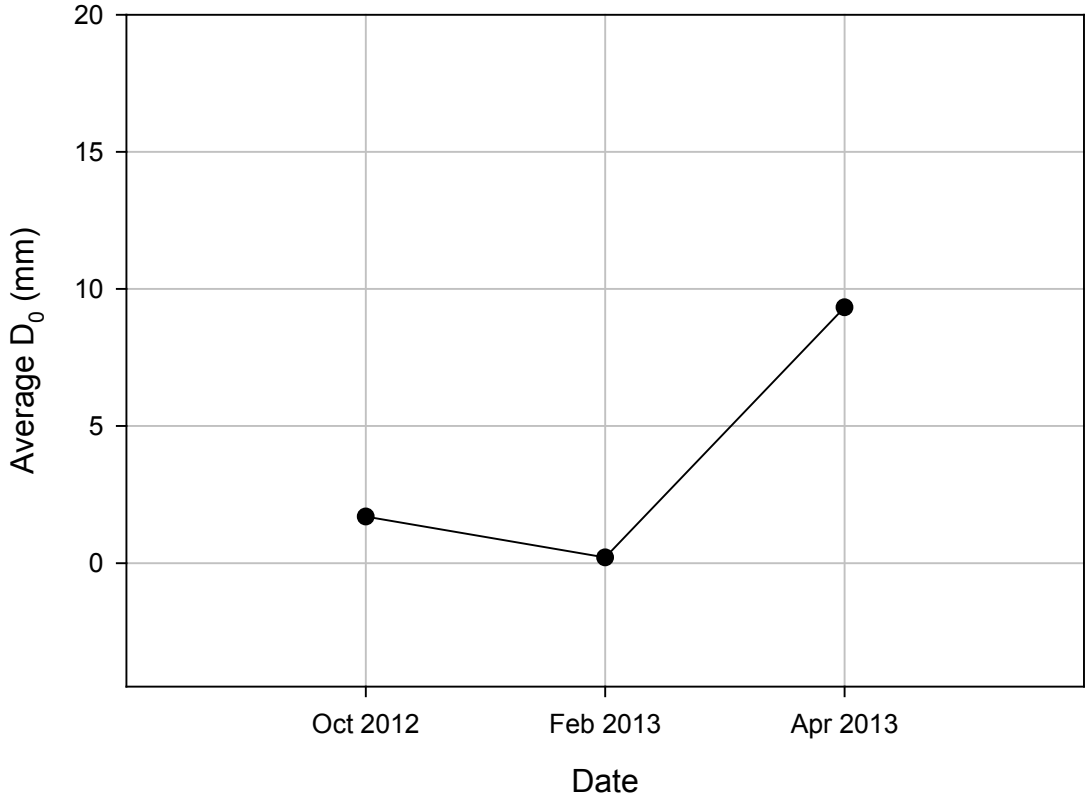

Figure 135. 2nd Street South seasonal D_0 variations

2nd Street North

The 6 inch to 18 inch layer of the 2nd Street North was stabilized with mechanically stabilized subgrade. The DCP profiles of April 2012, October 2012, and April 2013 are shown in Figure 136. The average CBR value of stabilized layer at October 2012 was less than the April 2013 value.

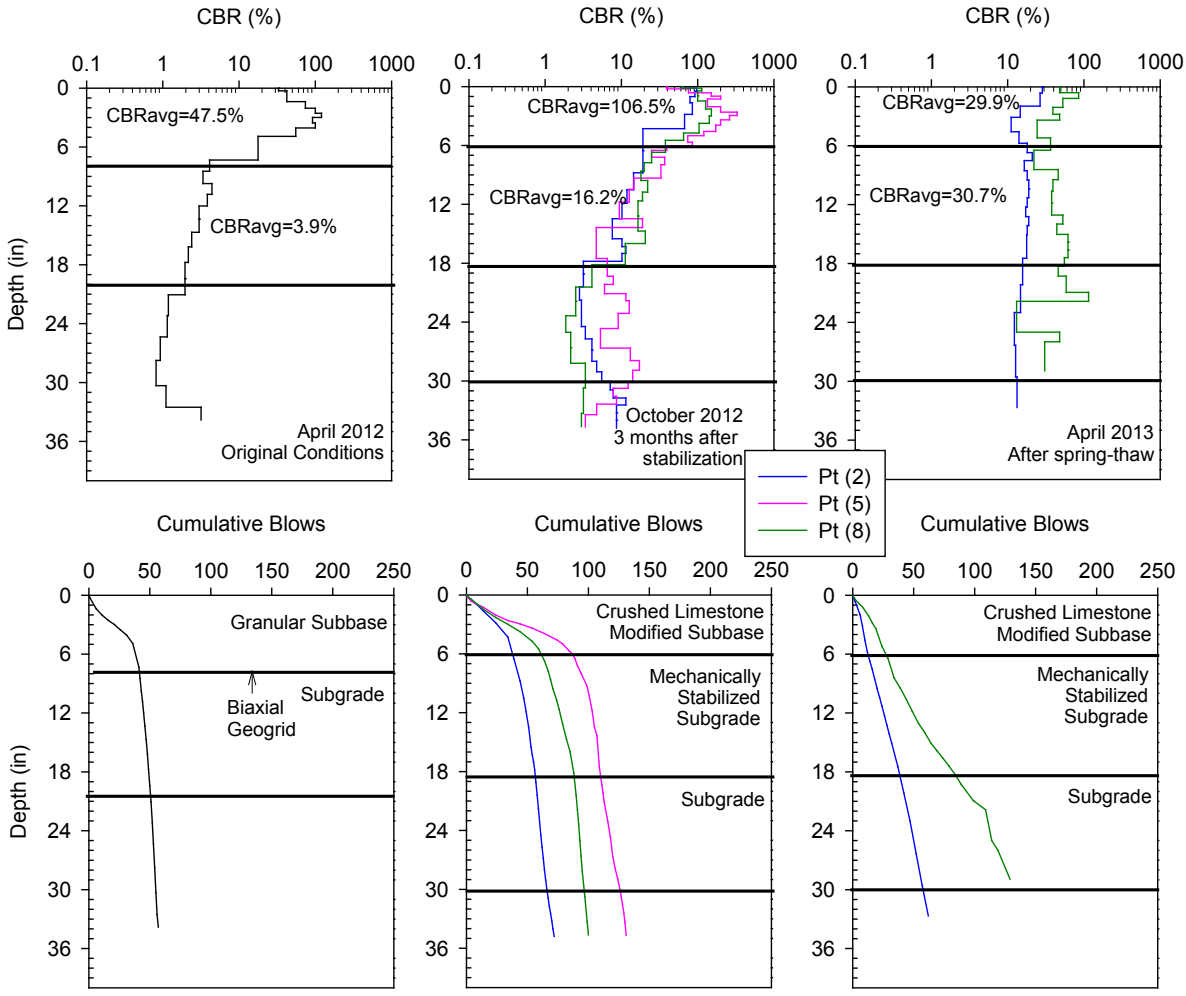

Figure 136. 2nd Street North seasonal DCP variations

The variation of D_0 with time is shown in Figure 137. It presents a decrease in D_0 at February 2013 followed by an increase at April 2013. This represents the effects of freezing and thawing to the soil stiffness.

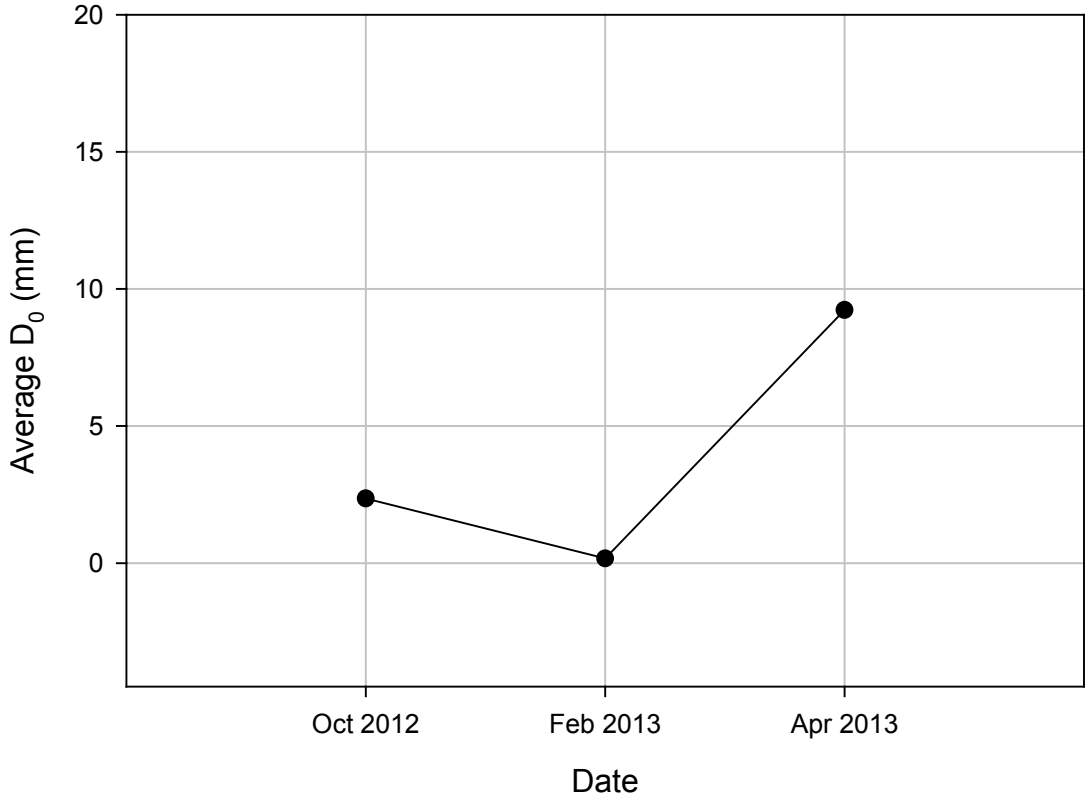

Figure 137. 2nd Street North seasonal D_0 variations

3rd Street South

Geocell and non-woven geotextile were used to stabilize the 3rd Street South. The DCP profiles of April 2012, October 2012, and April 2013 are shown in Figure 138. The average CBR value of stabilized layer of October 2012 was larger than the April 2013 value.

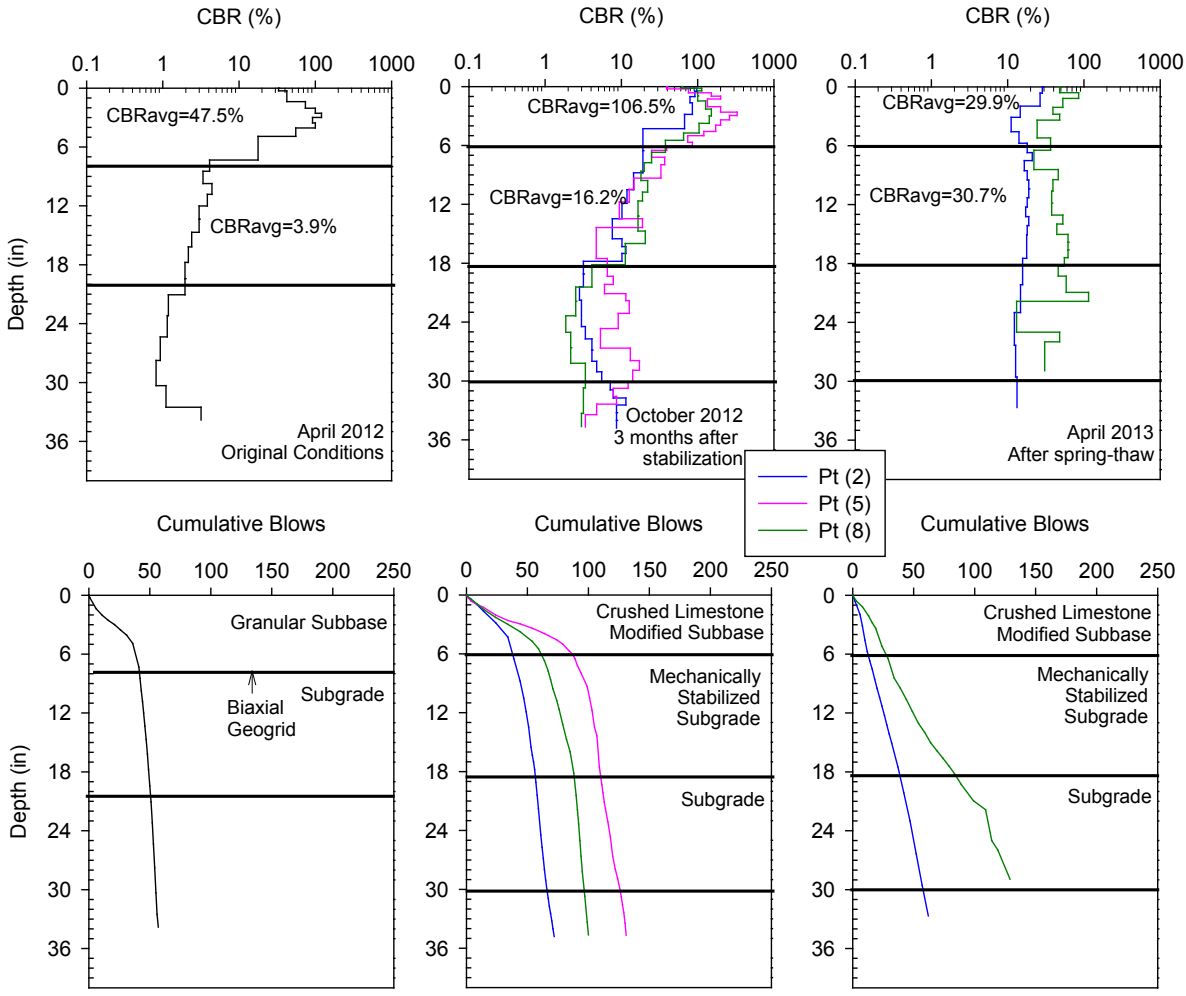

Figure 138. 3rd Street South seasonal DCP variations

The variation of D_0 with time is shown in Figure 139. It presents a decrease in D_0 at February 2013 followed by an increase at April 2013. This represents the effects of freezing and thawing to the soil stiffness.

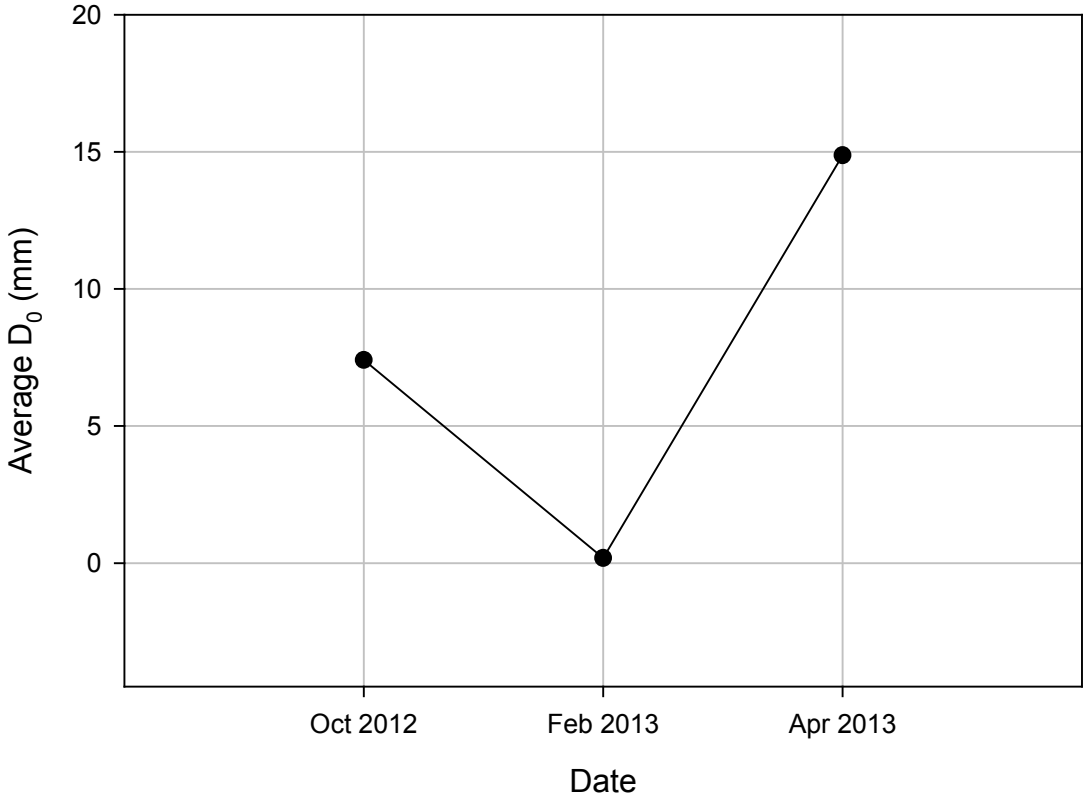

Figure 139. 3rd Street South seasonal D_0 variations

3rd Street North

Geocell and non-woven geotextile were used to stabilize the 3rd Street North. The DCP profiles of April 2012, October 2012, and April 2013 are shown in Figure 140. The average CBR value of stabilized layer of October 2012 was less than the April 2013 value.

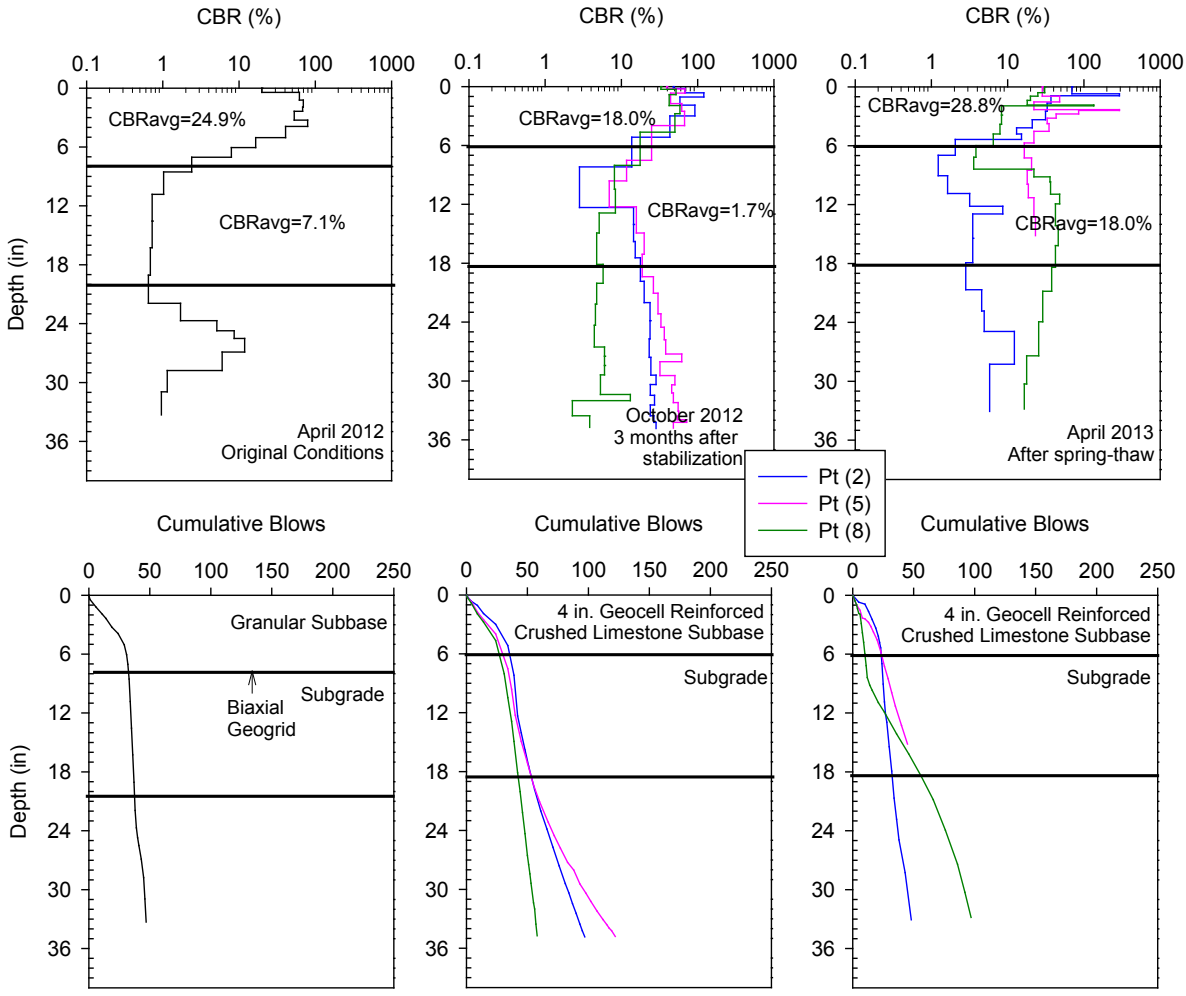

Figure 140. 3rd Street North seasonal DCP variations

The variation of D_0 with time is shown in Figure 141. It presents a decrease in D_0 at February 2013 followed by an increase at April 2013. This represents the effects of freezing and thawing to the soil stiffness.

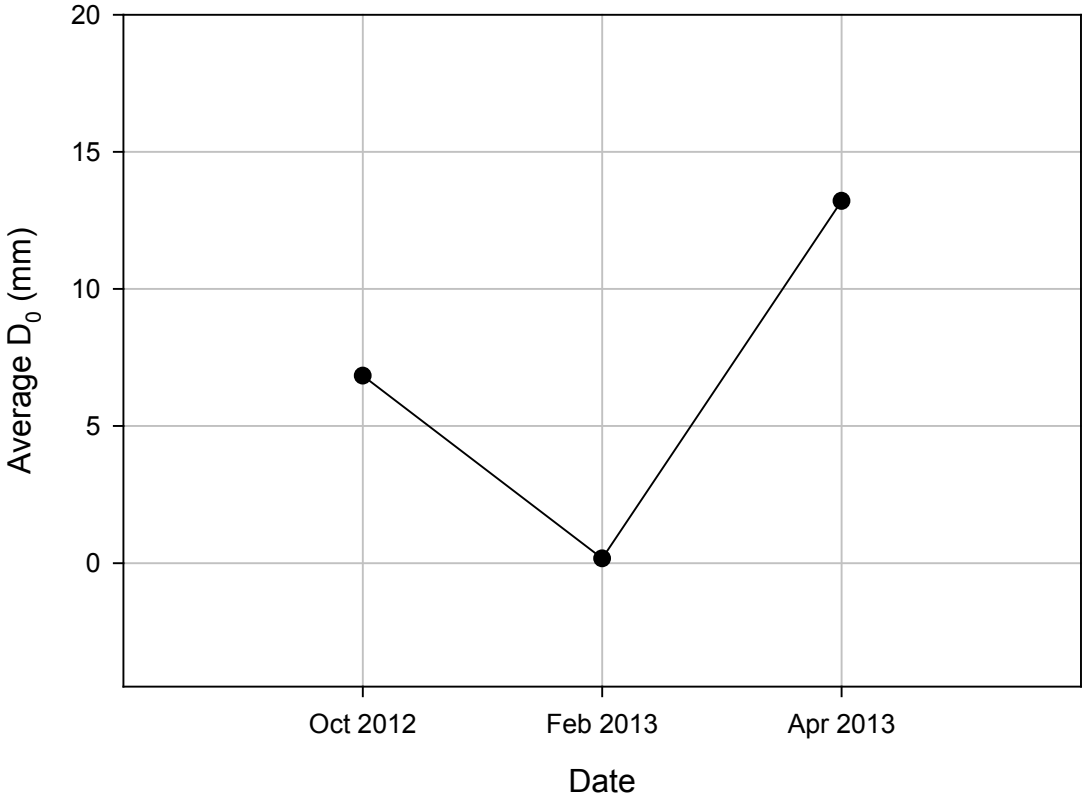

Figure 141. 3rd Street North seasonal D_0 variations

4th Street South

Woven geotextile was used to stabilize the 4th Street South. The DCP profiles of April 2012, October 2012, and April 2013 are shown in Figure 142. The average CBR value of stabilized layer at October 2012 was larger than the April 2013 value.

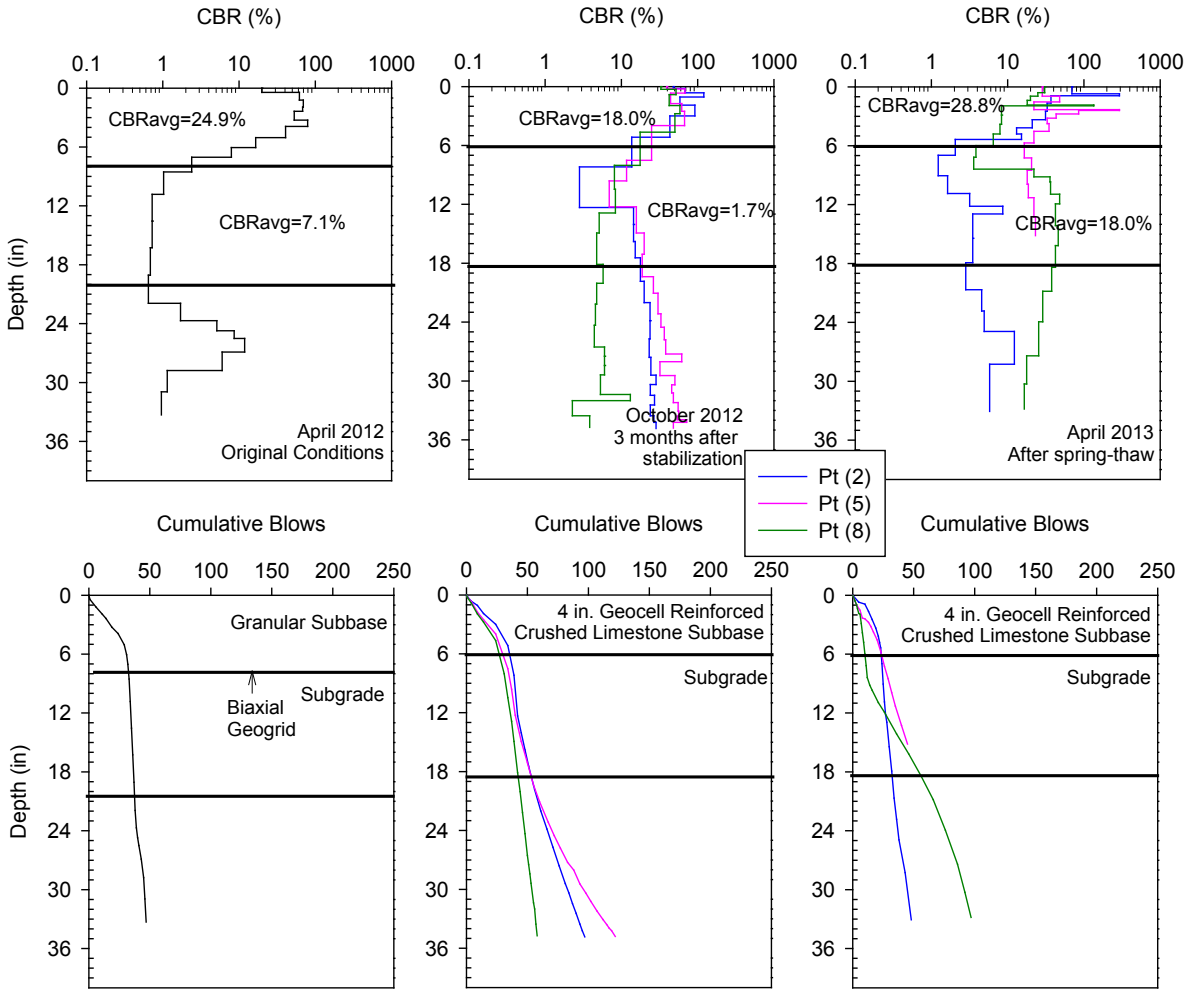

Figure 142. 4th Street South seasonal DCP variations

The variation of D_0 with time is shown in Figure 143. It presents a decrease in D_0 at February 2013 followed by an increase at April 2013. This represents the effects of freezing and thawing to the soil stiffness.

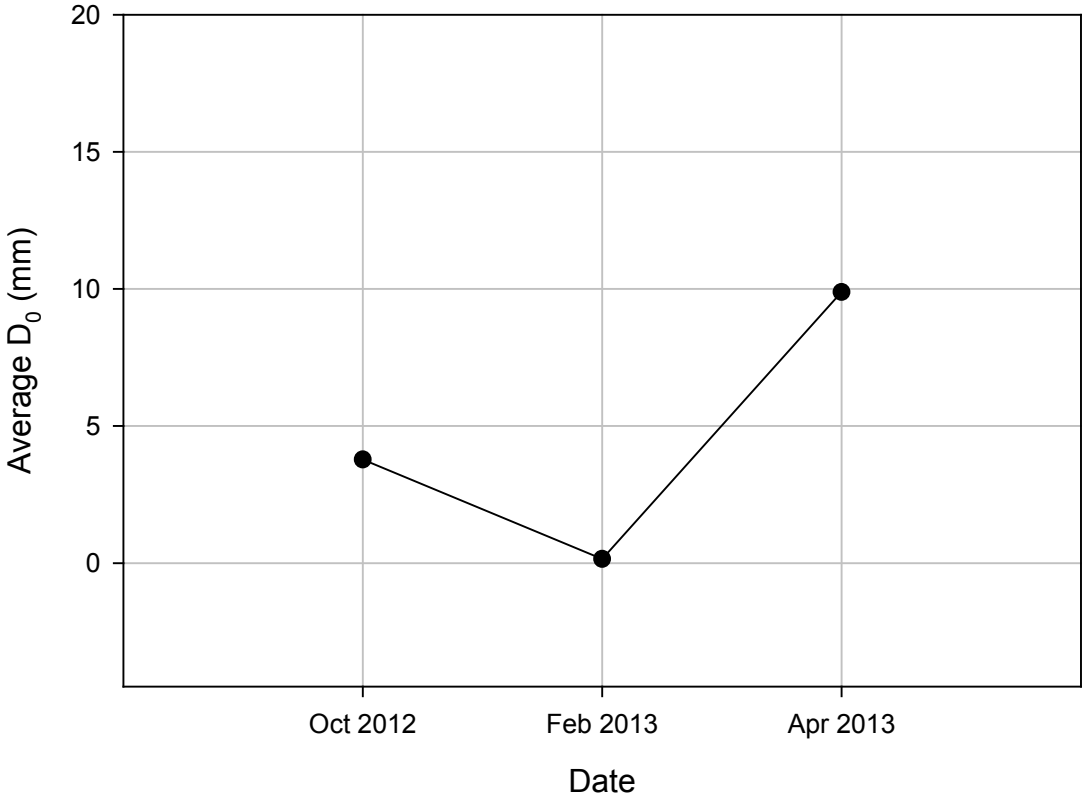

Figure 143. 4th Street South seasonal D_0 variations

4th Street North

Non-woven geotextile was used to stabilize the 4th Street North. The DCP profiles of April 2012, October 2012, and April 2013 are shown in Figure 144. The average CBR value of stabilized layer at October 2012 was larger than the April 2013 value.

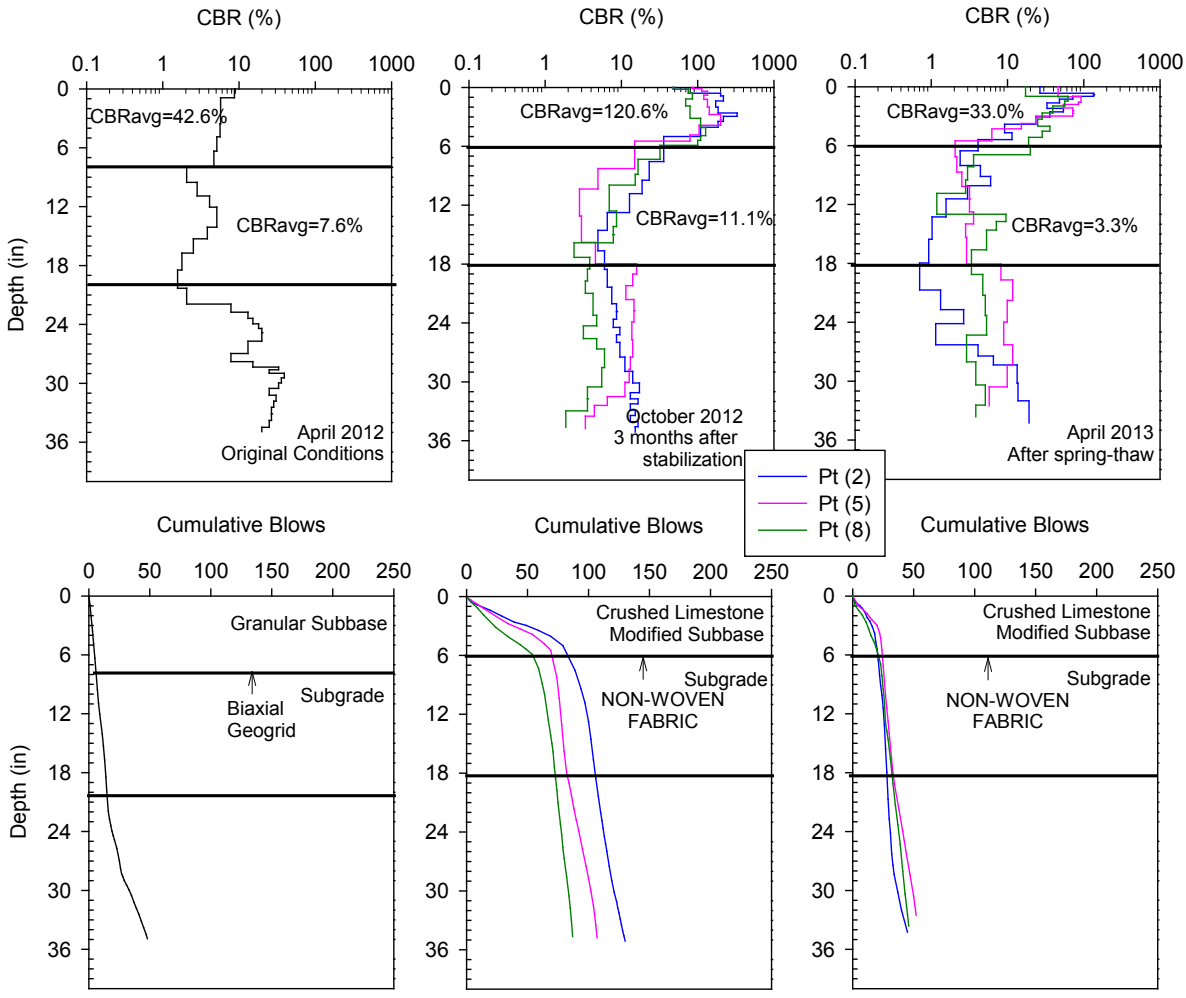

Figure 144. 4th Street North seasonal DCP variations

The variation of D_0 with time is shown in Figure 145. It presents a decrease in D_0 at February 2013 followed by an increase at April 2013. This represents the effects of freezing and thawing to the soil stiffness.

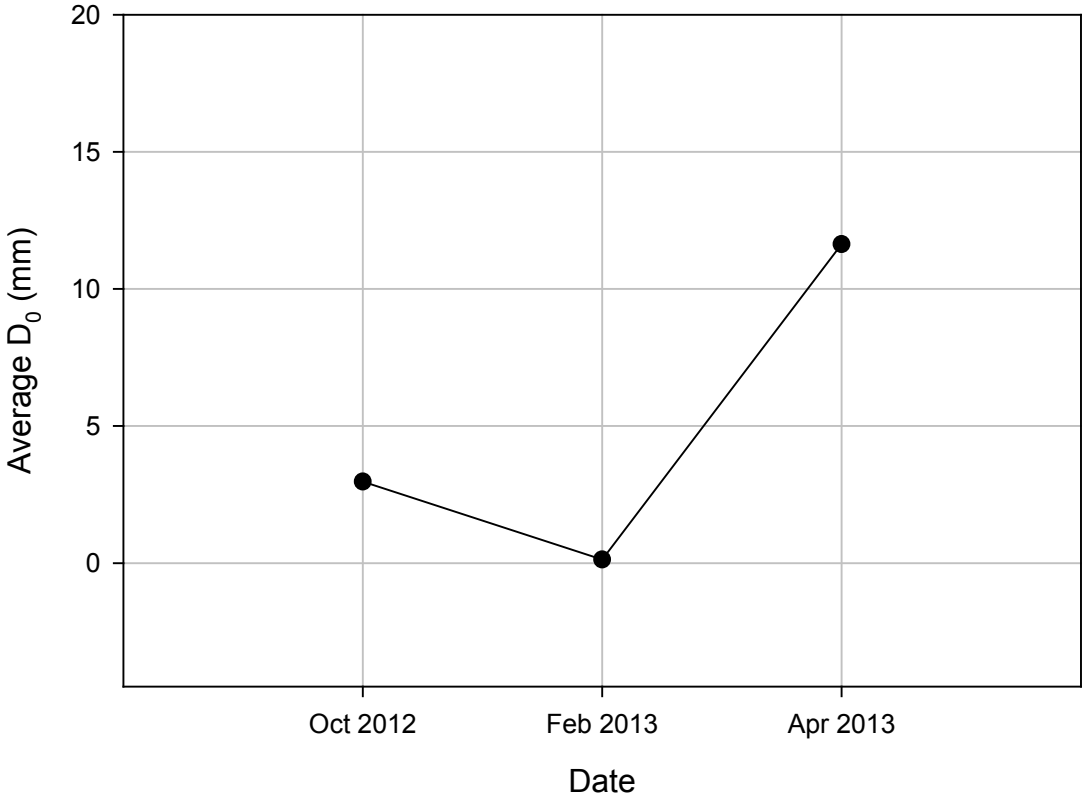

Figure 145. 4th Street North seasonal D_0 variations

5th Street South

Biaxial geogrid was used to stabilize the 5th Street South. The DCP profiles of April 2012, October 2012, and April 2013 are shown in Figure 146. The average CBR value of stabilized layer at October 2012 was larger than the April 2013 value.

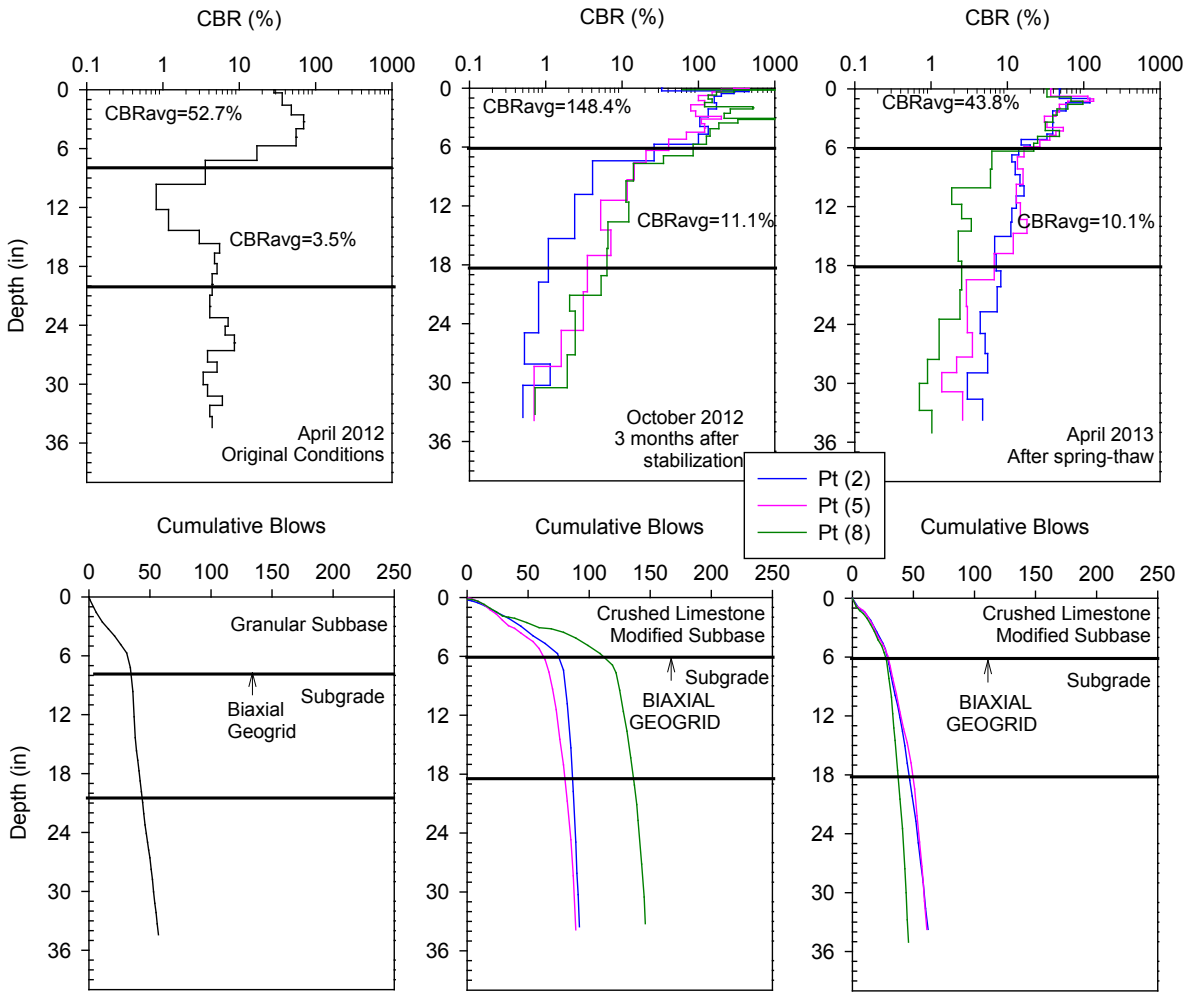

Figure 146. 5th Street South seasonal DCP variations

The variation of D_0 with time is shown in Figure 147. It presents a decrease in D_0 at February 2013 followed by an increase at April 2013. This represents the effects of freezing and thawing to the soil stiffness.

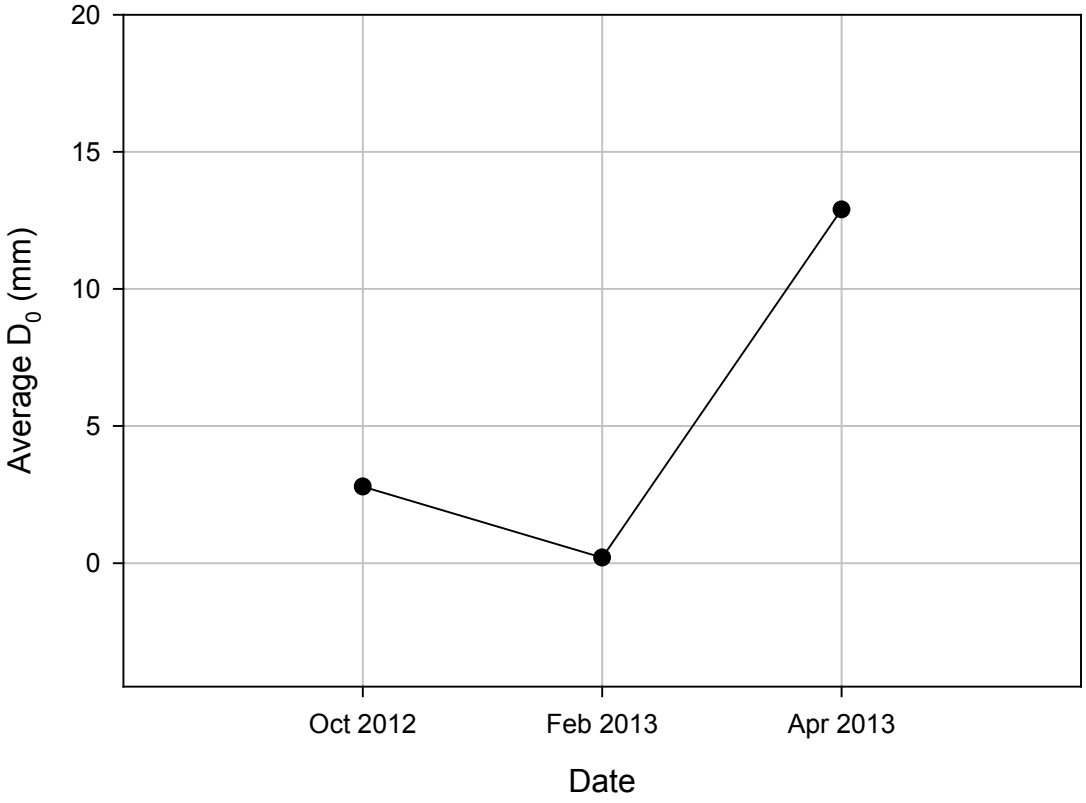

Figure 147. 5th Street South seasonal D_0 variations

5th Street North

Triaxial geogrid was used to stabilize the 5th Street North. The DCP profiles of April 2012, October 2012, and April 2013 are shown in Figure 148. The average CBR value of stabilized layer at October 2012 was larger than the April 2013 value.

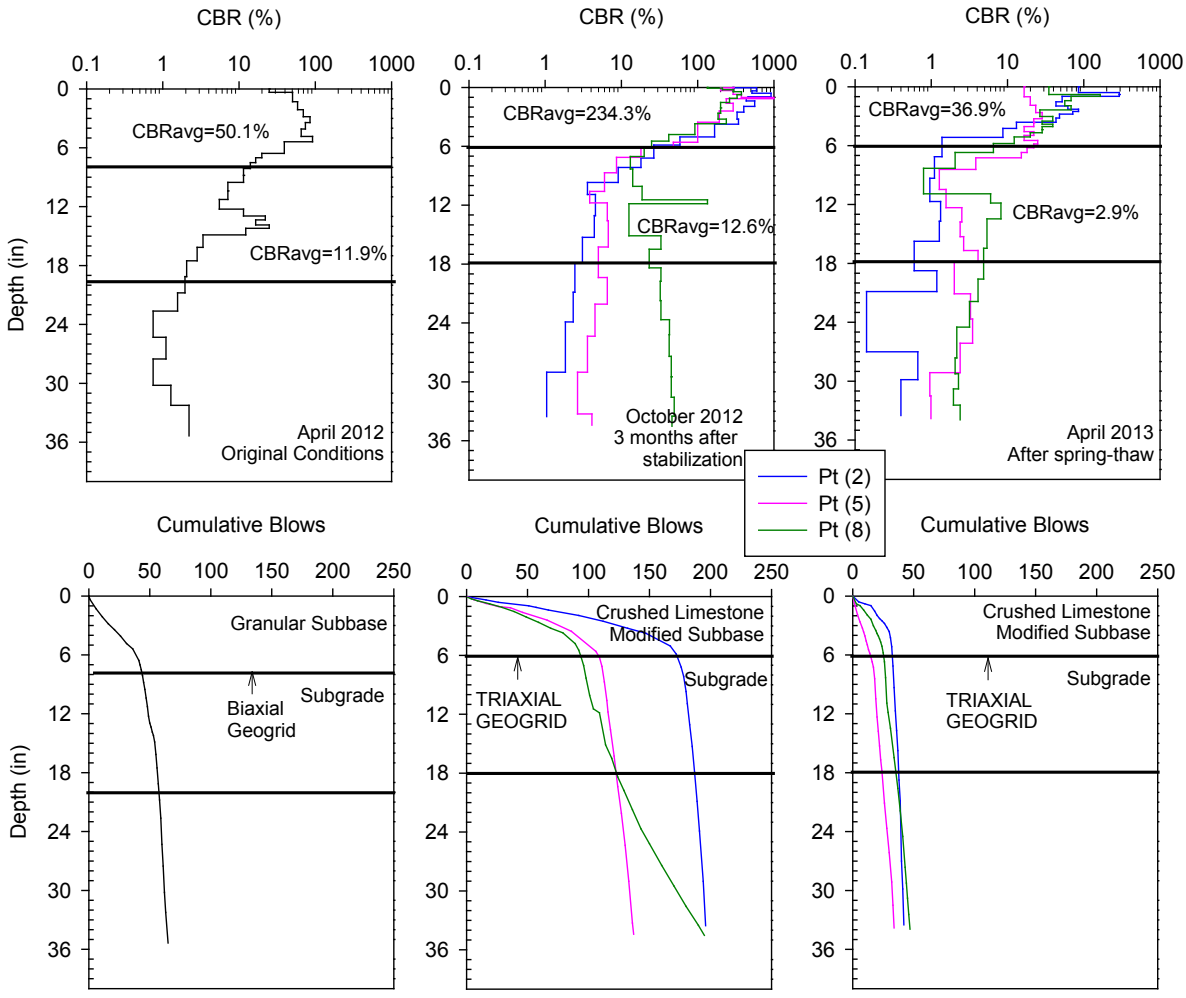

Figure 148. 5th Street North seasonal DCP variations

The variation of D_0 with time is shown in Figure 149. It presents a decrease in D_0 at February 2013 followed by an increase at April 2013. This represents the effects of freezing and thawing to the soil stiffness.

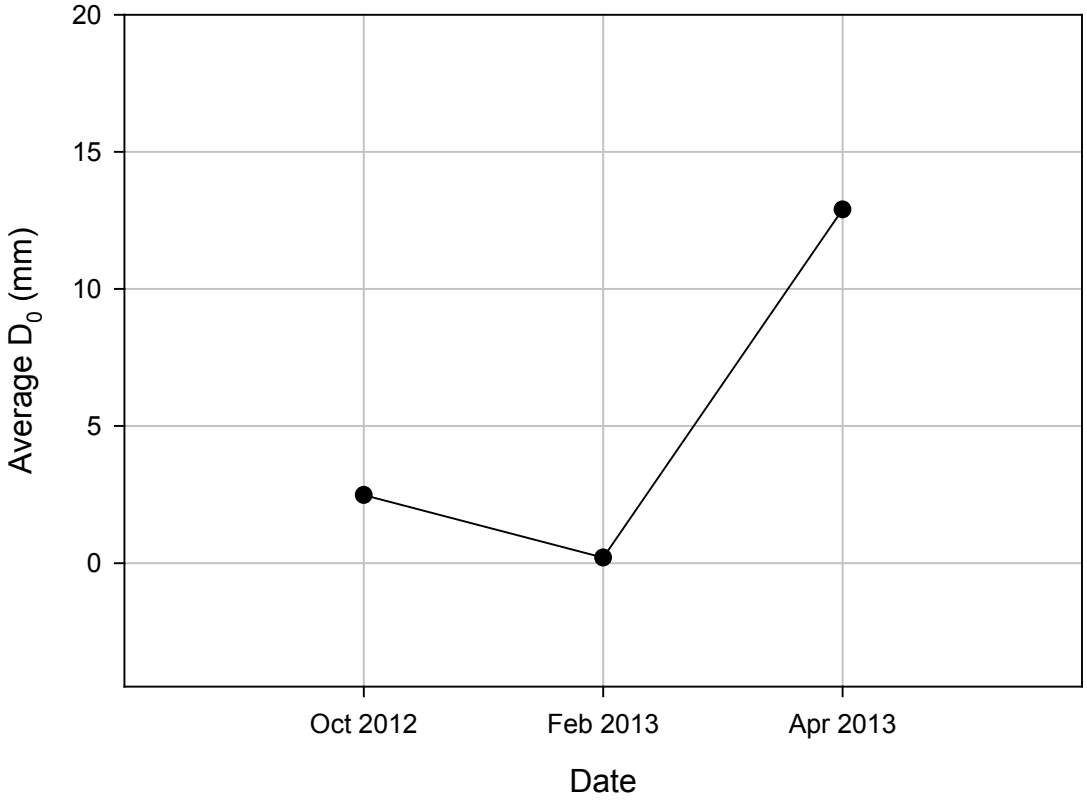

Figure 149. 5th Street North seasonal D_0 variations

6th Street South

Recycled subbase was stabilized with 5% cement + 0.4% MF fiber at the 6th Street South. The DCP profiles of April 2012, October 2012, and April 2013 are shown in Figure 150. DCP refusal was obtained for the stabilized layers at both October 2012 and April 2013.

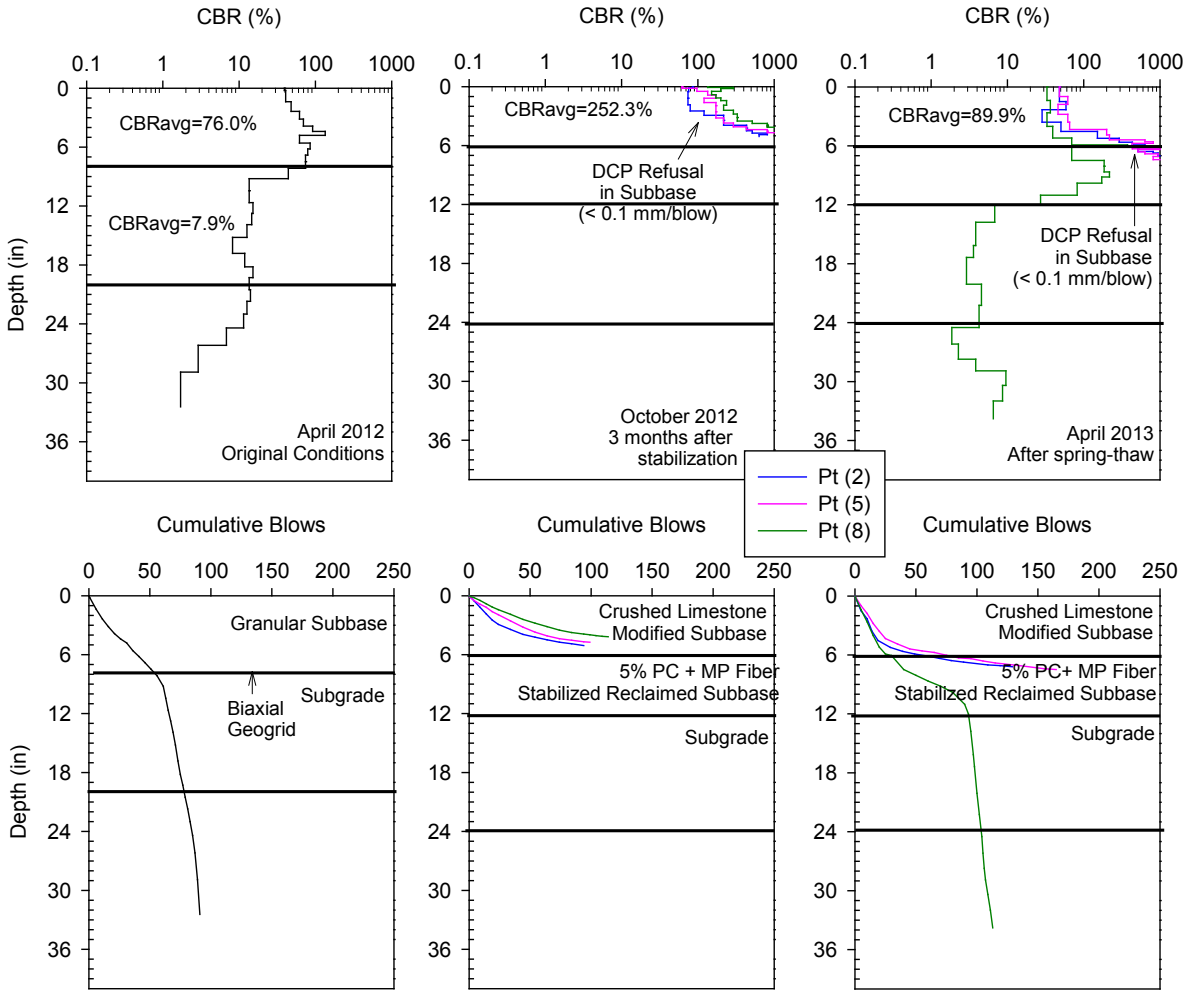

Figure 150. 6th Street South seasonal DCP variations

The variation of D_0 with time is shown in Figure 151. It presents a decrease in D_0 at February 2013 followed by an increase at April 2013. This represents the effects of freezing and thawing to the soil stiffness.

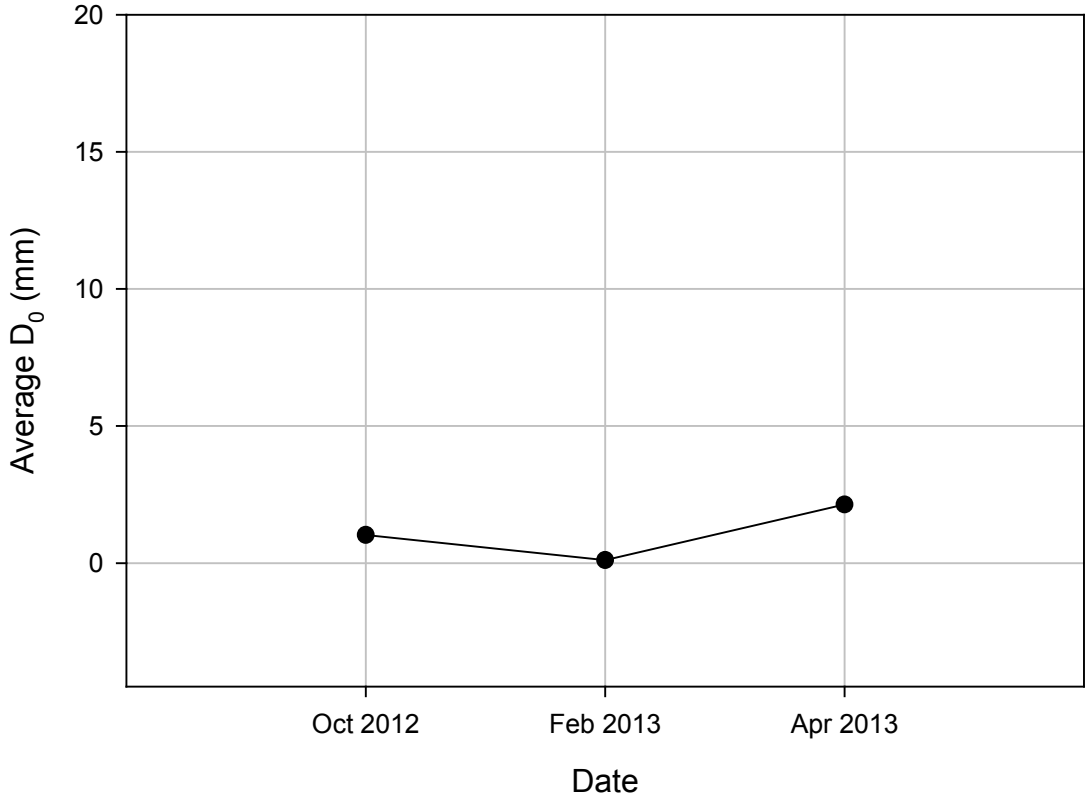

Figure 151. 6th Street South seasonal D_0 variations

6th Street North

Recycled subbase was stabilized with 5% cement + 0.4% PP fiber at the 6th Street North. The DCP profiles of April 2012, October 2012, and April 2013 are shown in Figure 152. The average CBR value of stabilized layer at October 2012 was larger than the April 2013 value.

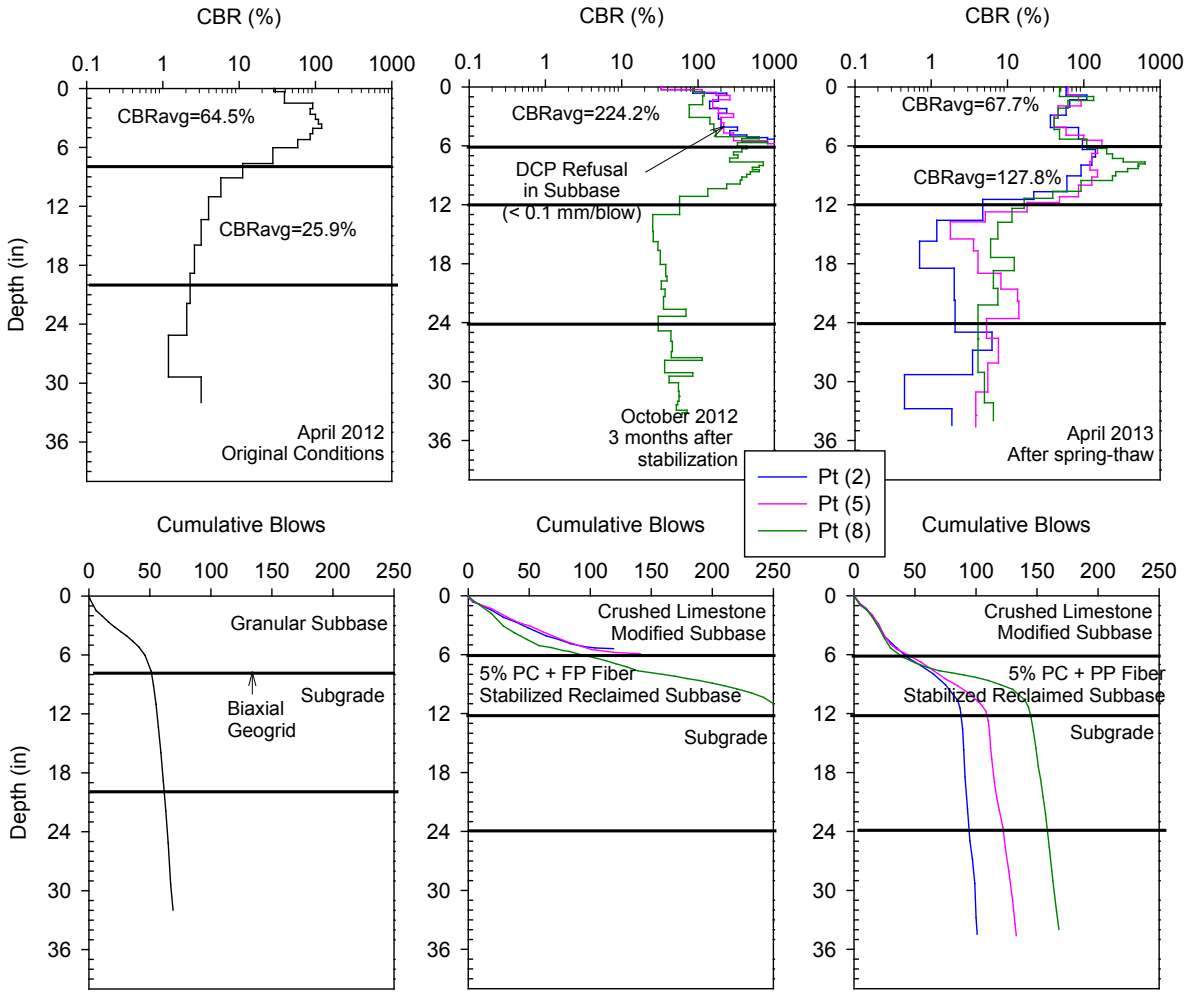

Figure 152. 6th Street North seasonal DCP variations

The variation of D_0 with time is shown in Figure 153. It presents a decrease in D_0 at February 2013 followed by an increase at April 2013. This represents the effects of freezing and thawing to the soil stiffness.

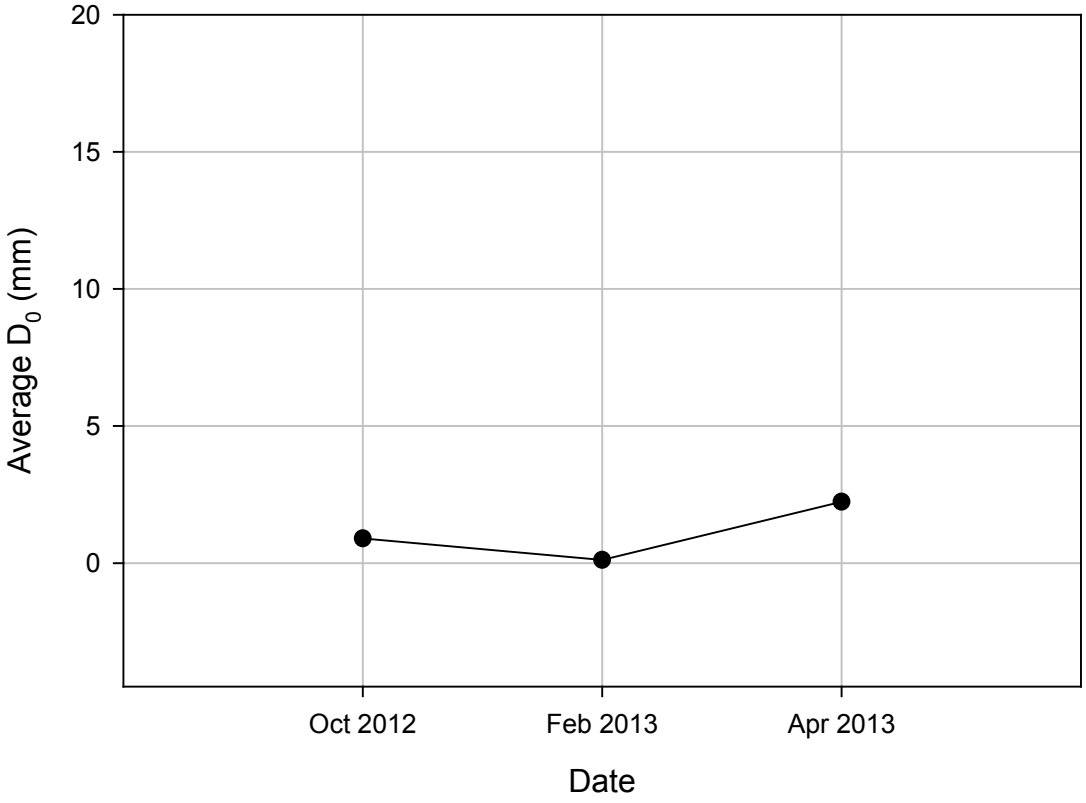

Figure 153. 6th Street North seasonal D_0 variations

7th Street South

Recycled subbase was stabilized with 5% cement at the 7th Street South. The DCP profiles of April 2012, October 2012, and April 2013 are shown in Figure 154. DCP refusal was obtained for the stabilized layers at both October 2012 and April 2013.

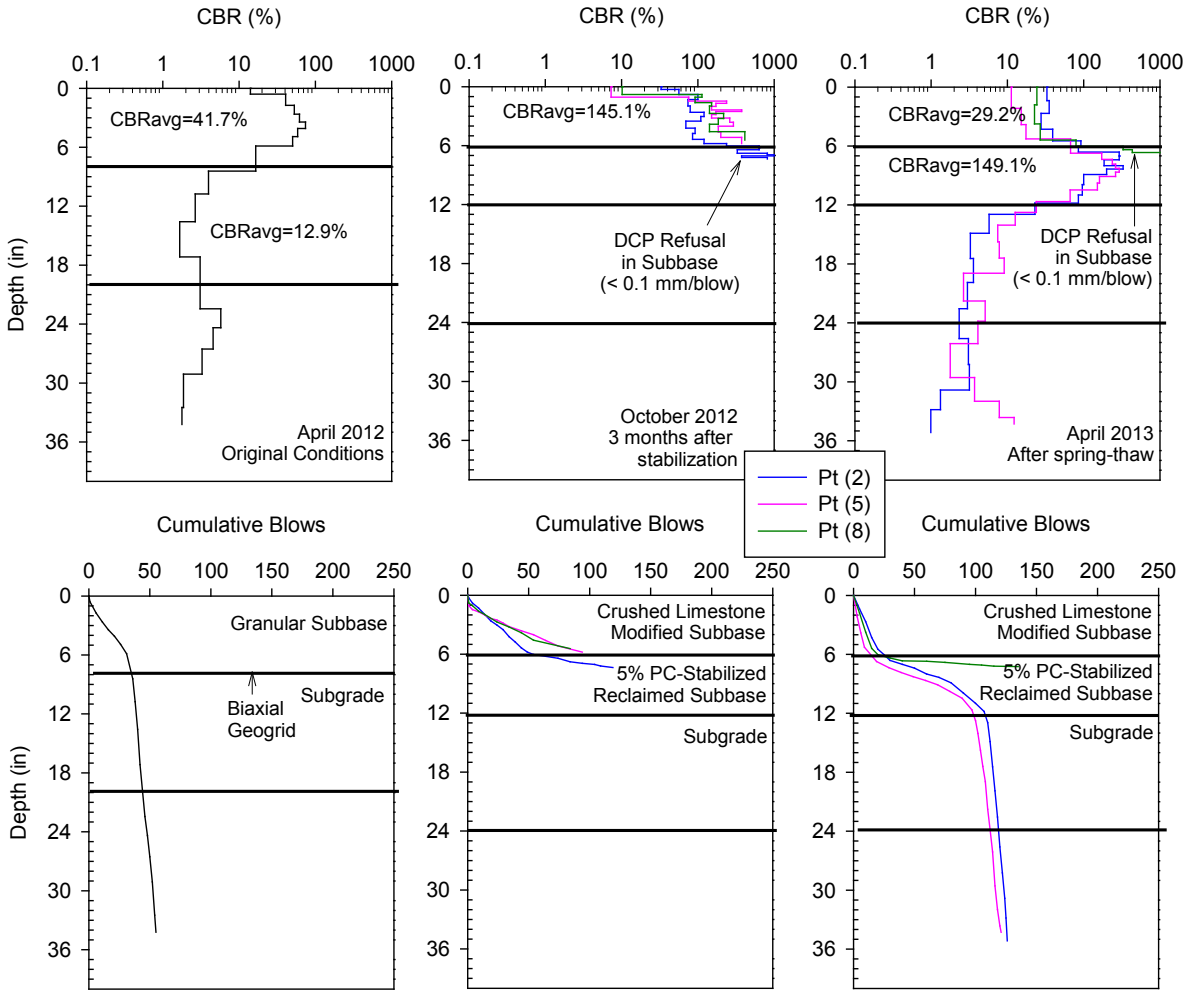

Figure 154. 7th Street South seasonal DCP variations

The variation of D_0 with time is shown in Figure 155. It presents a decrease in D_0 at February 2013 followed by an increase at April 2013. This represents the effects of freezing and thawing to the soil stiffness.

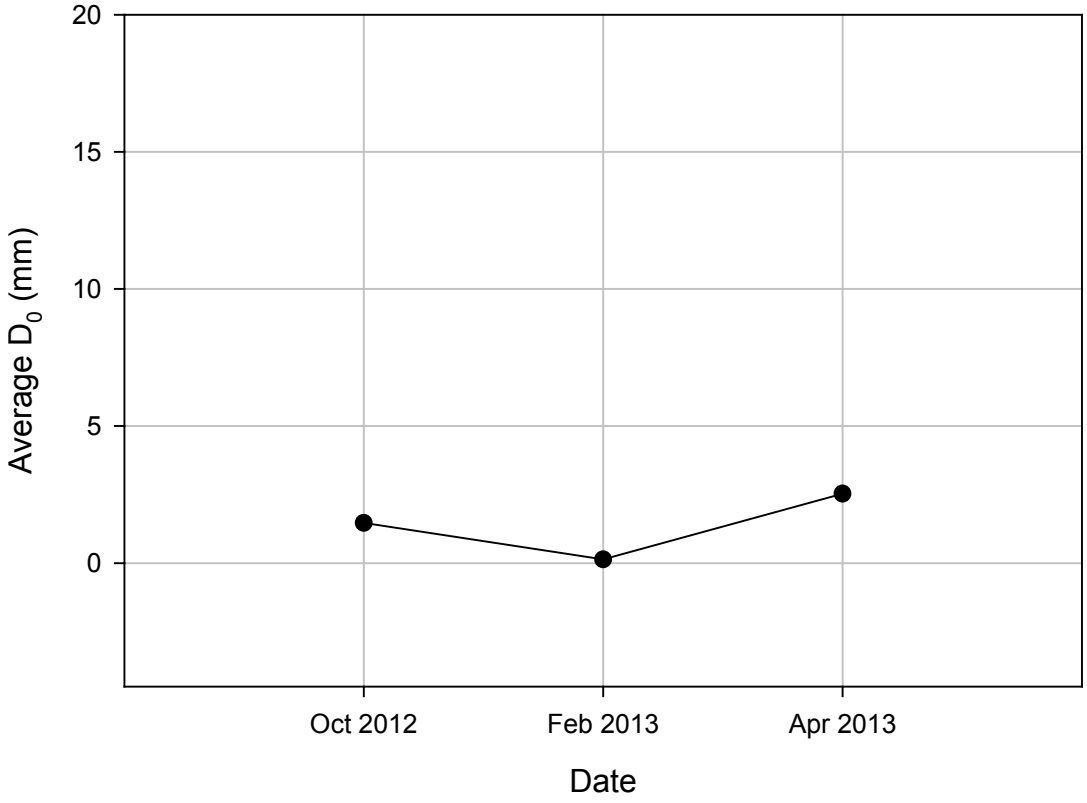

Figure 155. 7th Street South seasonal D_0 variations

7th Street North

Recycled subbase was stabilized with 5% cement at the 7th Street North. The DCP profiles of April 2012, October 2012, and April 2013 are shown in Figure 156. DCP refusal was obtained for the stabilized layers at both October 2012 and April 2013.

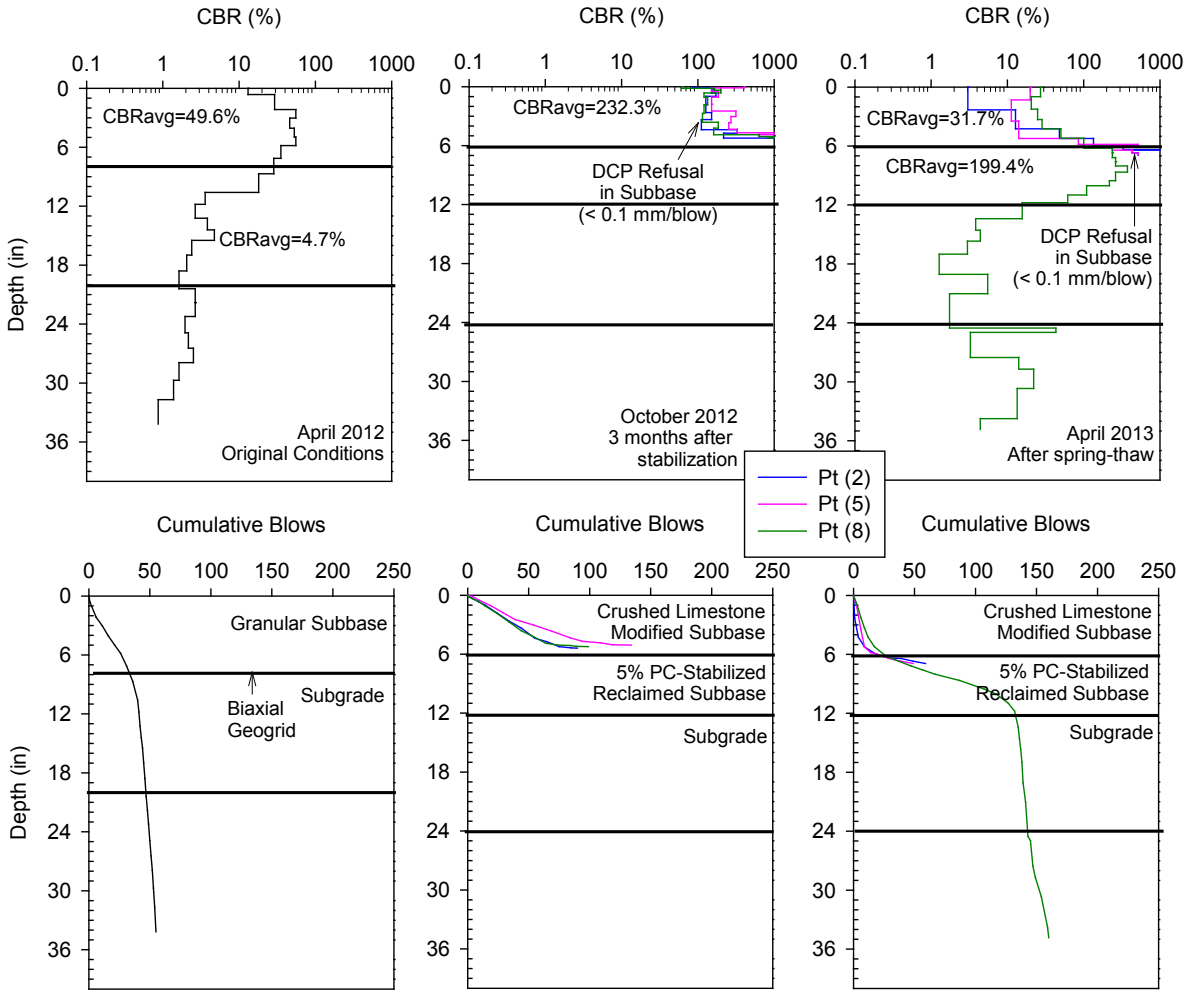

Figure 156. 7th Street North seasonal DCP variations

The variation of D_0 with time is shown in Figure 157. It presents a decrease in D_0 at February 2013 followed by an increase at April 2013. This represents the effects of freezing and thawing to the soil stiffness.

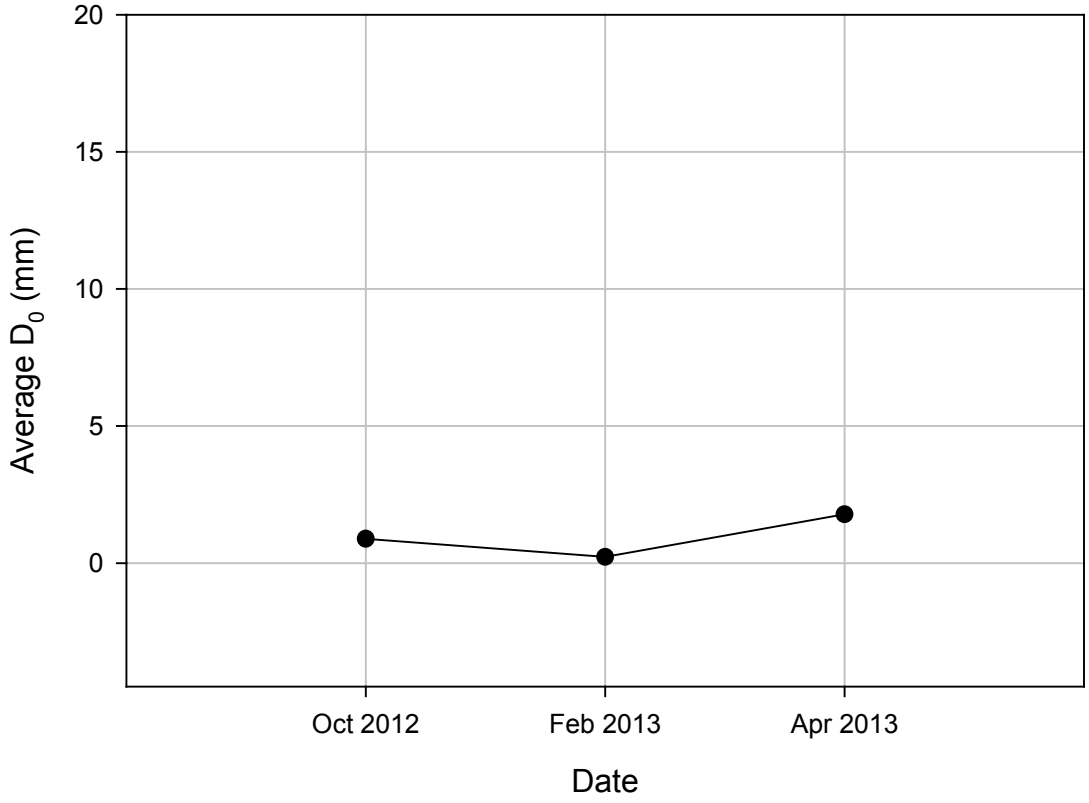

Figure 157. 7th Street North seasonal D_0 variations

8th Street South

The 6 inch to 18 inch layer of the 8th Street South was stabilized with compacted subgrade. The DCP profiles of April 2012, October 2012, and April 2013 are shown in Figure 158. The average CBR value of stabilized layer at October 2012 was larger than the April 2013 value.

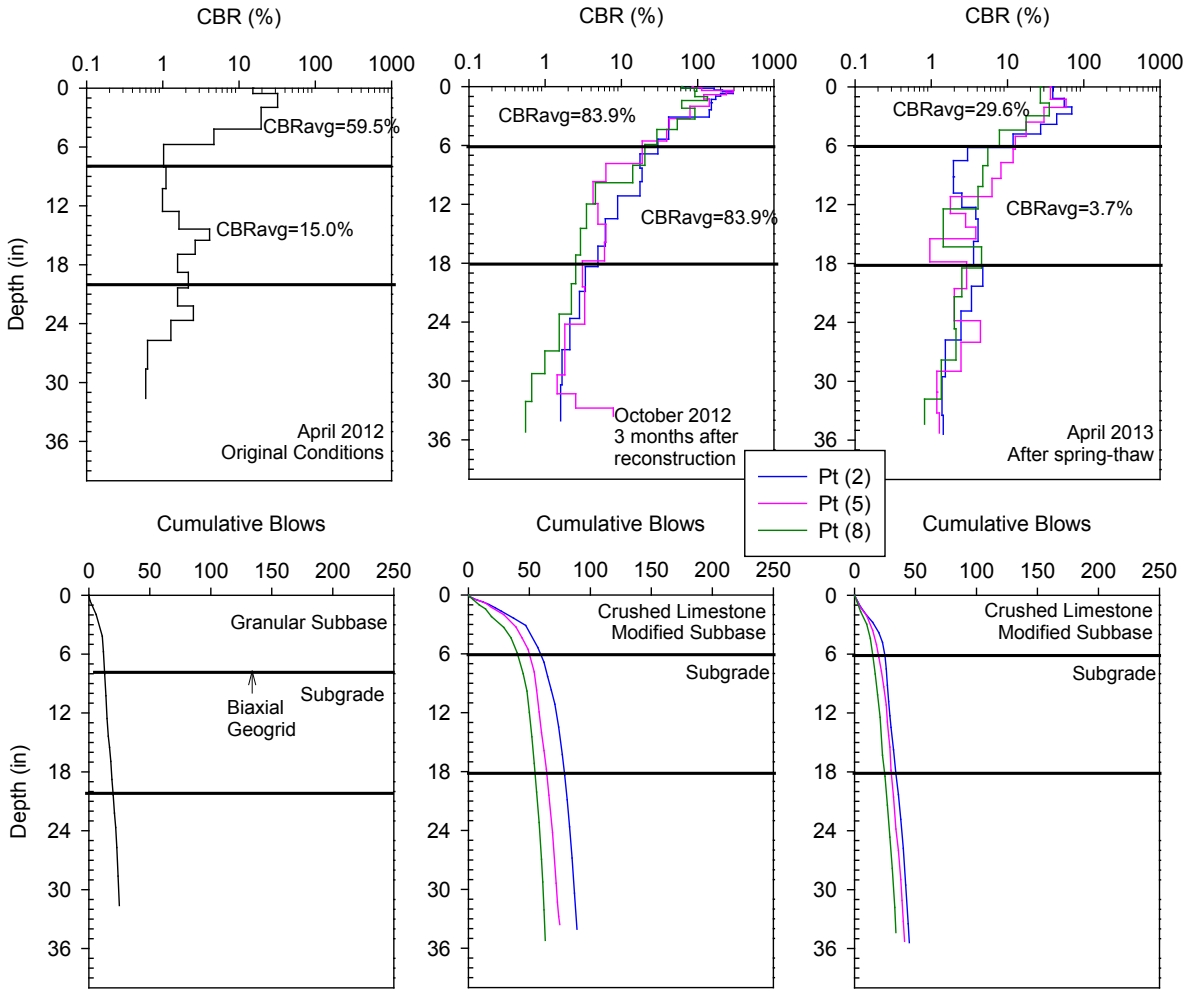

Figure 158. 8th Street South seasonal DCP variations

The variation of D_0 with time is shown in Figure 159. It presents a decrease in D_0 at February 2013 followed by an increase at April 2013. This represents the effects of freezing and thawing to the soil stiffness.

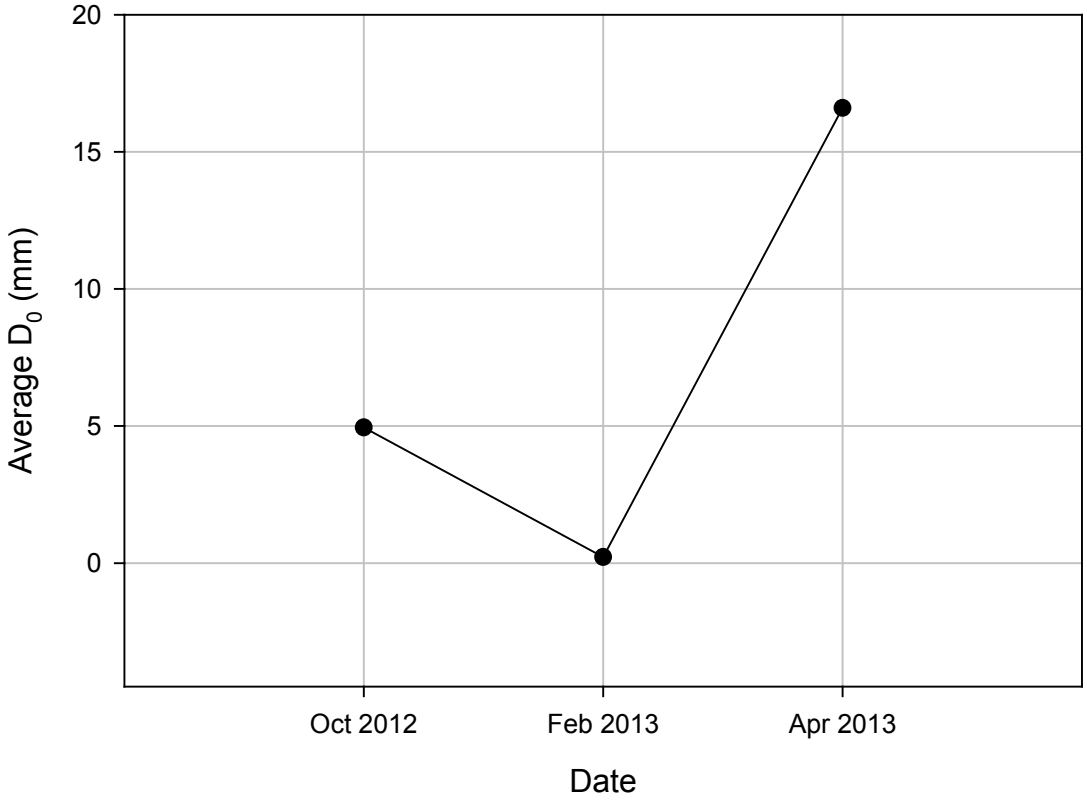

Figure 159. 8th Street South seasonal D_0 variations

8th Street North

The 6 inch to 18 inch layer of the 8th Street North was stabilized with compacted subgrade. The DCP profiles of April 2012, October 2012, and April 2013 are shown in Figure 160. The average CBR value of stabilized layer at October 2012 was larger than the April 2013 value.

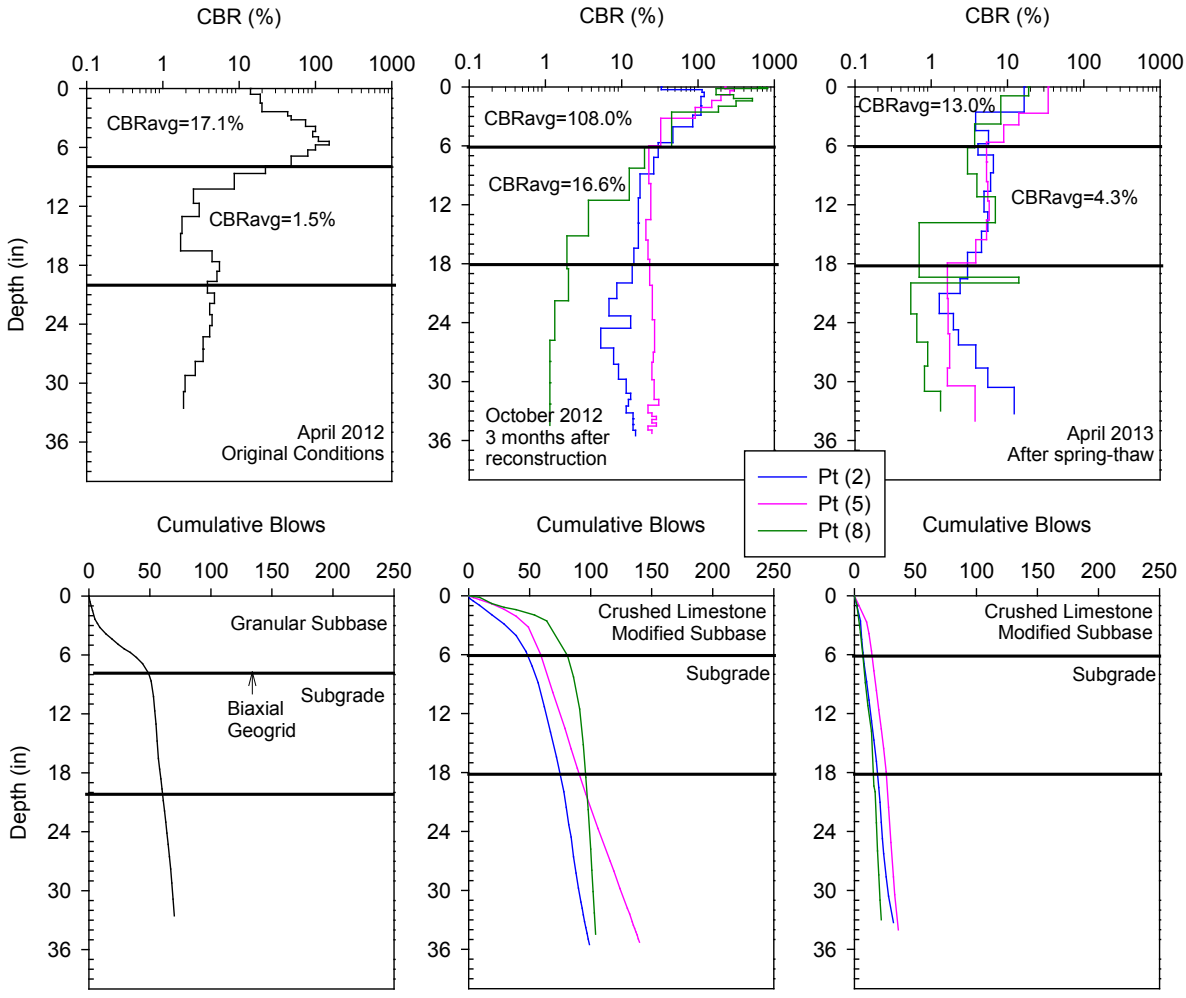

Figure 160. 8th Street North seasonal DCP variations

The variation of D_0 with time is shown in Figure 161. It presents a decrease in D_0 at February 2013 followed by an increase at April 2013. This represents the effects of freezing and thawing to the soil stiffness.

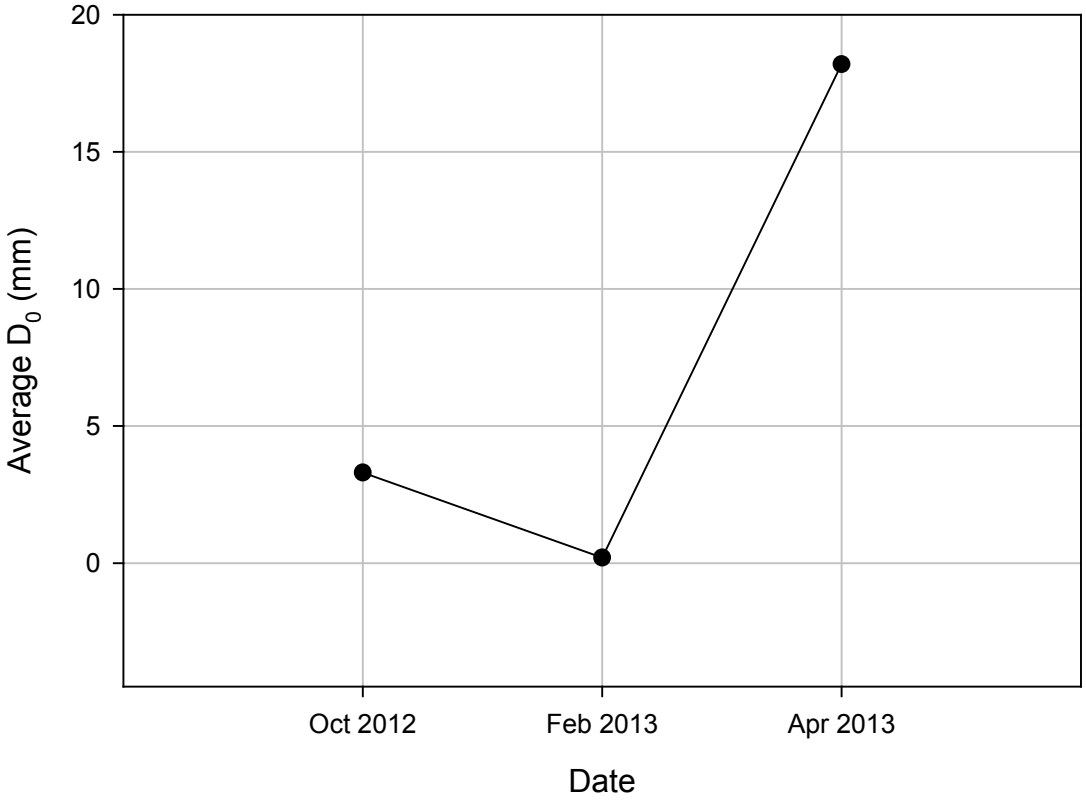

Figure 161. 8th Street North seasonal D_0 variations

9th Street South

The 6 inch to 12 inch layer of the 9th Street South was non-stabilized recycled subbase. The DCP profiles of April 2012, October 2012, and April 2013 are shown in Figure 162. DCP refusal was obtained for the recycled subbase layers at both October 2012.

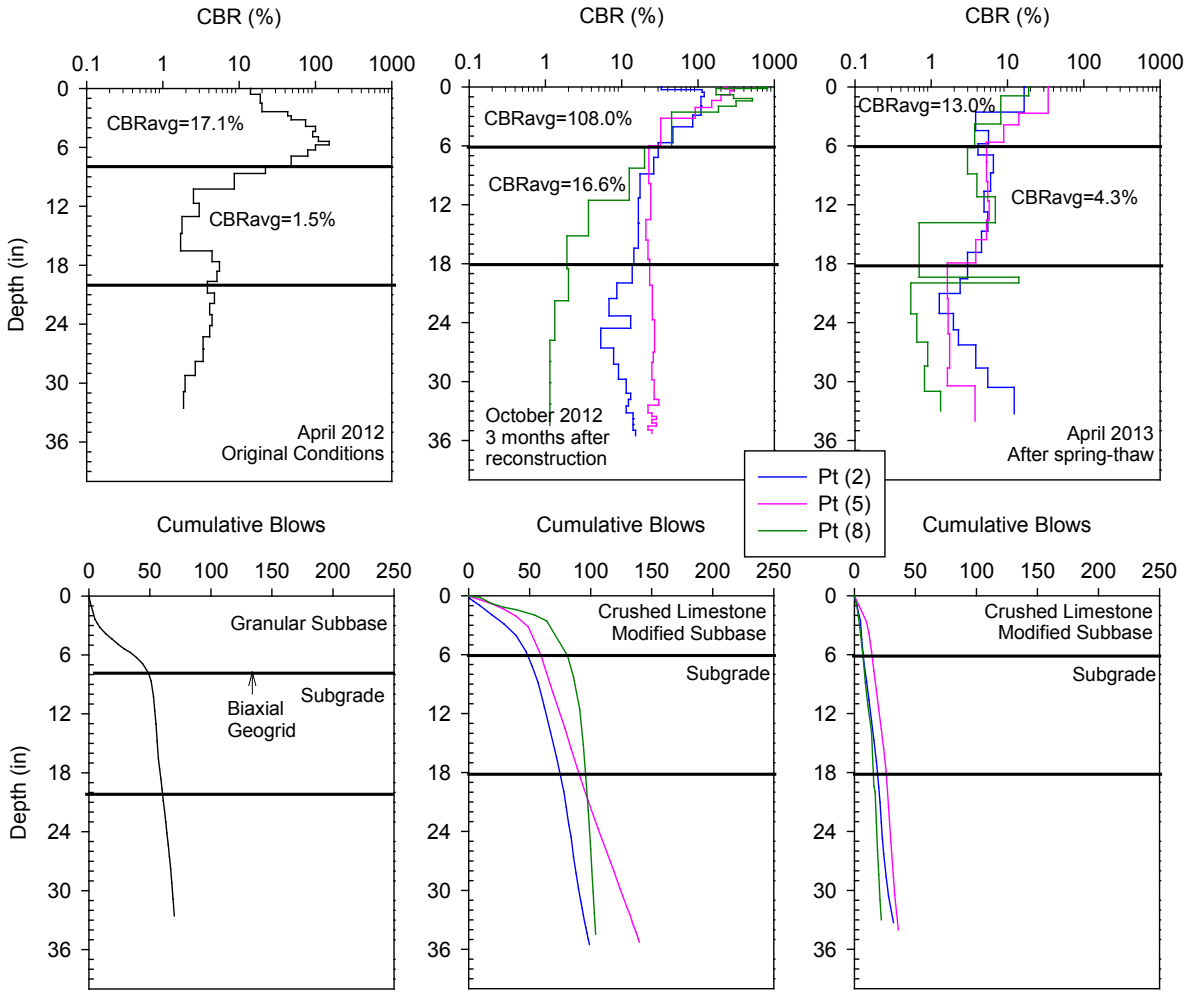

Figure 162. 9th Street South seasonal DCP variations

The variation of D_0 with time is shown in Figure 163. It presents a decrease in D_0 at February 2013 followed by an increase at April 2013. This represents the effects of freezing and thawing to the soil stiffness.

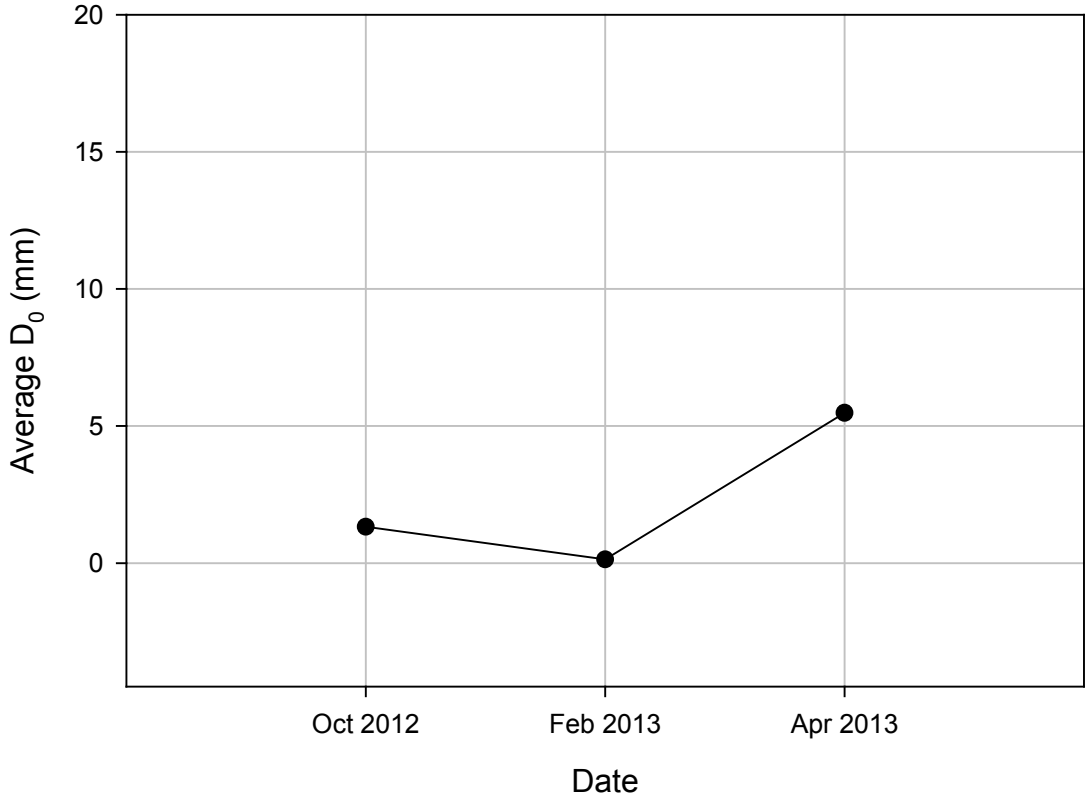

Figure 163. 9th Street South seasonal D_0 variations

9th Street North

The 6 inch to 12 inch layer of the 9th Street North was non-stabilized recycled subbase. The DCP profiles of April 2012, October 2012, and April 2013 are shown in Figure 164. The average CBR value at October 2012 was larger than the April 2013 value.

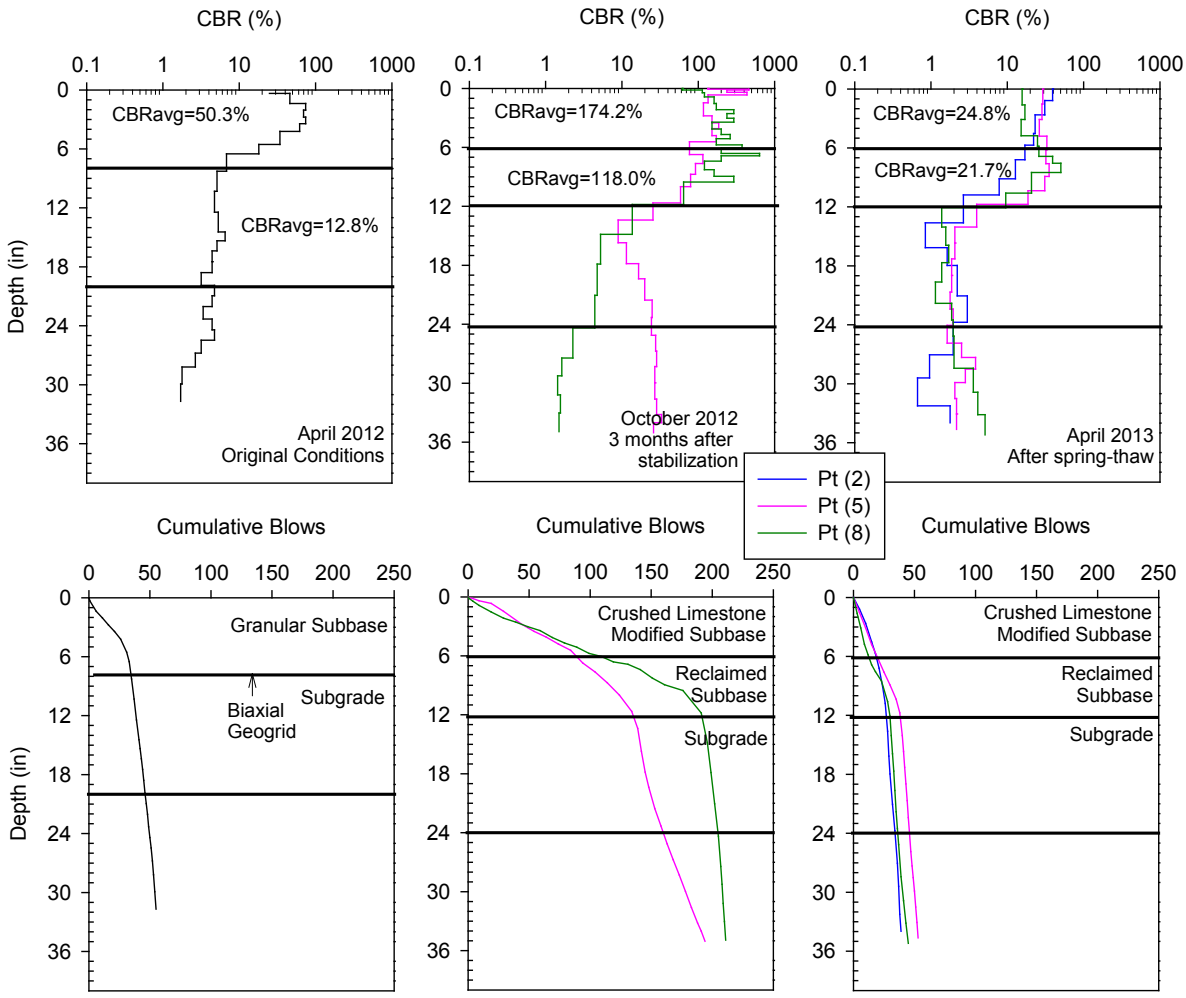

Figure 164. 9th Street North seasonal DCP variations

The variation of D_0 with time is shown in Figure 165. It presents a decrease in D_0 at February 2013 followed by an increase at April 2013. This represents the effects of freezing and thawing to the soil stiffness.

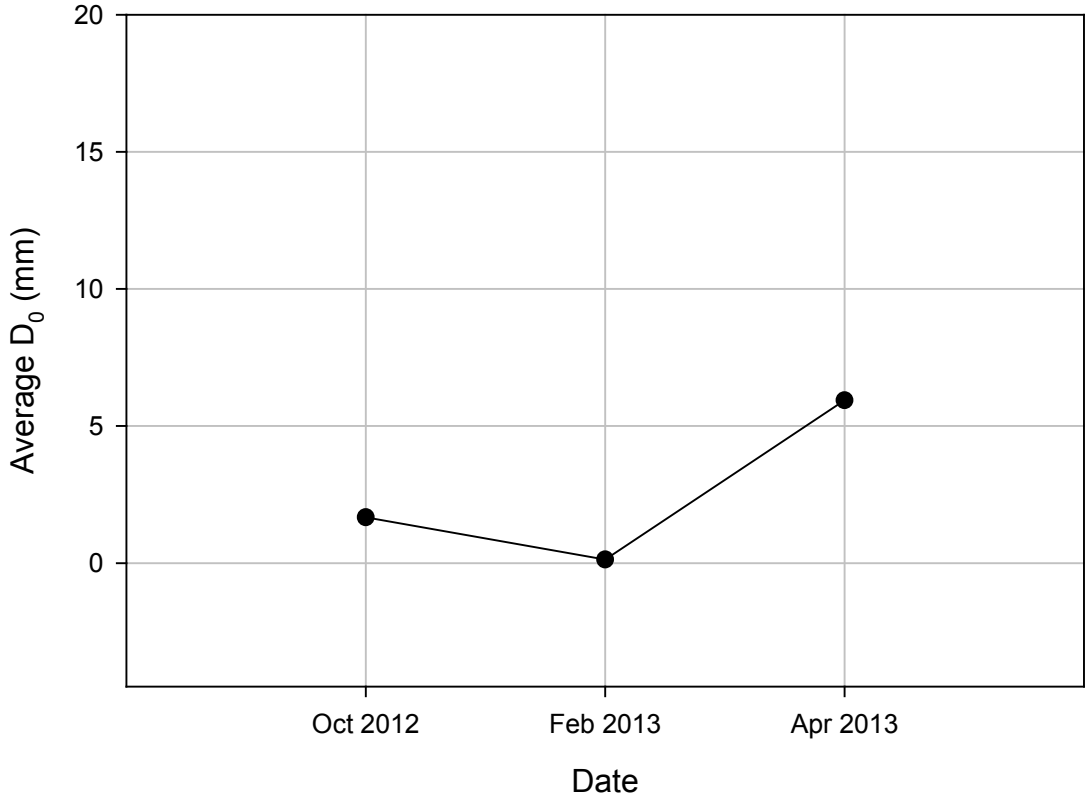

Figure 165. 9th Street North seasonal D_0 variations

10th Street South

Natural subgrade is under the 6-in crushed limestone modified subbase layer at the 10th Street South. The DCP profiles of April 2012, October 2012, and April 2013 are shown in Figure 166. The average CBR value at October 2012 was larger than the April 2013 value.

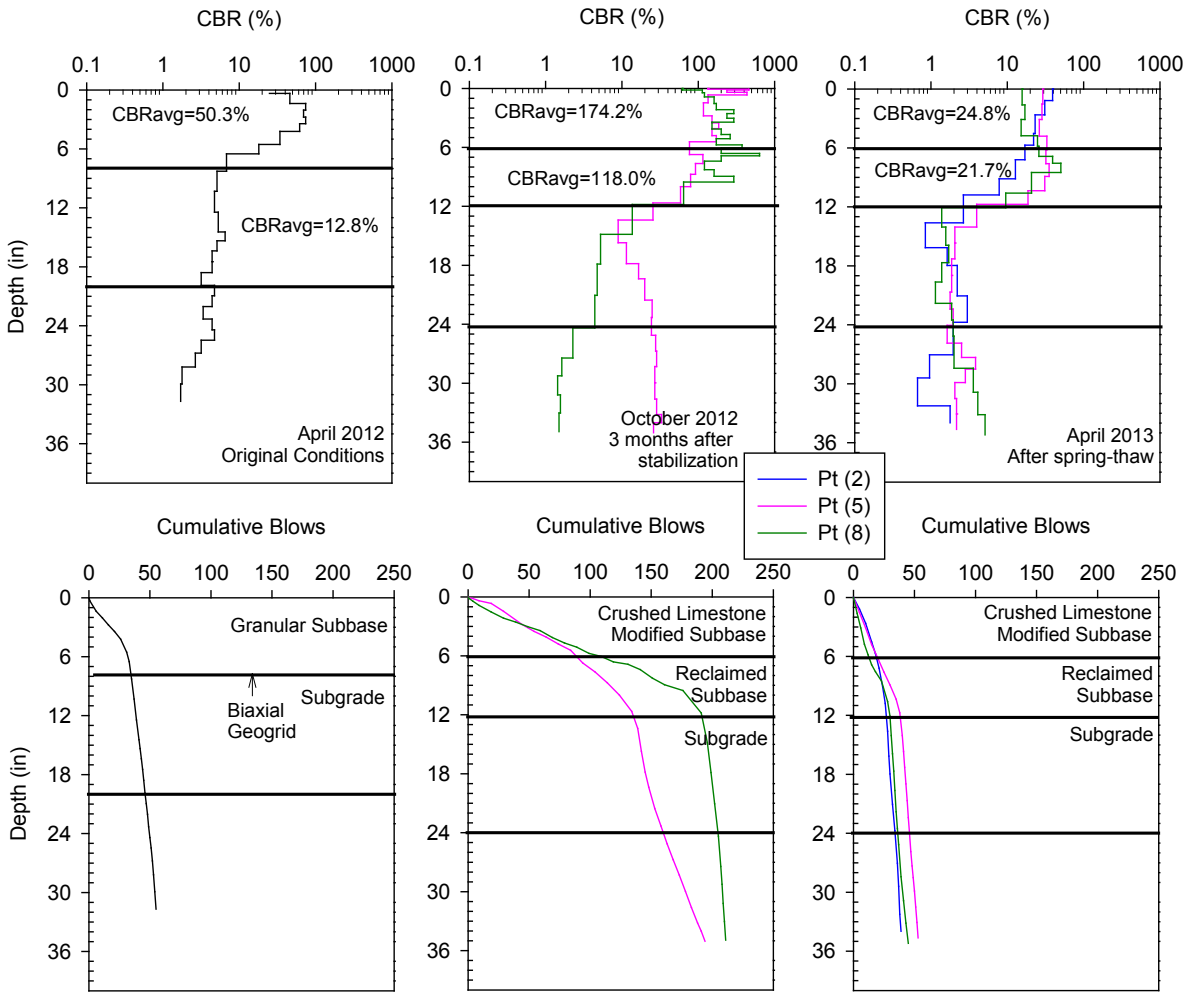

Figure 166. 10th Street South seasonal DCP variations

The variation of D_0 with time is shown in Figure 167. It presents a decrease in D_0 at February 2013 followed by an increase at April 2013. This represents the effects of freezing and thawing to the soil stiffness.

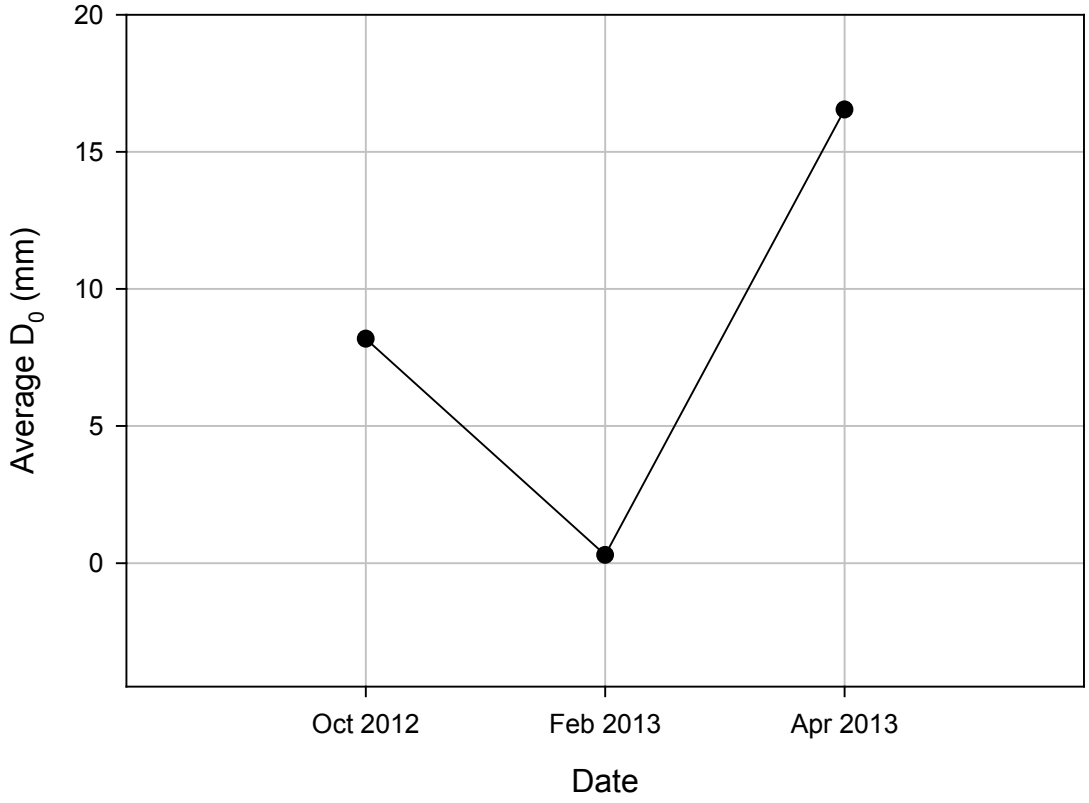

Figure 167. 10th Street South seasonal D_0 variations

10th Street North

Compacted subgrade is under the 6-in crushed limestone modified subbase layer at 10th Street North. The DCP profiles of April 2012, October 2012, and April 2013 are shown in Figure 168. The average CBR value of stabilized layer at October 2012 was larger than the April 2013 value.

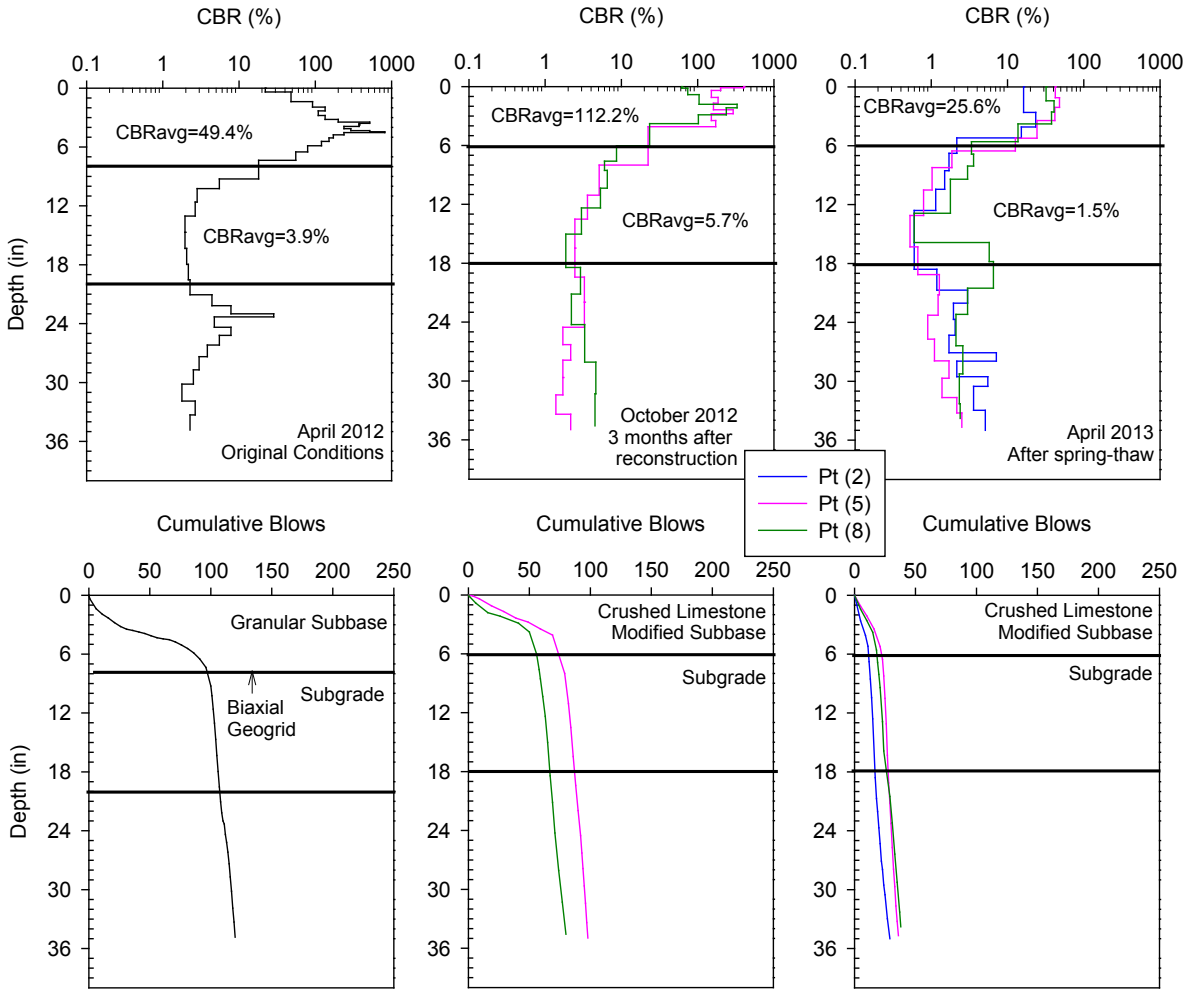

Figure 168. 10th Street North seasonal DCP variations

The variation of D_0 with time is shown in Figure 169. It presents a decrease in D_0 at February 2013 followed by an increase at April 2013. This represents the effects of freezing and thawing to the soil stiffness.

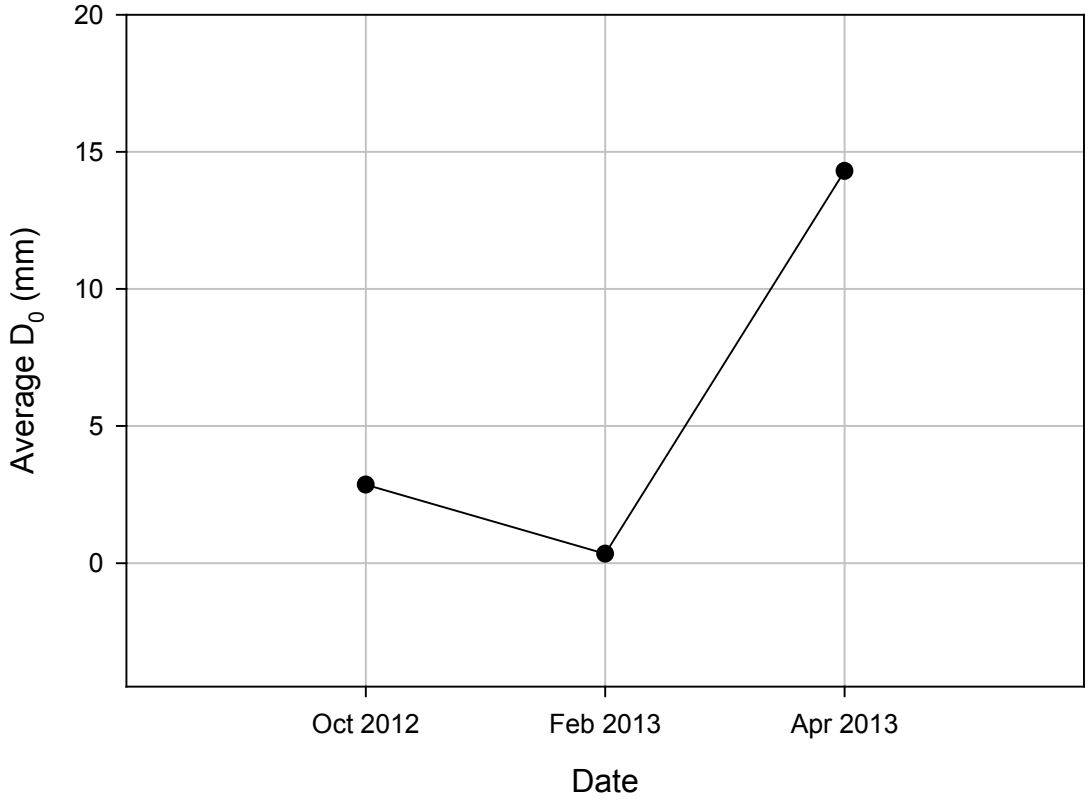

Figure 169. 10th Street North seasonal D_0 variations

11th Street South

The 6 inch to 18 inch layer of 11th Street south was subgrade stabilized with 20% Port Neal fly ash. The DCP profiles of April 2012, October 2012, and April 2013 are shown in Figure 170. The average CBR value of stabilized layer at October 2012 was larger than the April 2013 value.

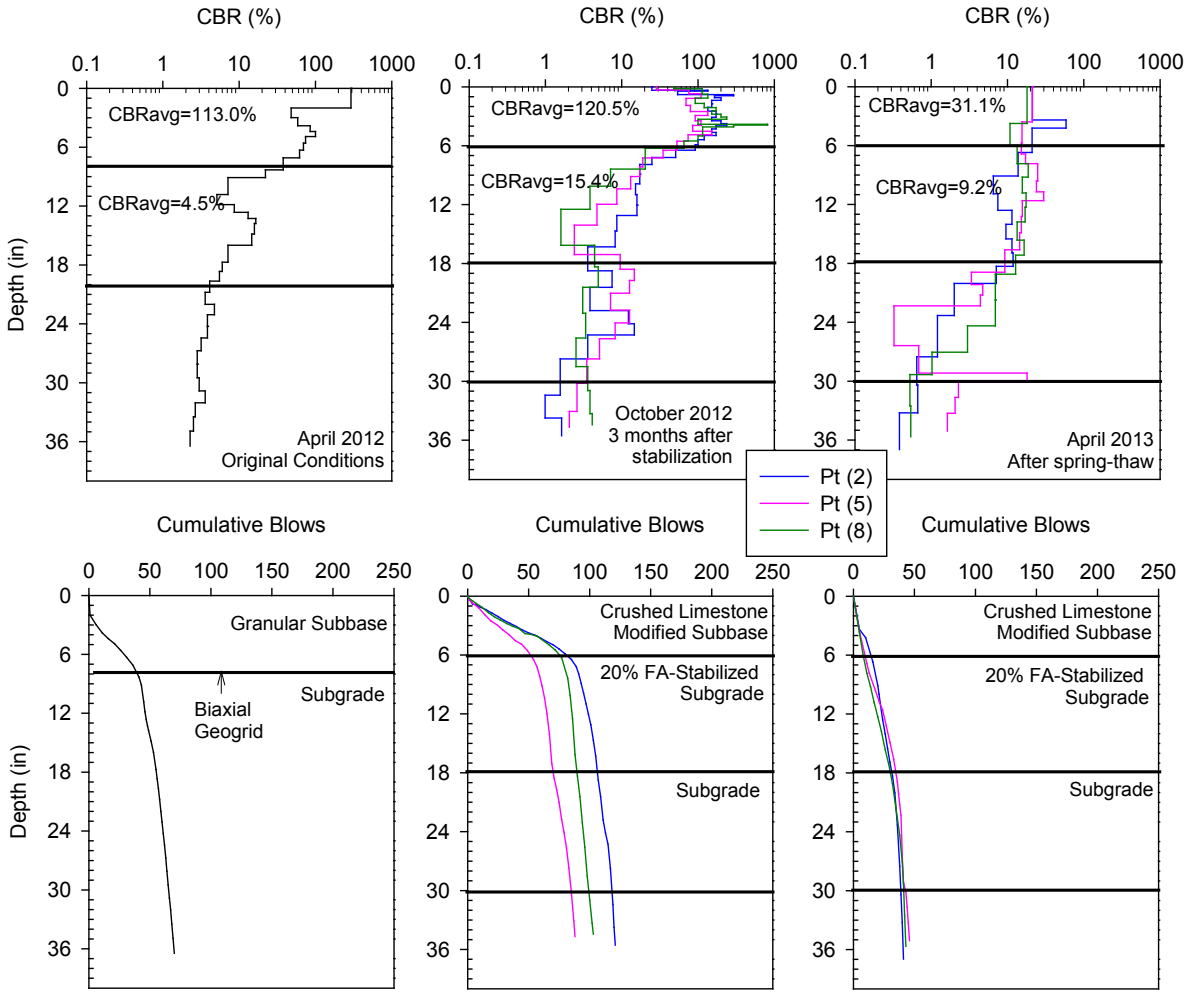

Figure 170. 11th Street South seasonal DCP variations

The variation of D_0 with time is shown in Figure 171. It presents a decrease in D_0 at February 2013 followed by an increase at April 2013. This represents the effects of freezing and thawing to the soil stiffness.

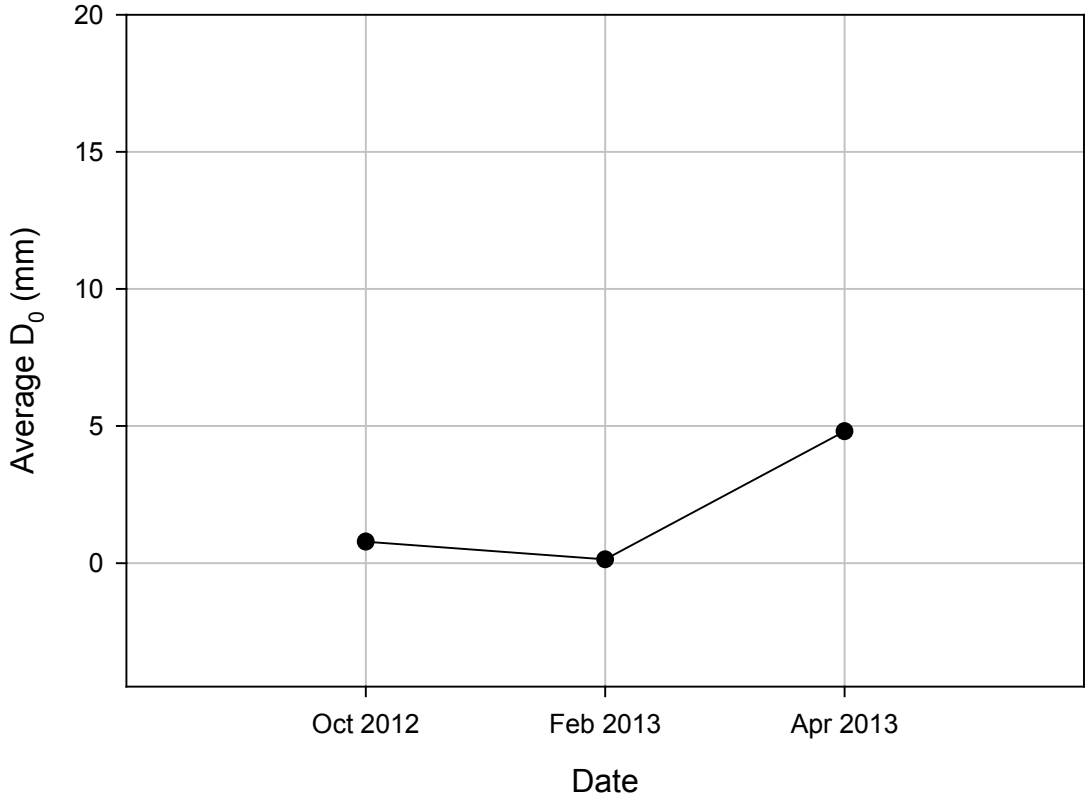

Figure 171. 11th Street South seasonal D_0 variations

11th Street North

The 6 inch to 18 inch layer of 11th Street North was subgrade stabilized with 10% cement. The DCP profiles of April 2012, October 2012, and April 2013 are shown in Figure 172. DCP refusal was obtained for the stabilized layers at October 2012.

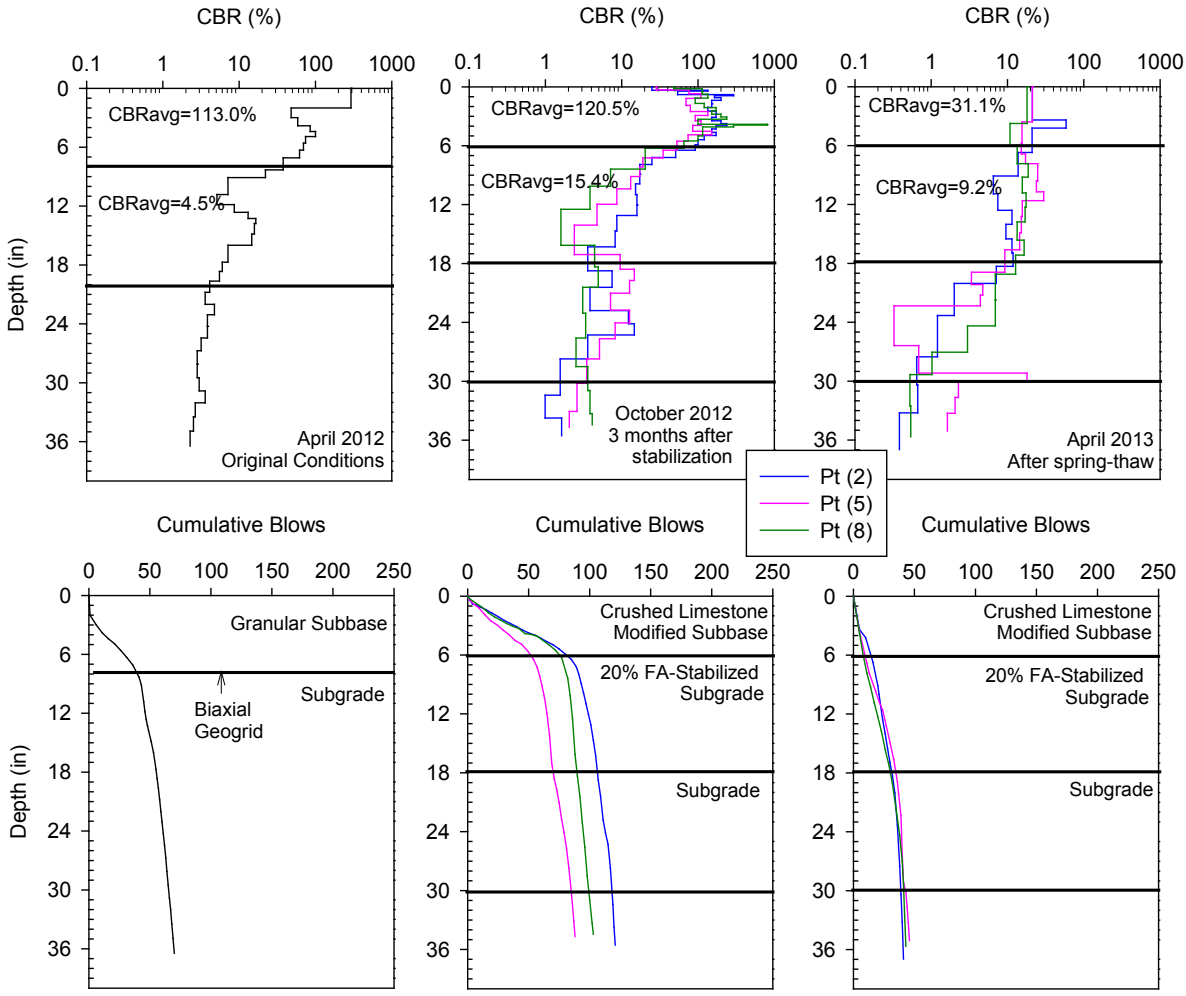

Figure 172. 11th Street North seasonal DCP variations

The variation of D_0 with time is shown in Figure 173. It presents a decrease in D_0 at February 2013 followed by an increase at April 2013. This represents the effects of freezing and thawing to the soil stiffness.

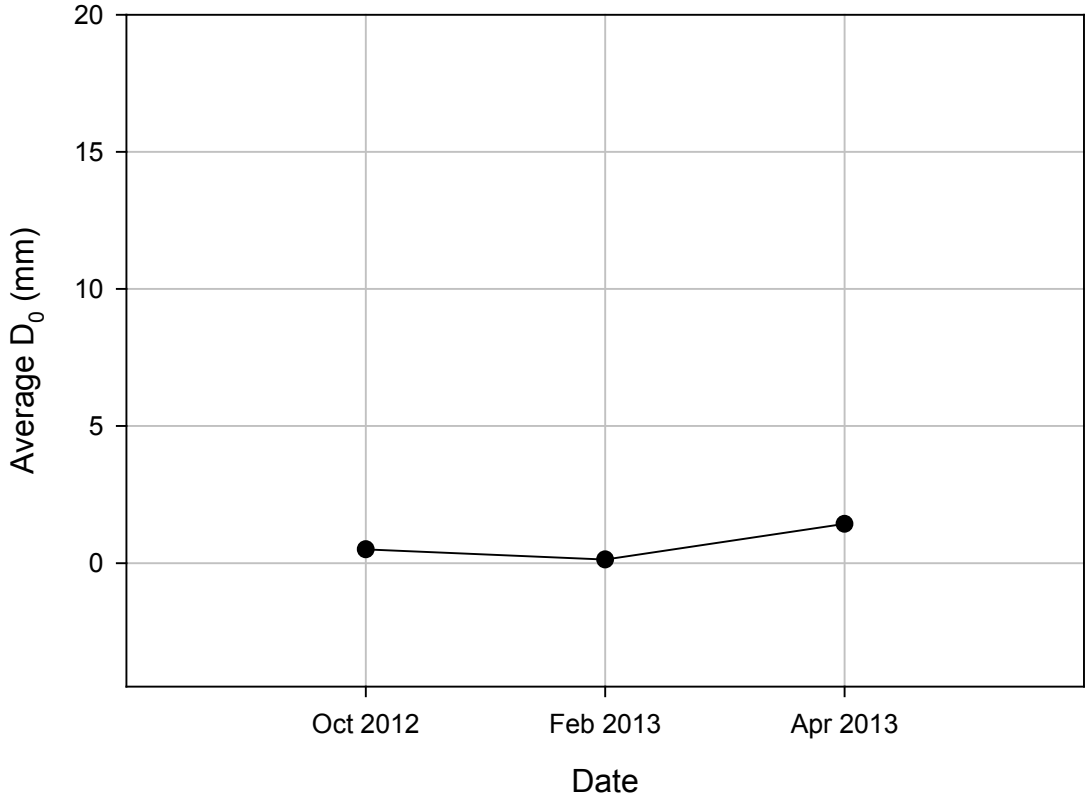

Figure 173. 11th Street North seasonal D_0 variations

12th Street South

The 6 inch to 18 inch layer of 12th Street South was subgrade stabilized with 10% Muscatine and Port Neal fly ash. The DCP profiles of April 2012, October 2012, and April 2013 are shown in Figure 174. The average CBR value of stabilized layer at October 2012 was larger than the April 2013 value.

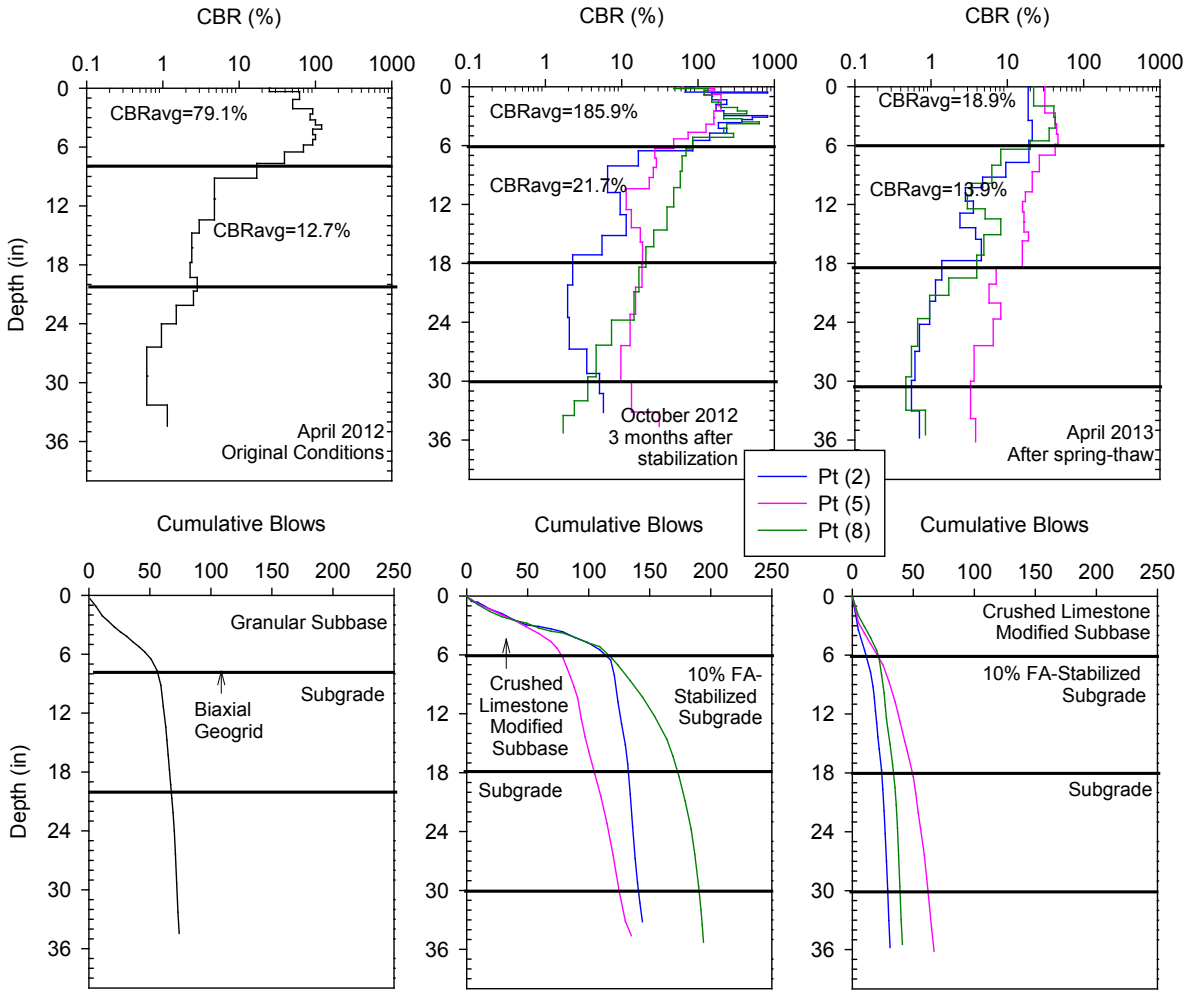

Figure 174. 12th Street South seasonal DCP variations

The variation of D_0 with time is shown in Figure 175. It presents a decrease in D_0 at February 2013 followed by an increase at April 2013. This represents the effects of freezing and thawing to the soil stiffness.

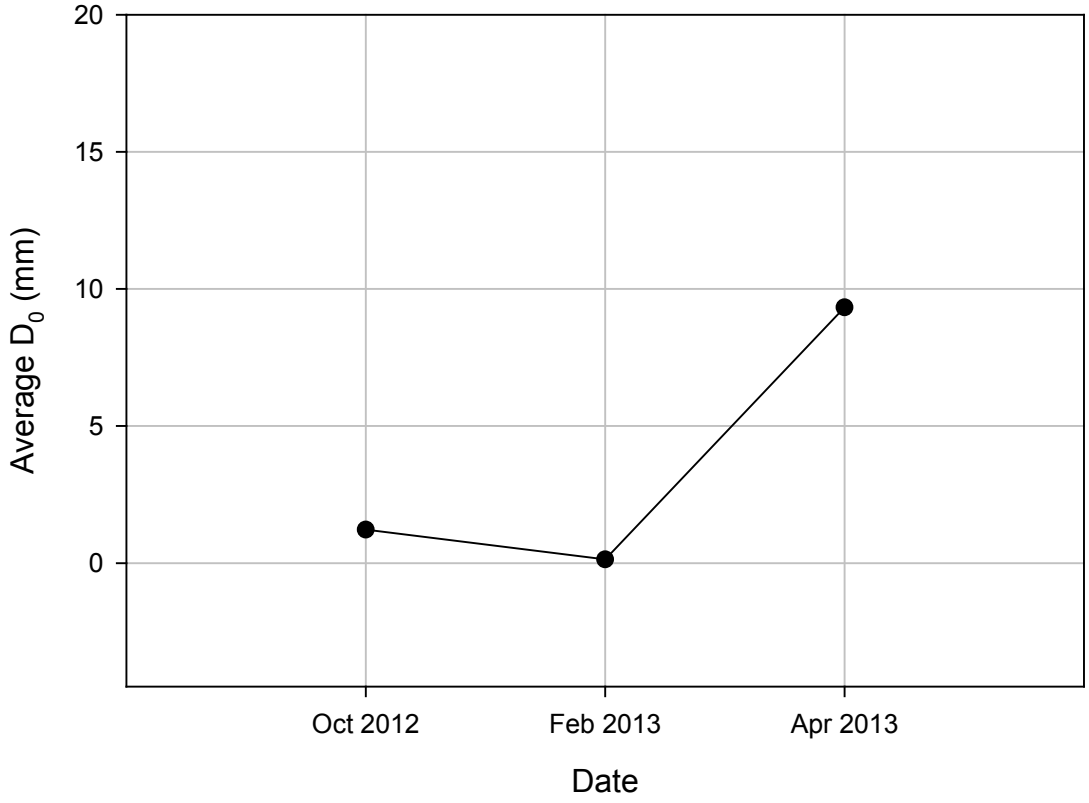

Figure 175. 12th Street South seasonal D_0 variations

12th Street North

The 6 inch to 18 inch layer of 12th Street North was subgrade stabilized with 15% Ames fly ash. The DCP profiles of April 2012, October 2012, and April 2013 are shown in Figure 176. The average CBR value of stabilized layer at October 2012 was larger than the April 2013 value.

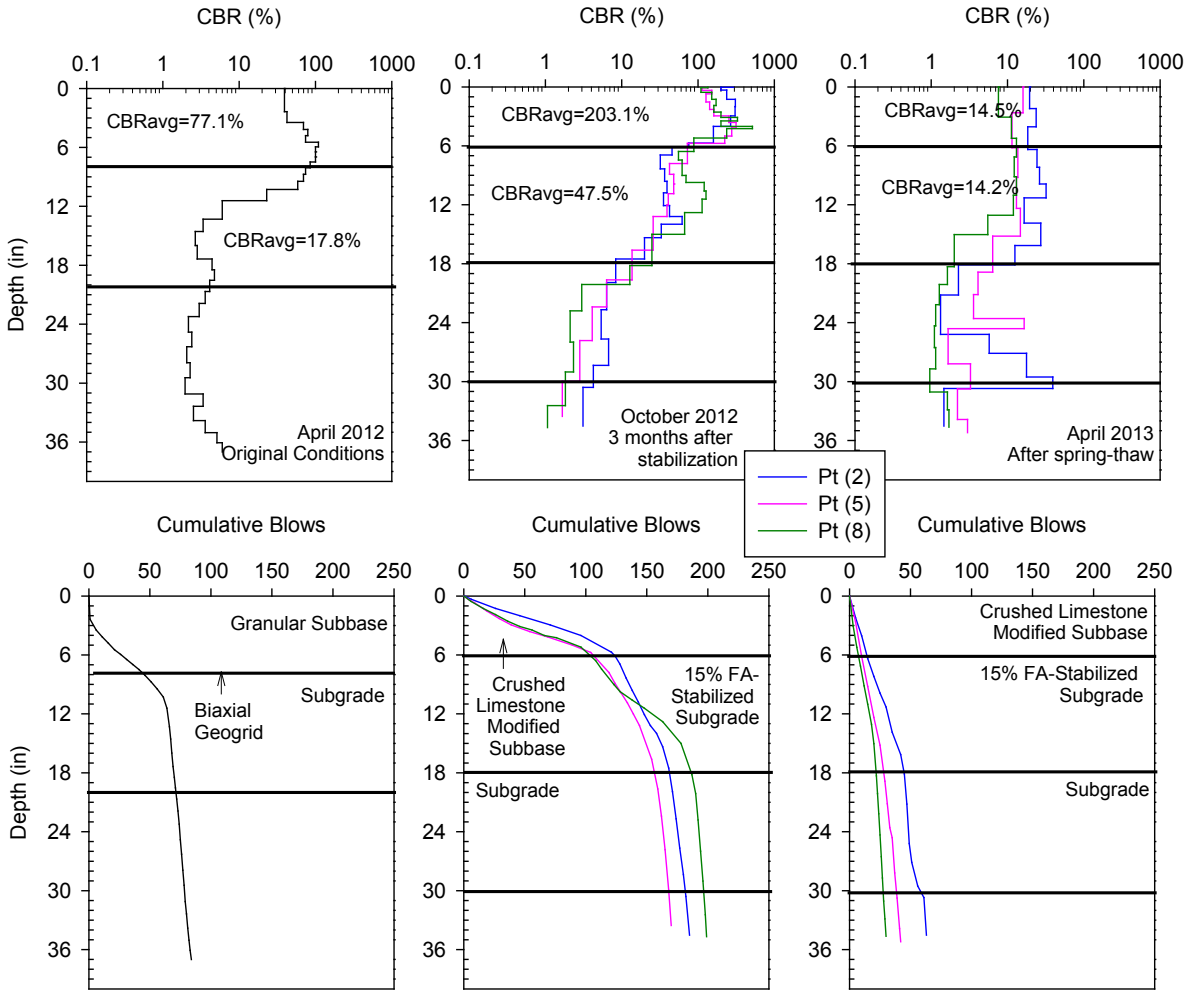

Figure 176. 12th Street North seasonal DCP variations

The variation of D_0 with time is shown in Figure 177. It presents a decrease in D_0 at February 2013 followed by an increase at April 2013. This represents the effects of freezing and thawing to the soil stiffness.

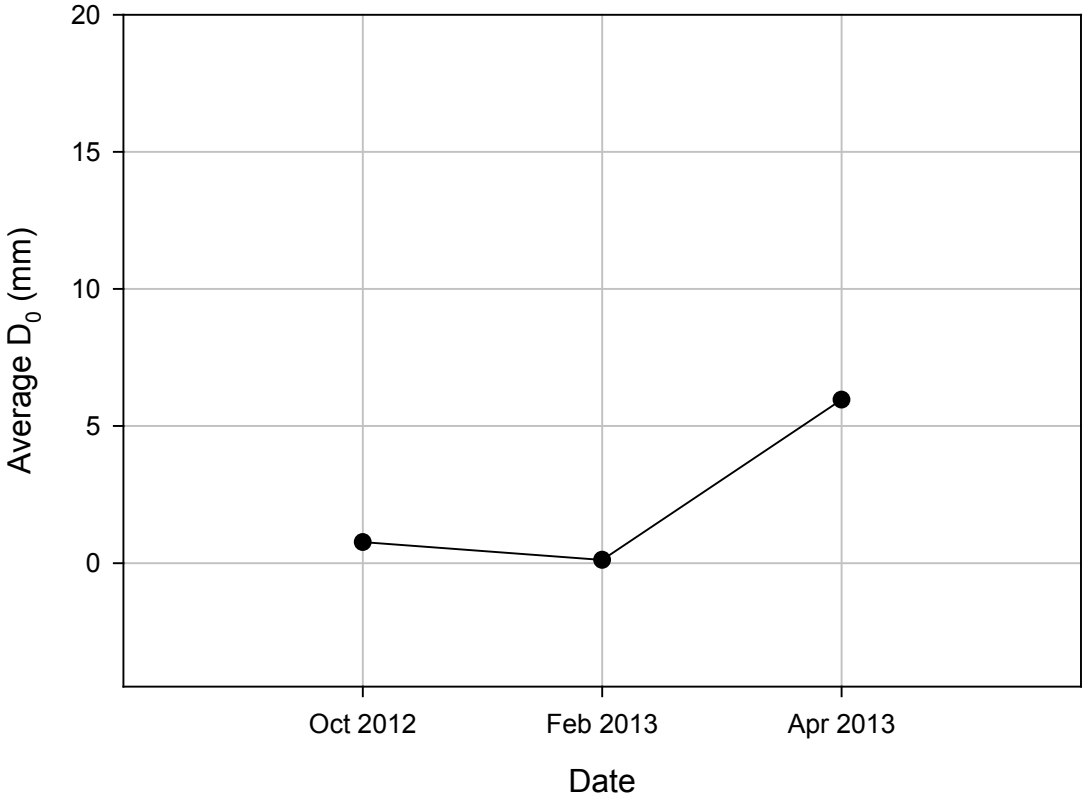

Figure 177. 12th Street North seasonal D_0 variations

Summary of in situ tests

The DCP tests were performed at all the 24 segments. The test results based on CBR values were determined to evaluate the soil stiffness. According to the results, cement stabilized recycled subbase and cement + fibers stabilized recycled subbase turned out to be more effective for controlling the freeze-thaw influence to soil stiffness. This point can also be correlated to the laboratory frost-heave and thaw-weakening tests. The stabilization effects on improving freeze-thaw performance of geomaterials were similar between laboratory tests and in situ tests. The average CBRs of each segment at October 2012 and April 2013 and the reduction factors for CBRs are summarized Table 65 and Table 66.

Table 65. Summary of CBRs and reduction factors of subbase layers from DCP tests

Time	October 2012		April 2013		Reduction factor	
Segment	South	North	South	North	South	North
1st St.	122.2	134.7	60.5	65.2	0.49	0.48
2nd St.	89.3	106.8	43.9	29.9	0.49	0.28
3rd St.	83.3	18.0	20.1	18.2	0.24	1.01
4th St.	88.5	120.6	46.0	33.0	0.52	0.27
5th St.	148.4	234.3	43.8	36.9	0.30	0.16
6th St.	252.3	224.2	89.9	67.7	0.36	0.30
7th St.	145.1	232.3	29.2	31.7	0.20	0.14
8th St.	83.9	108.0	29.6	13.0	0.35	0.12
9th St.	336.5	174.2	66.9	24.8	0.20	0.14
10th St.	122.2	112.2	26.9	25.6	0.22	0.23
11th St.	120.5	510.4	31.1	19.2	0.26	0.04
12th St.	185.9	203.1	18.9	14.5	0.10	0.07

Table 66. Summary of CBRs and reduction factors of subgrade layers from DCP tests

Time	October 2012		April 2013		Reduction factor	
Segment	South	North	South	North	South	North
1st St.	12.0	6.5	9.9	5.2	0.83	0.80
2nd St.	15.6	16.2	7.6	5.5	0.49	0.34
3rd St.	8.3	1.7	1.9	4.8	0.23	2.82
4th St.	20.9	11.1	6.6	3.3	0.31	0.30
5th St.	11.1	12.6	10.1	2.9	0.91	0.23
6th St.	-	318.1	109.9	127.8	-	0.40
7th St.	-	-	149.1	199.4	-	-
8th St.	83.9	16.6	3.7	4.3	0.04	0.26
9th St.	-	118.0	38.6	21.7	-	0.18

Table 66. Summary of CBRs and reduction factors of subgrade layers from DCP tests (continued)

Time	October 2012		April 2013		Reduction factor	
Segment	South	North	South	North	South	North
10th St.	11.3	5.7	2.5	1.5	0.22	0.26
11th St.	15.4	-	9.2	79.5	0.60	-
12th St.	21.7	47.5	13.9	14.2	0.64	0.30

The CBR values from laboratory and field were compared. Figure 178 shows a relationship between the laboratory and field CBR values. This result cannot exactly reflect the relationship between the two groups of CBR values. The laboratory CBR was not equal to the field CBR of the same material. The possible reasons caused the differences were: field construction conditions; different numbers of freeze-thaw cycles; different numbers of sample data.

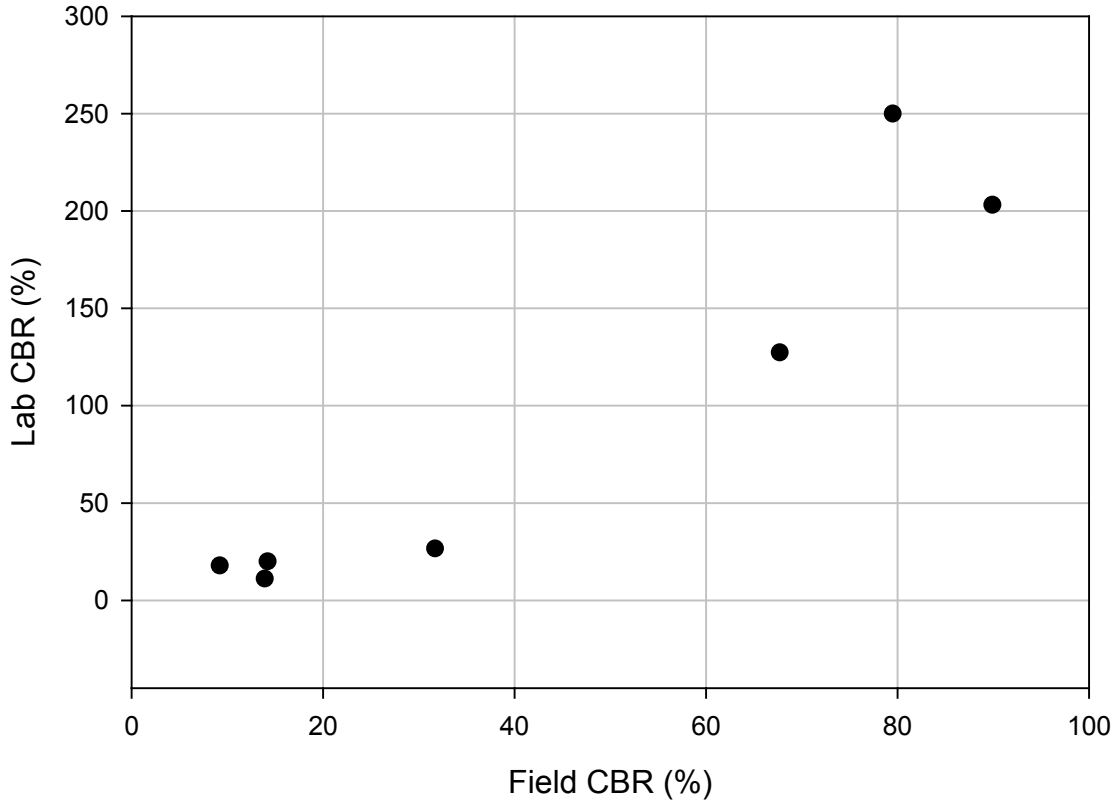

Figure 178. CBR values from laboratory and field tests

The CBR reduction factors based on laboratory and in-situ tests were compared. Table 67 summarizes the reduction factors from both laboratory and field. The factors that are less than 1.0 were plotted in Figure 179.

Table 67. CBR reduction factors for the stabilization methods both used in laboratory and field.

Stabilization method	Lab CBR reduction factor	Field CBR reduction factor
non-stabilized subgrade	0.21	0.22
15% Ames fly ash subgrade	0.27	0.30
10% Port Neal fly ash subgrade	0.75	0.64
20% Port Neal fly ash subgrade	0.62	0.60
10% cement subgrade	Refusal	Refusal
non-stabilized subbase	1.91	0.22
5.0% cement subbase	0.27	0.17
0.4% PP + 3.75% cement subbase	0.51	0.33
0.4% MF+ 3.75% cement subbase	1.42	0.36

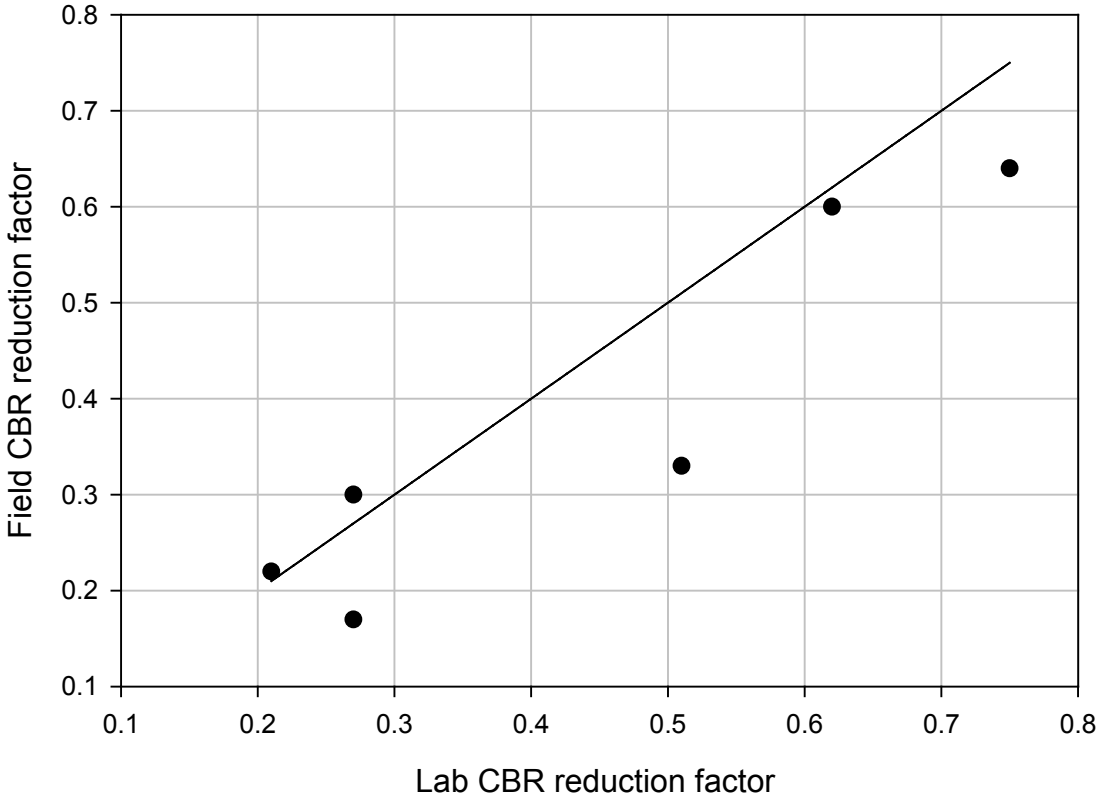

Figure 179. Field and Laboratory CBR reduction factors plots

The FWD measurement, D_0, resulted in the similar trend for seasonal variations. The relationship between after-thawing D_0 and before-freezing D_0 cannot be addressed from the comparison plots as in Figure 180.

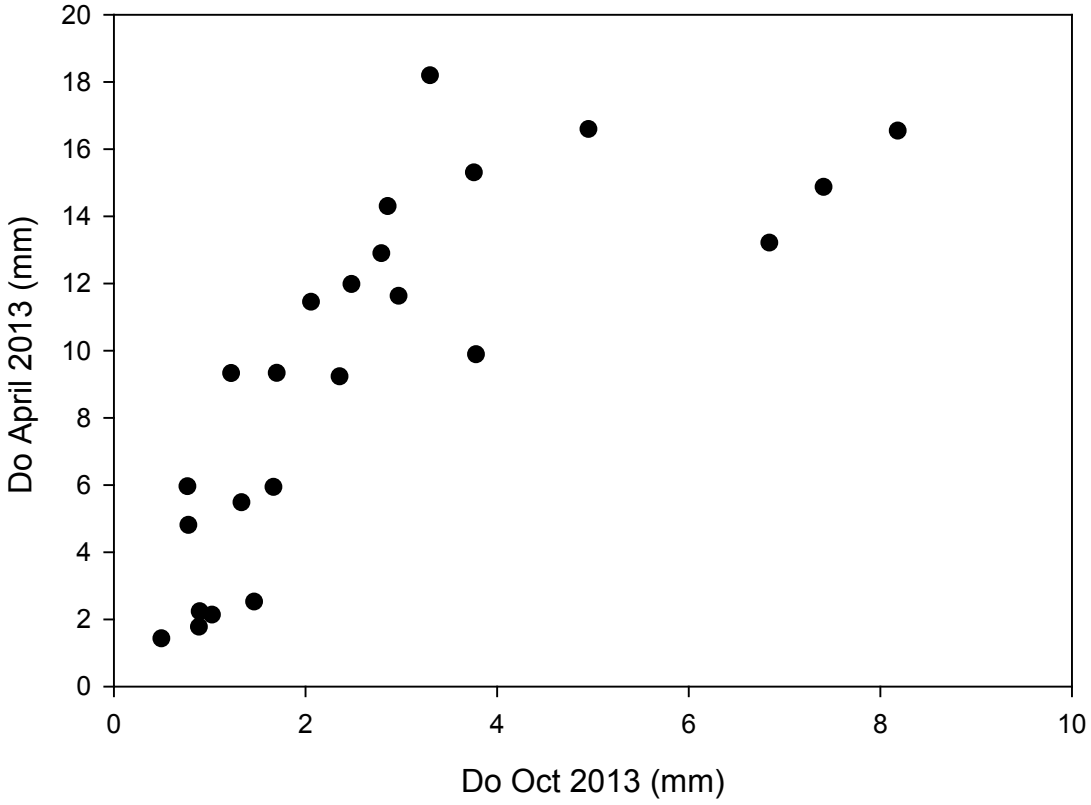

Figure 180. Deflections of after-thawing and before-freezing

The seasonal D_0 variations of all the 24 segments are presented in Figure 181. The during-freezing condition led to stiffer pavement than both of the before-freezing and after-thawing conditions. An obvious increase in D_0 was obtained from the April 2013 FWD results, which indicates the pavement was softer at that time than at both Oct 2012 and Feb 2013.

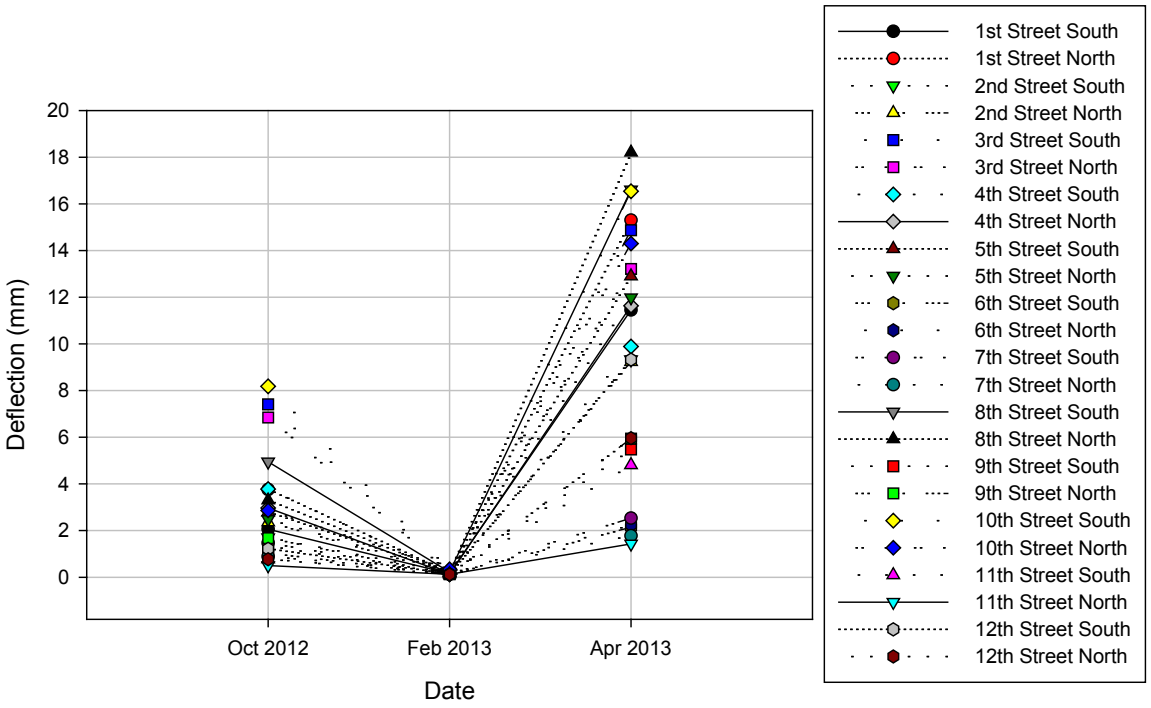

Figure 181. Summary of D_0 seasonal variations

Besides the deflection at the center of the loading plate, the deflections which are 12, 18, 24, 36, 48, and 60 inches behind the center of the loading plate were also recorded for each test. By plotting the deflections at these points, a deflection basin can be drawn (Figure 182) to observe the subsequent pavement response. From this figure, the load transfer efficiency of a pavement can also be determined. Figure 182 presents three deflection basins based on three seasonal periods at the same test location. The composite pavement after-thawing was softer than before and during freezing, and during-freezing pavement performed stiffer than the other two seasonal conditions. The during-freezing pavement also transferred the load more effectively than before-freezing and after-thawing conditions.

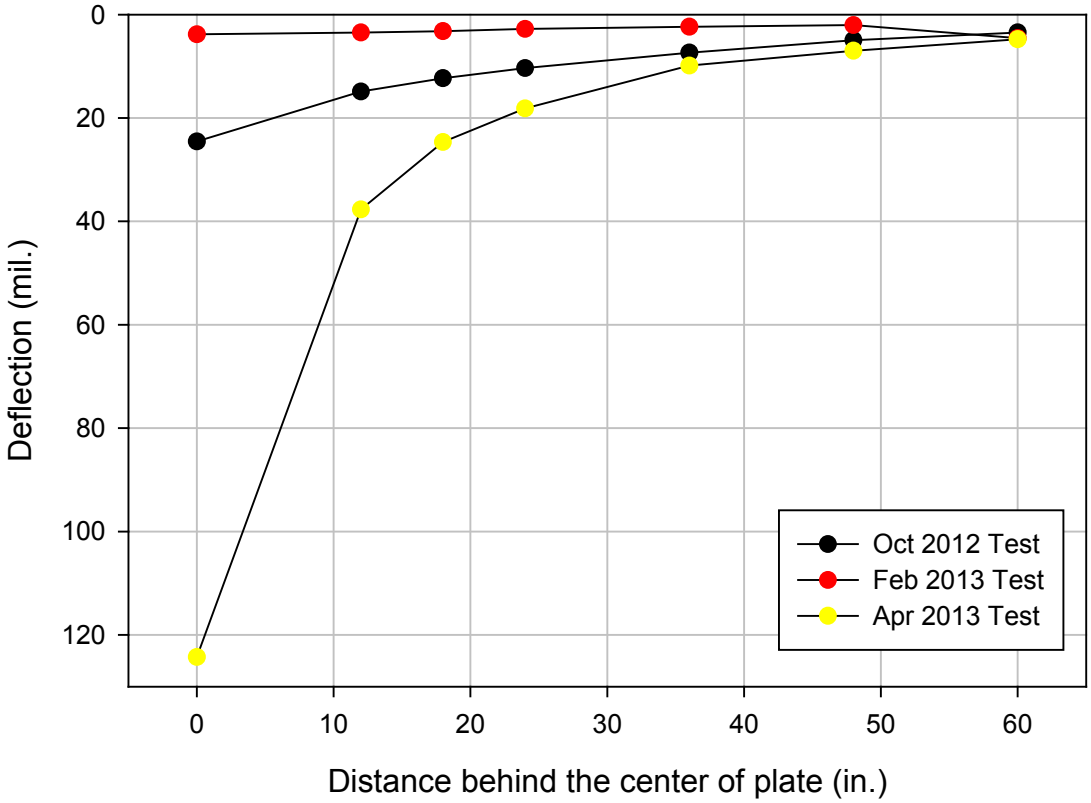

Figure 182. Defection basin at Station 350.0 ft. on the 12th Street north

CHAPTER 6. CONCLUSIONS AND RECOMMENDATIONS

This chapter presents an overview of the technical merit and scientific value gained from the study and an overview of the lessons learned. The conclusions are presented in two sections, conclusions based on frost-heave and thaw-weakening laboratory testing and those based on in situ testing, followed by recommendations for future research and practice.

The specific objectives of the study were to compare the stabilization effects of various stabilizers for geomaterials based on frost susceptibility and to associate laboratory results with in situ freeze-thaw performance. Frost-heave and thaw-weakening laboratory tests were conducted according to ASTM D5918 to determine freeze-thaw performance of sandy lean clay (CL) subgrade and silty sand with gravel (SM) subbase. Freeze-thaw performance of pavement systems with the same subbase and subgrade stabilization methods was determined through DCP and FWD testing. The test results from laboratory and in situ were evaluated and analyzed.

CONCLUSIONS

The CL had 11.43 mm/day frost heave rate and 1.4% CBR values that were high to very high frost susceptibility. Samples stabilized with different concentrations of fly ash and cement were tested. Of the four fly ash concentrations tested, 15% was the optimal fly ash content (as compared with 5%, 10%, and 20% fly ash) for controlling freeze-thaw performance. Of the three types of fly ash tested, the fly ash with the highest CaO contents was most effective in improving frost susceptibility. However, overall fly ash stabilization was not an effective method for decreasing the frost heave rates of the CL soil. Cement controlled both the heave rate and the CBR values change of this kind of soil effectively during freeze-thaw cycles.

The test results showed that the SM soil had 15.63 mm/day frost heave rate and 8.8% CBR values, and the frost susceptibility level of this soil ranges from medium to high. Fibers alone did not effectively decrease the frost heave rates or improve changes in soil stiffness. This finding differs from Hoover's (1982) conclusions but matched the conclusions reported in Tang et al. (2007). The proper amount of cement also controlled both the heave rate and the CBR values change of this SM soil. Regardless of the cost of materials and installations

and environmental friendliness, cement + fibers resulted in the optimal stabilization effects on improving the frost susceptibility of this kind of soil.

Compaction delay is an important factor influencing the stabilization effect. The longer compaction delay increased the frost heave rates and the stiffness changes of stabilized soils. Increasing the cure period from 7 days to 180 days improved the frost susceptibility of 15% fly ash stabilized loess samples.

The D_0 values that were directly measured from FWD tests were used to determine the stiffness of pavement systems. The test results showed that the values were lower under after-thawing conditions and were larger under frozen conditions. The D_0 seasonal variations trends were similar for the pavement systems with all kinds of stabilization methods and non-stabilized pavement systems.

The CBR values of each layer of pavement systems were calculated from the test results of DCP tests. Cement stabilized recycled subbase (SM) and cement + fibers stabilized recycled subbase turned out to be more effective for controlling the freeze-thaw influence to stiffness. Cement also resulted in higher CBR values than other stabilization methods for subgrade (CL) materials.

RECOMMENDATIONS FOR FUTURE RESEARCH

Performing this study raised several areas for future research:

- Perform frost-heave and thaw-weakening tests on fly ash + cement stabilized geomaterials to determine if cement can improve the fly ash stabilization effect on freeze-thaw performance.
- Decrease the cement content from 3.75% in the cement +fibers stabilized geomaterials to determine the optimum cement content.
- Conduct resilient modulus tests on the post freeze-thaw test samples to evaluate the soil stiffness changes under cyclic loading.
- Determine the effectiveness of geosynthetics (e.g., geocell, geotextiles, and geogrid) for improving the frost susceptibility of geomaterials.
- Conduct a study on the water movement in soil with different stabilization methods during freeze-thaw tests.

- Perform frost-heave and thaw-weakening tests on more geomaterials to evaluate the frost susceptibilities of other kinds of soils.

Results from this study and future research suggested here could ultimately be used to form a reference tool pavement designers could consult to effectively address frost susceptibility of pavement foundation geomaterials.

RECOMMENDATIONS FOR FUTURE PRACTICE

Results of this study suggest two related recommendations for future practice. First, in addition to accounting for major properties (e.g., shear strength, resilient modulus, and durability), pavement designers in cold regions should account for frost susceptibility as a factor that influences pavement serviceability, durability, and safety. Second, once the frost susceptibility of the pavement foundation materials is known, the pavement designers need to balance the initial cost of stabilizers that reduce frost susceptibility with the long-term costs associated with freeze-thaw damage.

WORKS CITED

Allen, T., Bell, J.R., and Vinson, T.S. (1983). Properties of geotextiles in cold regions applications. Corvallis, Oregon: Transportation Research Institute, Transportation Research Report 83-6.

ASTM. (2004). "Standard Test Method for Materials Finer than 75-µm (No. 200) Sieve in Mineral Aggregates by Washing." *Annual book of ASTM standards,* ASTM C117, West Conshohocken, PA.

ASTM. (2007). "Standard Test Method for Density, Relative Density (Specific Gravity), and Absorption of Coarse Aggregate." *Annual book of ASTM standards,* ASTM C127, West Conshohocken, PA.

ASTM. (2006). "Standard Test Method for Sieve Analysis of Fine and Coarse Aggregates." *Annual book of ASTM standards,* ASTM C136, West Conshohocken, PA.

ASTM. (1995). "Standard Specification for Fly Ash and Other Pozzolans for Use with Lime." *Annual book of ASTM standards,* ASTM C136, West Conshohocken, PA.

ASTM. (1963). "Standard Test Method for Particle-Size Analysis of Soils." *Annual book of ASTM standards,* ASTM D422, West Conshohocken, PA.

ASTM. (2003). "Standard Test Methods for Wetting and Drying Compacted Soil-cement Mixtures." *Annual book of ASTM standards,* ASTM D422, West Conshohocken, PA.

ASTM. (2003). "Standard Test Methods for Freezing and Thawing Compacted Soil-cement Mixtures." *Annual book of ASTM standards,* ASTM D422, West Conshohocken, PA.

ASTM. (2007). "Standard Test Methods for Laboratory Compaction Characteristics of Soil using Standard Effort." *Annual book of ASTM standards,* ASTM D698, West Conshohocken, PA.

ASTM. (2005). "Standard Test Method for CBR (California Bearing Ratio) of Laboratory-Compacted Soils." *Annual book of ASTM standards,* ASTM D1883, West Conshohocken, PA.

ASTM. (2006). "Standard Test Method for Unconfined Compressive Strength of Cohesive Soil." Annual book of ASTM standards, ASTM D2166, West Conshohocken, PA.

ASTM. (2006). "Standard Practice for Classification of Soils for Engineering Purposes (Unified Soil Classification System)." *Annual book of ASTM standards,* ASTM D2487, West Conshohocken, PA.

ASTM. (2005). "Standard Test Methods for Liquid Limit, Plastic Limit, and Plasticity Index of Soils." *Annual book of ASTM standards,* ASTM D4318, West Conshohocken, PA.

ASTM. (1996). "Standard Test Methods for Frost Heave and Thaw Weakening Susceptibility of Soils." *Annual book of ASTM standards,* ASTM D5918, West Conshohocken, PA.

ASTM. (2003). "Standard Test Method for Use of the Dynamic Cone Penetrometer in Shallow Pavement Applications." *Annual book of ASTM standards,* ASTM D6951, West Conshohocken, PA.

Beskow, G. (1935, 1991). "Soil Freezing and Frost Heaving with Special Applications to Roads and Railroads," in *Historical Perspectives in Frost Heave Research: The Early Works of S. Taber and G. Beskow.* Eds. Black, P.B., and Hardenberg, M.J. 37-158.

Bin-Shafique, S., Rahman, K., and Azfar, I. (2011). "The effect of freezing-thawing cycles on performance of fly ash stabilized expansive soil subbases." *Geo-Frontiers.* 2011: pp. 697-706.

Boone, IA. (2013). Google Maps. Google. <https://maps.google.com/maps?hl=en&tab=wl&authuser=0>. (November 4, 2013)

Brandl, H. (2008). "Freezing-thawing behavior of soils and unbound road layers." Slovak Journal of Civil Engineering. 3. 4-12.

Casagrande, A., Taber, S., and Watkins, W. (1931). "Discussion of Frost Heaving." *Highway Research Board, Proceeding,* Vol. 11, 165-177.

Cetin, B., Aydilek A., and Guney, Y. (2010). "Stabilization of recycled base materials with high carbon fly ash." *Resources, Conservation and Recycling,* 54(2010), 878-892.

Chamberlain, E.J. (1981). Frost susceptibility of soil: Review of index tests. U.S. Army Cold Regions Research and Engineering Laboratory Monograph 81-02.

Chamberlain, E.J. (1986). Evaluation of selected frost-susceptibility test methods. U.S. Army Cold Regions Research and Engineering Laboratory Report 86-104.

Chamberlain, E.J. (1987). A freeze-thaw test to determine the frost-susceptibility of soils. CRREL Special Report 87-1.

Chamberlain, E.J., and Carbee, D.L. (1981). "The CRREL frost heave test, USA." *Frost I Jord*, 22:53-63.

Chamberlain, E.J., Iskveer, I., and Hunsiker, S.E. (1990). "Effect of Freeze-Thaw on the Permeability and Macrostructure of Soils." *Proceedings International Symposium on Frozen Soil Impacts on Agricultural*, Range and Forest Lands, March 21-22, Spokane, WA, pp. 145-55.

Chen, X., and Wang, Y. (1988). "Frost heave prediction for clayey soils." *Cold Regions Science and Technology*. 15(1988), 233-238.

Cokca, E. (2001). "Use of Class C fly ashes for the stabilization of an expansive soil." *Journal of Geotech. and Geo-environmental Engg.*, 127(7):568-573.

Collins, R. W. (2011). "Stabilization of marginal soils using geofibers and nontraditional additives." M.S. Thesis, University of Alaska Fairbanks, Fairbanks, AK.

Crane, R.A., Guthrie, W.S., Eggett, D.L., and Hanson, J.R. (2006). "Roughness of Flexible Pavements with Cement-Treated Base Layers." In Transportation Research Board 85th Annual Meeting Compendium of Papers. CD-ROM. Transportation Research Board, National Research Council, Washington, D.C., January 2006.

Dempsey, B.J., and Thompson, M.R. (1973). "Effects of freeze-thaw parameters on the durability of stabilized materials." *Civil Engineering Studies*, Transportation Engineering Series No. 4, Illinois Cooperative Highway Research Program Series No. 136.

FHWA. (2000). "LTPP Manual for Falling Weight Deflectometer Measurements Operational Field Guidelines: Version 3.1." Long Term Pavement Performance Program, Pavement Performance Division, U.S. Department of Transportation, McLean, VA.

George, K.P. (1968). "Cracking in Cement-Treated Bases and Means for Minimizing It." In Highway Research Record 255, TRB, National Research Council, Washington, D.C., 1968, pp. 59-70.

Ghazavi, M., and Roustaie, M. (2009). "The influence of freeze-thaw cycles on the unconfined compressive strength of fiber-reinforced clay." *Cold Regions Science and Technology,* 61(2010), 125-131.

Gray, D.H., and Ohashi, H., (1983). "Mechanics of Fiber Reinforcement in Sand," *Journal of Geotechnical Engineering*, Vol. 109, No. 3, March, 1983.

Guthrie, W.S., Lay, R.D., and Birdsall, A.J. (2007). "Effect of Reduced Cement Contents on Frost Heave of Silty Soils: Laboratory Testing and Numerical Modeling." 07-2999, Transportation Research Board 86th Annual Meeting, Washington, D.C., January 2007.

Hazirbaba, K., and Gullu, H. (2007). "California Bearing Ratio improvement and freeze-thaw performance of fine-grained soils treated with geofiber and synthetic fluid." *Cold Regions Science and Technology,* 63(2010), 50-60.

Henry, K.S. (1990). Laboratory investigation of the use of geotextiles to mitigate frost heave. CRREL Report 90-6. U.S. Army Corps of Engineers.

Hoover, J.M., Moeller, D.T., Pitt, J.M., Smith, S.G., and Wainaina N.W. (1982). Performance of Randomly Oriented, Fiber-Reinforced Roadway Soils: A Laboratory and Field Investigation. Iowa Department of Transportation Project HR-211. Iowa State University College of Engineering, Ames, IA.

Janoo, V.C., Barna, L.A., and Orchino, S.A. (1997). Frost-Susceptibility Testing and Predictions for the Raymark Superfund Site. CRREL Special Report 97-31.

Janoo, V.C., Eaton, R., and Barna L. (1997). Evaluation of Airport Subsurface Materials. U.S. Army Corps of Engineering, Cold Regions Research and Engineering Laboratory Special Report 97-13.

Johnson, A.J. (2012). "Freeze-thaw performance of pavement foundation materials." M.S. Thesis, Iowa State University, Ames, IA.

Joint Departments of the Army and Air Force USA. (1985). Pavement Design for Seasonal Frost Conditions. Technical Manual TM 5-818-2/AFM 88-6, Chapter 4. Washington, D.C. U.S. Government Printing Office.

Konrad, J.M. (1988). "Influence of freezing mode on frost heave characteristics." *Cold Regions Science and Technology*, 15 (1988) 161-175.

Lee, W., Bohra, N.C., Altschaeffl, A.G., and White, T.D. (1995). "Resilient modulus of cohesive soils and the effect of freeze-thaw." *Canadian Geotechnical Journal*, 1995, 32(4):559-568, 10.1139/t95-059.

Norling, L.T. (1973). “Minimizing reflective cracks in soil-cement pavements: a status report of laboratory studies and field practices.” In Highway Research Record 2442, TRB, National Research Council, Washington, D.C., 1973, pp. 22-23.

O’Flaherty, C. A., Edgar, C. E., and Davidson, D. T. (1963). “The Iowa State Compaction Apparatus: A Small Sample Apparatus for Use in Obtaining Density and Strength Measurements of Soils and Soil-Additives.” Presented at the 42nd Annual Meeting of the Highway Research Board, Washington, D.C., January 1963.

Pavement Interactive. 2006. "Frost Action". <www.pavementinteractive.org/article/frost-action/#>. (November 4, 2013).

Penner, E. (1966). “Frost-Heaving in Soils.” National Research Council, Canada. Research Paper No. 295 of the Division of Building Research. Reprinted from Proceedings: Permafrost International Conference, November 1963, 197–202.

Penner, E. (1967). “Experimental pavement structures insulated with a polyurethane and extruded polystyrene foam.” Proceedings International Conference. Low Temperature Science, 1966, Sapporo, Japan, Vol. 1(2):1311-1322.

Penner, E., and Eldred, D. (1985). “Equipment and methods for soil frost action studies.” National Resource Council, Canada, Div. Building Res. Intern. Rep. 503.

Rosa, M.G. (2006). “Effect of freeze-thaw cycling on soils stabilized using fly ash.” M.S. Thesis, University of Wisconsin-Madison, Madison, WI.

Solanki, P., Zaman, M., and Khalife, R. (2013). “Effect of Freeze-Thaw Cycles on Performance of Stabilized Subgrade.” *Sound Geotechnical Research to Practice,* pp. 566-580.

Svec, O.J. (1989). “A new concept of frost-heave characteristics of soils.” *Cold Regions Science and Technology*, 16 (1989) 271–279.

Taber, S. (1929). “Frost Heaving.” *Journal of Geology*, Vol. 37, No. 5 (Jul.–Aug., 1929), 428–461.

TxDOT Designation. (1999). “Test Procedure for Freezing and Thawing Tests of Compacted Soil-cement Mixture.” TxDOT Designation, TEX-135-E.

Viswanadham, B.V.S. (2009). “Model studies on geofiber-reinforced soil.” *Geotide*, IGC 2009, Guntur, India.

Weather.com (2013). "Average Weather for Boone, IA - Temperature and Precipitation." <http://www.weather.com/weather/wxclimatology/monthly/graph/50036>. (September 11, 2013).

Wikipedia: The free encyclopedia. (2013). Wikimedia Foundation, Inc. <http://en.wikipedia.org/wiki/Portland_cement#ASTM_C150>. (November 4, 2013).

White. D.J., Becker, P., Vennapusa. P.K.R., Dunn, M., and White, C.I. (2012). “Soil stiffness assessment of stabilized pavement foundations.” presented at Transportation Research Board, 92nd Anuual Meeting, Washington, D.C., January.

Ystenes, M. (2011). “Frost heave – Telehiv.” <http://www.flickr.com/photos/ystenes/5606721032/>. (November 4, 2013).

Zaimoglu, A.S. (2010). “Freezing-thawing behavior of fine-grained soils reinforced with polypropylene fibers.” *Cold Regions Science and Technology*, 60 (2010) 63-65.

APPENDIX A. STRESS PENETRATION CURVES FROM AFTER FREEZE-THAW CBR TESTS

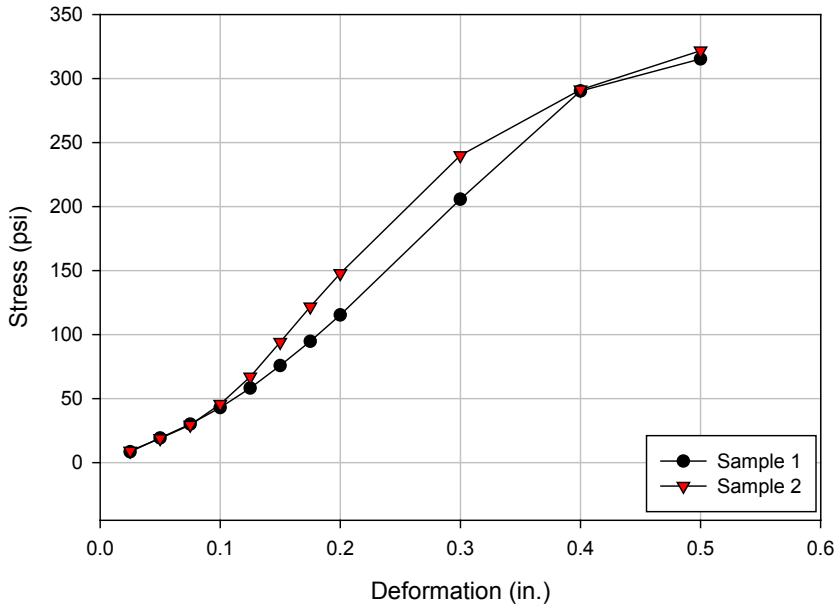

Figure 183. Non-stabilized recycled subbase stress penetration curves

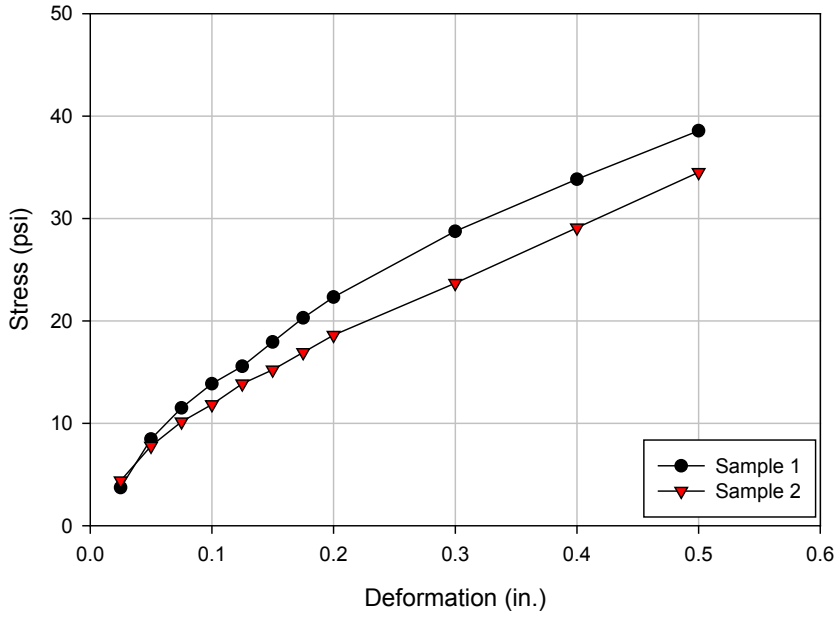

Figure 184. Non-stabilized subgrade stress penetration curves

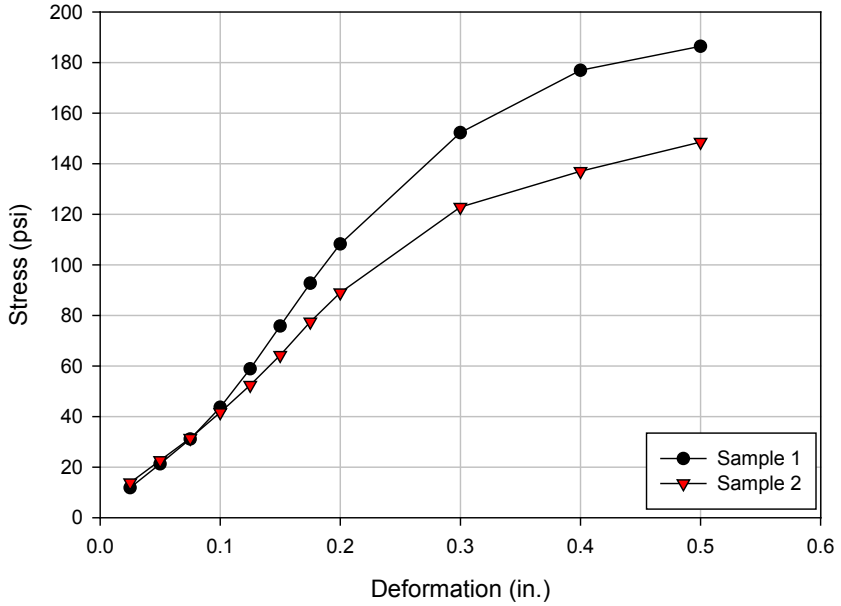

Figure 185. 5% Ames FA stabilized subgrade stress penetration curves

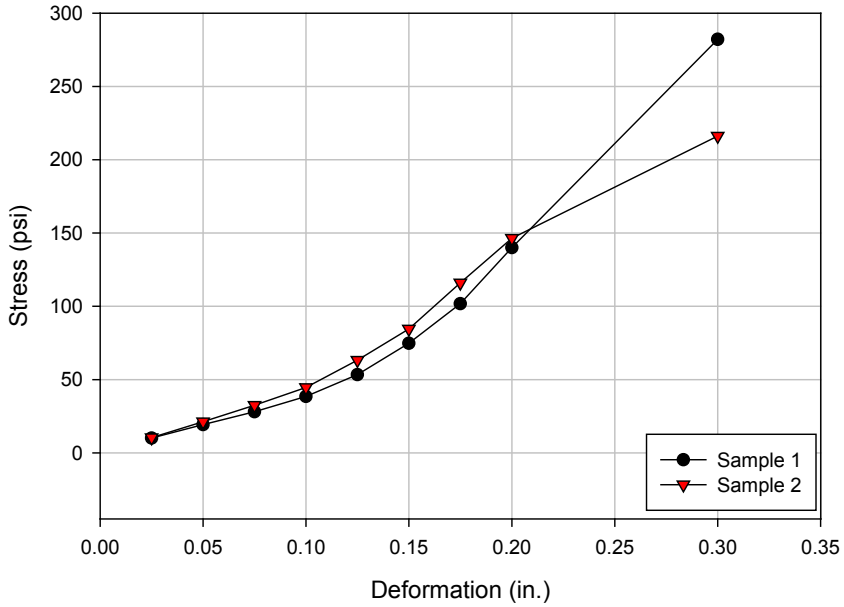

Figure 186. 10% Ames FA stabilized subgrade stress penetration curves

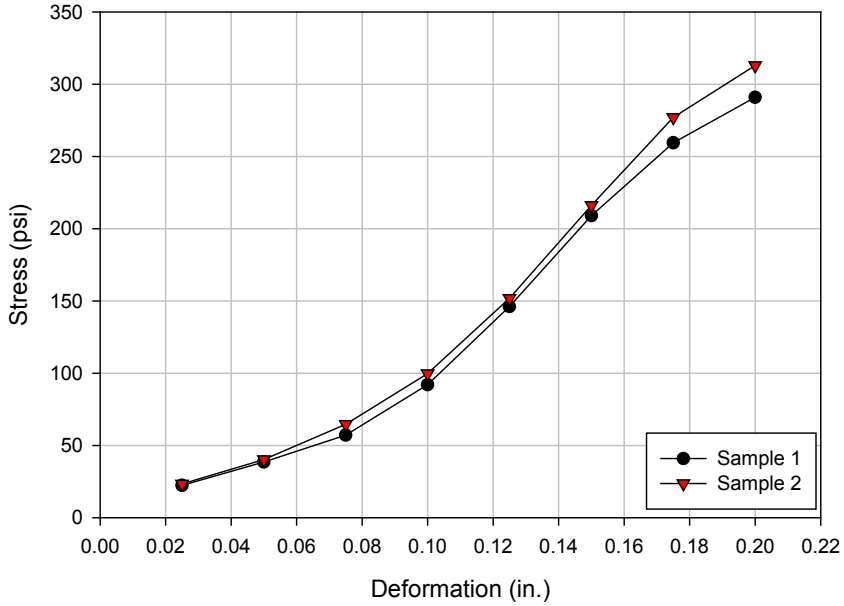

Figure 187. 15% Ames FA stabilized subgrade stress penetration curves

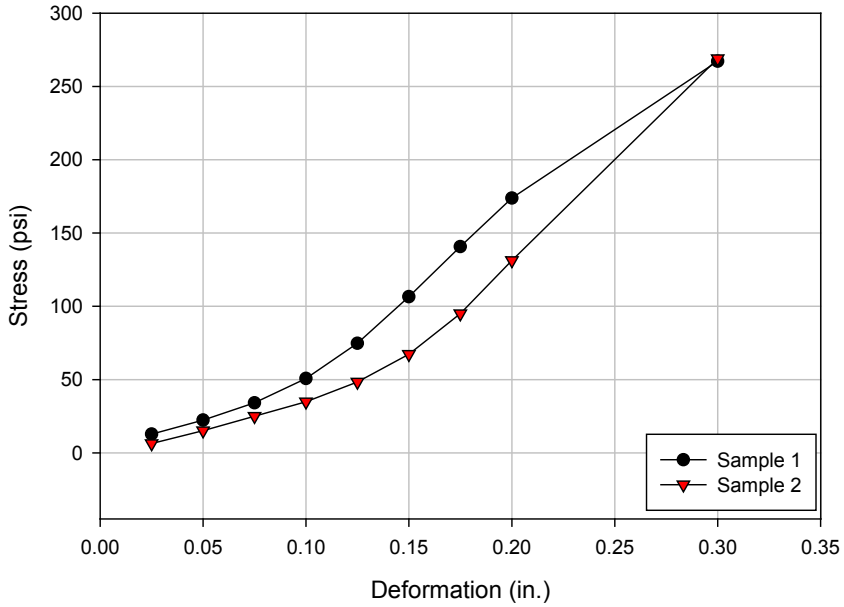

Figure 188. 20% Ames FA stabilized subgrade stress penetration curves

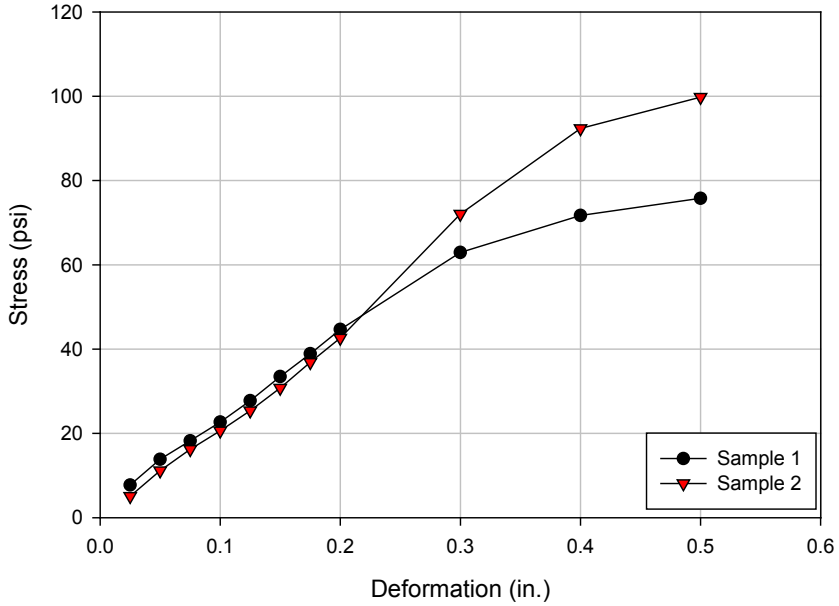

Figure 189. 5% Muscatine FA stabilized subgrade stress penetration curves

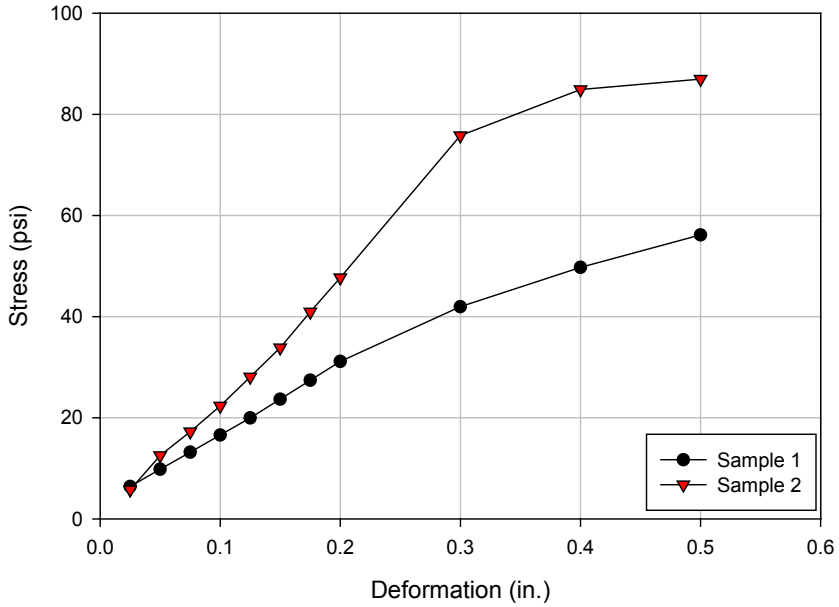

Figure 190. 10% Muscatine FA stabilized subgrade stress penetration curves

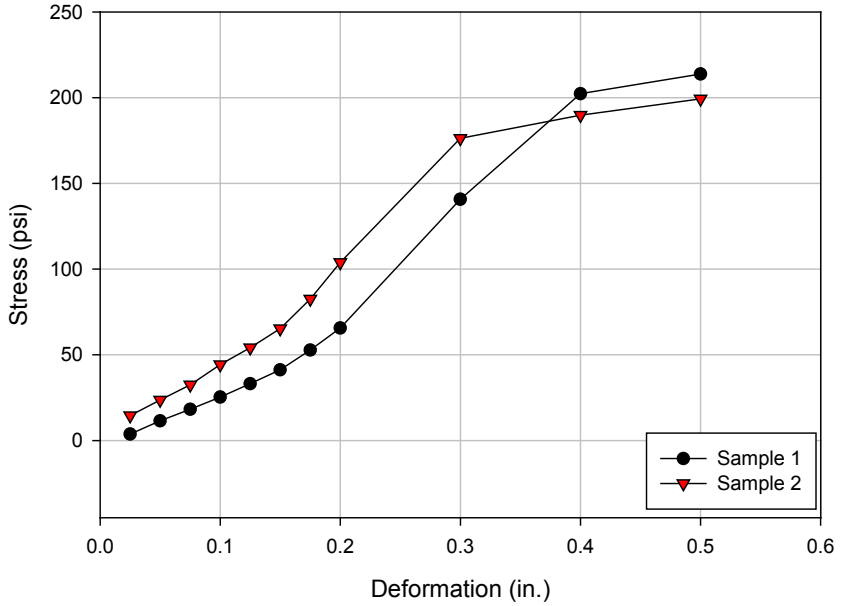

Figure 191. 5% Port Neal FA stabilized subgrade stress penetration curves

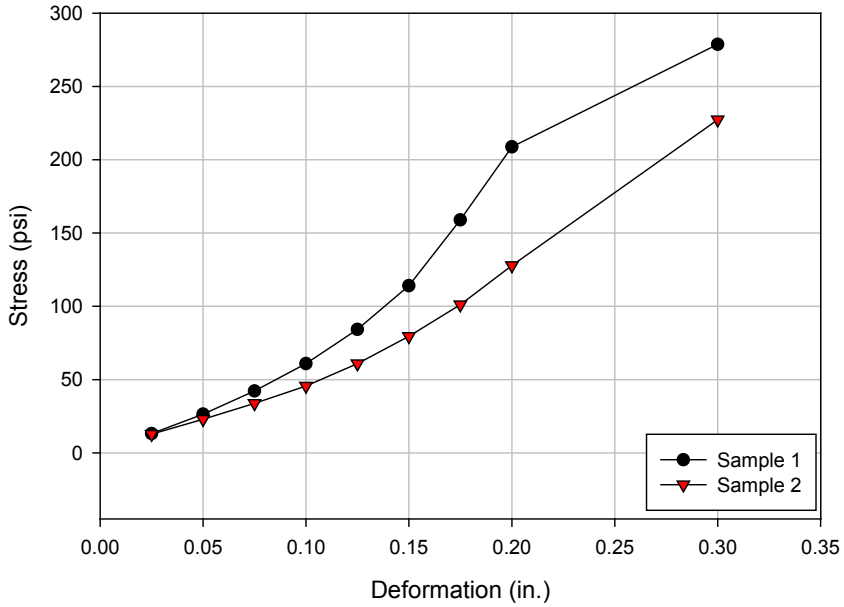

Figure 192. 10% Port Neal FA stabilized subgrade stress penetration curves

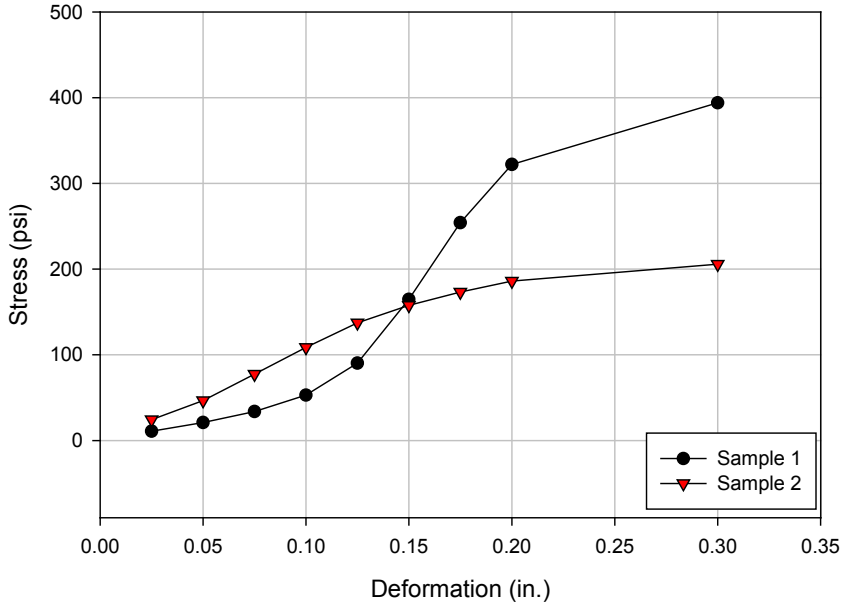

Figure 193. 15% Port Neal FA stabilized subgrade stress penetration curves

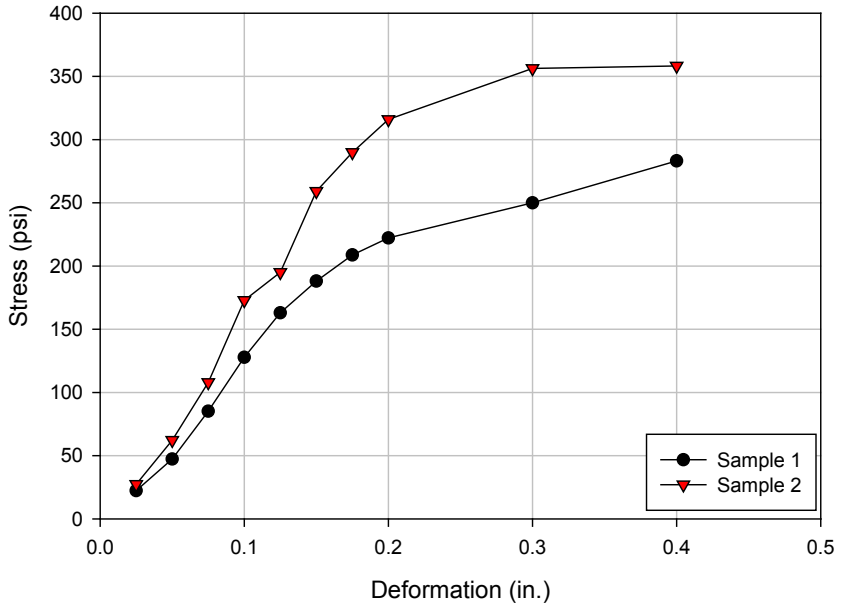

Figure 194. 20% Port Neal FA stabilized subgrade stress penetration curves

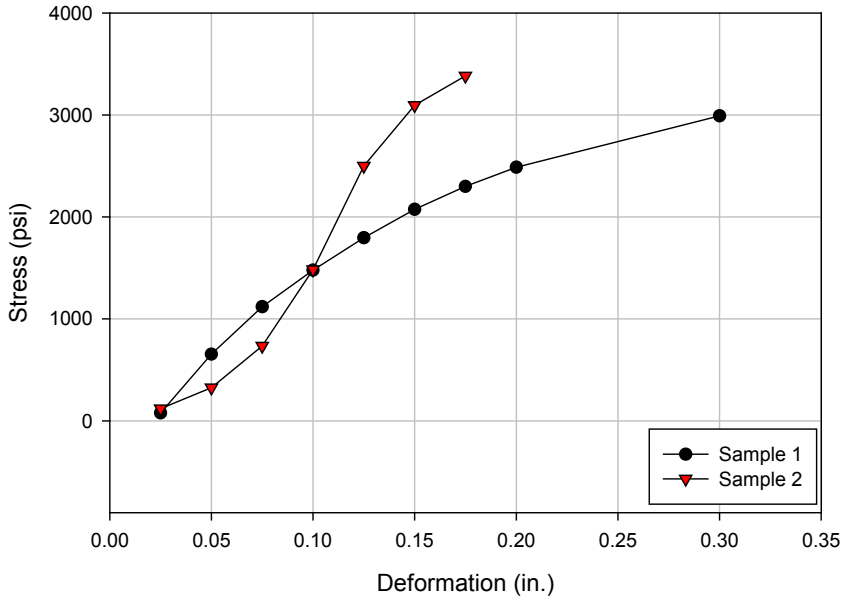

Figure 195. Cement stabilized subgrade stress penetration curves (sample 1: 5% cement; sample 2: 10% cement)

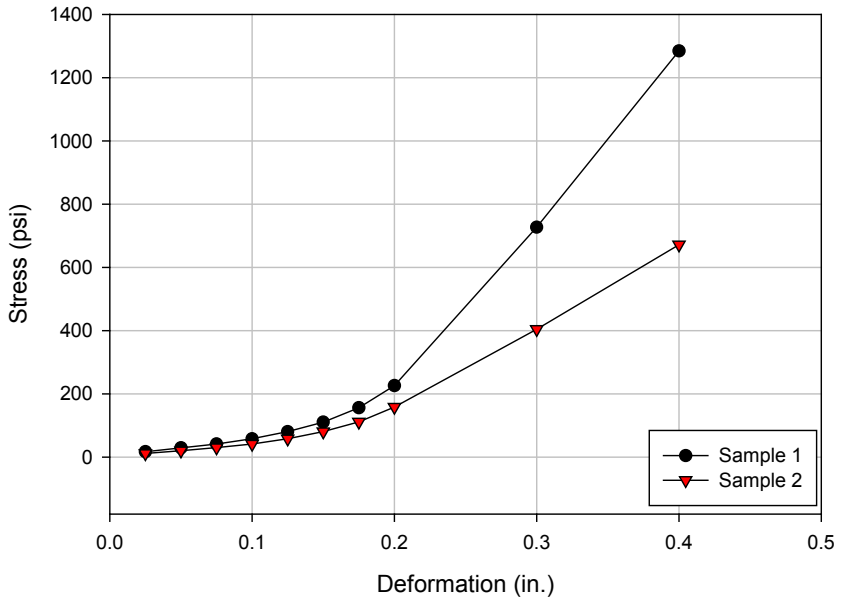

Figure 196. 2.5% cement stabilized recycled subbase stress penetration curves

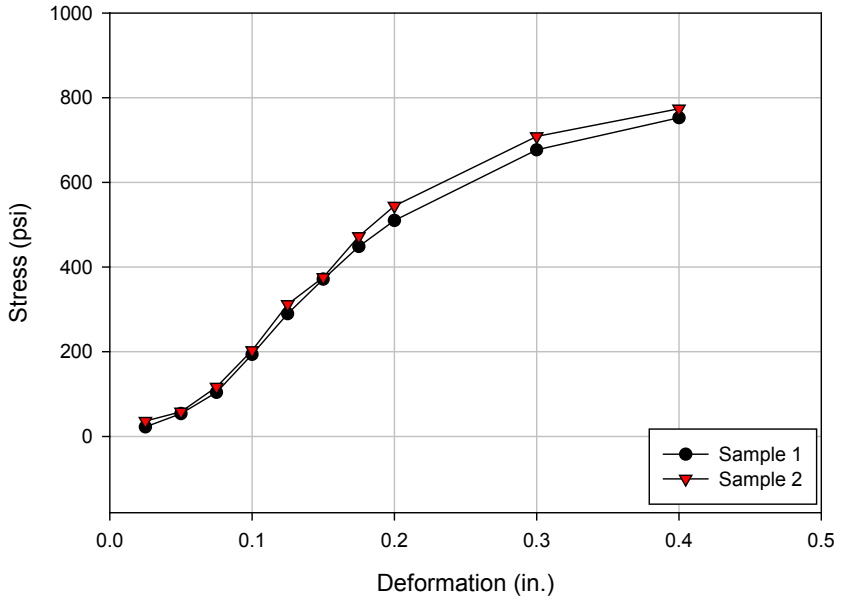

Figure 197. 3.75% cement stabilized recycled subbase stress penetration curves

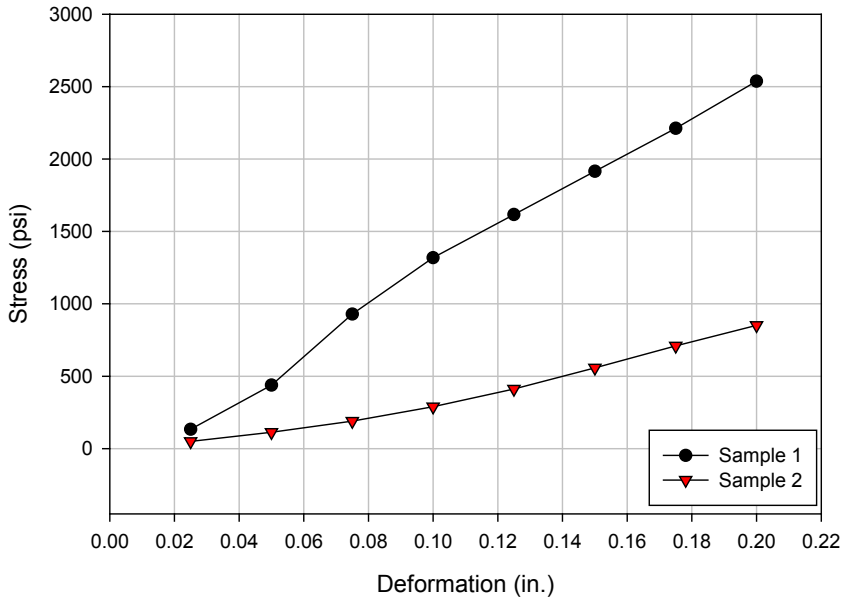

Figure 198. 5% cement stabilized recycled subbase stress penetration curves

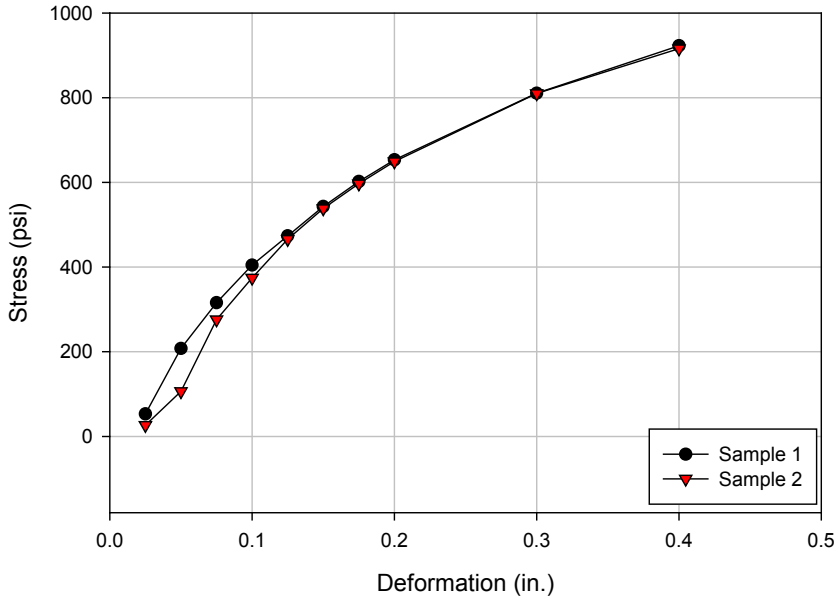

Figure 199. 7.5% cement stabilized recycled subbase stress penetration curves

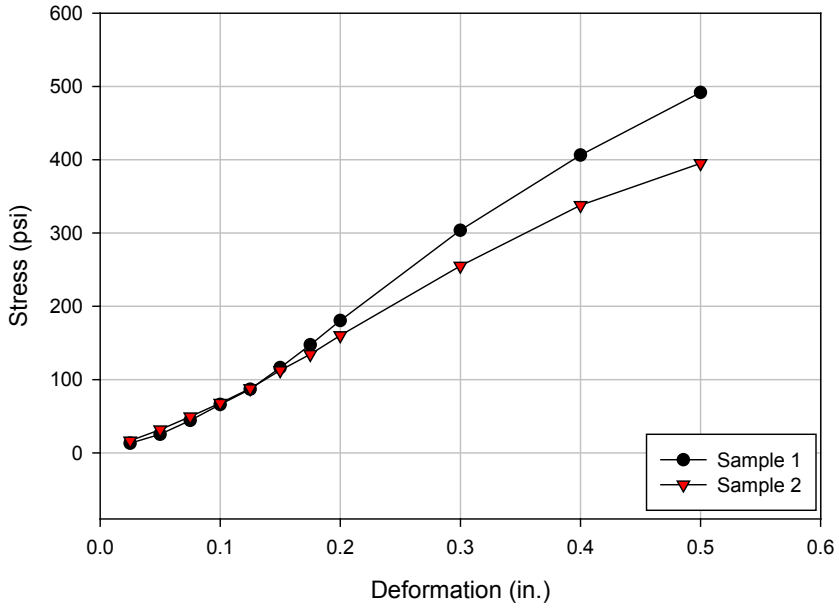

Figure 200. 0.2% PP fiber stabilized recycled subbase stress penetration curves

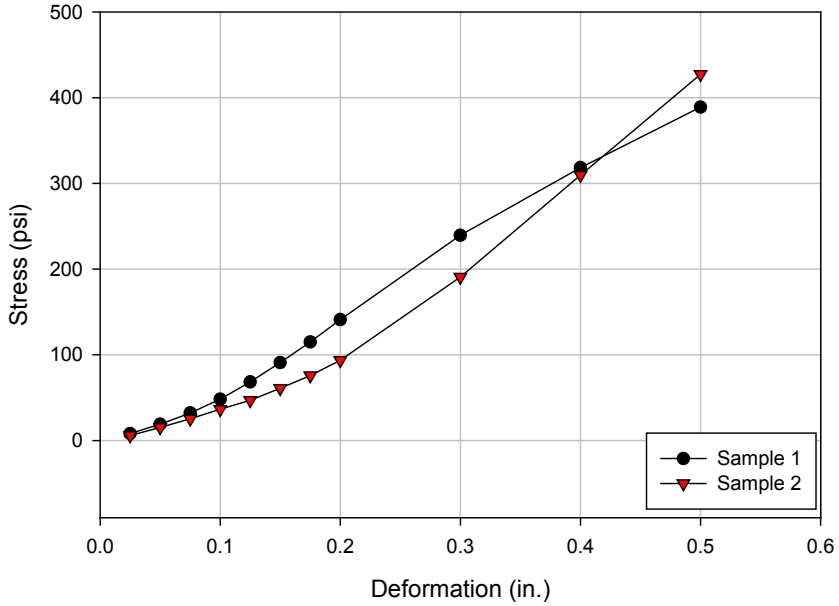

Figure 201. 0.4% PP fiber stabilized recycled subbase stress penetration curves

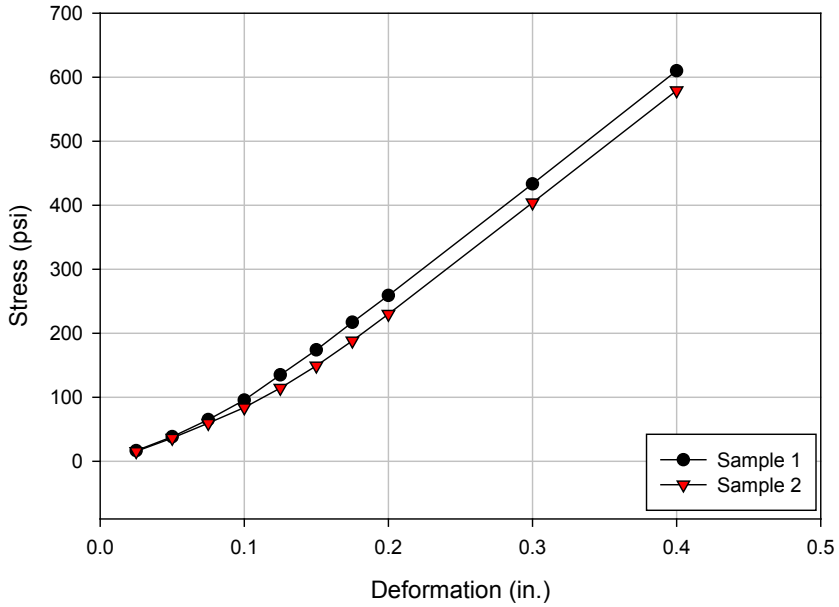

Figure 202. 0.6% PP fiber stabilized recycled subbase stress penetration curves

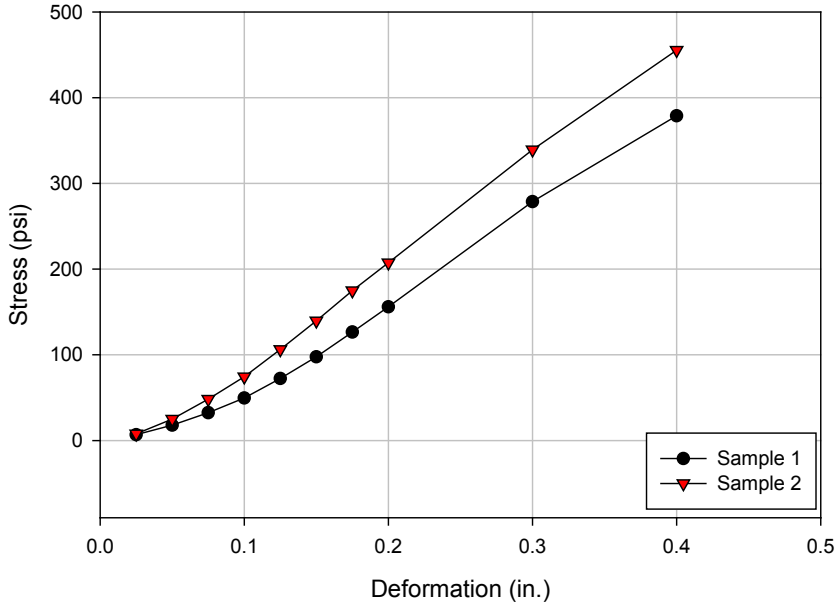

Figure 203. 0.2% MF fiber stabilized recycled subbase stress penetration curves

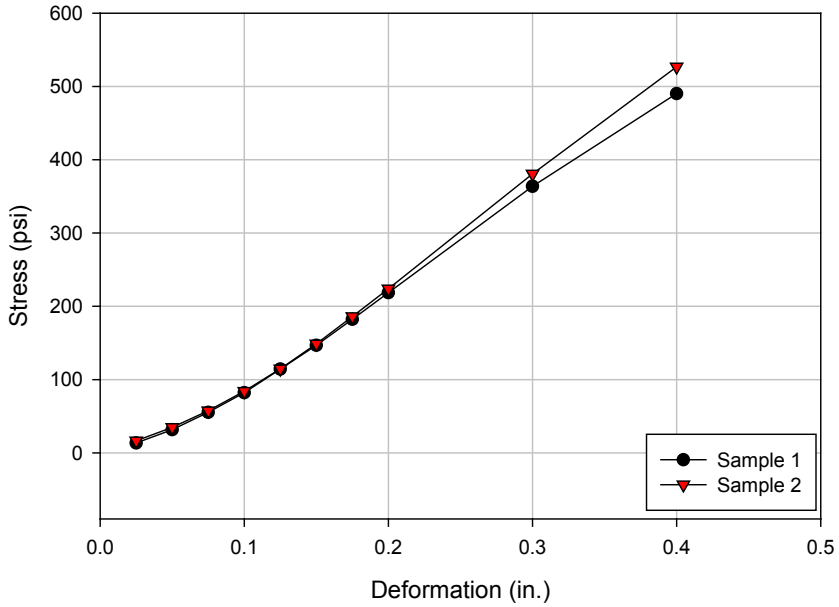

Figure 204. 0.4% MF fiber stabilized recycled subbase stress penetration curves

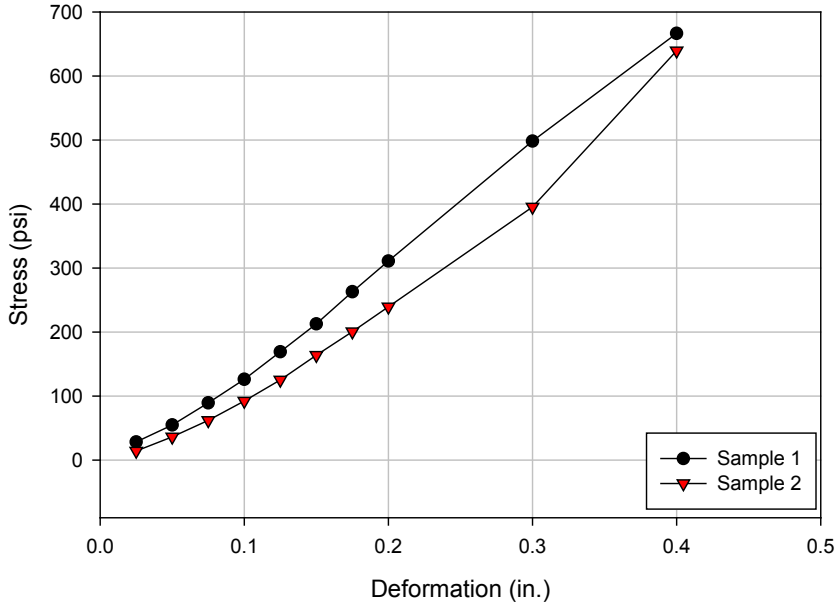

Figure 205. 0.6% MF fiber stabilized recycled subbase stress penetration curves

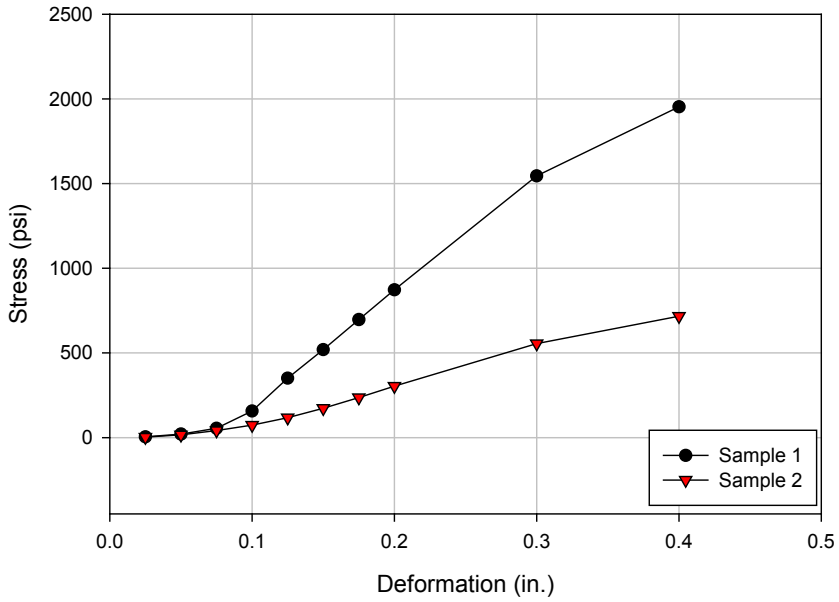

Figure 206. 3.75% cement + 0.2% PP fiber stabilized recycled subbase stress penetration curves (sample 1: no compaction delay; sample 2: 12-hr compaction delay)

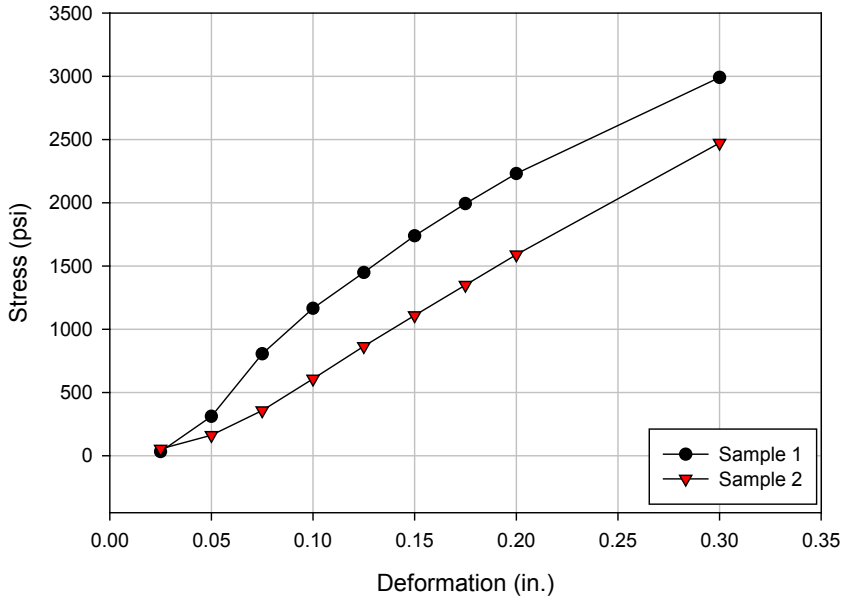

Figure 207. 3.75% cement + 0.4% PP fiber stabilized recycled subbase stress penetration curves (no compaction delay)

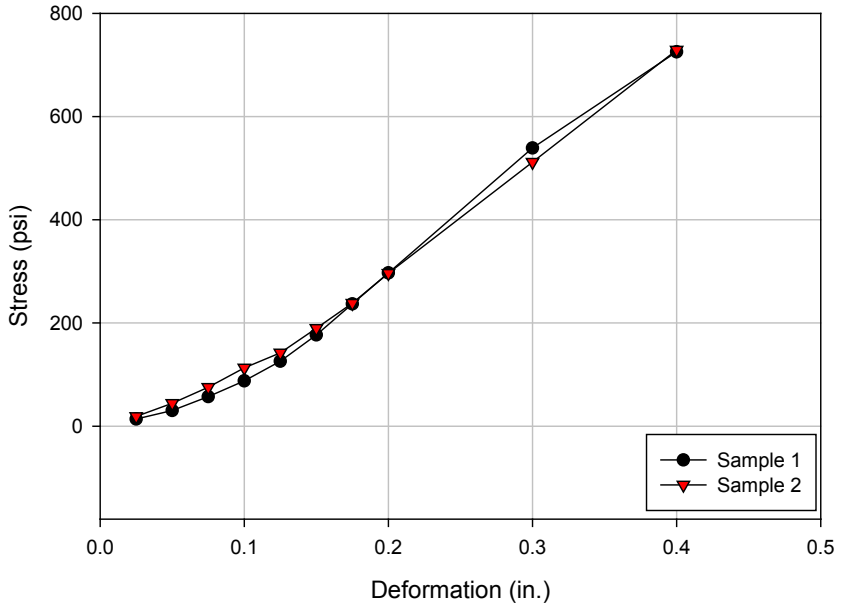

Figure 208. 3.75% cement + 0.4% PP fiber stabilized recycled subbase stress penetration curves (12-hr compaction delay)

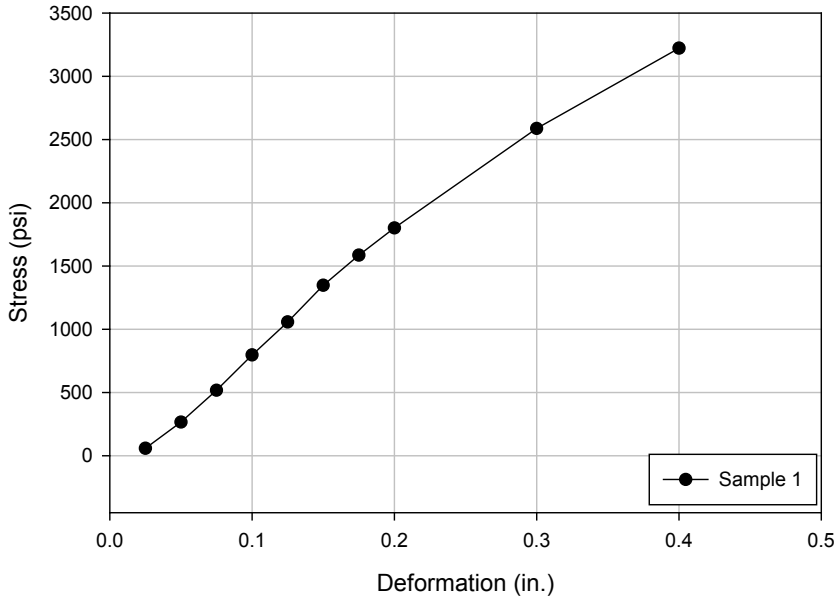

Figure 209. 3.75% cement + 0.6% PP fiber stabilized recycled subbase stress penetration curve

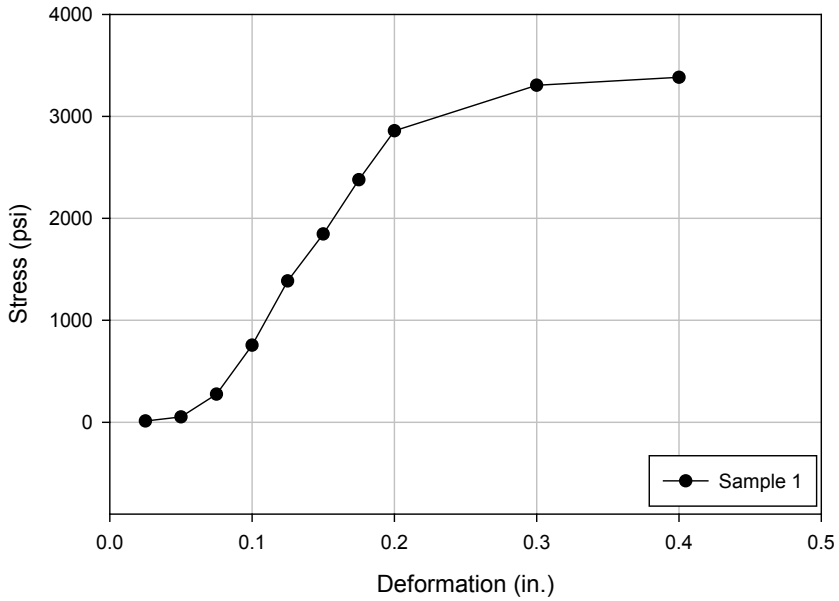

Figure 210. 3.75% cement + 0.2% MF fiber stabilized recycled subbase stress penetration curve

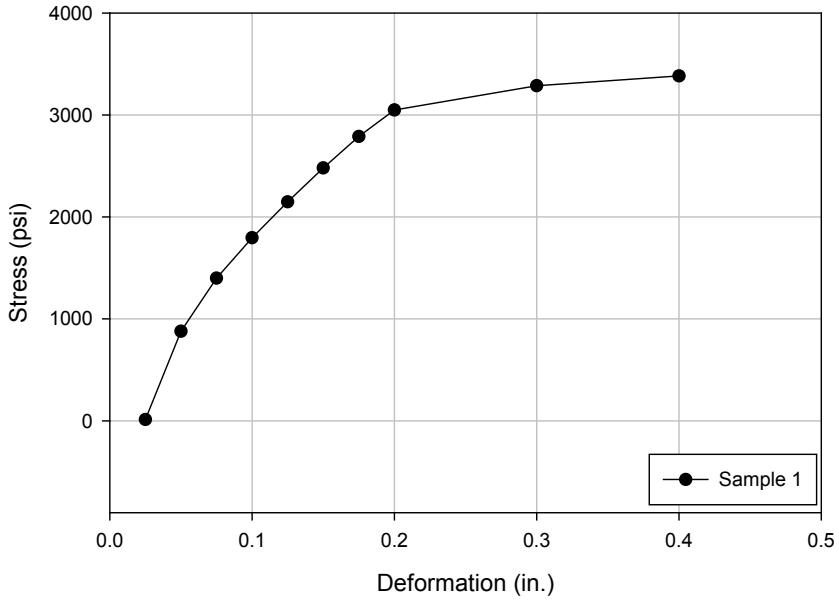

Figure 211. 3.75% cement + 0.4% MF fiber stabilized recycled subbase stress penetration curve

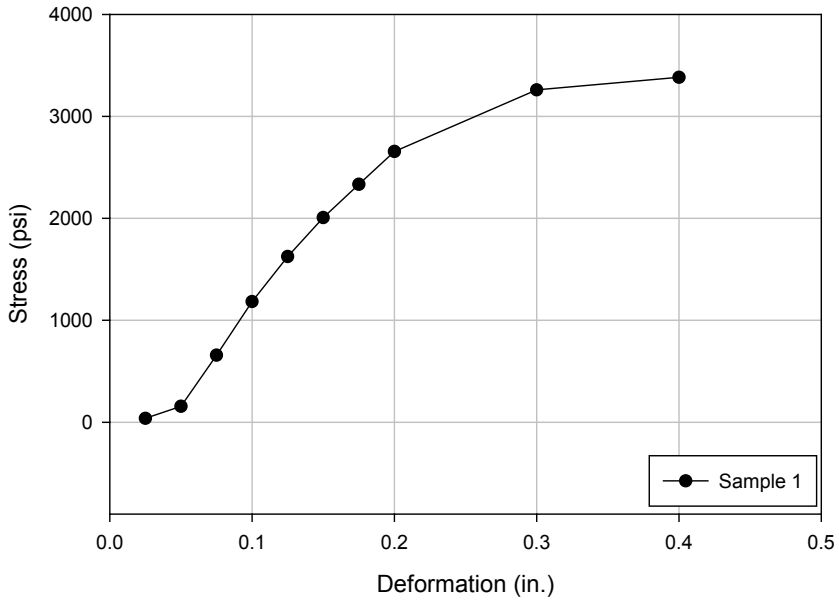

Figure 212. 3.75% cement + 0.6% MF fiber stabilized recycled subbase stress penetration curve

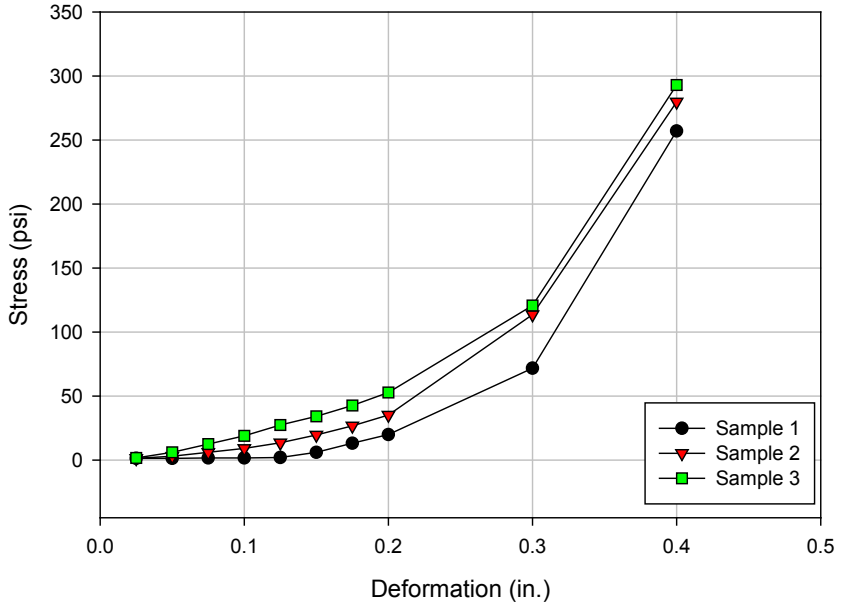

Figure 213. 90-day cured 15% FA stabilized western Iowa loess stress penetration curves

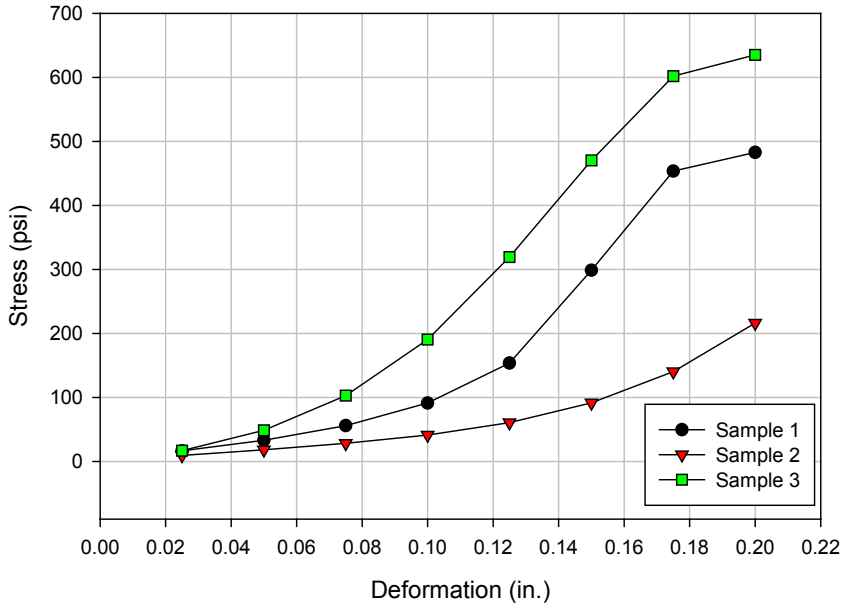

Figure 214. 180-day cured 15% FA stabilized western Iowa loess stress penetration curves

APPENDIX B. STRESS PENETRATION CURVES FROM BEFORE FREEZE-THAW CBR TESTS

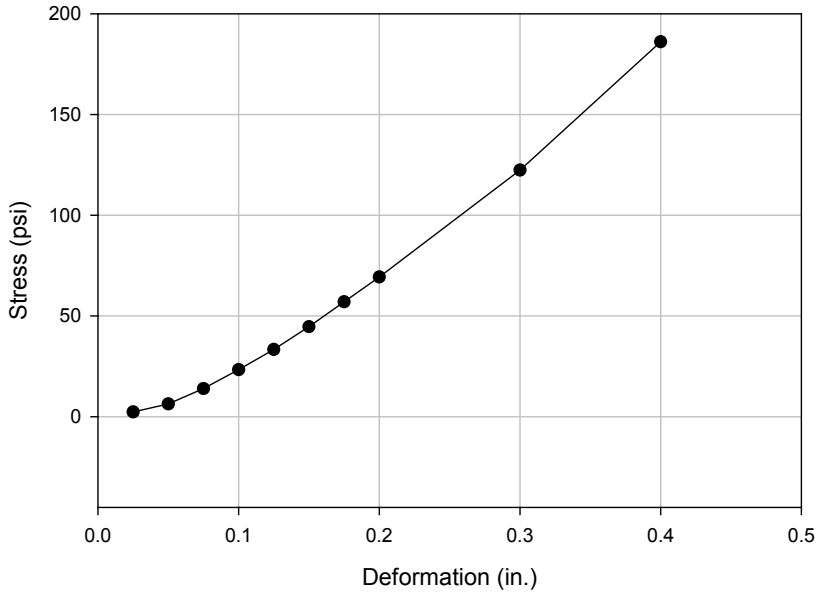

Figure 215. Non-stabilized recycled subbase stress penetration curve

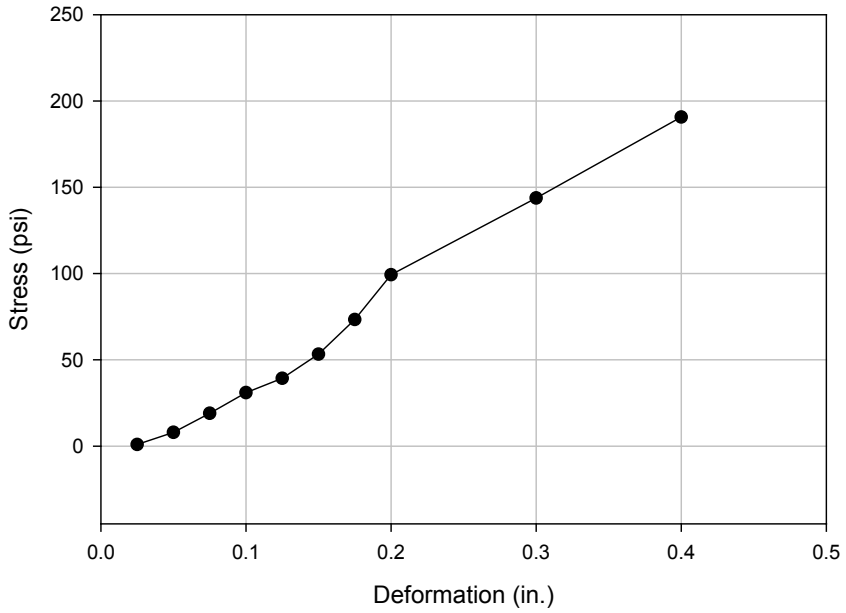

Figure 216. Non-stabilized subgrade stress penetration curve

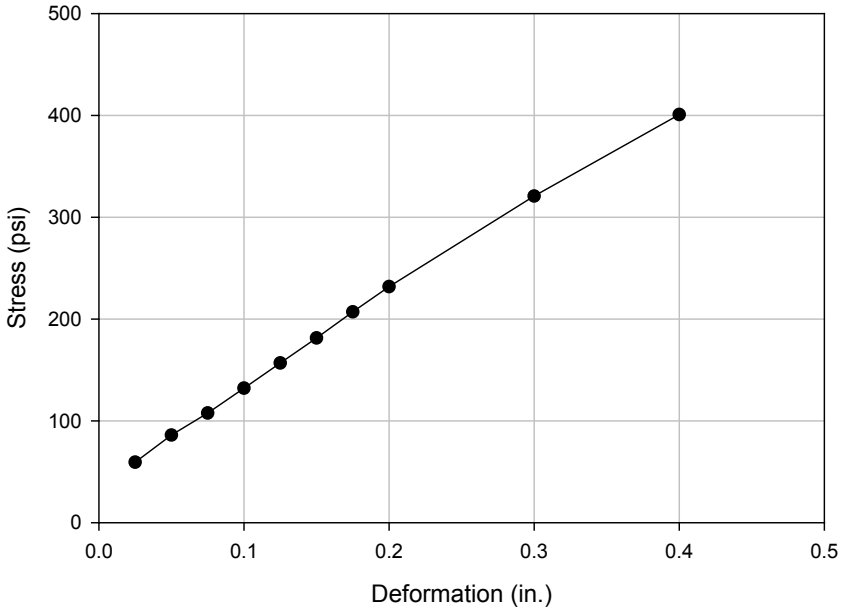

Figure 217. 5% Ames FA stabilized subgrade stress penetration curve

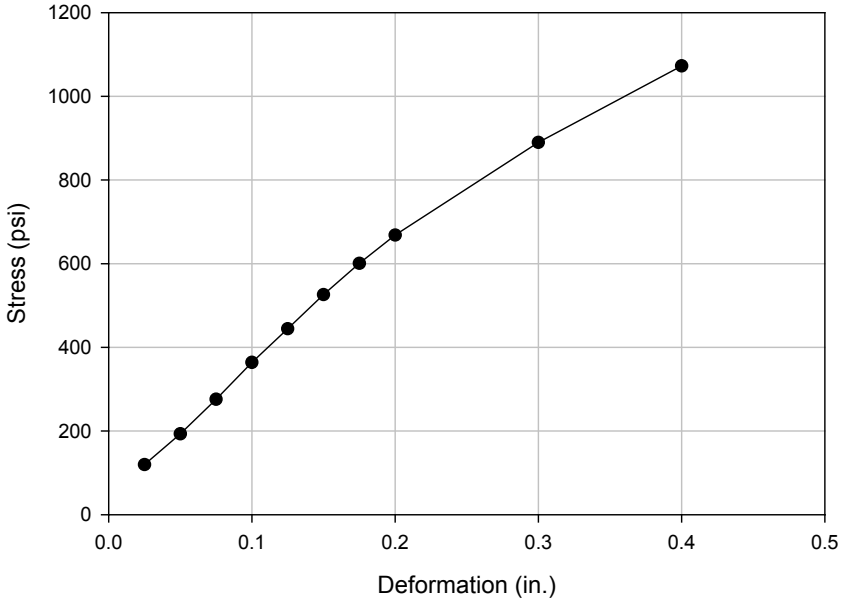

Figure 218. 10% Ames FA stabilized subgrade stress penetration curve

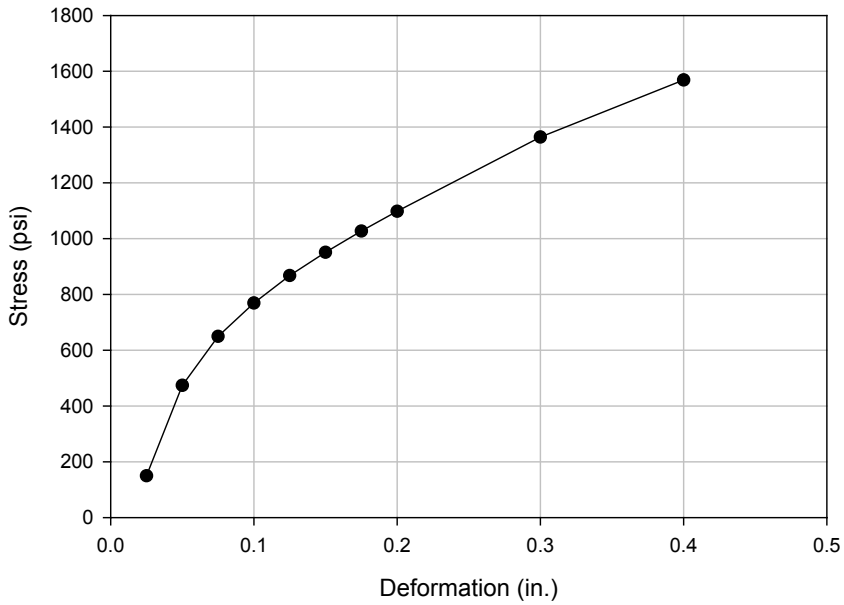

Figure 219. 15% Ames FA stabilized subgrade stress penetration curve

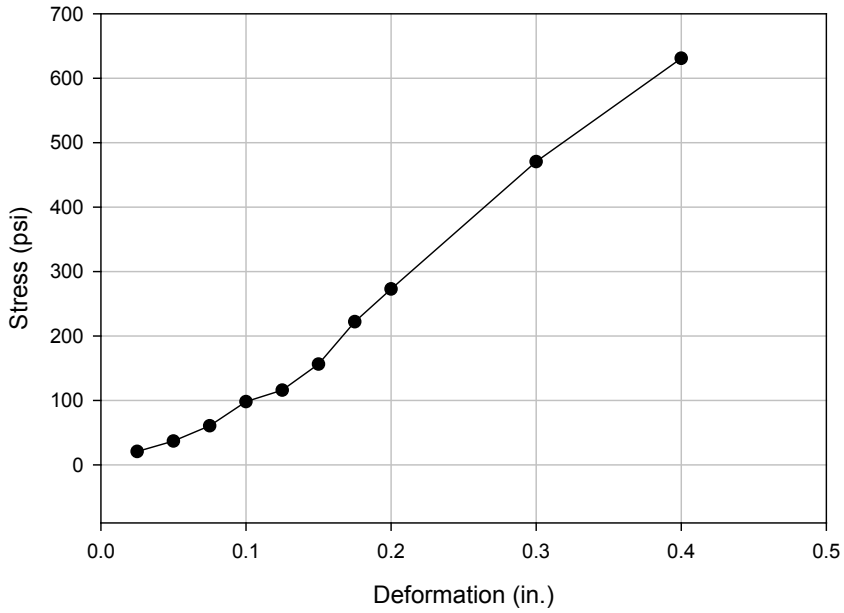

Figure 220. 20% Ames FA stabilized subgrade stress penetration curve

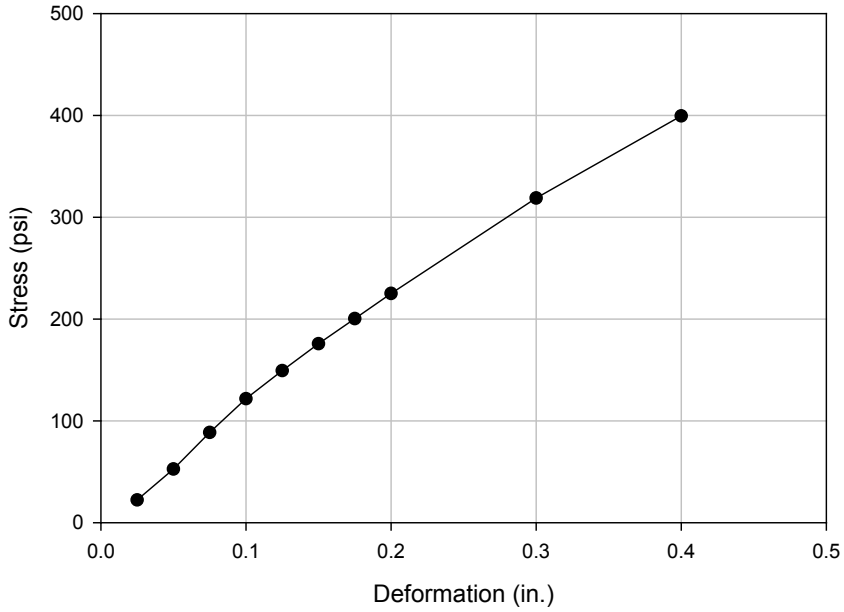

Figure 221. 10% Port Neal FA stabilized subgrade stress penetration curve

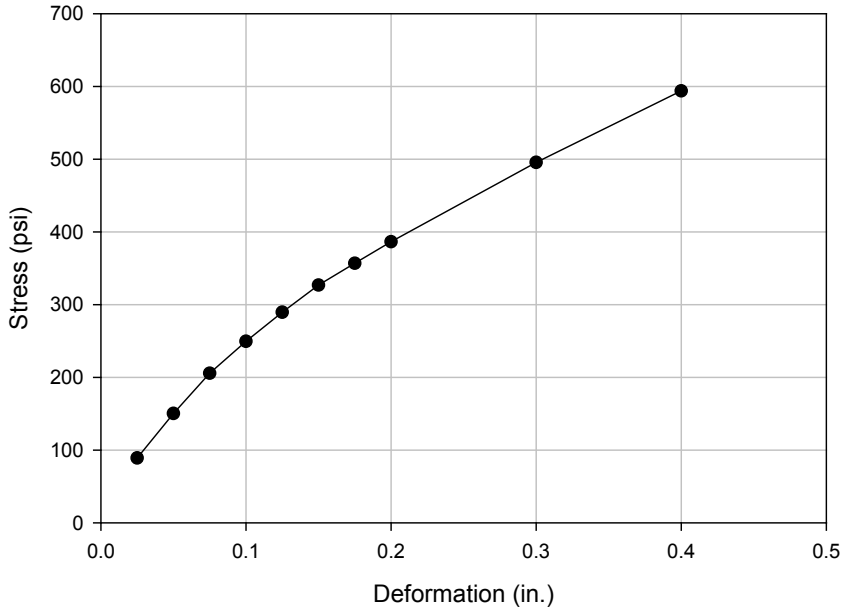

Figure 222. 15% Port Neal FA stabilized subgrade stress penetration curve

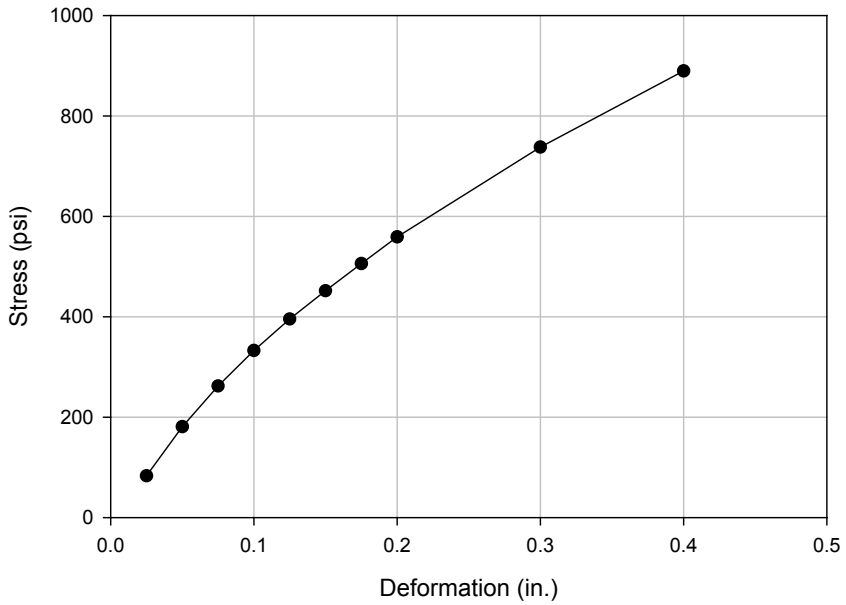

Figure 223. 5% cement stabilized subgrade stress penetration curve

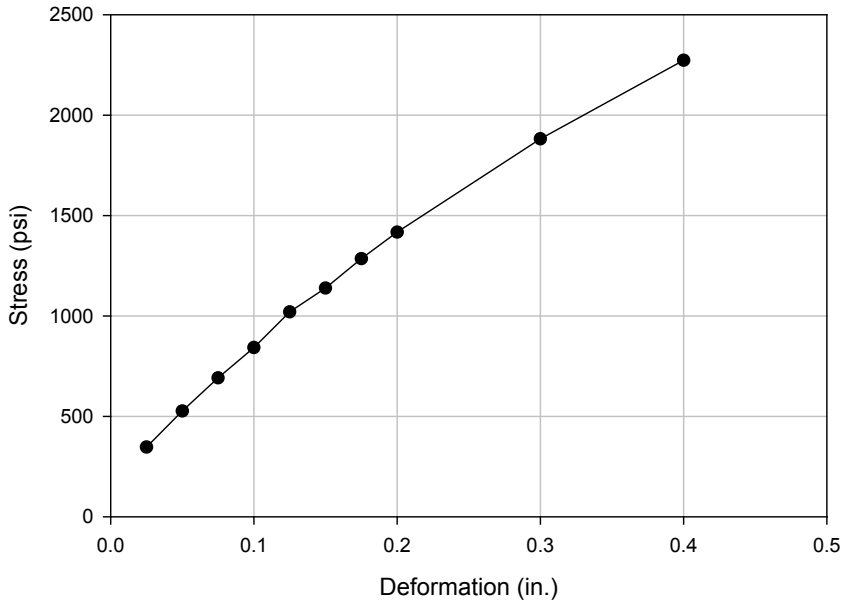

Figure 224. 10% cement stabilized subgrade stress penetration curve

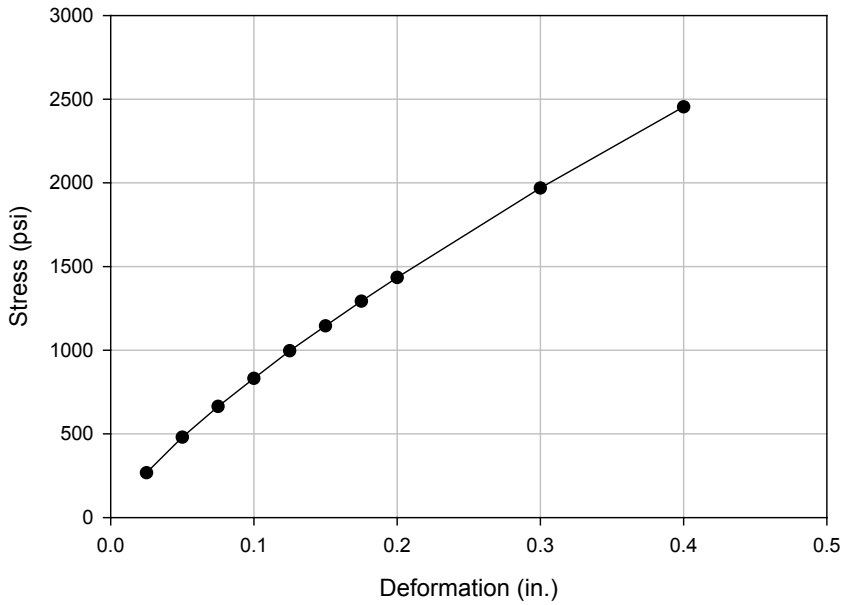

Figure 225. 2.5% cement stabilized recycled subbase stress penetration curve

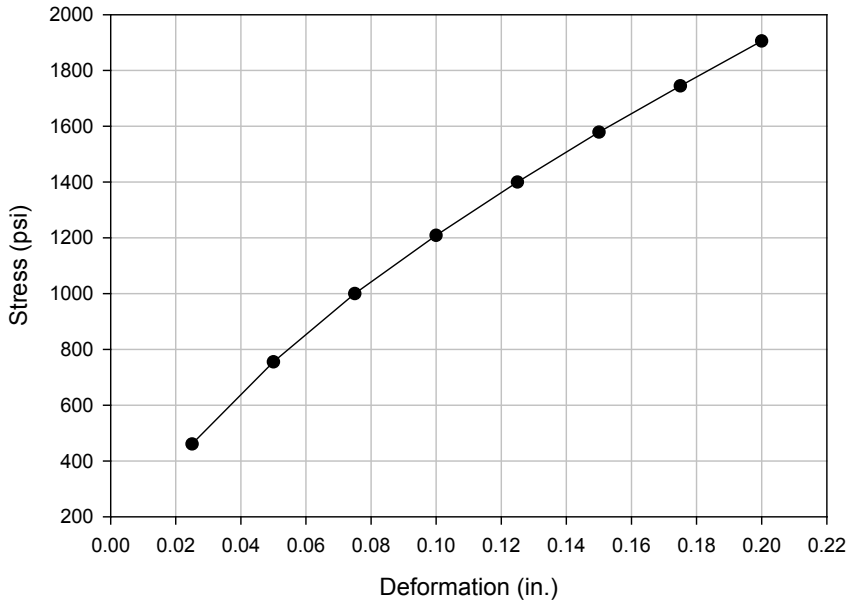

Figure 226. 3.75% cement stabilized recycled subbase stress penetration curve

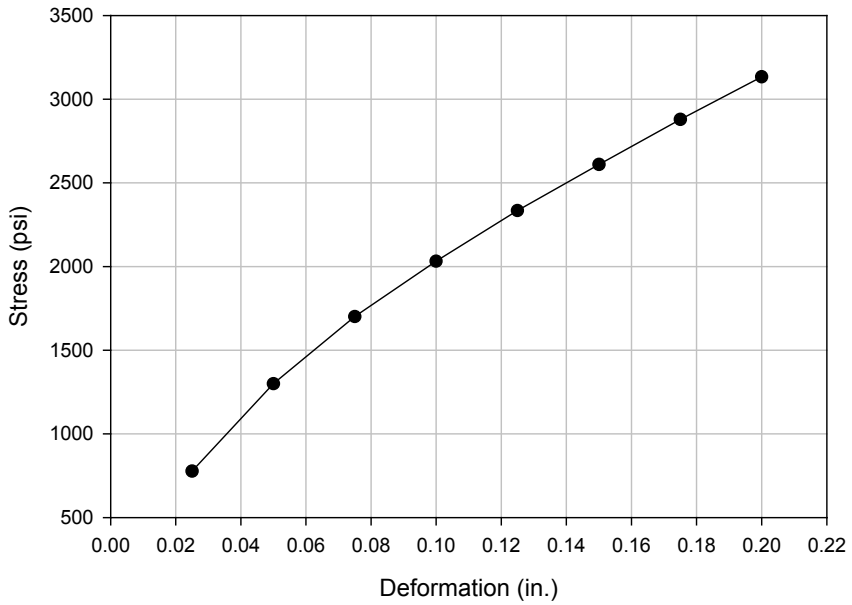

Figure 227. 5% cement stabilized recycled subbase stress penetration curve

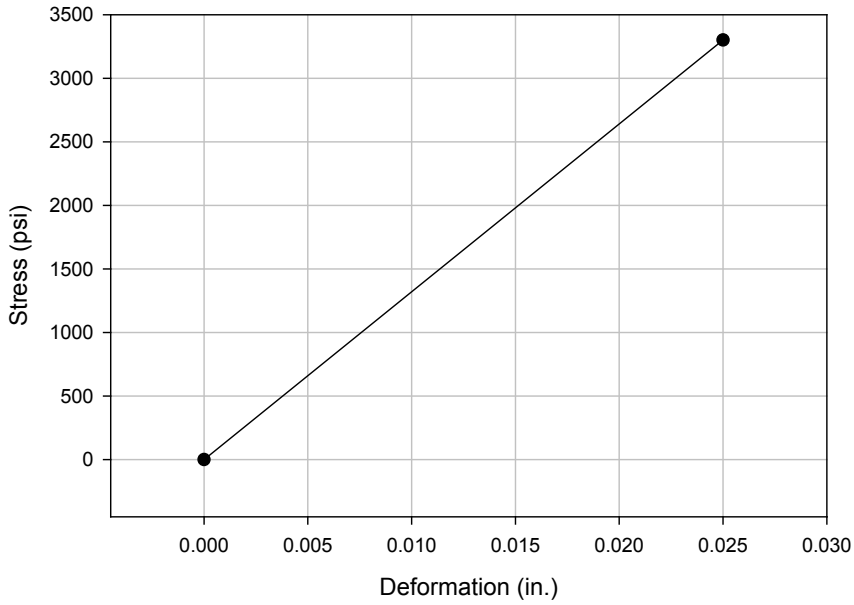

Figure 228. 7.5% cement stabilized recycled subbase stress penetration curve

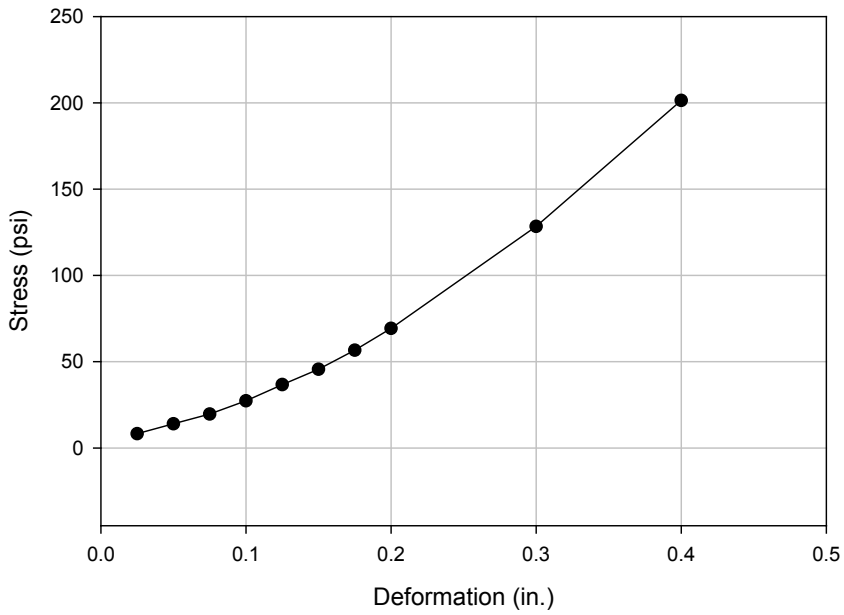

Figure 229. 0.2% PP fiber stabilized recycled subbase stress penetration curve

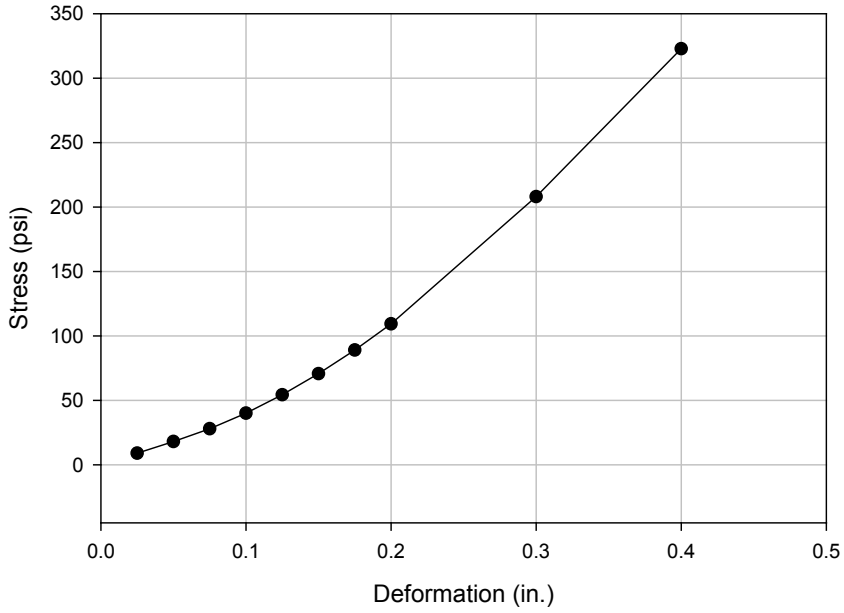

Figure 230. 0.4% PP fiber stabilized recycled subbase stress penetration curve

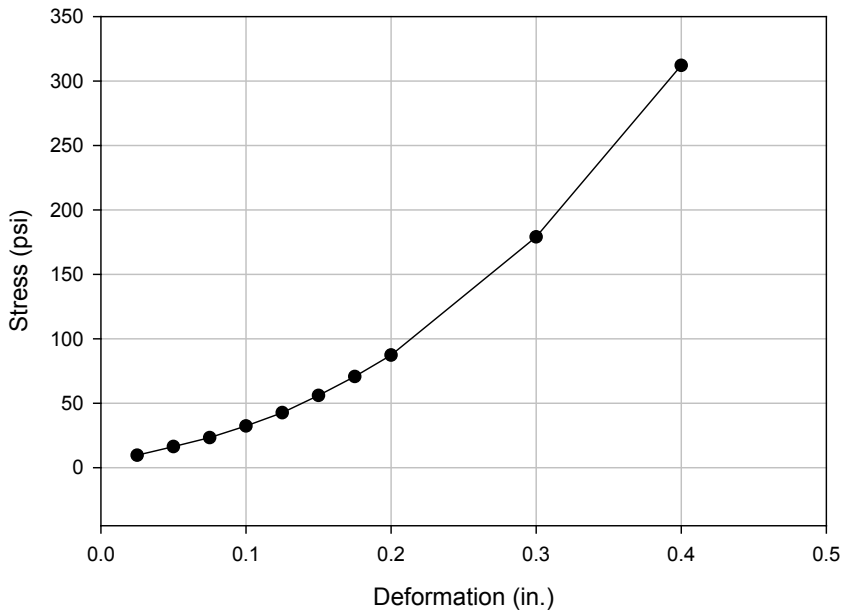

Figure 231. 0.6% PP fiber stabilized recycled subbase stress penetration curve

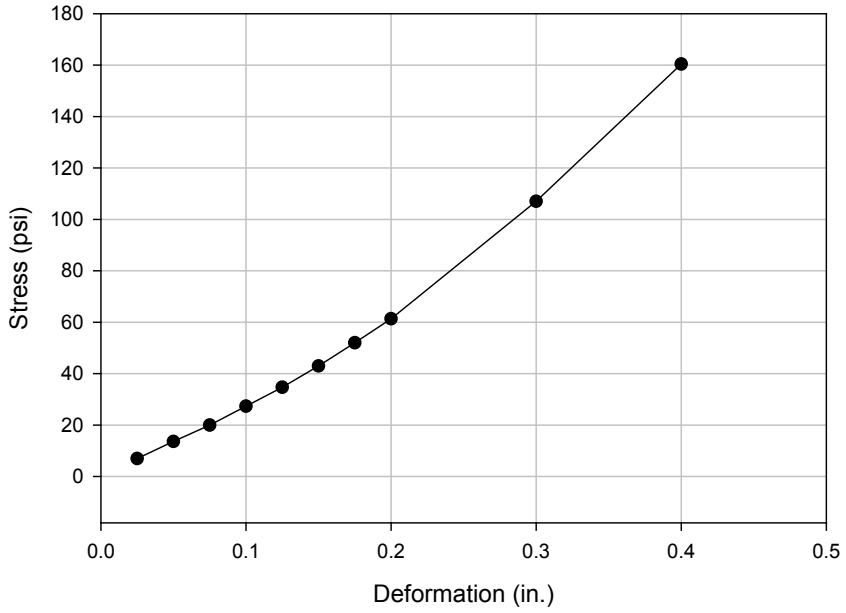

Figure 232. 0.2% MF fiber stabilized recycled subbase stress penetration curve

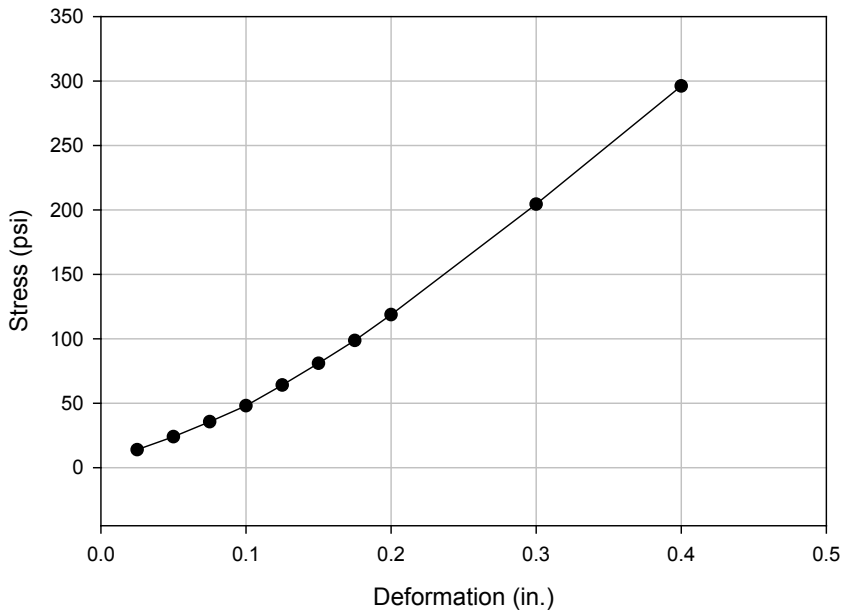

Figure 233. 0.4% MF fiber stabilized recycled subbase stress penetration curve

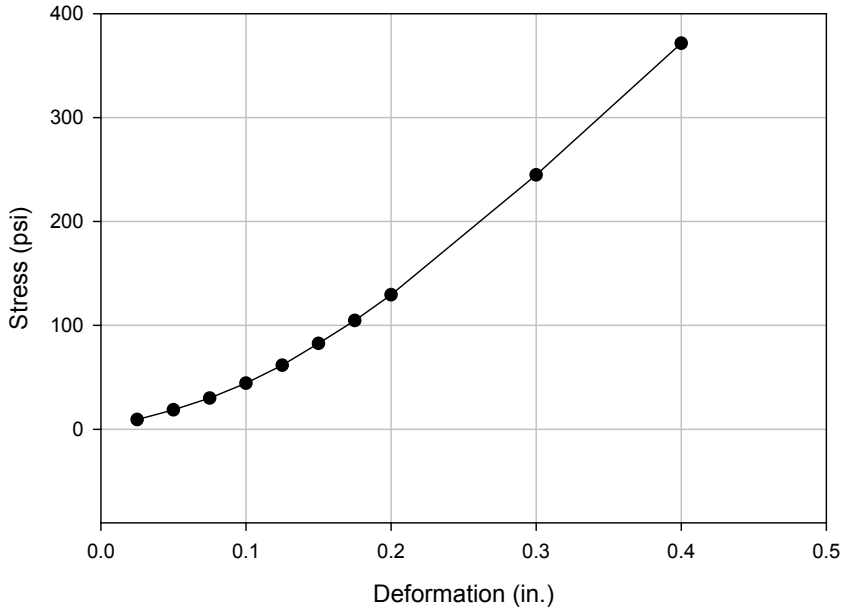

Figure 234. 0.6% MF fiber stabilized recycled subbase stress penetration curve

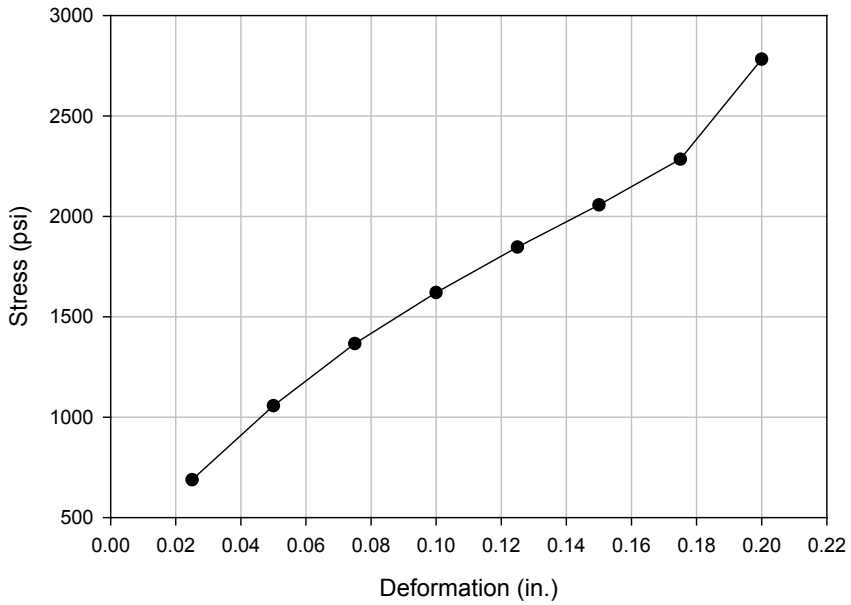

Figure 235. 3.75% cement + 0.2% PP fiber stabilized recycled subbase stress penetration curve

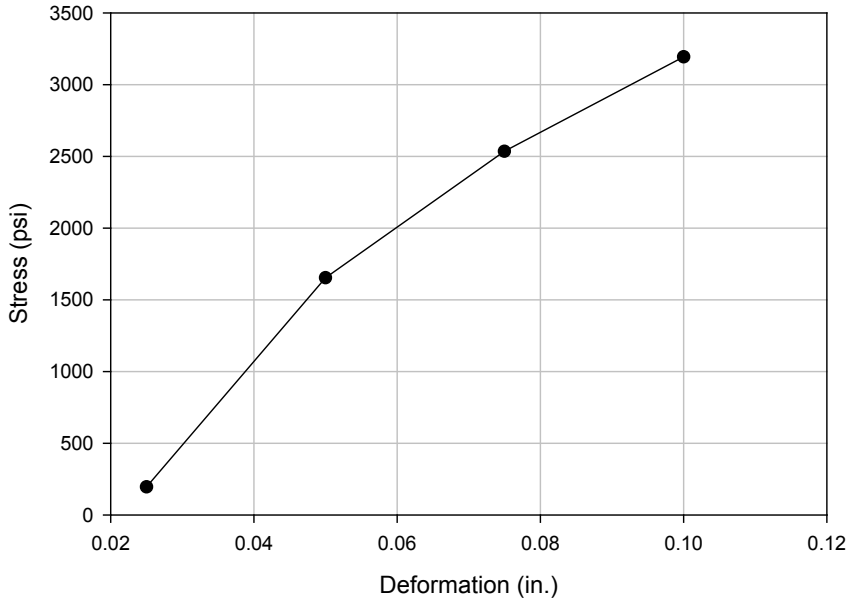

Figure 236. 3.75% cement + 0.4% PP fiber stabilized recycled subbase stress penetration curve

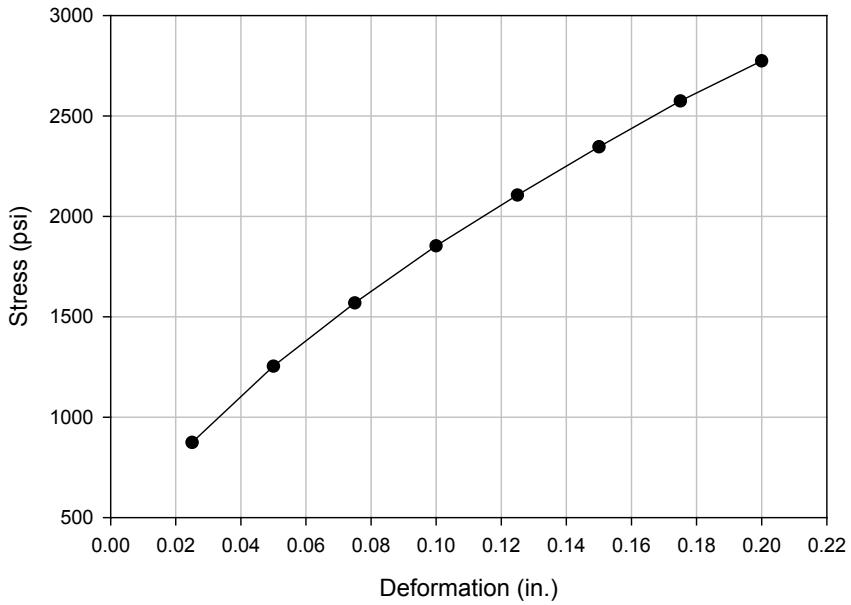

Figure 237. 3.75% cement + 0.2% MF fiber stabilized recycled subbase stress penetration curve

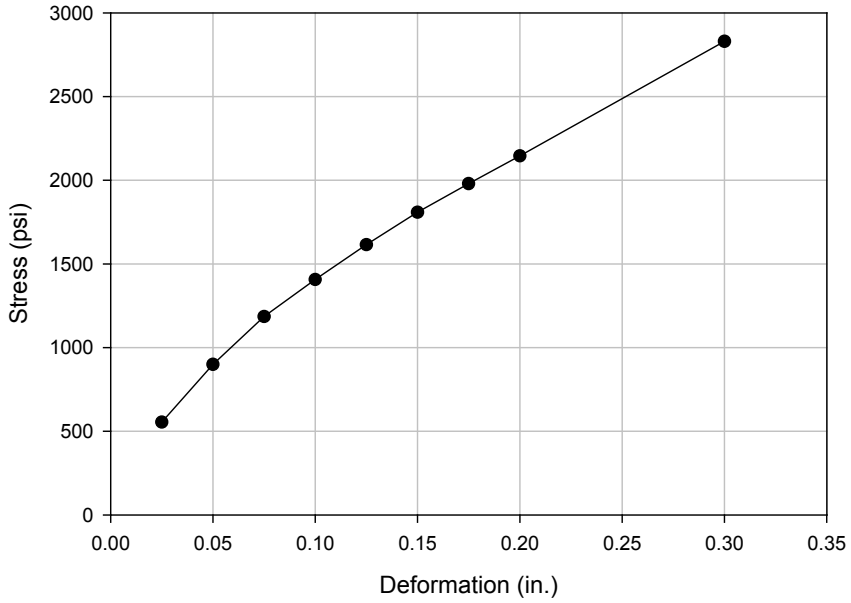

Figure 238. 3.75% cement + 0.4% MF fiber stabilized recycled subbase stress penetration curve

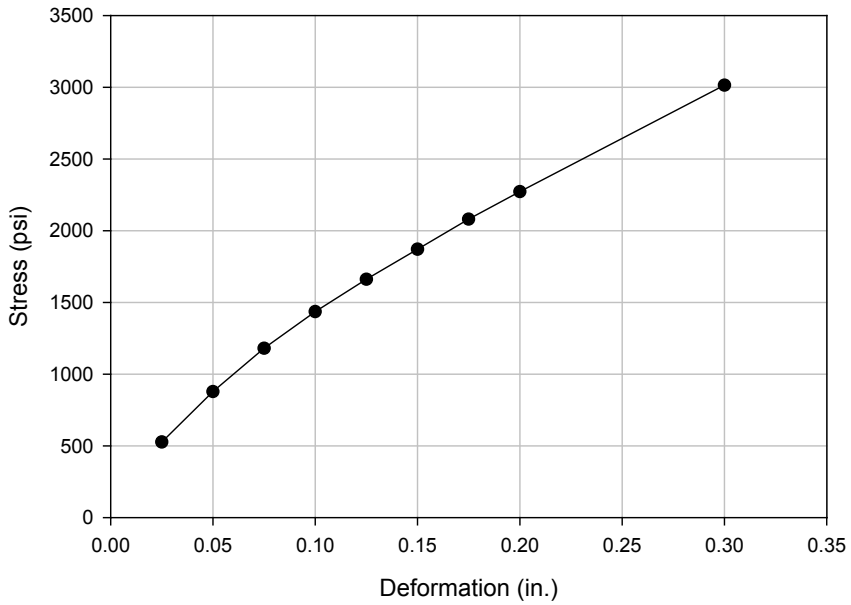

Figure 239. 3.75% cement + 0.6% MF fiber stabilized recycled subbase stress penetration curve

APPENDIX C. FROST-HEAVE AND THAW-WEAKENING TEST PROCEDURAL MANUAL

Material Preparation

1. Based on moisture-density tests, determine the optimum moisture content. Add sufficient water to the samples to reach the optimum moisture content.
2. Cohesive materials require approximately 6000 g per sample and cohesionless materials require approximately 7000 g per sample.
3. Separate into 4 samples and allow the samples to equilibrate overnight.
4. Take moisture content samples the day before compaction to verify accuracy.

Sample Preparation

5. Measure the mass of the top and bottom acrylic disks, the mass can be used for all four samples.
6. Measure the mass of the rings, membrane, and disks that will be used for each of the 4 samples.

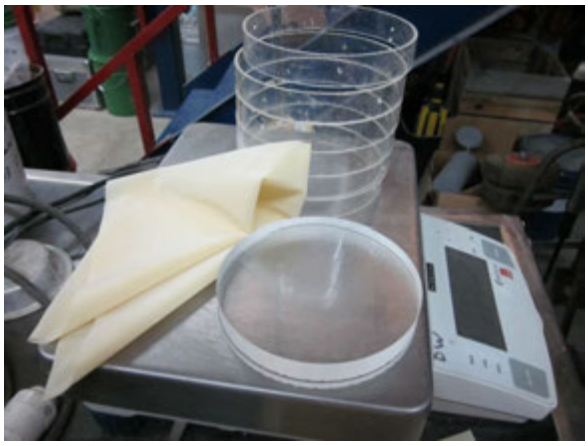

7. Wrap the membrane around bottom acrylic disk and place in the bottom of the sample mold with one half of the side walls removed.

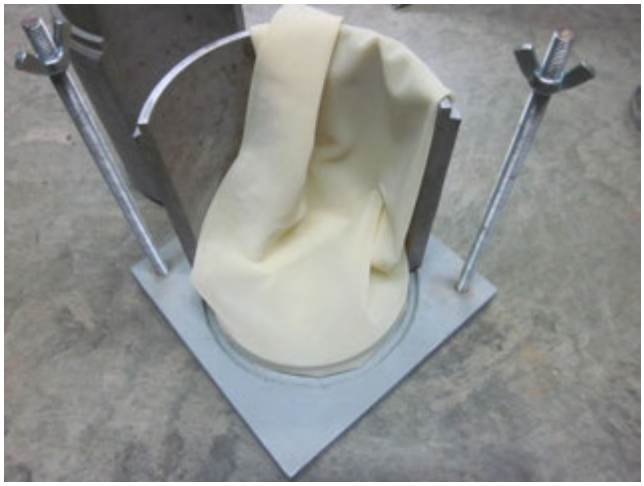

8. Place the 6 acrylic rings on the bottom acrylic disk, with the membrane inside of the rings. Align the thermocouple holes and notches vertically. The bottom ring should have a notch pointing down and the top ring should have a notch pointing up.

9. Place the other half of the side wall on the mold. Place 4 pipe clamps around the circumference of the side walls and tighten.

10. Place the collar on the mold and tighten the wing nuts

11. Stretch the membrane around the collar.

12. Compact material in 5 layers by applying 40 blows from a standard proctor hammer to each layer. Each layer should be nearly 1.2 in. thick.
13. Remove the membrane from the collar and remove the pipe clamps and side walls.

14. Fold back the membrane and trim the sample.

15. Place the top acrylic disk on the sample and measure the mass of the sample, rings, membrane, and disks.
16. Take a moisture content sample of each sample from the material that is remaining.

Sample Setup and Saturation

17. Place the porous stone and filter paper on the specimen base.

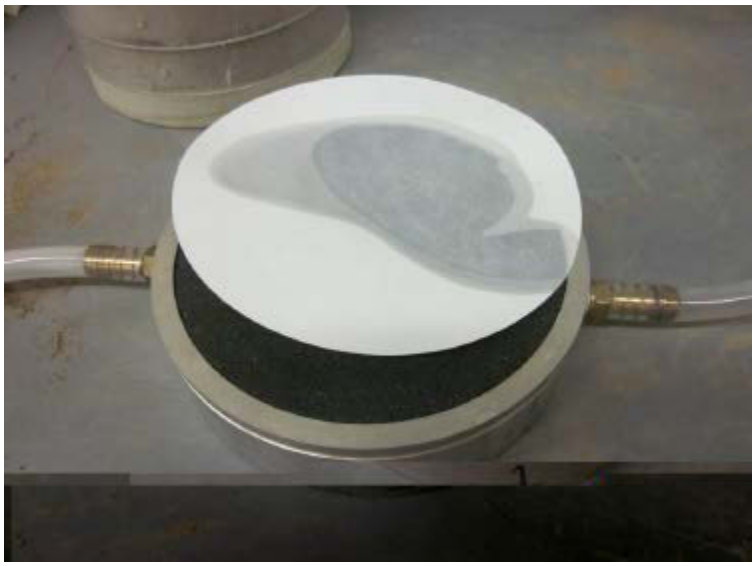

18. Remove the top and bottom acrylic disks from the sample and center the sample on the specimen base. For convenience, point the vertically aligned the thermocouple holes and notches toward the tubing coming from the water supply.

19. Roll the membrane around the specimen base and slide an O-ring over the membrane onto the specimen base. The O-ring should fit into the grooves in the specimen base. Place a pipe clamp around the O-ring and tighten.

20. Roll the membrane around the top of the sample and place a sheet of plastic wrap over the sample, secure with a rubber band. Place the surcharge weight onto the samples.
21. Connect the specimen base to the water supply.
22. Flush the air out of the water lines and clamp the tubing shut. Fill the water supply and seal it. It may be easier to seal the water supply if after flushing the lines; the line is not completely closed. By allowing the water to flow while sealing the water supply, the water level should move to the bottom of the glass bubble tube. Clamp the tubing shut.

23. Set the water head level to 1 in. by placing the bottom of the glass bubble tube 1 in. above the bottom of the sample. Mark the initial water level and measure the change in water level at the end of the saturation period.
24. Raise the bubble tube at a rate of 1 in. per hour for 8 hr, then set at 6 in. for 16 hrs.

Setup in Freezer

25. Disconnect the samples from the water supplies and remove the surcharge weights.
26. Puncture the membrane at the locations where the thermocouple will be placed.

27. Place the samples in the freezer on the bottom heat exchangers. Place the samples in the freeze according to the following arrangement.

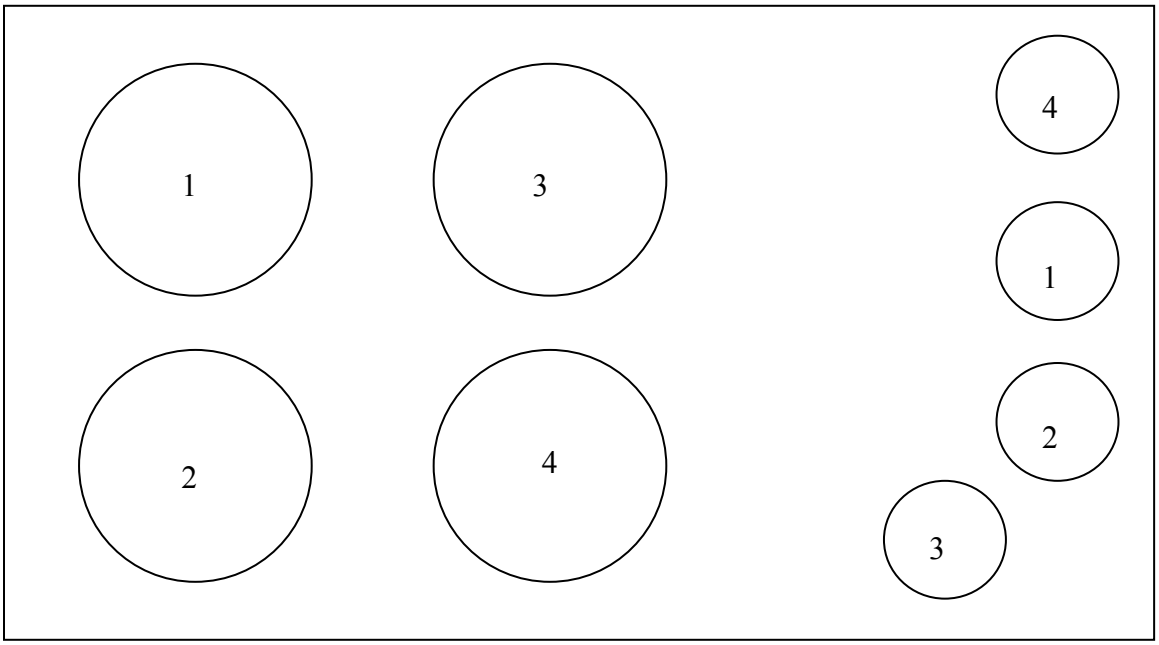

28. Place the top heat exchanger on the sample, seal with an O-ring, and reapply the surcharge weights.

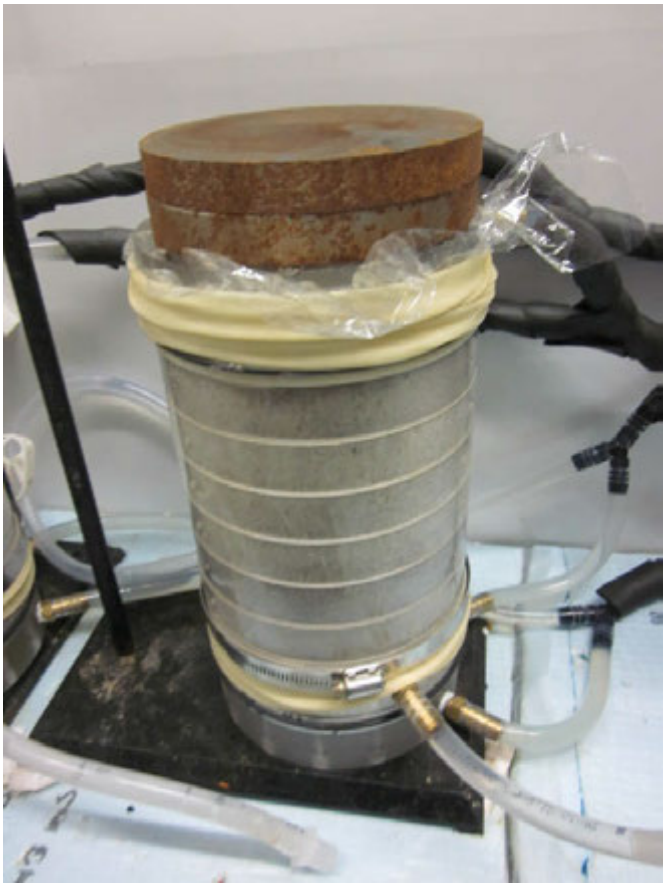

29. Place the water supplies in the freezer and re-connect to the specimen bases.

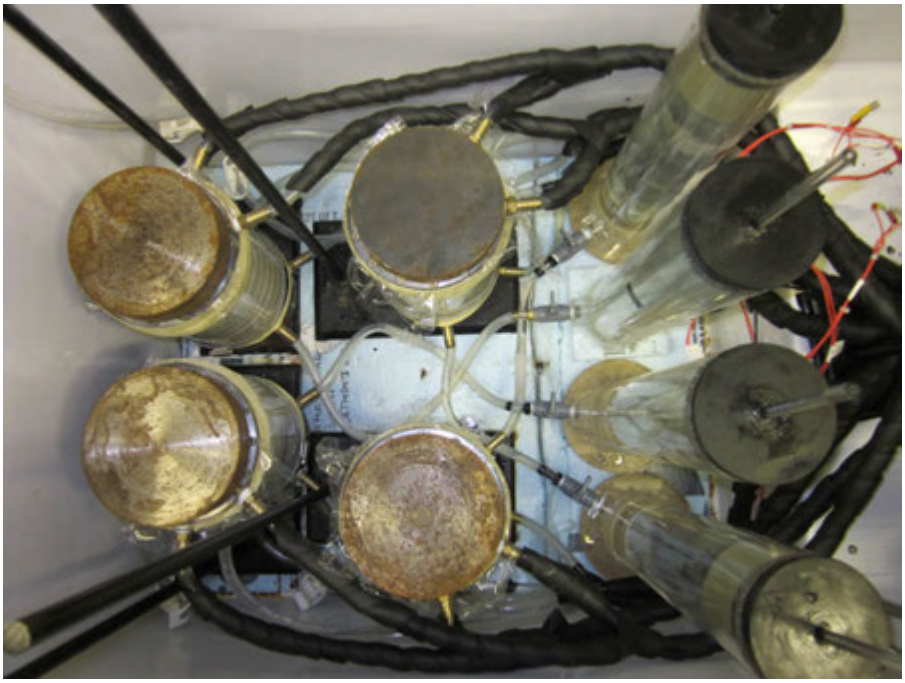

30. Purge the air from the water lines by allowing water to flow through the system. Set the head level 0.5 in. above the sample bottom, which is the same as setting the top of the bubble tube approximately 4.5 in. above the stopper. Mark the initial water level and measure the change in water level at the end of the testing period.
31. Connect the pressure transducer wires and wrap in electrical tape.
32. Dip the thermocouple tips in silicon adhesive and insert into sample. The numbers increase going down the sample (1 is on top and 8 is on bottom).

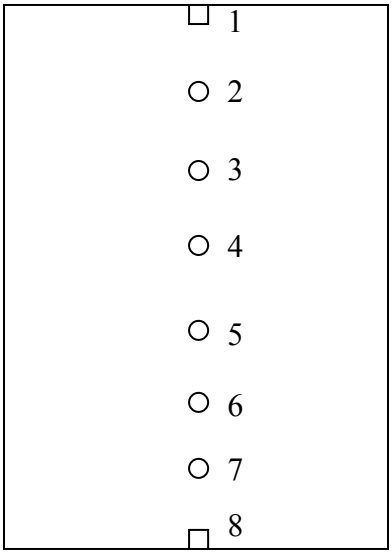

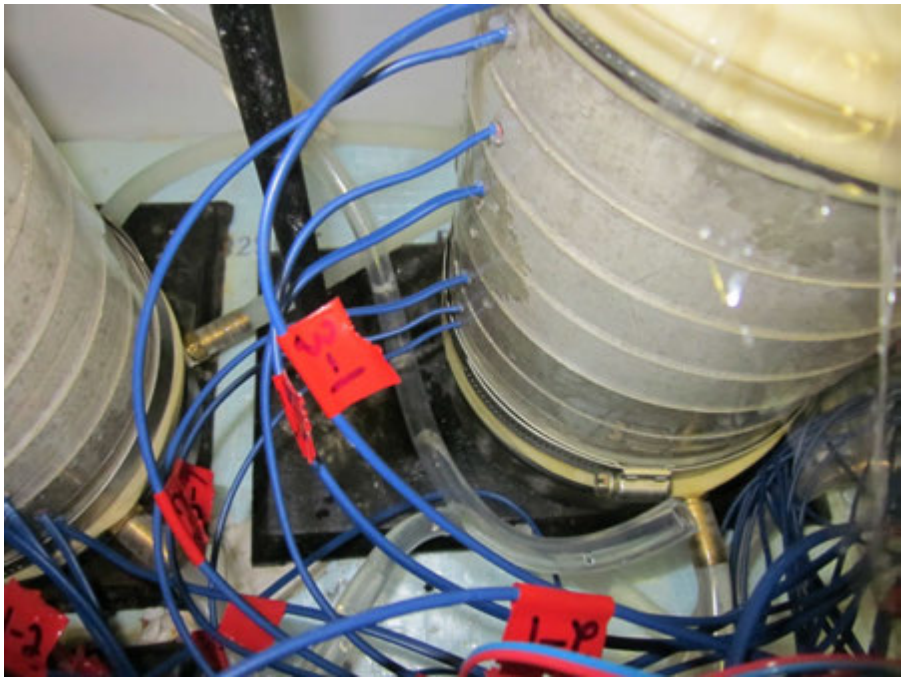

33. Turn on water baths and set the target temperature to 3°C. Turn on the freezer and place thermocouple in freezer. The following programs should be input into the top and bottom water baths:

Top Heat Exchanger		
Program Step	**Set Point (°C)**	**Duration**
1	3	960 min
2	3	480 min
3	3	1 s
4	-3	480 min
5	-3	1 s
6	-12	960 min
7	-12	1 s
8	12	960 min
9	12	1 s
10	3	480 min
11	3	1 s
12	-3	480 min
13	-3	1 s
14	-12	960 min
15	-12	1 s
16	12	960 min
17	12	1 s
18	3	480 min
19	3	1 s

Bottom Heat Exchanger		
Program Step	**Set Point (°C)**	**Duration**
1	3	960 min
2	3	480 min
3	3	480 min
4	3	1 s
5	0	960 min
6	0	1 s
7	3	960 min
8	3	960 min
9	3	1 s
10	0	960 min
11	0	1 s
12	3	960 min
13	3	480 min
14	3	1 s

34. Place the displacement sensors on top of the sample. Place the sensors high enough that the expected range of heave can be measured. The light on the top of the laser gives an indication of where the laser is in the measuring range. The light on top of the lasers mean the following:
    - Red means the laser is out of the measurement range
    - Green means the laser is in the measurement range
    - Orange means the laser is at the midpoint of the measurement range

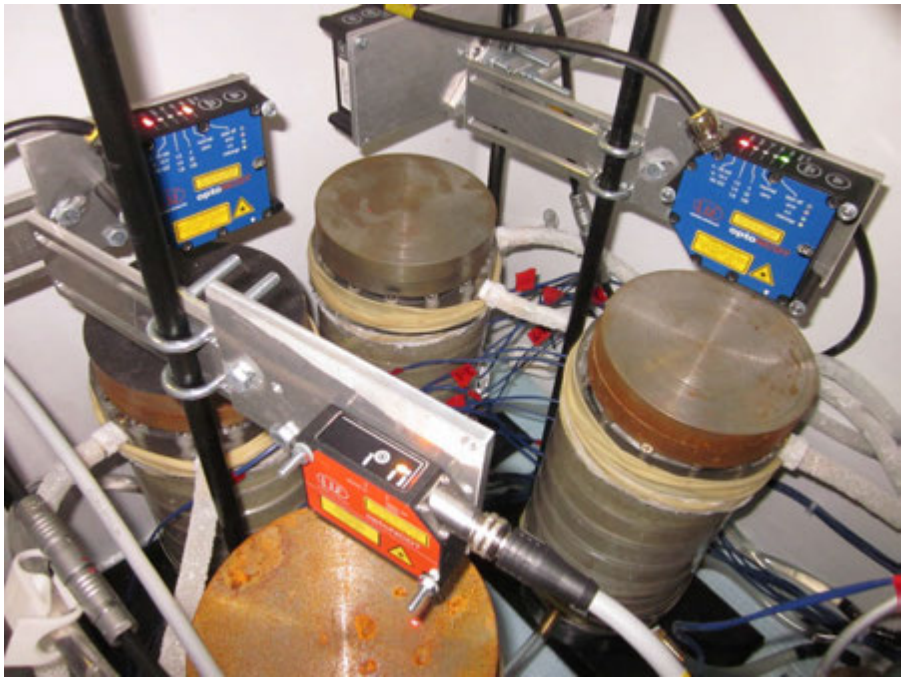

35. Observe the readings from the pressure transducers, thermocouples, and displacement transducers to make sure they are reasonable. Double check the water supply connections, the water supply valve is open the thermocouple placement,
36. Fill with granular insulation.

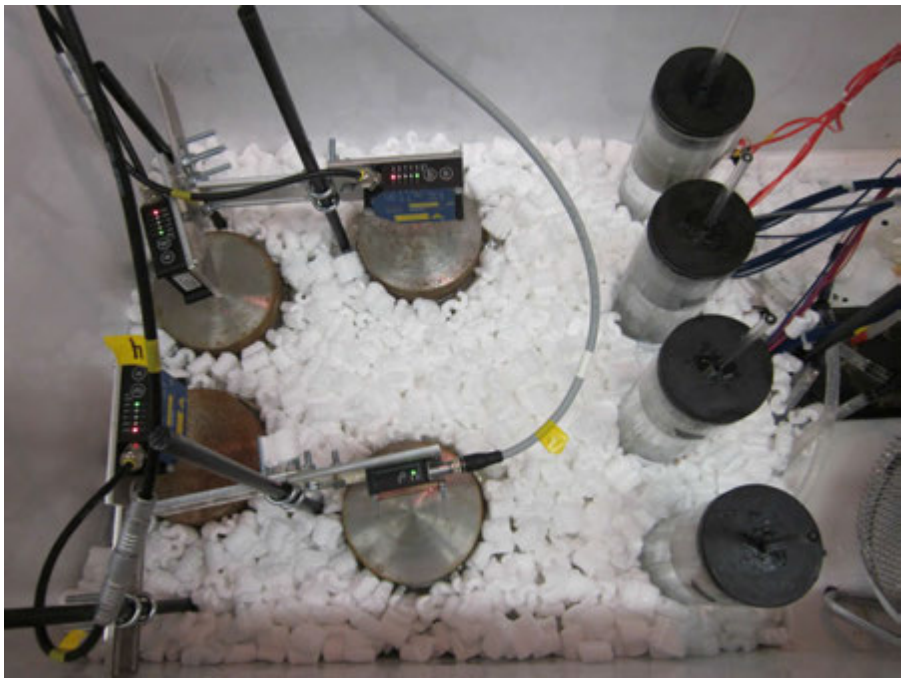

37. Place the thermocouple measuring the air temperature and the thermocouple for the freezer temperature controller into the freezer. Make sure neither

thermocouple is in contact with anything that may give a false air temperature reading.

38. Restart the data acquisition system and start the water bath programs.

Removal from Freezer and CBR

39. Remove the displacement sensors, granular insulation, and thermocouples.
40. Disconnect the samples from the water supplies and remove from the freezer.
41. Remove the pipe clamp from the samples and both O-rings and measure the mass of the sample, rings, and membrane.
42. Place 4 pipe clamps around the top 4 acrylic rings and place the CBR surcharge weights on the sample. Perform the CBR test.

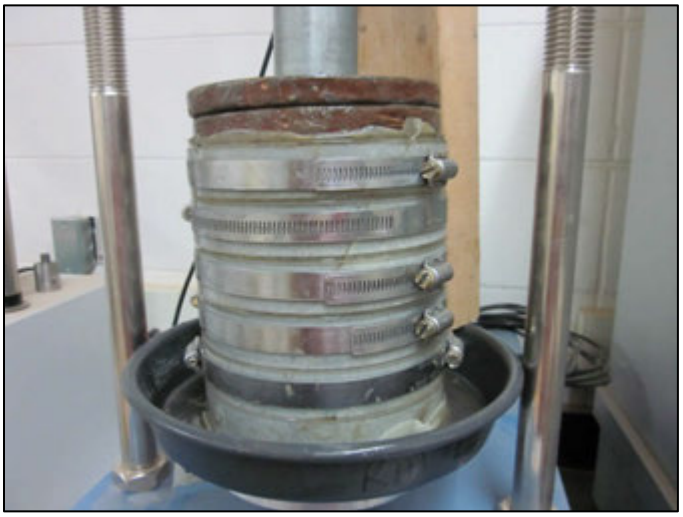

43. Take moisture content samples from the sample on 1 in. centers in the vertical direction to develop a moisture content profile.

ACKOWLEDGEMENTS

First and foremost I would like to thank my major professor, Dr. David White, for his guidance, encouragement, and patience. His financial support helped me to concentrate on this research and confidently to pursue a Master of Science degree. I am also thankful for Dr. Robert Horton, Dr. Peter Taylor, and Dr. Pavana Vennapusa. Their advising helped me to reach the goals of this research and professionally improved my thesis.

I am grateful for everyone who has helped me during my Master's study, especially the members at the Center for Earthworks Engineering Research at Iowa State University. I would like to thank Dr. Christianna White for her guidance on technical writing and Alex Johnson for sharing his previous experience.

At last, I would like to thank my deeply loving family, especially my parents who constantly pushed me to follow my dream and gave me great support on everything in my life.